STOCHASTIC PROCESSES IN THE HUMAN EYE MOVEMENT CONTROL SYSTEM

Thesis by

George Wood Beeler, Jr.

In Partial Fulfillment of the Requirements

For the Degree of

Doctor of Philosophy

California Institute of Technology

Pasadena, California

1965

(Submitted May 18, 1965)

PREFACE

The author of this thesis is a student in an interdisciplinary program at the California Institute of Technology administered under the joint supervision of the Electrical Engineering Department of the Division of Engineering and Applied Science, and the Division of Biology. For this reason, the thesis is intended to be read by members of both disciplines. In order to present a work that is compatible to both groups, two chapters of a review nature have been included following the introduction. It is hoped that the first of these review chapters will serve to acquaint the engineer with the biological and anatomical background of the human eye that is necessary to assess the experimental work reported in the latter part of the thesis. The other chapter is a rather detailed discussion of the instrumentation which was used during the experiments, and is intended to familarize the biologist with the data processing techniques which were used. It is sincerely hoped that both disciplines will find valuable information in this dissertation.

The author would like to acknowledge the advice, assistance, and guidance that he received from many people during his tenure at Caltech, but particularly that of:

Dr. Derek H. Fender, his advisor, under whose guidance he found his way through the research and education necessary to complete this work.

Dr. Patrick W. Nye, David S. Gilbert, and Gordon F. MacGinitie, who have served as "devil's advocates" at various times inconvenient to them throughout the course of the research.

F, Nl, and M, who have suffered the tribulations of being experimental subjects.

Dr. Gilbert D. McCann, for his reading of this manuscript and comments on it as it was produced.

Clark E. Albin, who steadfastly assisted in the laboratory work, and all the Biological Systems staff who have provided the group programming and equipment necessary for the data processing.

Simone J. DeMaria, M. Selby Butt, and Michael S. Cobb who assisted greatly in the preparation of this manuscript.

The author is indebted to the California Institute of Technology, and to the National Institutes of Health for their financial support of himself and this research.

This thesis is dedicated to Milton and Jane Greenfield, the author's parents, without whose faith and support this work would never have reached fruition.

ABSTRACT

Experiments have been performed to investigate several of the stochastic processes involved in the control of eye movements, particularly where these processes apply to saccades. Previous models have linearized the eye positioning system, and as a result some of the more important features have been lost in the analysis.

The experiments concentrated on four areas. The first of these was temporal prediction by saccades when tracking square wave target motions. This predictor function generates a response saccade approximately 100 msec before the stimulus step. The mean response time, however, never precedes the stimulus by more than 50 msec, and actually occurs after the stimulus when tracking either very short or long period square waves. These changes in mean response time are caused by a shift in the predictive lead at short periods, and by failures of the predictive mechanism at longer periods. This failure results in a delayed response 200 msec after the stimulus.

The second area investigated was the non-predictive saccadic response system. The investigation revealed that the sampled data effect previously reported is actually the result of the combination of a time delay and a refractory unit in the response mechanism. The characteristic times of these functions were investigated, along with the ability of the system to alter a response when additional retinal information arrives before the initial response saccade is elicited.

Thirdly, the role of spontaneous flicks in steady fixation tasks was investigated utilizing two-dimensional analysis. It was found that the majority of these events are of stochastic origin, whereas previous studies, analyzing only the horizontal components, indicated that the flicks are only used to correct fixation error. A generator

for the random flicks can be postulated, and the source of the spontaneous drift motion was identified.

Finally, experiments were performed on the perceptual effects of saccades. It was found that the visual system is incapable of detecting small target motions when they occur within ±40 msec of a flick. This suppression of movement detection by the saccades led to a re-evaluation of the efference copy mechanism, and the effect of this re-evaluation on eye movement control is discussed.

TABLE OF CONTENTS

CHAPTER I

INTRODUCTION

The function and control of human eye movements have for many years interested research workers in such diverse fields as experimental psychology, ophthalmology, and engineering. While the sources of these interests have been different - the psychologist seeking the behavioral implications of eye motion, the opthalmologist seeking the medical aspects of the sense organ, and the engineer attempting to represent, in formal terms, the system which controls the eye position - they have found common ground for research in this problem. For this reason, eye movements and perception form an ideal field for research in an interdisciplinary program such as the one of which the author is a member.

The motion of the eye can best be described, both from subjective and physiological points of view, in terms of the line of sight of the subject. The movement of this line about the visual field which the subject is persuing is accomplished in several ways - by body motion, changes in the posture of the head, and by pure rotation of the eye about its center. This thesis is concerned with only the latter method of moving the line of sight, although it is realized that the other modes of motion represent a large field of research which should at some time be explored. With this restriction, the motion of the line of sight can be described either by the rotation of the eyeball, by the motion of the point of intersection of the line of sight with the visual scene, or by the motion of the image on the retina. In the work that follows these measures will be regarded as synonymous, and the terms "movement" and "rotation" will be used interchangeably.

There are three regimes in which eye motion occurs, and these can be differentiated by their time courses as: slow, or drift, motion with a maximum frequency of about 2.5 cps; the flick or saccade, a form of step function; and, tremor, a small amplitude movement at higher frequencies than the drift. The first two of these components are observed both as controlled components, when the fixation position of the eye is being shifted, and as random motions perturbing the line of sight position from the desired location. The tremor, on the other hand, never appears to be controlled by the subject, and is probably a form of noise in the neuro-muscular system.

Functionally, each of the three forms of eye rotation can be ascribed a specific task. The four to twelve cps band of tremor has been shown to be beneficial to the maintenance of clear vision by providing repeated stimulation to the retinal receptors. The drift movements provide the eye displacement when the orb is tracking a target which is executing a simple slow movement; this is generally referred to as the smooth-following mode. The saccades, easily the most efficient of the eye movement components in terms of speed, are utilized in producing gross eye rotations. Voluntary saccades, those engendered in response to an external stimulus, fall into two functional categories. When a person is studying a large visual area, as in reading, the saccades serve to move the fixation position of the eye from one area of interest to the next. Thus, one function of the saccades is to produce large, rapid changes of the fixation position with respect to a stationary target. The second voluntary function is observed in the task of tracking target displacements which are too rapid to be followed by the drift component. In this mode, the saccades exhibit a response delay on the order of 200 msec, although there is deviation from this value under many tracking conditions. In addition to their appearance during voluntary tasks, many apparently spontaneous saccades are observed; these are generally refer-

red to as flicks. While the presence of these flicks in the eye control system represents a form of noise or inaccuracy in that system, they might well be of physiological benefit in the maintenance of clear vision.

On first consideration, it would appear that the control system which generates the voluntary eye movements has to be a highly complex system in order to encompass the broad range of functions of which the eye is capable. Investigation, however, has revealed that the saccadic and drift systems may be separated functionally and tested individually. Moreover, each of these two control systems can be broken down still further into predictive and non-predictive modes. In general terms, the eye position control system can produce a following response to a simple stimulus waveform,[1] such as a target position which is purely sinusoidal in time, with far less phase lag than the response to a complex target motion. This non-linearity, a measure of the adaptability of the control system, has frequently been studied separately from the overall response.

Studies of the eye movement control system have been made several times in the last six years, and three sub-systems have been fairly substantially modelled. Fender and Nye (25) produced a smooth-following model in 1961 which provides good measurements of the tracking of sine-wave stimuli, and thereby specifies the predicting mode of the drift system. Young (61) and Dallos (14) have both analyzed the smooth following system in response to unpredictable stimuli by using target motion waveforms composed of the sums of

[1] Throughout this thesis, except where otherwise stated, "stimulus" or "stimulus waveform" will always refer to the pattern of target motion; for example, a "horizontal sinusoidal stimulus waveform" implies that the target moves to-and-fro along a horizontal line in the visual field with a displacement x from some central position given by the simple sine function $x(t) = x_{max} \cdot \sin 2\pi ft$. The brightness of the target is, in general, constant.

non-integrally related sine waves. While the overall forms of their models are different, the resultant responses are quite similar, and either might be taken as a satisfactory model of that sub-system. Finally, Young (61) has modelled the saccade control system in response to unpredictable step stimuli as a sampled data system. This latter model is a good approximation to this sub-system over a limited range of conditions, but important exceptions will be noted in the work which follows.

The flick and drift components which appear as spontaneous rotations of the eye have also been studied in recent years. Much of this work, however, has been performed by analyzing only one directional component of the eye movements, the horizontal. These studies have tended to emphasize the role of the flicks as correctors of fixation errors created by random drift motion. Studies utilizing both directional components, however, reveal that the flicks represent substantial random movement during simple fixation tasks, and a re-evaluation of these roles is necessary.

There has been, then, substantial research on eye movements aimed at establishing the model, but obvious gaps exist in the available specifications, and more extensive analysis in these areas would appear fruitful. There are three major areas to be covered. First, no model has been derived for the saccade response when tracking a predictable stimulus. The response of the eye to pure square waves was shown by Stark, Vossius, and Young (56) to be highly predictive, but they did not evolve a model from those experiments. Secondly, Young's sampled data model for the saccade control system is not a good approximation to the control system response for stimulus steps which follow each other closely in time, and his system does not provide reasonable guides as to the form or origin of the sampler. A careful examination of saccadic tracking in the following regime where his model is insufficient, however, yields basic information on the nature of the sampler, and serves to identify some of the information processing procedures which are

performed on the stimulus input. At the same time, a depression of the perceptual sensitivity to various visual stimuli is correlated with the saccades and alters the responses of all of these systems; this is deserving of investigation. Finally, spontaneous eye movements, movements not correlated with any target motion, are observed during the performance of all visual tasks. As these motions appear to be random, a stochastic process should be introduced in order to describe the source of these motions, and explain the interaction of spontaneous flicks and drifts. It is known that the error produced by these random movements is limited, and therefore at least one of the components must also serve an error correcting function.

The attempt of this thesis is to provide some of the links missing from the human eye control system. Modelling itself is an intellectual exercise at best, unless it also serves as a guide to the understanding of the physiological structure of the system. Despite the fact that the physiology of the oculomotor system has been extensively investigated, its detailed function remains elusive. Wherever the evidence collected in this work serves as a guide to this structure or function, a comment or speculation to that effect will be made, for this is, in the end, the justification for the work.

CHAPTER II

GROSS ANATOMY AND KINEMATICS OF THE EYE

Introduction. - Specifications of the gross anatomy of the eye and descriptions of typical eye movements fill many volumes. It is not the intent of this chapter to survey the whole of this knowledge, for the interpretation of the results of the research to be presented here relies only on certain of these facts; the material in this chapter is chosen to present those facts, and others which are necessary to maintain an overall perspective of the problem. This information is divided into two sections, anatomy and kinematics. The former is a purely physical description of the visual system, as it is known, while the latter is a summary of the forms of eye movement which are observed when studying an eye performing monocular fixation.

Gross Anatomy of the Eye

General. - The primary components of the orb are shown as a cross-section of the left eye in Fig. 2.1. (15) The overall shape of the eye is a sphere approximately 25 mm in diameter with a secondary spherical bulge, the cornea, to the front. Light enters the orb through the cornea, passing through the pupil and the lens to form an image on the retina. The spherical, transparent surface of the cornea, combined with the refractive medium of the lens, provides the eye with its optical power, and real images of the outside world are formed on the photosensitive receptors of the retina at the back of the eye. The total power of this optic system is about 60 dioptres (dioptres = 1/focal length in meters), of which about 43 dioptres are associated with the corneal surface. The ciliary muscle changes the optic power of the lens by introducing a circumferential tension which changes the curvature of the refractive surfaces.

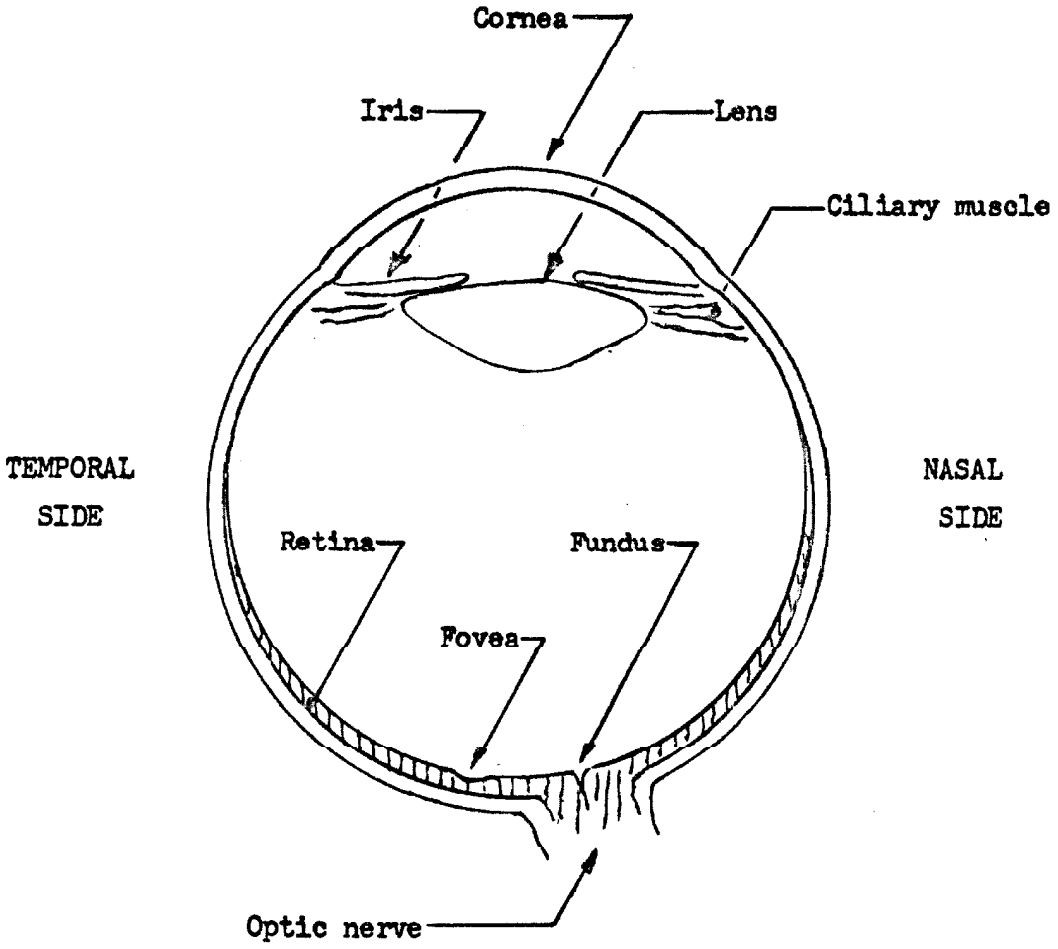

Fig. 2.1 - Horizontal section of left eye.

This muscle can produce a total change in the optic power of the eye of about eight dioptres.

In order to assess the visual effects of rotations of the orb, it is convenient to reduce the optical system of the eye to an equivalent system specified by a single optical power and two optical nodal points. Under this representation, the rear nodal point is about 17mm from the central portion of the retina. Thus, if the angle between the line of sight, and the line to any given target point changes by ω min arc (due either to eye rotation or target movement), then the image of that target point will move approximately 5ω microns on the surface of the retina. Owing to the fact that all eye movements are actually rotations of the orb, all motions and positions with respect to the eye will henceforth be specified in min arc or deg arc; this includes eye movements, target positions in space, and image locations on the retina. The image locations may be determined in linear dimensions from the simple relationship given above.

Two important features of the retina are indicated in Fig. 2.1. The first of these is the fovea. This region can be identified anatomically, as will be seen shortly, and can be shown experimentally to be the region of the retina on which the eye locates that area of the visual image which is under closest scrutiny. The fovea is located about 5 deg arc nasally and 1.5 deg arc below the optic (geometric) axis of the orb. The second retinal feature of note at this point is the fundus, or 'blind spot', where the axons of retinal neurons leave the eye and form the optic nerve.

The musculature which controls the position of the eye within its orbit is depicted in Fig. 2.2. (12) Three pairs of muscles, the members of each pair working in opposition, can provide all desired eye positions when utilized in the proper combination.

The primary information pathways to and from the orb are two nerve trunks which pass through the Annulus of Zinn. The first of

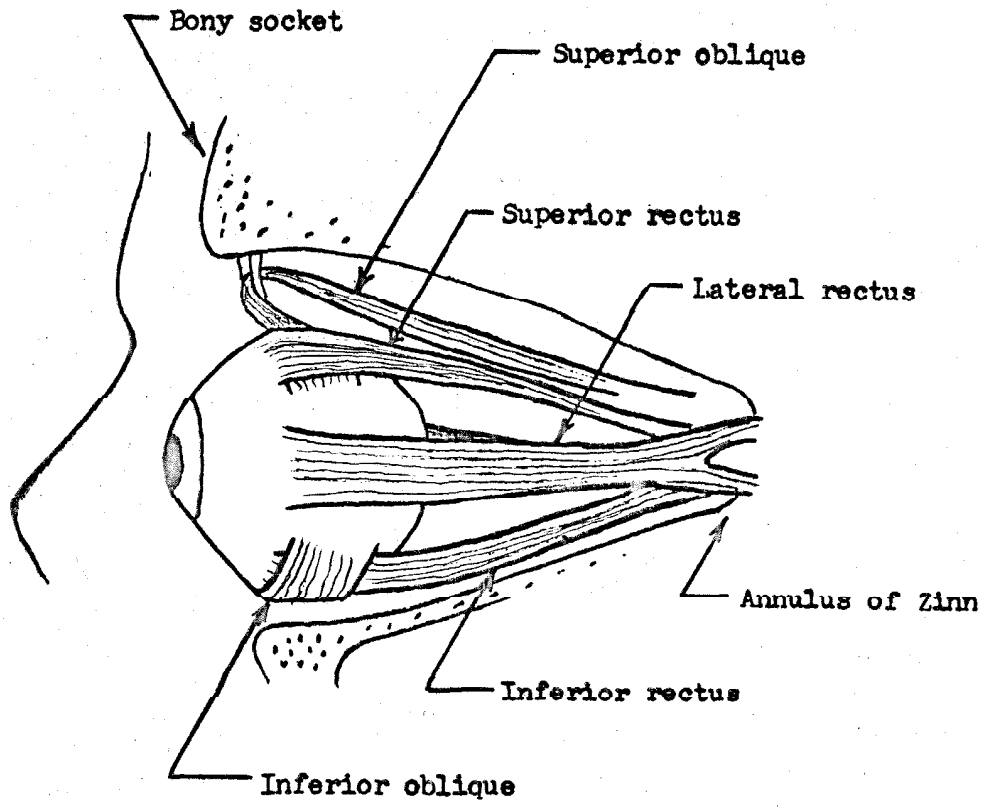

Fig. 2.2 - Side view of the left eye, showing five of the six extraocular muscles; redrawn from Cogan.

these is the optic nerve, which is primarily afferent and carries the information from the retinal receptors through the optic chiasma to the lateral geniculate bodies. The other nerve trunk is the oculomotor nerve, an efferent bundle, which carries the signals to control the extraocular muscles.

Within the general structure of the eye, two major areas need rather more detailed discussion for the purposes of this thesis - the receptive surface of the retina, and the motive system of the extraocular muscles.

The Retina

The receptors. - The retina is the surface which transforms the information of the visual image from light to neural impulses, and is composed of a layer of receptors and neurons spread over somewhat more than half of the inner surface of the eyeball. (15, 49) The receptors of the retina, numbering about 10^8, are divided anatomically into two classes, rods and cones. These two types of receptors differ radically in function, as will be seen shortly, and are distributed in a non-uniform manner over the retina. Typical retinal interconnections are shown in Fig. 2.3, from Polyak (49). These include both connections between neighboring receptors, and connections which provide some of the available information pathways from the receptors to the axons which comprise the optic nerve. It should be noted that the eye is engineered backwards from the way in which man would probably realize such a system. Light incident on the receptors from the front of the eye comes from below in Fig. 2.3, and must pass through the axons and neurons before striking the rods and cones. The rich interconnective network, of which only a small portion is indicated in Fig. 2.3, effects a great deal of data processing on the visual information before this information ever leaves the retinal level. This preliminary processing is a function about which little is known at present, but the fact that it occurs over the majority of the retina indicates that it probably serves to condense the incoming information and thereby

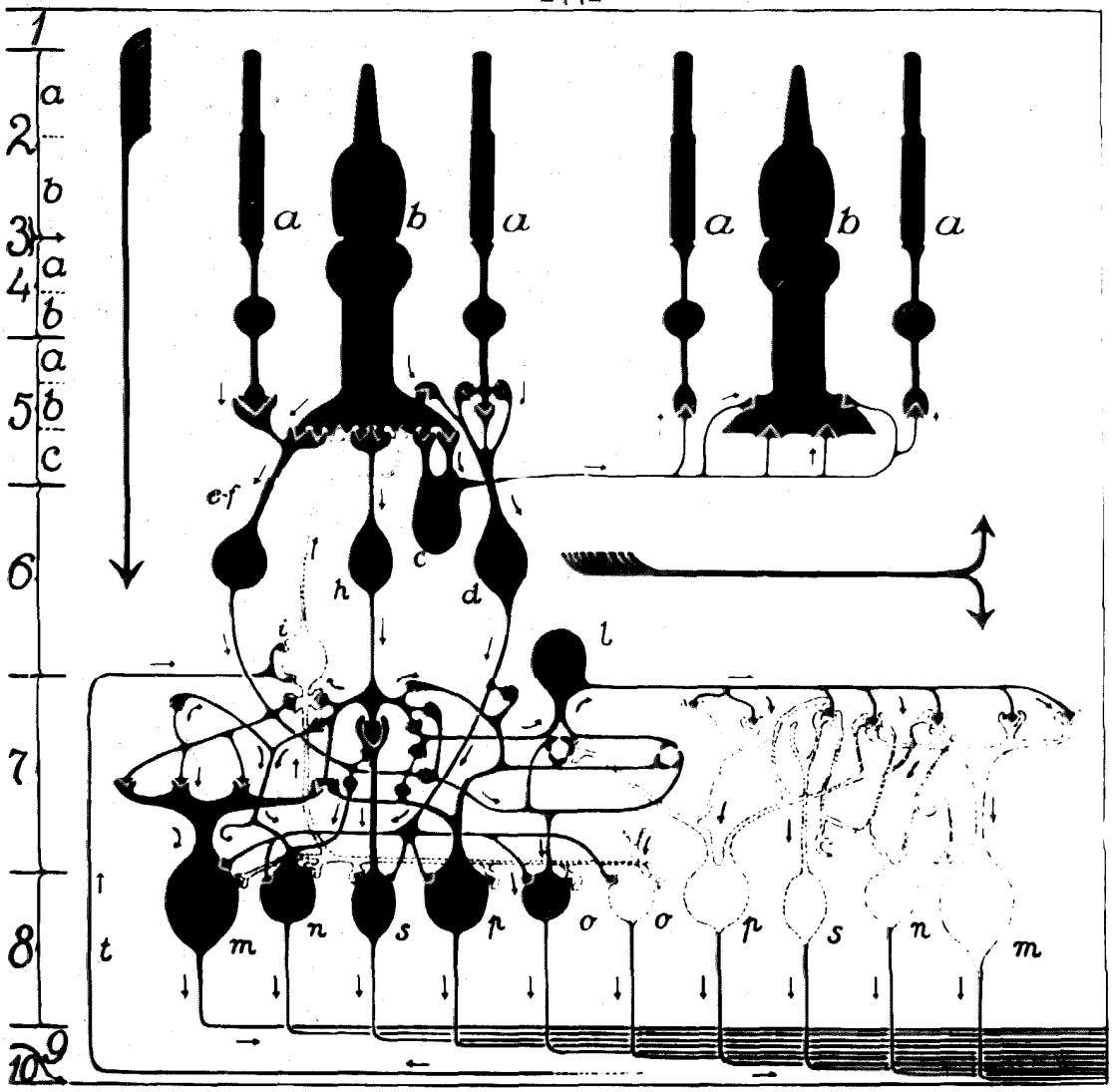

Fig.2.3 The structure of the primate retina reduced to its essentials, including the synopsis of the propagation of the retinal impulses from the photoreceptors to other parts of the retina, to the brain, and from the brain back to the retina (direction indicated by the arrows)

Labeling of the cells: (*a*, *b*) rods and cones, or the photoreceptors where the nervous impulses are generated by physical "light" (in the scheme only the left group of the photoreceptors is assumed to be stimulated by light); (*c*) horizontal cells by means of which the impulses are transmitted to the surrounding rods and cones; (*d*, *e*, *f*, *h*) centripetal bipolar cells of the mop, brush, flat, and midget varieties, which "transmit" the impulses from the photoreceptors to the ganglion cells, the bipolars serving as "analyzers"; (*i*) centrifugal bipolar cell, a variety of the "amacrine cells," which probably receives the impulses from the centripetal bipolars, from the ganglion cells, and also from the brain by way of the centrifugal or efferent fibers (*t*) and transmits them back upon the photoreceptors (*a*, *b*); (*l*) an "amacrine cell" which possibly intercepts a part of the bipolar impulses and spreads them over the surrounding territory; (*m*, *n*, *o*, *p*, *s*) ganglion cells which receive impulses from the centripetal bipolars and transmit them to the brain along their axons called "optic nerve fibers." (Figure and caption from Polyak.)

reduce the number of axons that are necessary in the optic nerve.

The fovea. -One identifying characteristic of the foveal region is to be seen in Fig. 2.1, a depression in the retinal cross-section. Of more importance, however, is the fact that the relative receptor density changes in the neighborhood of the fovea. At the periphery of the retina the receptive surface is entirely composed of rods, but the concentration of rods decreases and that of the cones increases from the periphery towards the center of the fovea, until at the center of the fovea only the cones remain. The relationship between this receptor density and the ability of the eye to perform its visual task is seen quite clearly in Fig. 2.4, after Polyak (49). Here, two curves are plotted as a function of the angular distance from the center of the fovea. The solid line is the cone gradient expressed in terms of the number of min arc subtended by a cone, and the dashed line is the visual acuity plotted as the resolvable visual angle. It can be seen, then, that the fovea, composed entirely of closely packed cones, is also the most sensitive portion of the retina in terms of the ability to resolve small targets.

Definition of the actual area of the fovea is difficult, and varies from author to author depending on which of many conventions is adopted. Three of these conventions are worth noting at this point. Davson (15) and Polyak (49) have used two different physiological characteristics to define the foveal area. Davson defines an "outer fovea" of approximately 80 min arc diameter in which the receptors are virtually all cones. Polyak, on the other hand, notes in his histological studies an area inside Davson's "outer fovea" in which the receptors appear to have a one-to-one neural connection with axons of the optic nerve. Polyk calls this the "central bouquet of cones" and determines a diameter for this region of about 15 min arc. The third convention relates to properties of the eye motion when fixating a stationary small target. The eye moves even during these steady fixations, but the error which the eye position system allows is limited.

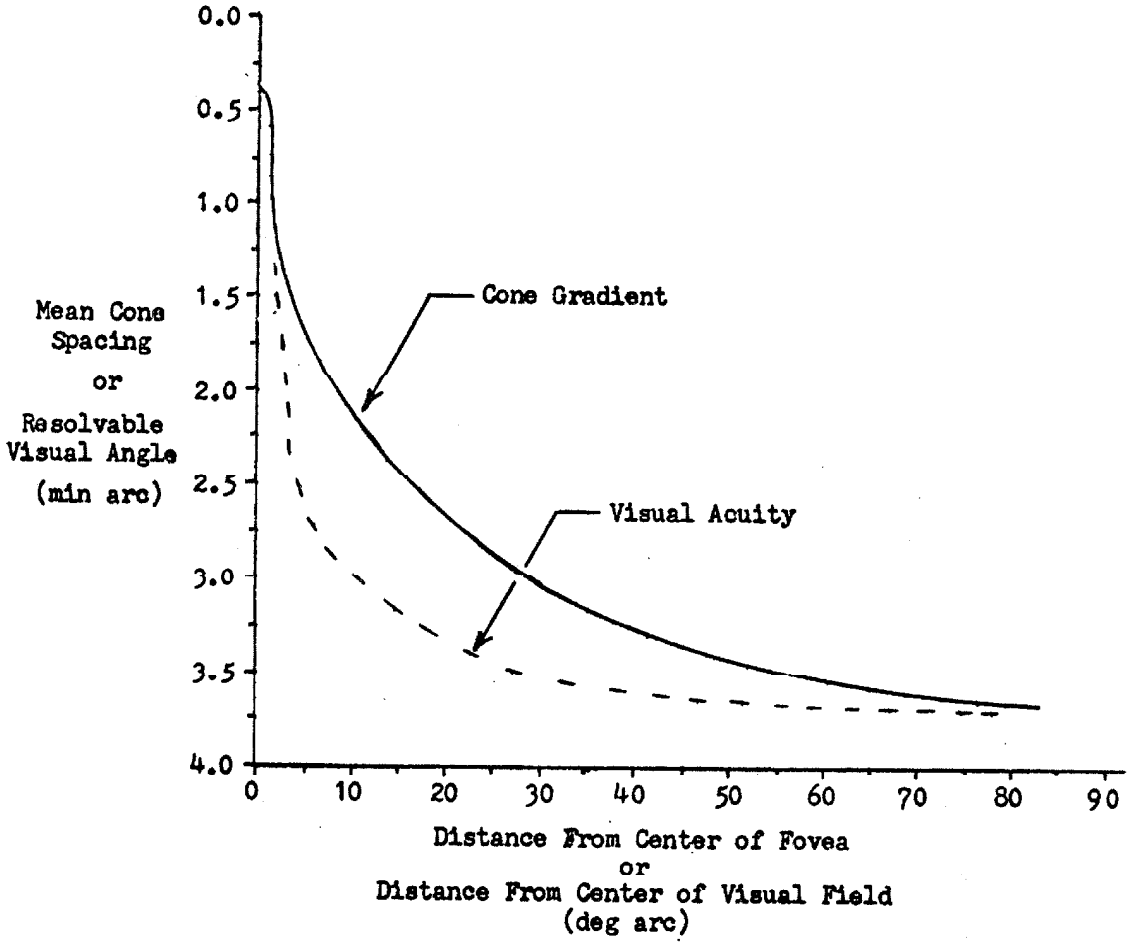

Fig. 2.4 - Comparison of the cone gradient and visual acuity, redrawn from Polyak.

The supposition is that the positional control is used to retain the image being fixated on the area of the retina which has the greatest acuity, the fovea, and that the error actually observed is therefore a measure of the foveal size. The measure obtained with this convention is very similar in size to Polyak's "central bouquet".

Receptor functions. -It was noted above that the rods and cones differ in their functional usage, and the primary difference is one of sensitivity. (49) The rods are sensitive to much lower light intensity levels and thus are used primarily in scotopic (night) vision. In photopic (daylight) vision, however, the rod response saturates, and the visual function is taken over by the cones, thus providing the eye with the ability to function over a range of target luminance levels that varies by a factor of 10^7. Man being a diurnal animal, the majority of his experience is involved with photopic vision, and it is not surprising, therefore, that the cones are the receptors which fill the fovea - that portion of the retina having the highest acuity.

The visual tasks performed during the experiments reported in this thesis were all concerned with tracking or fixating small targets illuminated at the photopic level. For this reason, the cones, and specifically, those cones in the foveal region, are the receptors which are transmitting the information necessary to perform these tasks.

The transfer function which relates the nervous impulses on the optic nerves to the illumination incident on a given receptor is not known, although a great deal of good experimental investigation has been carried out in an attempt to determine it. Most of this research is beyond the scope of this thesis, but some of the experimental results have a direct bearing on the functions of eye movements in maintaining vision, and will be presented here.

First, reference to experiments on other mammals (3, 4, 30, 31, 35) indicates that much of the visual information is transmitted by neural units of the on-off type at higher levels than the

retina; that is, these units respond only to changes in luminance level rather than to a particular level. Figure 2.5 was redrawn from Baumgartner (4) to illustrate the response of an "on" unit in the optic tract of the cat. The upper line in this sketch represents the activity of the unit, the signal being contained in the impulses shown as vertical strokes across the line. The receptive field of this unit is illuminated by a diffuse light which is switched on and off as indicated by the lower line in the figure. When the light is switched on, there is a sudden burst of activity in this ganglion cell, but the activity decays to a noise level within 800 msec. Moreover, the activity is inhibited when the illumination is again switched off. "Off" units perform the same relative function to an inverted stimulus form; that is, they respond to a decrease in luminance and are inhibited by an increase. In short, these units will only produce a meaningful response if the luminance level is changed, and the pattern of neural information arising from the distribution of light on the retina will rapidly fade out unless the image is moved across the retina so that spacial gradients in luminance levels are translated into temporal gradients at any given receptor.

Secondly, retinal receptors, like all neural elements, probably suffer an adaptation effect that reduces the strength of their output as the time of exposure to the stimulus increases. Under this condition, it is necessary to bring new receptors to bear on the image at periodic intervals of time, if clear vision is to be maintained.

The extraocular muscles

It has already been stated that this chapter will discuss both the anatomy and the kinematics of the eye. The musculature, although it is the medium through which the kinematics are effected, is anatomical and therefore is discussed in the first section of the chapter. Figure 2.6 shows the top view of the left eye, with four of the six extraocular muscles visible. It is readily apparent from this figure that the muscles which effect the eye position control do not lie in

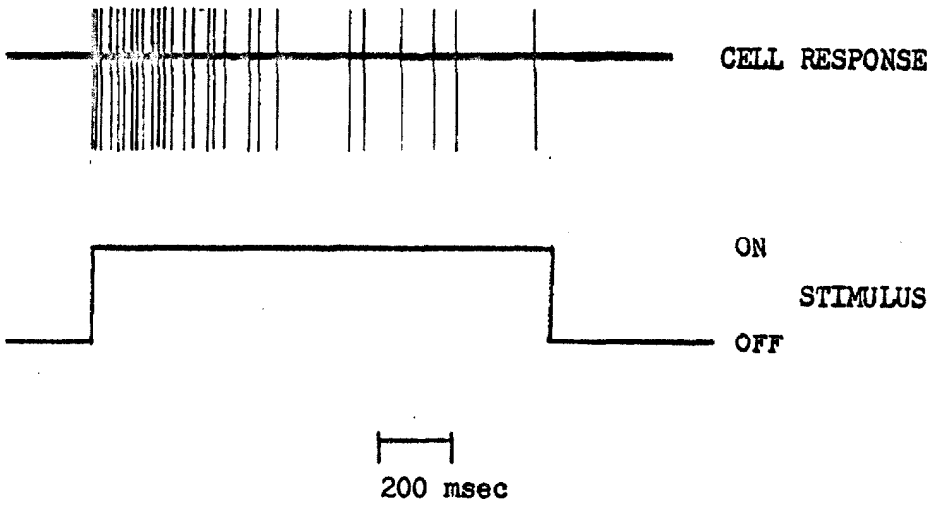

Fig. 2.5 - Response to diffuse light from a ganglion cell in the optic tract of a cat, redrawn from Baumgartner.

mutually perpendicular planes. It is convenient for the purposes of the discussion that follow to introduce a coordinate system in which eye positions can be expressed, and this introduction follows, even though logically it falls under the general term kinematics.

Coordinate system. -In all eye movements, the position of interest is the direction in which the line of sight is pointing; this primary axis is the line drawn from the fovea through the rear nodal point and projected into space from the front nodal point. In order to specify the direction of this line, a set of reference axes is needed, and, as spherical coordinates are to be used, a center of coordinates. The center of coordinates in this case will be defined as the center of the orb. The reference axis is defined when the subject is erect, with his head facing along a line perpendicular to the plane of his body, and he is fixating on a point in this line that is located at infinity; in this condition, the line of sight is aligned with the reference axis.

Given the reference axis, and center of coordinates above, a sphere is drawn concentric with the orb, and marked with the standard geo-spherical coordinates so that the reference axis intersects the equator of the sphere at the prime meridian. In this system the nasal (medial) direction and the elevation (up) represent positive rotations as shown in Fig. 2.7 for the left eye.[2] This system is two-dimensional, as the target plane used in the experimental work reported later is the infinite plane. The eye, however, possesses one more degree of rotational freedom than is accounted for in this system. This is a torsional rotation using the line of sight as the

[2] The system here does not represent a standard in this type of work. In fact, all three logical orientations of the polar axis have been used at times. The experimental work to be presented, however, is involved with eye positions which never deviate more than $\pm$ 2 deg arc from the reference axis, and either of the two polar orientations that place the reference axis on the equator are equivalent in this region. The orientation used was chosen because it simplifies one of the terms in the muscle-position transformation that is derived later.

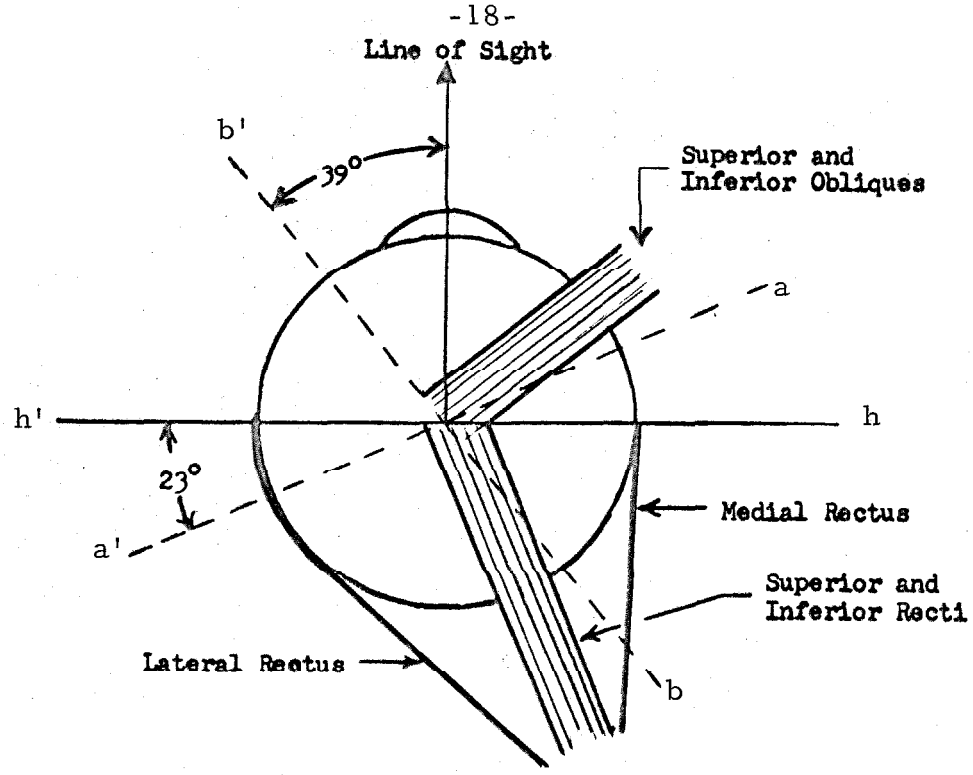

Fig. 2.6 - Left eye seen above, showing extraocular muscles and principle axes. (See also Fig. 2.2)

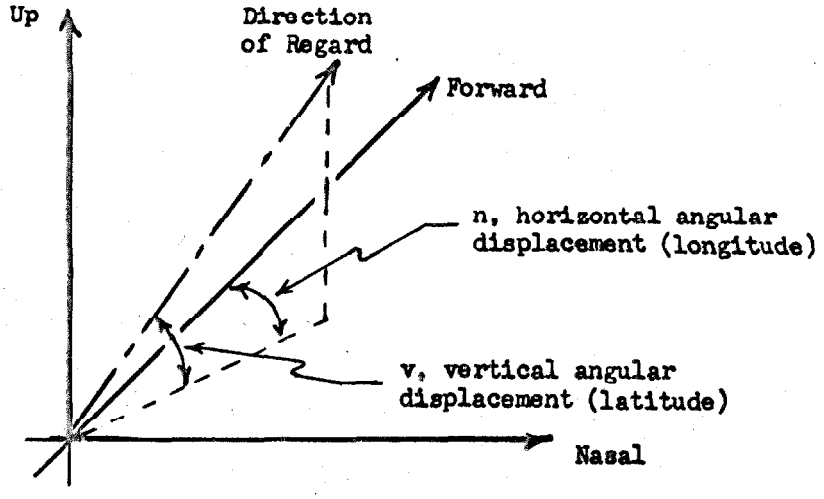

Fig. 2.7 - Geo-spherical coordinate system used in the muscle-position transformation. The 'north pole' is up, and the forward direction intersects the 'equator' at the 'prime meridian'.

rotational axis. In order to measure this rotation, which produces no change in the position of the line of sight, it is convenient to imagine an arrow scribed on the retina with its tail at the center of the fovea. The orientation of this arrow is chosen such that its image on the coordinate sphere points temporally, parallel to the equator, when the eye is in the primary, or reference, position. The torsional angle is then defined as the clockwise angle from the coordinate equator to this vector (arrow).

Muscle-position transformation. -Using this coordinate convention, it is now possible to analyze the actions of the various pairs of extraocular muscles in terms of the eye motions they produce. The principle defining planes have been shown along with the extraocular muscles in Fig. 2.6. In this figure, the horizontal line h-h', a vertical line perpendicular to the paper through the center of the orb, and the line of sight are the three axes around which the eye movements are defined. In order to produce pure eye rotations, rotations which change only one of the position coordinates, it would be necessary for the three pairs of muscles to terminate on diameters of the eyeball perpendicular to these axes, and to pull in a direction perpendicular to the axis in question. All three pairs of muscles roughly fulfill the first criterion, but only one pair, the medial and lateral recti, fulfill the latter. This pair produces pure horizontal rotation about the vertical axis. From the figure it will be seen that the majority of rotation about the horizontal axis, h-h', results from the action of the superior and inferior recti. (See also Fig. 2.2.) The tendons of this muscular pair are inserted into the globe at the vertical poles, but the direction in which they pull is at an angle of 67 deg with the axis h-h' rather than perpendicular to it. The result is that these muscles produce pure vertical rotation about an axis a-a' which intersects the principle horizontal axis h-h' at an angle of 23 deg. The third pair of extraocular muscles is comprised of the superior and inferior obliques. The tendons for this pair are inserted into the eyeball at

about the same places as those of the superior and inferior recti, but their plane of action intersects the line of sight with an angle of about 51 deg, with the result that they produce pure torsional motion about an axis b-b' which intersects the line of sight at a 39 deg angle.

The fact that the superior and inferior recti and superior and inferior obliques act "off axis" means that contractions of these muscles produce orb rotations about all three principle axes, with a few exceptions. If the eye is turned temporally 23 deg, then the superior and inferior recti produce pure vertical motion, and if the eye is turned nasally 57 deg, this same pair produces pure torsion. Similar positions for pure motion exist for the obliques. The total transformation between muscle contractions and eye positions is given in Appendix I. This transformation is an approximation to the real case in that the assumptions which must be made when deriving it idealize the muscles and their insertions, but the approximation is quite sufficient for eye positions within the region of interest of this thesis. The result of the transformation within this region is shown in Fig. 2.8. The axes of this figure represent the resultant eye positions. The curves represent the loci of eye positions resulting from constant muscle tension in the medial and lateral recti, while the hash-marks on these curves represent increments of tension in the superior and inferior recti sufficient to produce pure vertical rotations of one deg were the eye rotated temporally 23 deg. The obliques are assumed to maintain their reference tension, and the plot is calculated for the left eye. As can be seen from Fig. 2.8, the muscular effects are mutually perpendicular at the origin of this plot. A derivation in Appendix I shows that the pairs of recti may be treated as though they produce independent rotations if their action is restricted to a region of three deg arc radius around the reference axis.

The reference position, defined above, (also called the neutral position or the "position of physiological rest") is that position in which the subject will align his eyes to fixate a target if he is given the

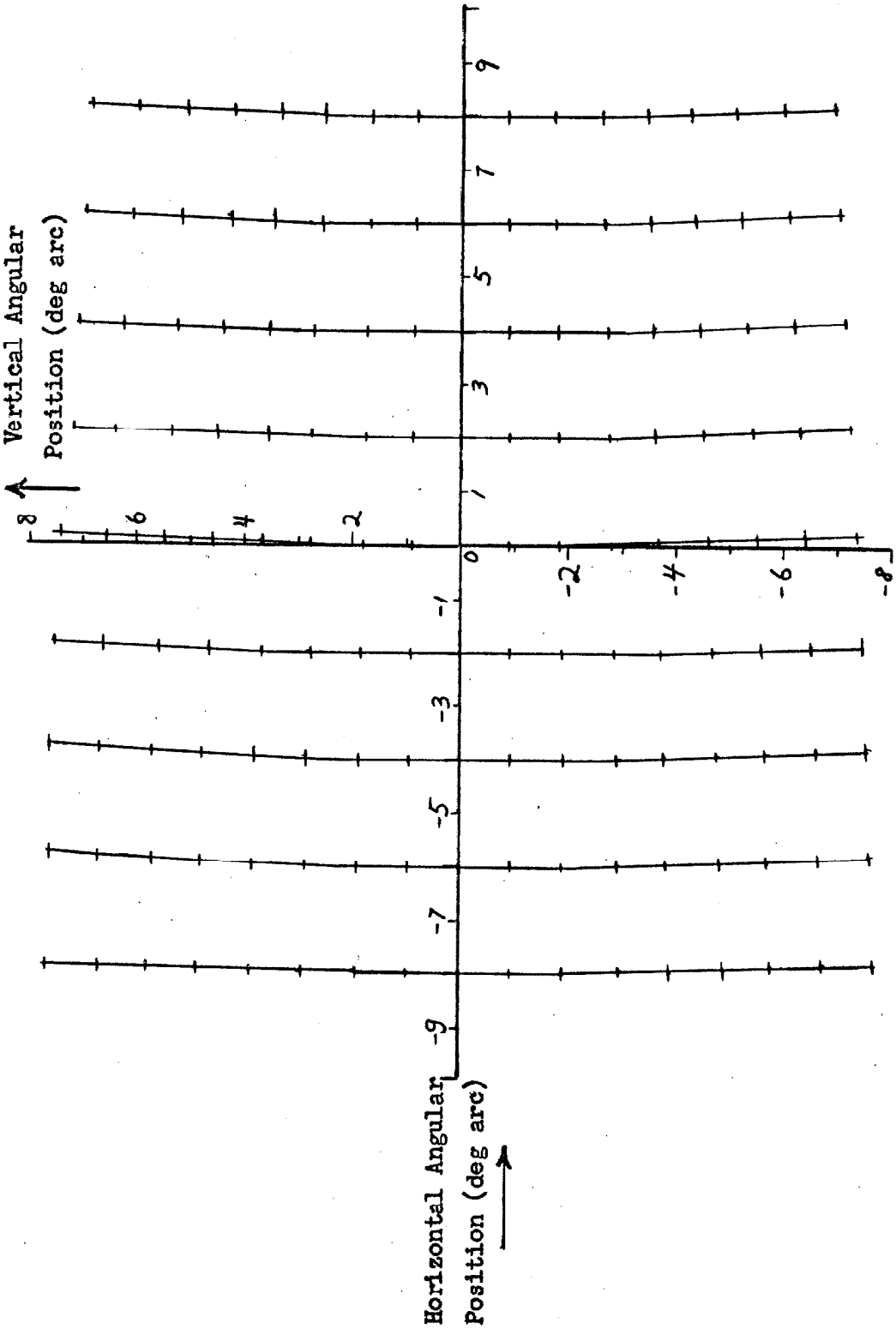

Fig. 2.8 - Orb position resulting from specific muscular contractions. See text for complete interpretation of plot.

freedom to move either himself or the target. This is not, however, the position which the eye would take up if all innervation to the extraocular muscles were removed. Under these latter conditions, the eye position would be entirely determined by the elasticity of the muscles, the position referred to as the "paralysis position", or the "position of anatomical rest". No average determination of this position has been made, except that it is slightly temporal and up from the neutral position. (12)

Physiology of the extraocular muscles. -A recitation of the details of a subject as complex as the physiology of the extraocular muscles would be out of place in this thesis, but two aspects of the afferent and efferent information pathways related to these muscles are of interest.

The first of these arises from the fact noted in the section above that the natural position of the orb and the position determined by the elastic properties of the muscles are not the same. Thus, a constant innervation is needed to maintain the proper tone of these muscles even when they are in the so-called neutral position. Further, the fact that the various pairs of muscles are inserted at opposite ends of diameters of the orb means that they work in opposition, and thus must be reciprocally innervated to produce pure rotations of the eyeball. During reciprocal innervation, the agonist (muscle towards which the eye is turning) receives increased activity, while the signal to the antagonist is reduced. Electromyographic studies confirm these facts. (40, 44) In addition, such studies show that during the most rapid eye movements, flicks, the antagonist is inhibited completely so that the maximum force of the agonist may be effected. (57)

The second interesting aspect of the muscular physiology is the fact that even though sensory units are found in the extraocular muscles, there is apparently no signal transmitted from these muscles which can provide the cortex with information about the

position of the orb. (10) In spite of this fact, the human is capable of differentiating between retinal image motions which arise from target displacements in space and image movements which are the result of eye rotation. In order to explain this ability in the absence of sensory information from the extraocular muscles, the theory of efference copy has been promulgated. This theory assumes that the command signals (efferent) to the extraocular muscles are also sent to that region of the cortex which evaluates the position of the retinal image. It is assumed that the muscles respond faithfully to the command signals, and that these command signals can therefore be used to determine the eye position; this permits the effects of eye rotations of the retinal image location to be differentiated from the effects of target motion.

Kinematics of the Eye

Background. -Kinematics, the study of motion in the abstract, is used in reference to the eye to denote the form of eye movements. (59) Eye motion during tracking tasks, or when the subject is moving his point of regard around a stationary field, is clearly a beneficial phenomenon, but the presence of eye movements during the fixation of a small, stationary target, and the presence of uncorrelated eye movements during tracking tasks, are not readily explainable phenomena. Moreover, the orb exhibits three distinct classes of motion, each having an origin that is apparently independent of the others. The object of this section is to describe these classes of movement, and to attempt to identify what function they serve outside of the straightforward task of tracking a moving target. As this study is not a new one, a brief historical comment on these classifications would appear to be in order.

Helmholtz in his well-known Treatise On Physiological Optics (28) was one of the first researchers in human vision to note that the eye appeared to move in jerks as well as to execute slow drifts. Further, by the careful observation of after-images, he was able to

report that both of these forms of motion were present when the eye was simply fixating a single point. Although he did not have sensitive position measuring apparatus available, and although the physiological foundation of the visual receptors was not well explored, Helmholtz arrived at conclusions about the perceptual benefits of eye movements which are strikingly similar to what is believed some 90 years later on far stronger evidence. The following quotation from an English translation describes the observation of after-images during fixation, and concludes with an explanation of the phenomena observed:

> Sharply defined negative after-images of the objects develop, which coincide with the objects as long as the gaze is held steady. . . The little deviations of its [the eye's] position. . . are revealed by parts of the negative after-images flashing up on the edges of the objects, first on one side and then on the other. This wandering of the gaze serves to keep on all parts of the retina a continual alternation between stronger and weaker stimulation. . . and is evidently of great significance for the normality and efficiency of the visual mechanism. . . . Strong negative after-images are, indeed always an indication of high degree of retinal fatigue. (28)

Despite the fact that more accurate measuring techniques have identified one more form of eye rotation than Helmholtz observed, and have permitted precise specification of the two classes he observed, the evidence to follow will show that his primary conclusions as to why spontaneous eye movements are present were correct.

Eye Movement Classification

The concern of this thesis is with the three classes of eye movements that can be observed by testing one eye only. During the experimental sessions from which the data to be presented were drawn, the subject's left eye was tested with the vision of the right eye obscured by a patch; the subject's head and body positions were fixed; and the target appeared optically to be located at infinity. For these reasons conjugate movements (both eyes), vergence movements (to bring the eyes to bear simultaneously on the same target), and compensatory movements (resulting from motion of the subject), served no useful function during the experiments. The movements

that are left are those which can be observed while testing a single eye performing monocular tasks, and these fall into three classes which can be identified by their frequency composition, or time course - tremor, drift, and flick (or saccade). (1,17, 22, 52)

Tremor. - Tremor is the smallest and fastest of the eye motions observed in the human. It is seen in all regimes of vision, and during all types of tracking tasks, but is too small to be regarded as a form of response. Rather, it appears to be a form of noise in the eye position control system, and to be a completely uncontrolled function.

Fender (24) used special recording techniques which allowed the optical elimination of all flicks and drifts with amplitudes greater than one min arc from his records, leaving only the tremor. Fig. 2.9 shows a recording of the tremor made in this manner. The results of a spectral analysis performed on this type of record are presented in Fig. 2.10 (also after Fender). The tremor is seen from this figure to possess appreciable power at all frequencies up to about 100 cps. In addition to being a high frequency component, the tremor is identifiable by its amplitude. Many researchers have investigated the tremor and the agreement as to the amplitude of the this motion is surprisingly good. In general, the median peak-to-peak amplitude is taken to be on the order of one min arc. (1, 17, 24, 52, 53)

The source of the tremor has not been precisely identified. The frequency, as high as 80 cps, and the very small amplitude, median muscle length change on the order of five microns, of this motion tend to belie any conjecture that it might be controlled either consciously or subconsciously. It has already been noted that the extraocular muscles are maintained in a continuously tonic state. Thus, it is entirely possible that the tremor arises from an imperfection in the maintenance of tone, specifically, from incomplete fusion of the individual twitches which comprise this tone.

Drift. - Drift is the slowest of the eye motions under consideration,

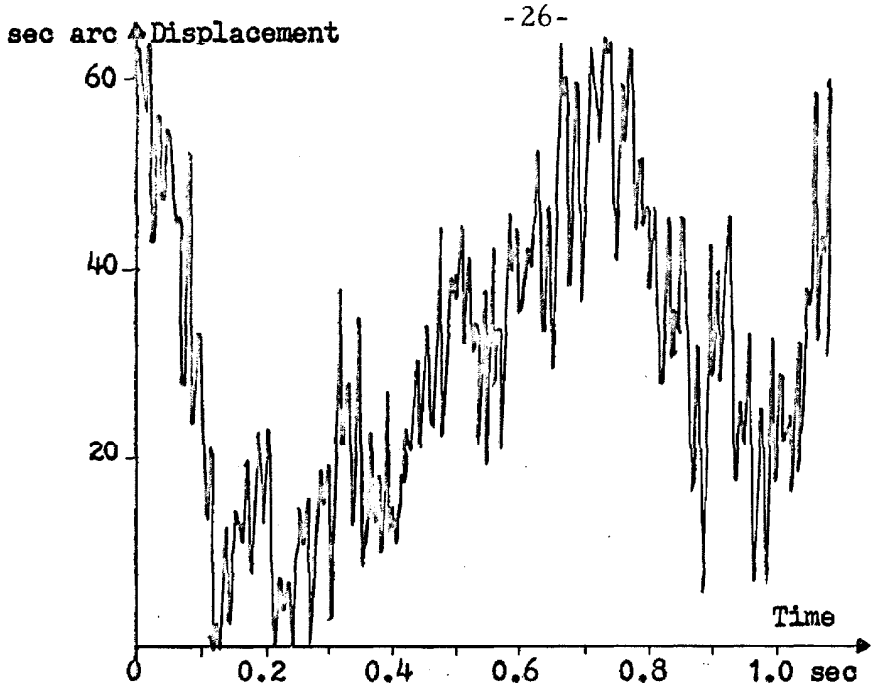

Fig. 2.9 - Recording of eye tremor, redrawn from Fender.

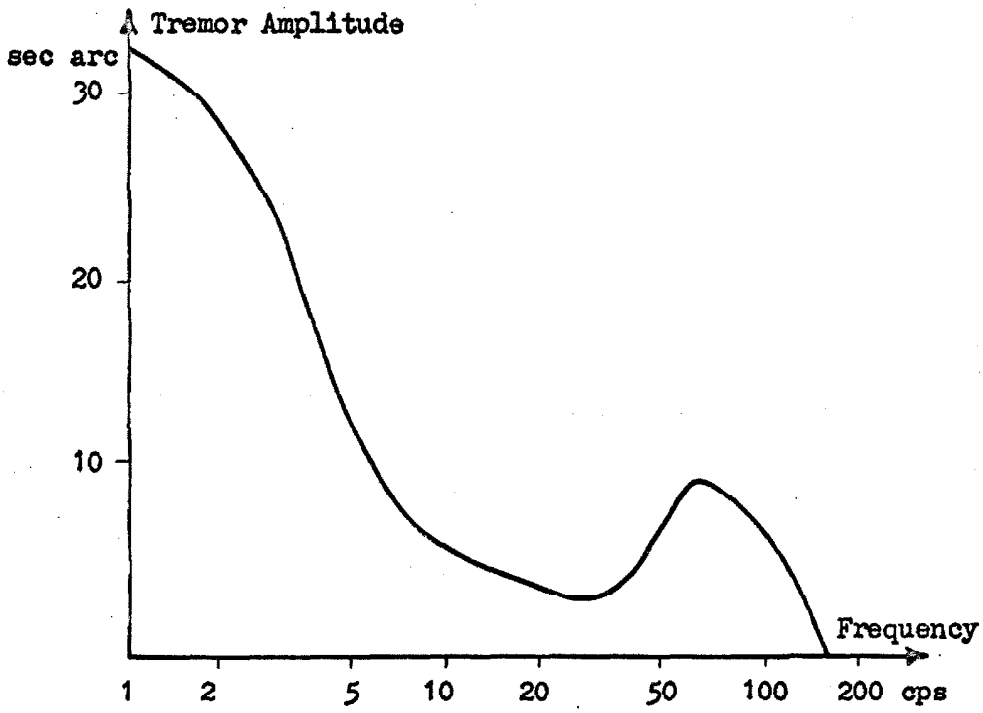

Fig. 2.10 - Tremor amplitude spectrum, redrawn from Fender.

and is observed both as the response to a stimulus movement, and as an apparently spontaneous motion that is uncorrelated with the stimulus movement. Records of horizontal eye movements elicited in response to three visual tasks, sine-wave following, square-wave following, and steady fixation, are shown in Fig. 2.11. In each record segments of drift have been identified, as have the rapid flicks which separate these segments. (Tremor would appear on these records as a small perturbation on the eye position which would widen the traces. No attempt has been made to reproduce this effect in tracing the original records for Fig. 2.11.) Reference to individual traces in this figure will reveal both the correlated and uncorrelated drift components.

In the response to the sine-wave stimulus (Fig. 2.11a) the majority of the eye displacement is accomplished by the drift segments. These drift segments are not, however, totally correlated with the stimulus; that is, they do not represent a response that differs only in amplitude and phase from the stimulus, although the average over many response cycles can be so characterized. The form of drift (smooth-following) response shown in Fig. 2.11a is maintained for sine-wave stimulus frequencies up to about 2.5 cps (25), and this fact has been used to specify the upper frequency limit of the drift.

Uncorrelated drift appears in the response traces of Fig. 2.11b and Fig. 2.11c. In the former trace, the correlated response to the square-wave stimulus is provided by the flicks, while the latter trace is taken from a visual condition which calls for no response motion at all. Nevertheless, eye position changes resulting from the drift are apparent in both records. Consideration of this spontaneous drift is provided in detail in Chapter VIII.

Flick or saccade.[3] - The flick is the more rapid of the large eye

[3] In much of the literature, the terms flick and saccade have been used interchangeably in reference to this eye movement component. More recently, however, the term flick has been used when the component occurs spontaneously, and the term saccade when it occurs in response to an external stimulus.

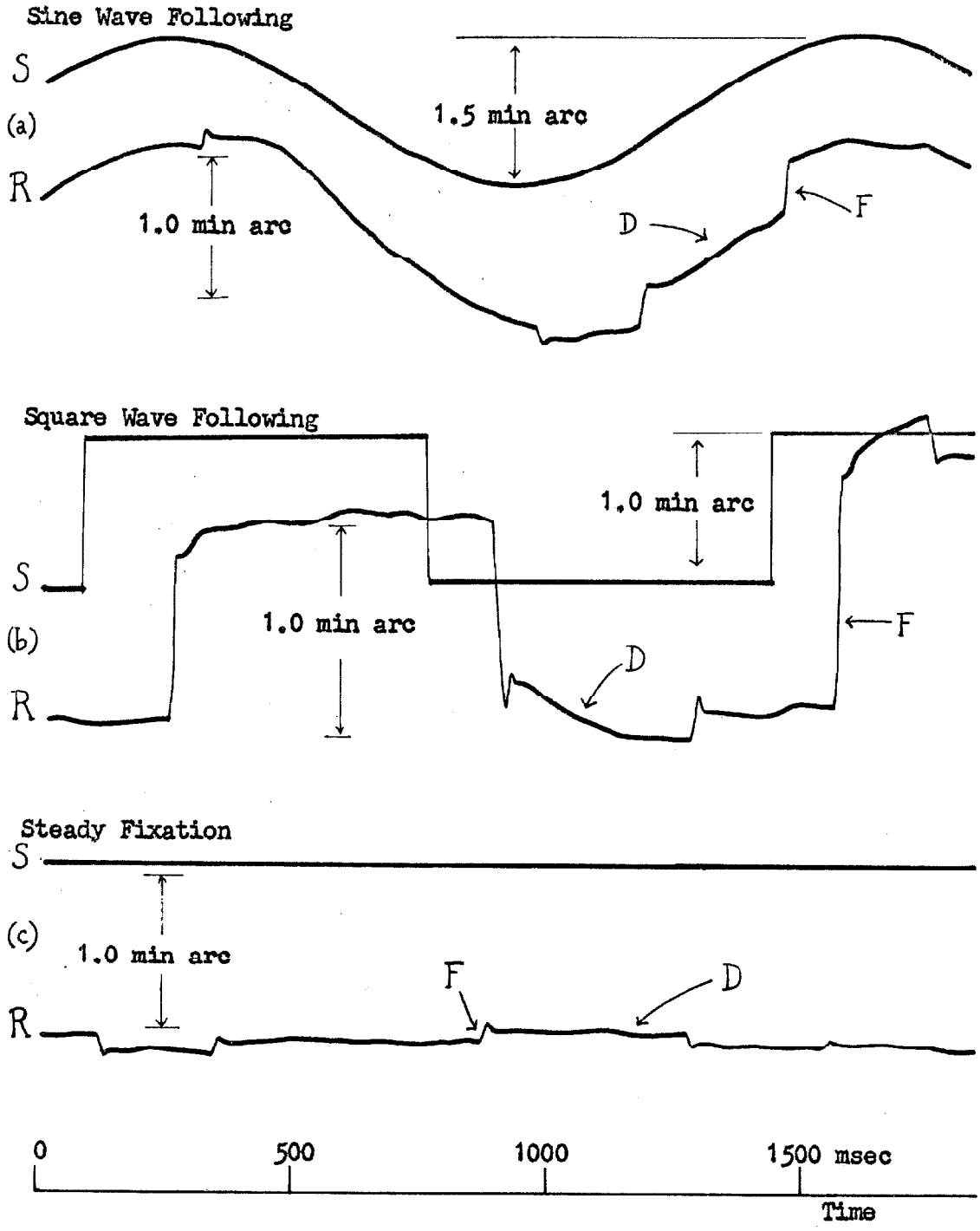

Figure 2.11 - Typical eye movement responses in tracking tasks. Flicks (F) and drift segments (D) are indicated.

movement components, representing a step function in the eye position; like the drift, the flick appears both spontaneously and in response to stimulus motions. The flicks shown in the eye movement traces of Fig. 2.11a and 2.11c are all spontaneous; in the former figure the correlated portion of the eye response is in the drift segments, and the stimulus in the latter figure requires no following response. The correlated response to the square-wave stimulus (Fig. 2.11b) is the large flicks that occur shortly after each stimulus step. Yet even in this following regime spontaneous flicks can be observed during the intervals between stimulus steps. The term spontaneous as used here, and in relation to the drift, is meant to imply that these components are not correlated to the stimulus motion, and are not consciously controlled. They may, however, be subconsciously controlled so that the fixation position error which arises from these spontaneous components is limited. This form of control mechanism is considered in Chapter VIII.

The primary characteristic of a flick is its time course, as flick amplitudes vary from as small as three min arc to as large as 30 deg arc. The largest of the saccades occur during tracking tasks, or when the subject is surveying a large visual scene, whereas the spontaneous flicks referred to above appear to be limited in amplitude and seldom exceed 30 min arc. The characteristic time course of these flicks, and of saccades smaller than about two deg arc, is shown in Fig. 2.12, which shows the position and velocity of the eye as a function of time during the course of two types of flick, "overshot" and "undershot". An overshot response is one in which the motor system, while attempting to produce a step position change, actually passes the final resting position, and performs a decaying oscillation around that final level. (The derivative for this plot was obtained mathematically after the flick position was sampled in time and transmitted to digital computers. This form of data processing is discussed in detail in the following chapter.) Saccades larger than about

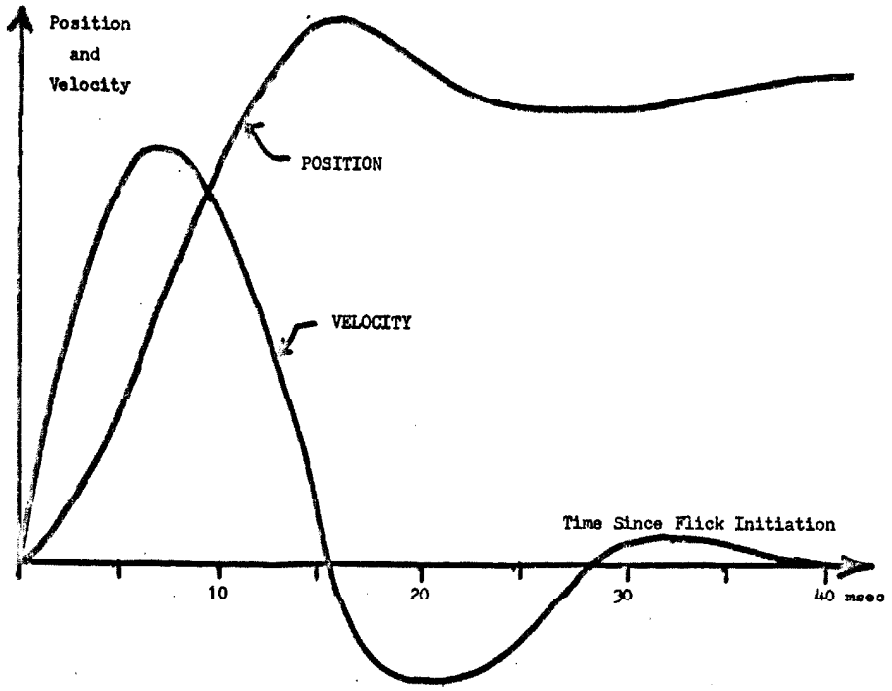

Fig. 2.12b - Overshot flick.

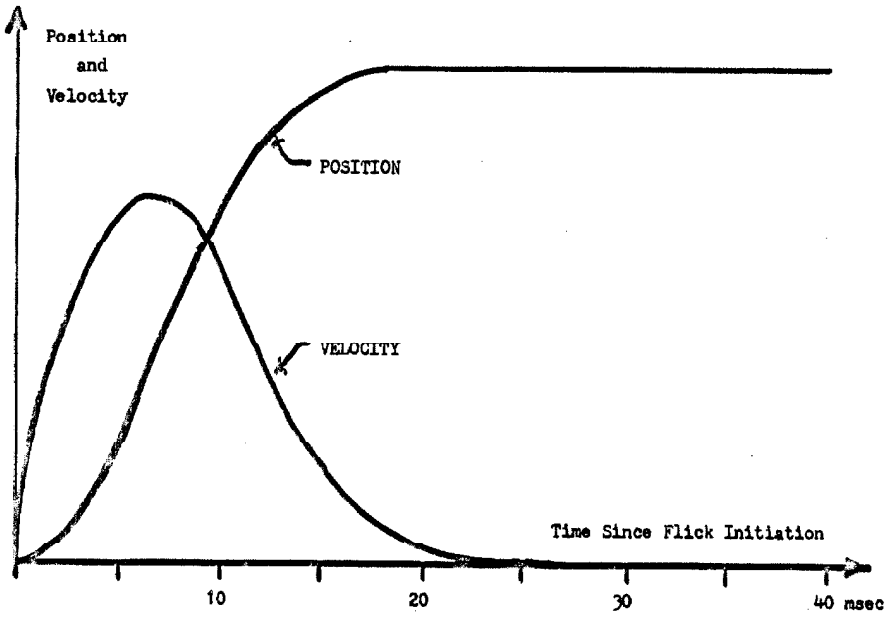

Fig. 2.12a - Undershot flick.

Figure 2.12 - Unscaled plots showing time course of flicks.

two deg arc tend to be somewhat slower than is shown in Fig. 2.12, because the orb reaches a terminal velocity which prevents it from achieving any given final position in a constant time period. The discussion that follows is strictly applicable, therefore, only to flicks and saccades smaller than two deg arc. The peak displacement for both undershot and overshot flicks is attained in 15 to 20 msec. At this point, the undershot flick (Fig. 2.12a) has reached its final position, whereas the overshot flick (Fig. 2.12b) attains its final position about 30 msec after its inception. The peak velocity for both the undershot and the overshot flicks is achieved about eight msec after the start of the flick.

The overall muscular innervation pattern that produces these flicks is not well known. As noted earlier, the initiation of a flick is marked by greatly increased activity in the agonist, and total inhibition of the antagonist. Beyond this point in the time course of the flick, there is little agreement, and less experimental evidence, on the innervation. Two arguments are presented; one is that the eye proceeds on a "ballistic" path and ultimately stops due to a combination of the elastic and frictional properties of the extraocular muscles; and the other argument is that the flick is terminated muscularly by inhibition in the agonist, and increased activity in the antagonist. Although this is an important question that has yet to be resolved, it is unimportant to the arguments that are to follow. The salient feature of the innervation patterns for flicks is that they represent quite complex impulse patterns at the muscles, Thus, a "random" flick represents a more sophisticated process than does random drift, which could simply be fluctuations in the tonic level of some of the muscles.

Physiological Benefits of Movement Components

In the discussion of the various eye movement classifications, the functions of these components in following target motions were pointed out, but it was also noted that components of each of the three

classifications could be observed which were uncorrelated with the target motion. Although these uncorrelated components may well be accidental, arising as a result of noise in the eye position control system, there is a great body of evidence that they do serve a useful physiological function in the maintenance of clear vision. (19, 20, 24)

This fact arises from the nature of the receptors themselves. First, evidence was presented earlier in this chapter that many of the neural pathways in the optic tract require changes in the incident illumination in order to produce a response. Secondly, neural units suffer fatigue, or adaptation - their output decays with continued stimulation. The eye movements have been shown to meet these situations by providing the receptors on the image boundaries with changing illumination, and by continually bringing fresh receptors to bear on these boundaries.

The experiments that have been used to test this assumption have involved optically eliminating the effect of eye movement on the image position at the retina. (11) Perception of the image fails periodically in this "stabilized" condition for as much as 90 percent of the total viewing period. (20) Simulated eye movements of each of the three classes were then imposed on the image position externally, and the effect of each in terms of target visibility was measured. This effect is generally measured by the so-called visibility factor, defined as the proportion of the total viewing time that the target is perceived. The results of these experiments are summarized in the following sections.

Tremor. - The fact that the mean tremor amplitude (one min arc) is of the same order of magnitude as the mean receptor spacing (40 sec arc) in the fovea led to the supposition that the tremor component of the eye motion is responsible for sweeping pattern boundaries across individual receptors, and thereby providing the requisite on-off signal. Verification of this effect was sought by imposing a simple sinusoidal target motion on the stabilized image; a range of amplitudes

and frequencies of this sinusoid was used, and the effects on the visibility factor were noted. The results showed that the most efficient tremor components in this respect were those in the peak-to-peak amplitude range from 0.6 to 1.6 min arc, with a frequency range from 4 to 12 cps. (20) Tremor components that satisfied these conditions were found to increase the visibility factor to about 100 percent.

In this context, it is worthwhile noting that simulated eye movements are not the only mechanisms which can regenerate a faded, stabilized retinal image. Even with no eye movements, simulated or real, perturbing the retinal image position, the image is perceived by the subject periodically. This implies that either the stabilization fails periodically (mechanical slippage in the stabilization apparatus), or that the image fading is not purely a function of the photoreceptor stimuli. Recent experiments by Lehmann, Beeler, and Fender (38), in which the electro-encephalogram was correlated with the image visibility, support this latter assumption. Centrifugal fibers to the retinal receptors are known to exist (49), and these have been shown to affect the retinal sensitivity (33).

Drift. - The effects of drift on image visibility have been measured by imposing image motions of known velocity. The effects were not as clear-cut as the results for the tremor, however, for the regeneration benefits of drift were found to be proportional to the imposed image velocity. Fender (24) argues that the function of the drift is to continually bring fresh receptors to bear on the target. This being the case, it might be assumed that drift, if added to simulated tremor, would reduce the tremor amplitude necessary to produce maximum viewing efficiency. This experiment has unfortunately not been performed.

Flicks. - Simulated flicks in the form of imposed step displacements of the retinal image were found to be quite efficient in regenerating a faded, stabilized retinal image, if these flicks were larger than 2.5 min arc. (20) While this indicates that the flicks are

capable of maintaining clear vision, they probably do not serve this function in practice, because the mean spontaneous flick rate for some subjects is lower than one per second, and this rate would not be an efficient image regenerator. Rather, this function is probably served by the tremor. The flicks are, however, capable of fulfilling the role that was postulated above for the drift - that of bringing fresh receptor areas to bear on image boundaries. This possibility is discussed further in Chapter VIII.

Conclusion

As was noted in the introduction to this chapter, the information just presented is only a collation of the facts that are needed about the eye and its motive system in order to assess the experimental evidence to be presented later. Generally speaking, each of the points that have been brought up in this chapter will be referred to at a later point in this thesis.

CHAPTER III

STIMULATION, MEASUREMENT, AND AUTOMATED PROCESSING OF EYE MOVEMENTS

Introdution. -Experimental procedure can, in general, be broken down into two broad categories - the measurement of the experimental parameters, and the processing of these parameters to provide meaningful measures of the effects being tested. The first of these categories can be further divided into the problems of stimulating the experimental preparation, and measuring the response, although the separation of these factors is not always discreet. This chapter describes the general techniques that were adopted during the research for this thesis. Although several distinct experiments were performed, the majority of the apparatus and methods were applicable to all of them; as each experiment is discussed in the following chapters, only the detailed variations of apparatus and procedure will be mentioned.

Measurement of Eye Movements

The problem. -The experiments performed in support of this dissertation were all involved with measuring the eye movements of a subject, or his perceptual functions, in response to a precisely defined stimulus under conditions that produced minimum interference with these movements and functions. The meeting of any one of the requirements, however, involved a compromise with the other two, and thus a statement of the criteria involved is necessary.

The form of the eye movement components that were of interest to the experimenter specified the measurement criteria that were to be met. In brief, the experiments performed required measurements of both the flick and the drift components at amplitudes up to about

$\pm$ 2 deg arc. The smallest component amplitudes that were of interest were on the order of one min arc, so that the sensitivity of the system had to be better than that amount. Further, the time course of these components was needed. The measurement of drift, then, required that a DC system be employed, while the specifications of the flick required a minimum high frequency limit of 200 cps. Finally, the system had to be capable of measuring both the horizontal and vertical components of the eye position.

Presentation of the desired stimulus functions presented a problem that could not be entirely separated from the measurement method. Specifically, there were experiments where it was desireable to control the position of the image on the retina, rather than the position of the target in space. In order to accomplish this without mechanically limiting the eye position, it was necessary that the eye movements be added into the desired target motion, so that the subject was incapable of displacing the image on his retina by his own eye movements. This condition is generally referred to as a stabilized retinal image. The alternate visual condition, normal vision, wherein the retinal image position is the natural function of the eye position, was also used.

The final requirement placed upon the system was that it produced minimum interference with the normal visual processes. The primary question was one of comfort, for no subject who is in pain, particularly in an area as sensitive as the eye, is capable of full concentration on the task at hand, and as a result the validity of the observations would be suspect. Secondly, the measurement system should not interfere with the normal visual and positional functioning of the eye. This meant that the optical characteristics of the cornea and lens should suffer no interference, and that the extraocular muscles should be free to move in the normal manner with little or no additional loading. Lastly, the measurement system should not conflict with the stimulus. This required that no light of wavelengths

to which portions of the eye are sensitive be incident on the eye due to the measurement technique.

In the past, many solutions to these problems have been attempted and championed by researchers in this field. Some of these are worthy of mention here as a background to the technique adopted for this work. Comments as to the success or failure of each solution will be given where necessary.

Available Methods

Mechanical. - Two of the earliest experimenters to use some technique for measurement of the eye position, other than direct observation of the eye or after-images, were Huey (32) and Delabarre (16). These men, working at the turn of the century, simultaneously, but apparently independently, developed a mechanical system to measure the eye position. This process involved fitting a plaster cast to the eye, and then attaching a lever system that recorded the eye position on a smoked drum. The disadvantages of this system are obvious, and less painful methods were soon adopted.

Direct photograpy. - The desire to avoid interference with the eye functions led Dodge and Cline (21) in 1901 to switch to motion-picture photography of the eye, wherein the position was measured from the photographs. The accuracy obtainable at that time is questionable, but the technique was improved over the years as optics, films, and high speed cameras improved, until Byford (8) in 1961 achieved a resolution of several hundred cycles, and a sensitivity on the order of 30 sec arc. The major drawback to any photographic technique, however, is the time and labor involved in translating the film record into a measure of eye position.

Reflection techniques. - The availability of good photo-electric devices since 1945 has led many researchers to make use of the reflectivity of the eye in providing optical measuring techniques which require no attachments to the subject. Lord and Wright (39) used

the surface of the cornea as a spherical reflector. Parallel light reflected from the cornea appears to come from a point source located midway between the surface and the center of curvature of the cornea. As the focus of this corneal-reflex is well forward of the center of rotation of the eye, this virtual point source moves with the eye, and may be tracked with photomultipliers. They used an ultraviolet light source, and arranged the incident beam to fall on the fundus in an attempt to eliminate visual interference. Unfortunately, the lens of the eye fluoresces in ultraviolet light (15), with the result that the visual field is perfused with blue light under their experimental conditions.

The difference in reflectivity between the white sclera and the darker iris also provides an optically locatable portion of the orb, and several techniques utilizing this fact have been devised; of these, two are representative. The technique adopted by Young (61) involved measuring the reflected luminance from two circles of light, one incident on the scleral-corneal edge at each side of the eye, as shown in Fig. 3.1a. The differential of the reflected intensities is a linear function of the eye position for small movements. The resolution of this technique, however, is limited to 15 min arc, and the cadmium sulfide photocells used by Young set an upper frequency limit on the order of 10 cps. In order to increase the accuracy and response speed, Rashbass and Westheimer (51) utilized a flying spot scan. A small beam of light was swept across the scleral corneal edge, and on towards the pupil until it passed the point where it created a corneal reflex (the virtual point source used by Lord and Wright); the reflected light was measured by phototubes. The eye position was then taken to be proportional to the time between the drop in reflected intensity at the scleral edge, and the pulse of reflected intensity caused by the corneal reflex. (See Fig. 3.1b) This system had the advantage over that used by Lord and Wright of eliminating possible contamination of the records by head movements. Using this method, Rashbass and

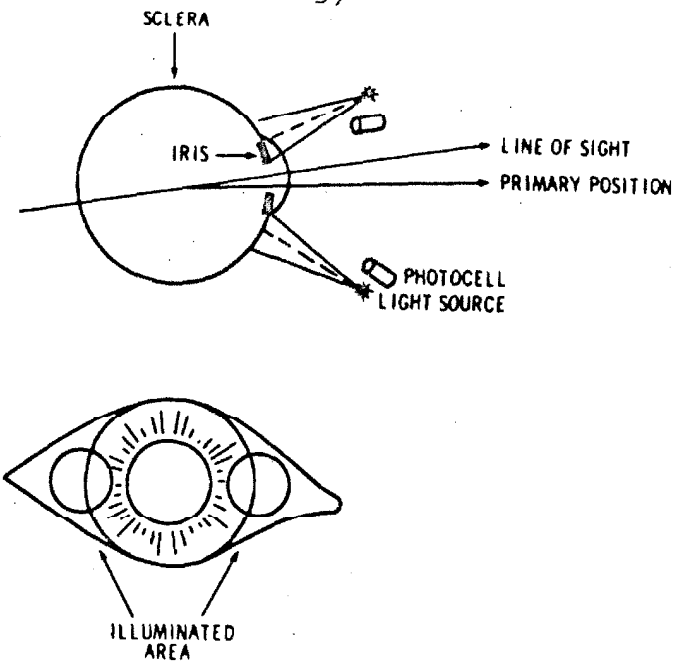

Fig. 3.1a - Position measuring system used by Young. Horizontal eye position is proportional to the differential of the light reflected from the two illuminated areas.

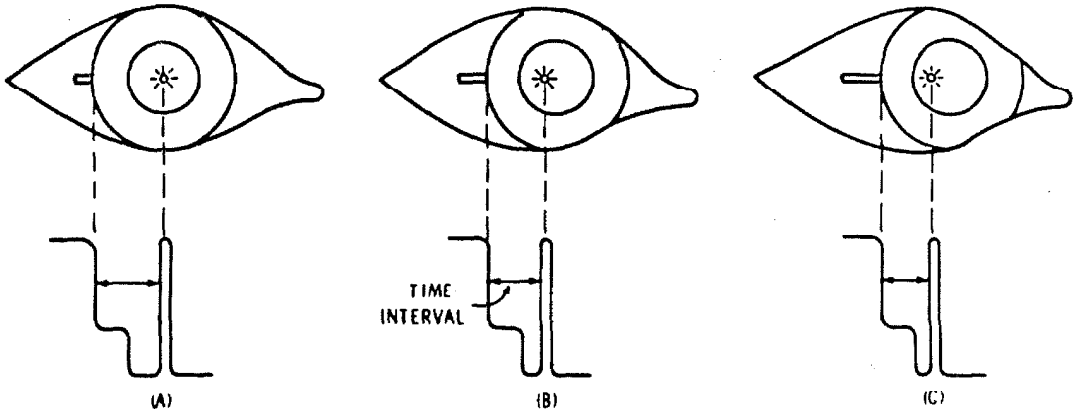

Fig. 3.1b - Position measuring system used by Rashbass and Westheimer. Schematic shows light reflected from the eye as the illuminating beam sweeps from the sclera past the corneal reflex. Horizontal eye position is proportional to the time interval indicated.

Westheimer achieved a resolution of six min arc, and an upper frequency limit of 100 cps. Both this method, and that of Young, however, are restricted to measuring horizontal eye positions, as the eyelids obscure both the upper and lower scleral-corneal edges.

Contact lens techniques. -The widespread development of well-fitting contact lenses in the 1930's proved a boon to experimenters in eye research. As soon as one has a comfortable instrument "platform" attached with fair rigidity to the subject's eye, high quality optical components can be attached to the orb. The first experimenter to use an attachment of any sort on the eye was Orschansky (48) in 1898. He attached a spherical metal cap to the subject's eye and imbedded a small mirror in this cap. He then reflected light from this mirror and recorded the resultant beam rotations on photographic plates. This method has been refined considerably since that time, and the system described by Fender (23) is one of the most common in use today. The technique is principally the same, except that great care is taken in fitting the contact lenses, and the mirror is placed quite carefully so that it is perpendicular to the visual axis of the eye, thus assuring that the full eye movements are measured, and that no components of horizontal eye motion are introduced into the vertical recording, or vice versa. (41) The system described by Fender used a moving film strip for recording, but subsequent changes in that system have included the use of photocells to measure the angular position of the reflected beams.

One of the major problems of the technique utilizing reflected beams is the difficulty of leading this beam out of the optical apparatus without interfering with the stimulus system. To alleviate this problem, Byford and Stuart (7) positioned a small lamp on the end of a stalk protruding from the contact lens. Tracking the motion of this lamp with photomultipliers provided an accurate measurement (down to three sec arc) of the eye position with a readily adjustable system.

Stimulus presentation methods. -It was noted above that any measurement technique used should be compatible with the desire to produce stimulus positions correlated with the eye position. Many of the techniques which provide an electrical output have been combined with electronic control systems to move the target in step with the eye, but these designs have been less than satisfactory because of the difficulty in obtaining a measure of the error between the target position and the eye position that could be used in a feed-back loop. In this regard, the contact lens techniques have shown a distinct advantage over all the other methods, for the same mirror which provides the position measurement can be incorporated optically into the stimulating system, and thus add the eye rotations directly into the beam being viewed by the subject.

The Apparatus

As a result of the arguments presented above, the author adopted a system that is a hybrid of Fender's and Byford's techniques. The major objection to this method, or to any method which requires the use of contact lenses, is the limitation on the number of subjects available for experimentation. The lenses, being precisely fitted to the individual eye, are expensive, and not all available subjects are capable of wearing, or willing to tolerate them. The result is that the experiments were necessarily limited to a small group of subjects, few of whom were naive to the experiment in progress. Great care was taken in experimental design, therefore, to ensure that the subject's knowledge of the research had minimal influence on the results. The subject pool that was available to the author consisted of four men, including the author, his advisor, and two students. Each of the experiments described later in the thesis was performed on at least three of these four subjects.

The experimental apparatus can be broken down into three sections; the attachment to the subject, the contact lens; the method

of measuring the eye position; and the optical system that projected the stimulus to the subject. A discussion of these follows in order.

Contact lens. - The heart of the experimental apparatus used is the contact lens worn by the subject. In order to assure that the accuracy of the measurements is better than one min arc, the lens must be fitted so as to ride on the subject's eyeball with a maximum slippage that is less than this amount. The contact lens used was designed to provide this stability with a minimum of discomfort to the subject.

The lens, shown in Fig. 3.2, is built up of a combination of three roughly spherical surfaces. The largest diameter surface is the outer or scleral portion; this section is molded from casts of the subject's eye, and is made as large as possible to take maximum advantage of deviations of the sclera from a true spherical surface, for it is such deviations which prevent the lens from rotating freely on the eye. In practice, these lenses cover about 1.7π radians solid angle on the subject's orb. The scleral portion of the lens extends forward on the subject's eyeball to a point just short of the limbus.

The limbus is the only portion of the surface of the eyeball that has sensory innervation, and therefore should not be contacted by the lens if the subject is to be comfortable. For this reason, the second spherical surface of the contact lens is an annular arch over the limbus that ends at a ring of contact with the cornea. The smallest diameter spherical surface is the corneal bulge. The diameter of this lens surface is slightly smaller than that of the cornea, with the result that the only contact between the lens and the cornea occurs on the ring where the limbal arch ends.

A lens designed as described above makes good mechanical contact with the eye at all possible points, but this would not be sufficient to provide the required stability were it not for the negative hydrostatic pressures that are developed behind the lens by osmotic

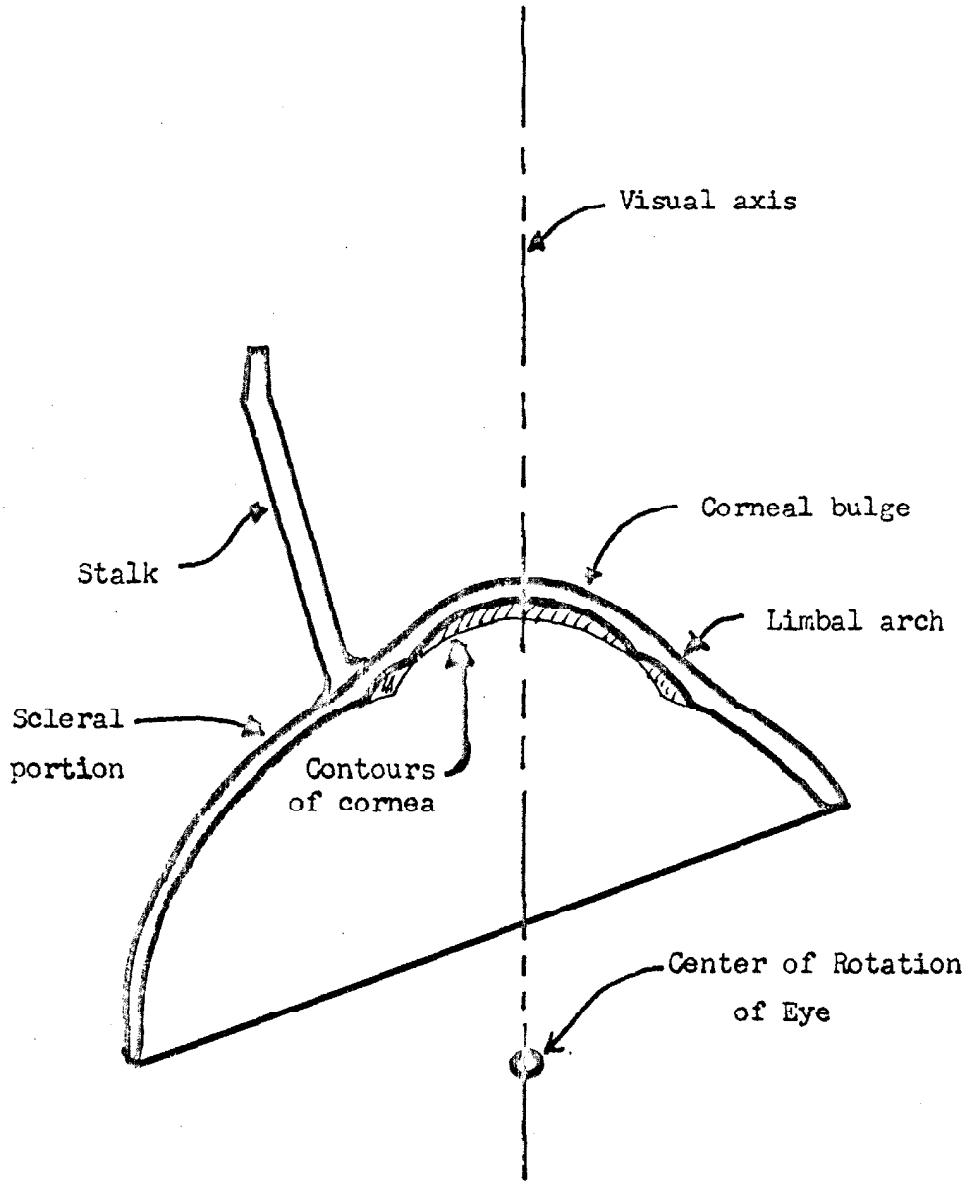

Figure 3.2 - Cross-sectional view of left eye contact lens, showing placement of stalk.

action. The lens is worn with some buffer solution (generally two percent sodium bicarbonate) filling the space between the lens and the eye. After about ten minutes of wearing, during which time the scleral fit has held the lens in position, a pressure differential of some 20 mm Hg is developed behind the lens, pulling the lens down into the conjunctiva (the membrane that covers the sclera), and providing a firm seat on the sclera. In this condition, the lens is quite stable. Fender (27) has reviewed the evidence on the stability of this type of lens, and concludes that the slip is less than one min arc for movements of less than one deg arc from the central position, and less than one percent of the total excursion for movements as far as nine deg arc from the center.

The lenses used weigh approximately 1.1 gm, and represent a moment of inertia about the center of the eye of 0.55 gm.cm^2. The moment of inertia of the lens increases the total moment that must be driven by the extraocular muscles by 12 percent, but Robinson (54) has shown that the moment of inertia of the eyeball has negligible effect on the flicks, the eye movements most easily affected by this moment of inertia. Using Robinson's figures, it can be shown that the contact lens causes an increase in the flick rise time of less than two percent. Thus the contact lens may be assumed to produce a negligible change in the dynamic characteristics of the orb. All the lenses provided for the experimental subjects were corrected optically to produce 20-20 vision. The refractive task of the cornea is taken over by the contact lens when a buffer solution is used (the refractive powers of the lens, buffer solution, and cornea being approximately equal), with the result that the corneal astigmatism of the subject is automatically corrected.

The contact lens, then, provides a stable, non-interfering platform on the eye from which to measure the eye position. In order to separate the optical components that provide these measurements from the disruptive influences of the eyelids and tears, a small (two mm

diameter) stalk is glued to the surface of the lens. (See Fig. 3.2) The stalk protrudes forward 15 mm and is affixed to the lens on the line where the eyelids meet in normal closure. In this position, the stalk does not prevent normal blinking, and the end of the stalk is well clear of the subject's eyelids and vertical cheek line. The tip of the stalk is located 24 mm forward, and 4 mm temporally from the center of rotation of the eye.

Position measurement. - The eye position measurement system used is very similar to that described by Byford and Stuart (7), and is depicted in Fig. 3.3. The light source is a small medical lamp (0.03" diameter and 0.10" long) mounted on a small cone that fits snugly over the tapered end of the contact lens stalk. The lamp is powered through strands of 44 gauge wire, which is light and flexible enough that it can be allowed to dangle from the stalk without affecting the subject's eye motions. When the subject is placed in the apparatus, his head is fixed rigidly in place by the combination of a molded dental bite, and a molded forehead rest. In this position, the lamp rotates above the photomultiplier tube assembly when the eye rotates. The photomultipliers measure the linear (tangential) component of the lamp rotation, but this is proportional to the angular displacement for positions less than three deg arc from the center, with an error less than 0.5 percent.

The photomultiplier is positioned under the subject's eye such that the lamp is on the axis of "tube 1" (see Fig. 3.3).[4] A distance A below the lamp a knife edge occludes half of the rectangular tube. At the bottom of the tube, a distance B below the knife edge, is placed a rectangular mask, and the photocathode of the photomultiplier tube.

[4] The description presented of the photomultiplier assembly covers only the horizontal (tube 1) channel, but is equally valid for the vertical channel. The image of the lamp in the 45 deg mirror is located on the axis of "tube 2", and this image moves horizontally as the eye performs up-and-down rotations about the horizontal axis.

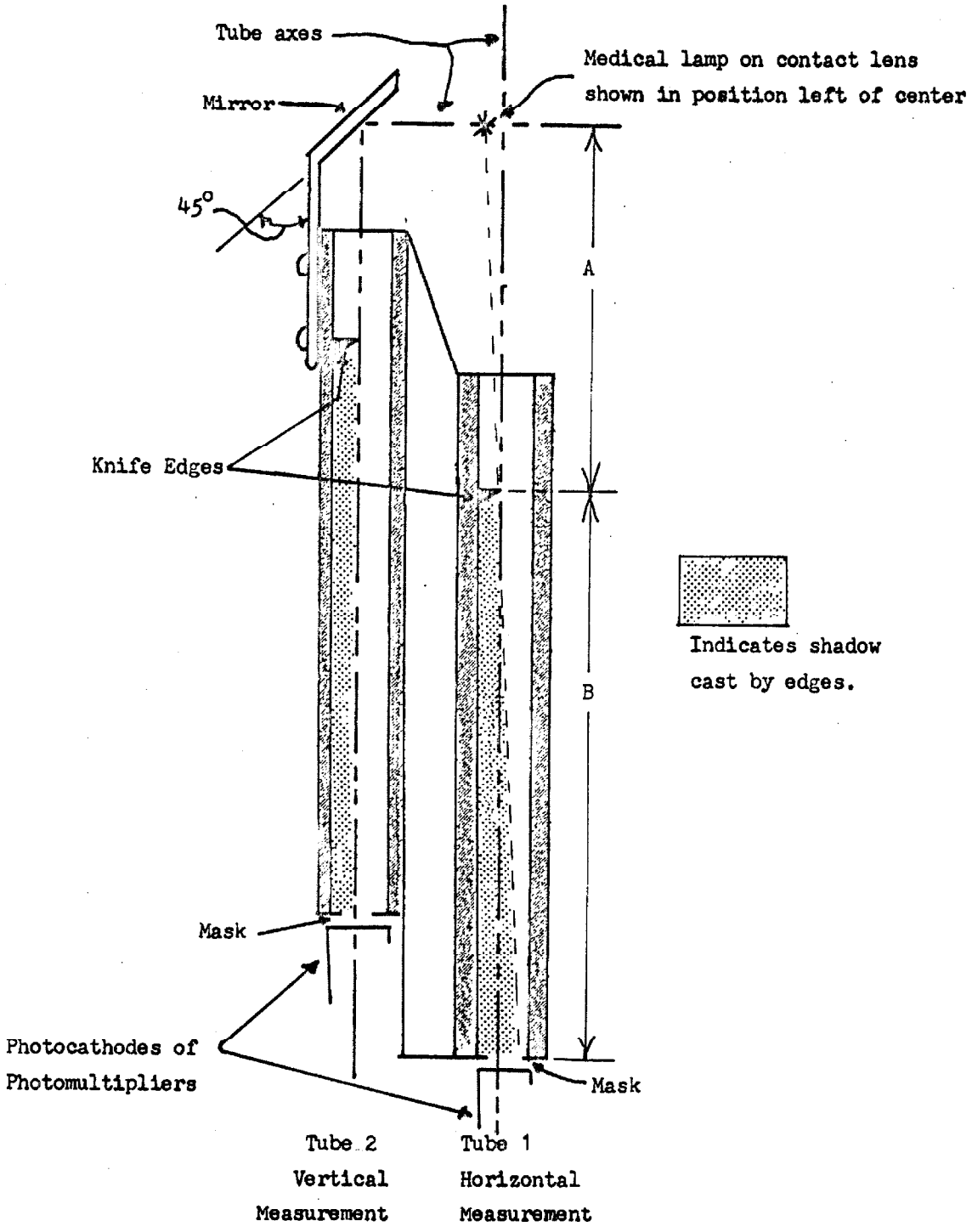

Figure 3.3 - Schematic diagram of the eye position measuring system. Cross-sectional view.

The rectangular mask serves to prevent variations in the tube sensitivity that might arise at the edge of the photocathode. In the central position, with the lamp on the tube axis, the knife edge casts a shadow over half of the photocathode. Any displacement of the lamp moves the shadow of the knife edge, and linearly increases or decreases the amount of light impinging on the photocathode.

The transformation from eye rotation to the photomultiplier tube output voltage can be represented as follows. An angular rotation of ω min arc at the eye displaces the lamp a distance $X = K_1\omega$, where K_1 is approximately .007 mm/min arc. A lamp displacement X produces a change in the shadow position at the photocathode of $Y = (B/A) \cdot X$. The shadow displacement, Y, is directly proportional to the differential light input to the photomultiplier tube, and the tube output voltage is similarly related to the light input. Thus, a single constant K_2 (volts/mm) can be used to relate the differential output voltage to the shadow position, yielding the final form for the output voltage, V, as:

$$V = K_1 \cdot K_2 \cdot (B/A) \cdot \omega \text{ volts.}$$

One of the advantages of this system lies in the factor (B/A) in the preceeding equation. Shifting the vertical position of the knife edge varies this ratio permitting the increase of either the sensitivity or the range of the system; a value of approximately two was used in the experiments.

In order to test the measurement system, a one inch diameter sphere whose angular position could be controlled to better than one min arc was placed in the system where the subject's eye would normally be positioned, and a contact lens was mounted on this sphere. The resultant calibration curve is shown for both the horizontal and vertical channels in Fig. 3.4. It can be seen that the assumption of linearity is good for positions out to 60 min arc either side of center. In all of the experiments in which larger than 60 min arc motions were recorded, the function of interest in the eye position recordings

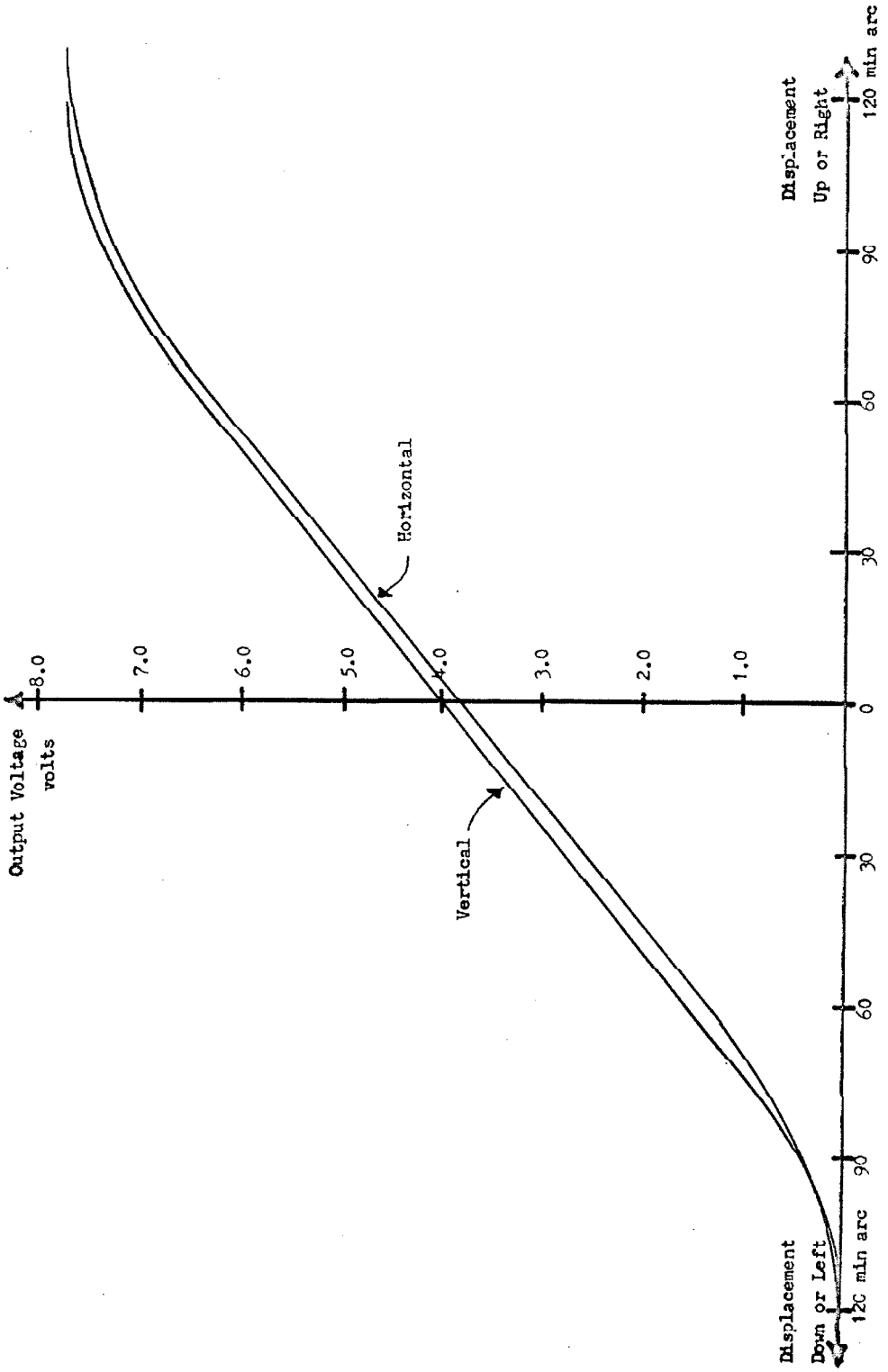

Figure 3.4 - Calibration curves of eye position measuring system, showing the photomultiplier output voltage as a function of the eye position.

was the time of occurrence of the flicks, and these times were saved in histograms whose cell size was several times greater than the error which might be introduced by the system non-linearity.

In order to avoid variations in the gain of the measurement system which might arise due to inaccurate setting of the high-voltage power supply, of the lamp current, or of the amplifiers that followed the photomultipliers, an automatic calibrator was built into the system. This was done by using a remote relay to displace the photocathode mask a known distance, thereby effectively incrementing the shadow displacement. The result is a simulated eye movement of known amplitude which can be measured on the records and used to calculate a voltage to eye position calibration factor. This calibrator was pulsed automatically at the beginning and end of each experimental run, and thus relieved the experimenter of a great many tedious adjustments.

Optical system. - The primary optical system that was used in all the experiments is essentially that which was described by Clowes and Ditchburn. (11) The total system is shown in schematic form in Fig. 3.5, but it is more readily understood if considered in three sections (labelled A, B, and C in the figure) which can be separated according to function. As this is a telecentric system, two beams, a target beam and a source beam, will be referred to. While these two beams can not be separated physically, they do exist as independent optical entities.

The first stage of the system (A) is the projector. It is in this stage that the target is located physically, and that the target illumination is controlled. Two identical, independent projection paths are provided in this stage. These allow the generation of two different target functions, which are then merged into a common stimulus beam at the beamsplitter, BS1. The primary source is the ribbon filament of a 200 watt projection bulb, which is imaged on the pinholes, P. Immediately in front of the pinholes are placed neutral density wedge

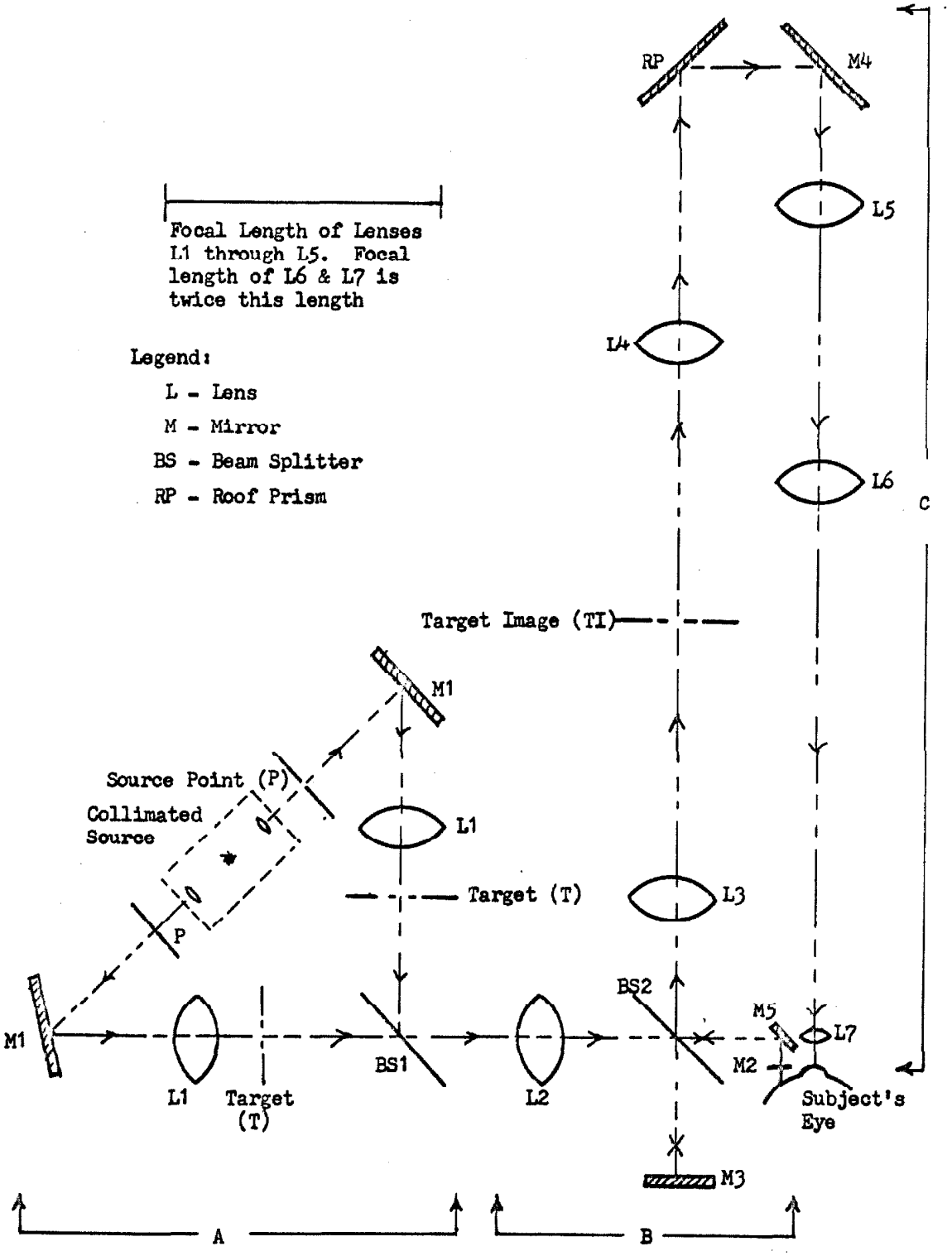

Fig. 3.5 - Schematic showing layout of primary optical system. See text for complete description.

filters (2.5 db/inch) which provide continuous, accurate stimulus intensity control. The pinholes are located (via the mirrors, M1) at the focal point of the collimating lenses, L1. The targets are placed in the parallel source beam thus created. Any controlled target motion that is used in an experiment is introduced at this point by simply displacing the target perpendicular to the source beam. The target image plane will ultimately be viewed at infinity, with the result that linear motion of the physical target can be described as angular rotation of the final visual target. If it is desired to include portions of the eye movements in the target position, these components will be optically added to the target beam in the later stages of the system.

The second stage of the system provides for the addition to the target position of a component that is twice the angular eye position. The real target in the projector stage is located at one focal point of the lens L2, while the contact lens mirror, M2, is at the other focal point. (For the purposes of this discussion, the path from beamsplitter BS2 to mirror M3 is assumed to be occluded.) Thus at the surface of the mirror M2, the target beam is parallel while the source is focused to a point. Rotation of the eye produces angular displacement of the target beam, but does not disturb the orientation of the source which has an image in the surface of M2. Finally, the lens L3 is located (via beamsplitter BS2) one focal length from the contact lens mirror, with the result that the light exiting from this stage has the source beam parallel, and the target beam converging to a real target image at the point TI.

The final stage in the system is the viewing stage. Lens L4 is so located that the target image at TI is at one of its focal points, and the roof prism, RP, is at the other, creating a parallel target beam and a source image at that prism. This source image is placed (via mirror M4) at the focal point of the lens L5, which forms the objective lens of a telescope (lenses L5, L6, and L7) of magnifying power 1/2. The telescope is focused at infinity (the target beam is parallel on entry),

and presents the image to the subject in Maxwellian view with the source beam focused on the front nodal point of the eye in order to achieve maximum intensity.

The production of a stabilized retinal image, one that remains fixed on the subject's retina regardless of his eye movements, can best be understood with reference to Fig. 3.6, which shows only that portion of the optical system involved in this function. The whole optical system has been laid out such that the magnifying power is unity up to the point at which the beam enters the telescope. Further, the effect of the contact lens mirror is to add twice the angular displacement (from the central position) of the eye into the target beam. If the target beam leaves the projector with an angular position 2α from the central position (due to linear motion of the target in the projector), and if the eye position is an angle ω from the center, then the entrant target beam to the telescope is at an angle of $(2\alpha + 2\omega)$, and on leaving the telescope is simply $(\alpha + \omega)$ with respect to the center line. The mirrors in the system and the roof prism provide the proper number of reflections to make the angular sign correct. However, the eye was rotated by an angle ω already, and thus the angular displacement on the retina remains simply α, the experimenter controlled angle, in spite of the subject's eye movement. The optical paths showing the equivalent target beam for the center position, and for an eye rotation ω are indicated in Fig. 3.6 by a solid and dotted line respectively.

The system in the configuration described above will only produce the stabilized vision condition. It is a simple matter, however, to produce normal vision, where no eye movement component is added into the target position so that the subjects eye motions control the retinal image position in the normal manner. To achieve this, the path from beamsplitter BS2 to the contact lens mirror is occluded, and the path from that beamsplitter to the stationary mirror M3 is opened. The two mirrors, M2 and M3, are at conjugate points in the

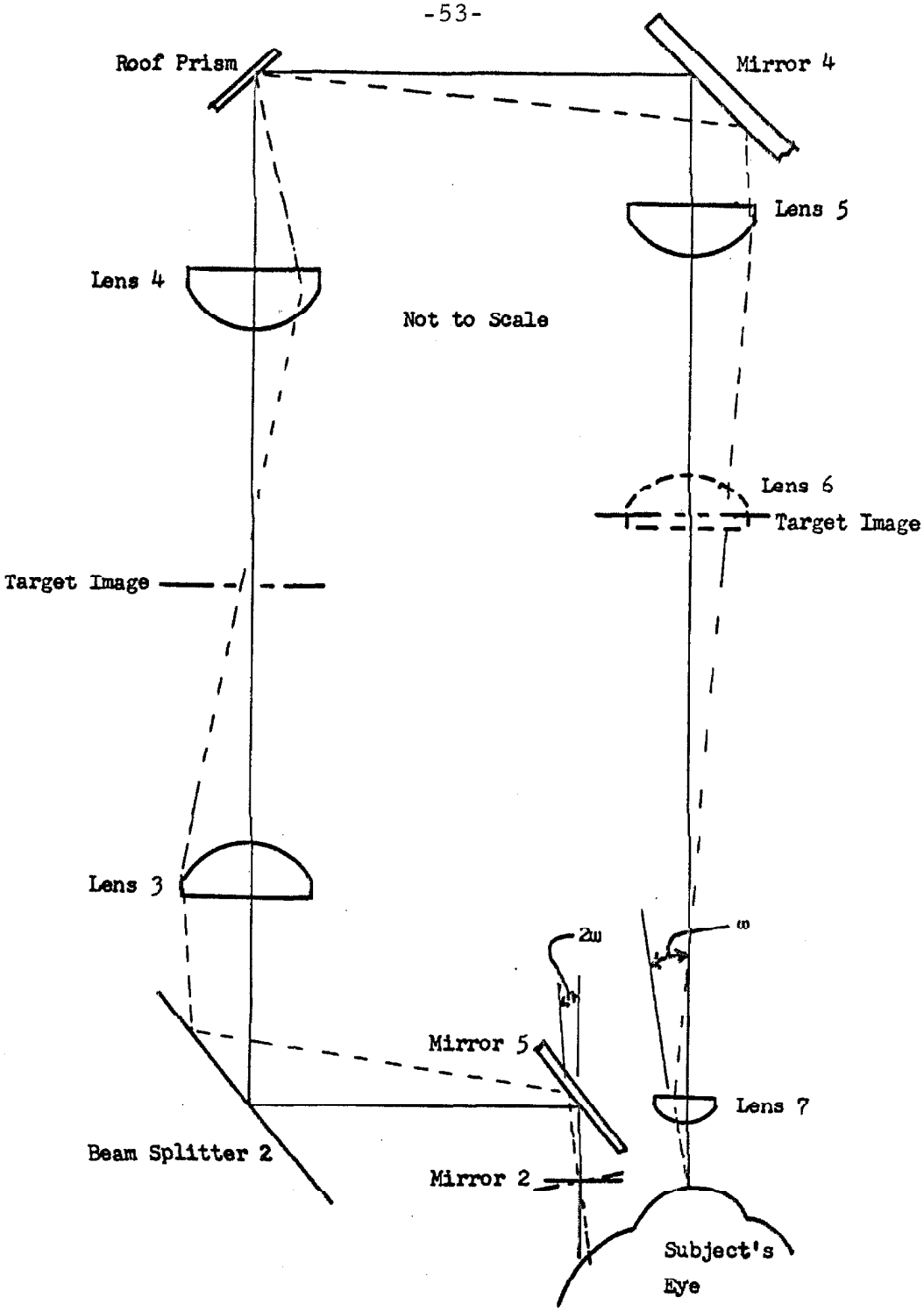

Fig. 3.6 - Partial schematic of optical system demonstrating stabilizing function. Solid path is central beam, and dotted path is beam displaced an angle ω, owing to an eye rotation of the same amount. See text for complete discussion.

system with respect to the beamsplitter, with the result that the functions of the contact lens mirror are taken over by the fixed mirror, providing a complete system in which the target position is not affected by eye movements.

Data Processing Techniques

The systems just described fulfill the requirements of the first of the two categories of experimental procedure - the measurement and control of the parameters. The completion of the research, however, requires that these parameters be reduced to a meaningful set of measures of the process under investigation. Any experiment that tests a system whose responses possess low order reproducibility must be predicated on the ability to reduce large amounts of data down to an average or statistical measure of the system processes. The human eye and its motor control comprise such a system in that no meaningful characterization of these units can be obtained from a single stimulus presentation. Rather, a highly reproducible stimulus must be presented repetitively, and a statistical determination of the response must be performed. The laboratory equipment that was used to provide these stimuli, and to handle the resulting data was chosen to minimize the labor and expense of performing the experiments. Although each experiment performed during the preparation of this thesis involved pieces of apparatus unique to that experiment, a great many of the techniques were common to all the experiments; the more important of these are described below.

Flick detector. -Because the work to be reported later is primarily concerned with the flick component of the eye movements, it proved useful to have an analog device that could detect the occurrence of a flick and produce an output pulse signifying this event. During many of the experimental sessions the simple occurrence of a flick was the response sought from the eye. In these sessions the flick detectors created a significant decrease in the amount of analog data that had to be considered, for they eliminated the necessity of searching long analog records for the flicks, which comprise less than five

percent of the total time of any eye movement record.

The flick detectors are two identical units, one working on the vertical component of the eye motion, and the other processing the horizontal. These units use the positional output voltages of the photomultiplier apparatus as their inputs, and produce a pulse on any one of four output lines (corresponding to up, down, nasal, or temporal) whenever a flick component of greater than three min arc occurs in the direction corresponding to that channel. The circuits used, and a discussion of the design of the flick detectors is given in Appendix II. Briefly, each of the units consists of a combination differentiator and low pass filter followed by pulse shaping networks. Whenever a flick component occurs at the input, the output of the differentiator consists of a pulse whose sign is dependent on the direction of that component. This pulse is passed through a differential amplifier whose positive and negative outputs go to separate Schmitt triggers; each of the two Schmitt triggers represents one of the two directional channels of the flick detector unit. The Schmitt triggers are used simply as threshold devices that respond only to negative pulses, thereby effecting the directional separation of the flick component. The remainder of the pulse-shaping circuitry was designed so that the overshoot of a large flick would not be detected as a smaller flick in the opposite direction.

The purpose of the low pass amplifier included in the flick detectors is to eliminate false detections of high-frequency tremor motion. However, as the sensitivity of the Schmitt triggers is increased to detect smaller flicks, the number of false detections must also increase. Moreover, blinks are frequently detected as gigantic flicks. Tests performed by visual inspection of experimental records show that less than one percent of the total number of detections are false, except in cases where fatigue is causing the subject to blink excessively. When this situation occurred, the experiments were terminated as a matter of course.

Recording devices. - The majority of the reduction performed on the experimental data was done with the digital computer complex available at Caltech. The data transmission link from the laboratory to these computers is fully automated, and is discussed below. Although this link is capable of transmitting the experimental data "on-line" (during the course of the experiment), many of the experiments required that multiple channels of data that were not compatible with the multiplexor be transmitted from each experimental run. As a result, some form of intermediate data storage was necessary in the laboratory. This intermediate storage was provided by a seven channel, magnetic, analog tape recorder. Plug-in amplifiers in this recorder permit either AM or FM recording modes on any of the seven channels.

In typical use, two of the channels were set aside for control tracks, and the other five were reserved for analog data. The primary control track was a clock track on which a fixed frequency square wave was recorded at the time the experimental data was recorded on the other channels. During the subsequent data playback, this track provided correlation between the timing during the experiment and the timing during data transmission, thereby effectively eliminating variations in the playback timing which might occur due to tape transport speed changes during either recording or reproduction. Furthermore, the tape transport speed of the tape recorder may be varied by powers of two from 1 7/8 to 60 ips. This allowed the playback and data transmission function to be performed at a higher tape speed than was used for recording, thus minimizing the additional time.

Digital computation. - The digital computer complex in the Caltech Computing Center has been engineered specifically to provide normal computing in parallel with such special functions as data collection from remote terminals in the laboratories. The basic system links an IBM 7094 with an IBM 7040 via a large capacity disc memory unit. The 7094 performs all the computation, while the 7040 acts as a

dispatcher for the system. In addition to performing the normal input-output functions required for any computer system, the 7040 simultaneously communicates with substations in various laboratories and will accept and store digital data from these substations for later processing.

The substation in the Biological Systems (Biosys) Research laboratories consists of two units, a teletypewriter and a special purpose data digitizer. The teletypewriter permits the user to control the data collection function of the 7040, allowing for variable format in the transmitted data. In addition, data processing in the 7094 can be initiated from this typewriter once the data collection is complete.

Biosys data terminal. -A special purpose, plugboard programmed, hybrid computer has been developed for the Biosys group, which permits a variety of data transmission, and experimental control modes. (13) The experimental control function of the Biosys data terminal (BDT) can be exercised simultaneously with data transmission, permitting "on-line" experiments, but for the sake of clarity the discussion to follow will separate these modes.

In those experiments which used the digital computers for data reduction, the BDT provided the control that was necessary to ensure a uniform, reproducible experimental regimen. This function is initiated by the experimenter, but runs independently of his control thereafter, unless he chooses to terminate the experiment. During the course of the experiment, the BDT provides the clock track to be recorded on the analog tape, and can initiate certain simple functions in the laboratory at precise times relative to the start of the experiment. In many of the experiments to be reported, for instance, the BDT started the stimulus function, provided precisely timed calibration steps in the eye movement measuring apparatus, and terminated the experiment after a predetermined span of time. The

great advantage of a system such as this was that it permitted a standard data format for each individual experiment, thereby simplifying the creation of the data reduction programs used on the computers.

In the experiments that were performed, two modes of data conversion and transmission were used. The first of these modes is simple analog to digital (A/D) conversion. The A/D converter accepts an input voltage in the range between plus and minus one volts (also the analog tape recorder limits) and converts this into a twelve bit binary integer for use in the computer. The conversion rate is generally controlled by the recorded clock (or some submultiple thereof), but this rate is limited to a maximum of 10^4 samples per second. In addition to the straightforward conversion of a single data channel, the BDT permits the multiplexing of from two to six channels. In this mode, one sample is sent from each of the channels sequentially at a sample rate proportionally higher than the basic sample rate for a single channel. Moreover, the BDT provides for the logical gating of A/D conversion either on a time basis, or on the basis of another recorded function. Using this capability, the experimenter can segregate portions of his data for analysis without being obliged to deal with masses of uninteresting data.

The second mode of operation that was used for data transmission is the time of event (TOE) mode. This method has application in experiments where the timing of a specific event is of importance rather than the shape of a given waveform. A prime example of this, of course, is the occurrence of a flick in a record of human eye movements. In order to transmit TOE, the BDT counts the recorded clock pulses in an 18 bit binary counter. Whenever an event, such as a pulse from the flick detector, occurs, the BDT transmits the current value of the counter. The result is a list at the digital computer of the times at which these events occurred. In general,

the events that were detected by the system were restricted to the crossings of a preset threshold by an analog voltage.

Data handling programs. -The system described above provided for the collection of the data by the 7040, which stored this data on digital magnetic tape. The final step in the experimental procedure was the reduction of this data by programs in the 7094. The specialized format of the data tape, however, makes it difficult for the average experimenter utilizing a simplified programming language, such as Fortran, to process the data efficiently. In order to minimize the time and trouble needed to retrieve this data from tape and convert it to the normal 7094 format, special data handling programs have been written for the Biosys group. These permit the programmer access to any specific data sample (A/D or TOE), or group of samples, in either a fixed or floating point format. This recovery is performed with a simple subroutine "call", and the user need never worry about tape position or word format.

CHAPTER IV

EYE MOVEMENT CONTROL SYSTEM MODELS

Introduction. - The preceding two chapters have been concerned with very general aspects of the research which was performed - the system being studied, and the methods used to investigate that system. It was noted in Chapter I that the intent of this thesis is to expand the existing knowledge of the system which controls human eye movements, particularly where that system is concerned with the saccade component. In order to present a unified view of the control system, however, certain background information is necessary. This chapter will discuss the problem of modelling the eye motion system from three points of view. The first of these is concerned with known physiological and psychophysical aspects of the system, and how these aspects can be applied to a basic model of this system. The second section will discuss the existing models, their strong points, and their faults. The final portion of the chapter will point up those areas of the model about which little or nothing is known, for it is at these areas that this thesis and its supporting research are aimed.

Throughout this chapter certain functions of the control system are ascribed to the cortex. No precise localization is implied by such a reference. Rather, the control system is undoubtedly distributed throughout much of the visual and motor areas. Reference to the cortex is intended to imply only the general level of the activity under consideration.

Basic Model

At this point, it is important to stress once more that this thesis is concerned with a restricted portion of the overall visual system. Within the human visual system there are many neurological control systems which have been studied, i. e. pupillary control, accommodation control, eye movements. (9 , 14, 25, 55, 61) Moreover, the control of eye movements alone can be further subdivided. The function of interest in this work is specifically the eye movements of a subject who is performing a monocular fixation task during which the target is constrained to motions in the plane at infinity. The visual information available to the subject is restricted to that provided by the stimulus in the tested eye by the simple expedient of occluding the vision of the other eye. In this condition, disjunctive and conjugate eye movements are of no benefit to the system. The model derived in this section is intended to show the essential information pathways that are available to the eye positioning system, and their probable interrelationship.

Retinal information. - The information pathway that is constituted by the retina, the retinal ganglion cells, the optic tract, and the lateral geniculate bodies is highly complex, but two forms of information passed through this route can be extracted.

The information regarding the position of the image on the retina is undoubtedly of greatest importance to the system. It was shown in Chapter II that the area of highest resolution on the retina is the fovea, and that a subject will tend to position his eye so that the fovea coincides with the portion of the image in which he is interested. A determination of the relative position error between the fovea and the point of interest is probably not made at the retinal level, but this determination can easily be made at higher levels. In addition to image position information, the cortex probably receives information from the retinal level concerning the velocity of the image across the

retina. Microprobing studies in mammals (4, 31) have detected such signals both in the optic tract, and in the lateral geniculate bodies.

Cortical processing. -The vast majority of the information processing in the system being studied takes place in the cortex, and the available histological evidence is insufficient to allow one to ascribe specific functions to specific areas of the brain. Despite this fact, experimental results have permitted the identification and separation of several types of processing.

First, it is in the cortex, that the conscious desires of the subject are effected as he determines which portion of the retinal image is to be fixated at the fovea. In the tracking tasks to be reported later, the subject was instructed to fixate a point source of light, and this simple instruction determined the reference point from which the error position of the eye could be evaluated. It is known that the areas of the retina are mapped at the lateral geniculate bodies and the visual cortex (31, 49), and this mapping permits the cortical determination of image position error once the point of interest has been chosen. Several researchers (25, 50, 61) have noted a "dead zone" around the fovea in which the target may be fixated without eliciting eye movements. This means that the cortex does not require eye motion unless the image-fovea position disparity is greater than this dead zone. It should also be noted that if image velocity information is not obtained from the retina, it can be derived from the image map at the cortex. Regardless of the task chosen or of how the information is obtained, the cortex translates this information into two simple factors, the velocity and position which the eye is to assume.

The motion of the orb is produced by two distinctive components, the drift and the saccades, and it has been shown (50) that these components are driven independently by the velocity

and position of the retinal image. Thus, the second function of the cortex is to generate the appropriate smooth-following and saccadic eye movements from image velocity and position information. The command signals which result from this computation are then fed to the extraocular muscles, which in turn produce the appropriate rotation of the orb.

Efference copy. -It was shown in Chapter II that the sensory system of the eye has no centripetal pathway from which the cortex can deduce the position of the eyeball; yet the human is capable of discriminating between retinal image motion which arises due to motion in the visual field, and image changes which are due to eye movements. The efference copy theory has been proposed to resolve this apparent anomaly. According to this theory, the efferent information, the command signals to the extraocular muscles, is sent back to that portion of the cortex which is involved with describing the eye movements to be performed. This efferent information is thought to be sufficient to describe the eye position.

It can be argued that the efference copy is of little value to the cortex when the subject is performing the simple task of tracking a point target. In such a situation, the fixation task can be reduced to the problem of maintaining the coincidence between the fovea and the point of interest. Regardless of whether image motion is produced by an error in eye movements, or by target motion, the corrective motion which the eyeball must perform is the same. It is only in situations where the cortex is specifically concerned with evaluating the motion of visual stimuli, for instance while trying to maintain a given direction of gaze with respect to the head, that the efference copy is of benefit.

Proprioceptive information. -Sensory formations such as Golgi tendon organs and muscle spindles are found throughout the extraocular muscles. (12) To date, however, no specific functions of these sensory pathways have been determined. Christman and Kupfer (10) show that this information is probably not used to evaluate eye position, and Whitteridge (60) shows that it does not maintain muscle tone as happens in much of the skeletal muscle. These facts have led to the speculation that these units serve to feed velocity signals back to the cortex, and such a loop has been included in some of the models proposed in the past (25, 26).

Basic model. -The various information pathways described above can be combined into a general model of the eye movement control system as shown in Fig. 4.1. The cortex contains the great majority of this system, for it performs both the evaluation of the desired eyeball motion, and generates the primary command signals to the muscles. Moreover, the system shown is capable of virtually any tracking mode desired. The cortical decision box is assumed to combine the information from the retina, proprioceptors, and efference copy with the conscious desires of the subject and produce signals from which the command units generate the eye movements. This decision unit is, however, capable of quite sophisticated modes of operation. For instance, it will be shown that for certain simple stimulus wave forms the cortex can predict the future course of the target and thereby reduce the phase lag which would normally exist in the tracking system. Such capabilities make the reduction of this model into a simple signal flow chart somewhat difficult. However, the specification of any given stimulus wave form and a determination of the predictability of that wave form makes such a reduction feasible. In the later sections of this chapter various models are presented as they have been derived by other researchers. In each of these cases, a signal flow diagram, and subsequently, a control system model, have been extracted because a complete stimulus

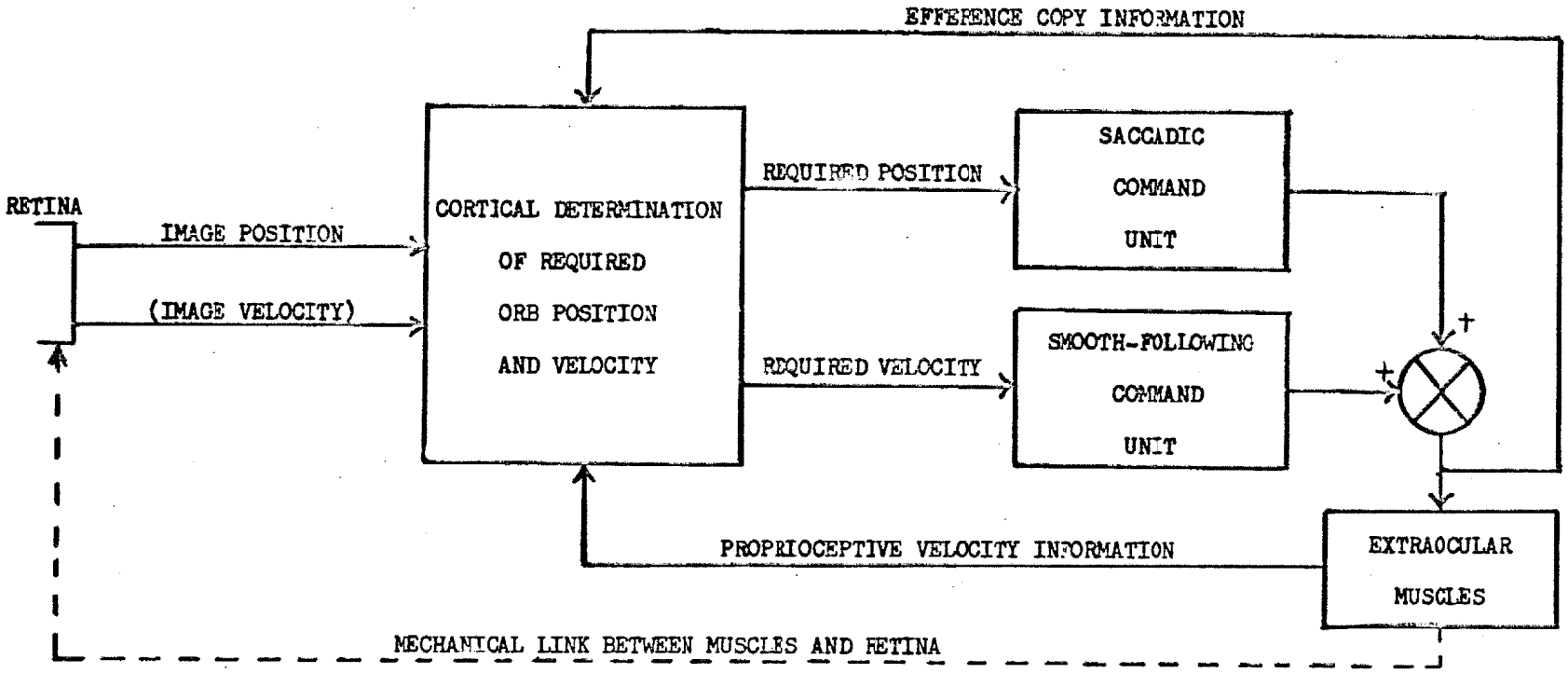

Fig. 4.1 - A general model of the oculomotor control system illustrating information pathways.

specification permitted the reduction of the cortical decision unit to a mathematical equivalent.

Previous Models

During the past six years, various attempts have been made to model the human eye fixation system. (14, 25, 34, 50, 53, 61) Of these attempts, four are representative, and serve to specify basic portions of the system. In this section, each of these models will be discussed, their applicability noted, and objections raised where necessary.

Smooth-Following Model

Experiment. - The first model of the human eye movement control system was published by Fender and Nye (25) in 1961. Their intent was to use the basic frequency response of the eye to derive the equivalent servo-mechanism. The experimental apparatus which was used for their experiments was identical to that described in the preceding chapter, and permitted them to test the eye in conditions of abnormal feedback. Although it was not discussed in detail in Chapter III, the system can be altered to produce visual conditions other than simply stabilized or normal vision. In particular, Fender and Nye created a condition of enhanced visual feed-back in which the image on the retina moves when the eye rotates, but the image is displaced twice as far on the retina as it would be in the normal vision condition. Their experiment then consisted of presenting to the subject a stimulus that consisted of a single frequency sine wave and instructing him to track that stimulus with his eye. In order to produce the frequency response curves, they extracted from the eye movement recordings the amplitude and phase of the first harmonic[5]

[5] Pursuant with standard mathematical definitions, the author uses the term "first harmonic" to refer to the fundamental of a wave form; in the case of eye movement responses to sine wave stimuli, this is the component at the same frequency as the stimulus.

of the response, and averaged these values over many cycles of stimulus. Using this method, they extracted frequency response curves for several subjects in all three visual conditions - normal, stabilized, and enhanced.

Model. - The basic model which Fender and Nye produced is shown in Fig. 4.2. The primary feedback loops which they employ can be identified with those postulated in the preceding section of this chapter. Their "retinal image feedback loop" is simply the mechanical link between the extraocular muscles and the retina; and their "oculomotor feedback loop" is simply a manifestation of the efference copy mechanism. The derivation of the feedback factors which they included is complex, and as several objections can be raised to these loops, discussion of this derivation is withheld here.

Objections. - The primary objection to be raised against this model is that it purports to measure the control system characteristics for all following regimes, whereas in fact, it represents the response to a special class of stimuli - predictable[6] sine waves. Stark, Vossius and Young (56) clearly show that the response to an unpredictable wave form possesses far greater phase lag than the response to a predictable stimulus. This fact was also noted by Fender and Nye, as they determined that the responses they were measuring represented a less than minimum phase system. In an attempt to resolve this point, they included the efference copy feedback loop. This loop is probably spurious to tracking functions in

[6] At this point, some attempt should be made to define what is meant by predictable stimuli. No determination of the predicting capabilities of these systems has ever been made, but the typical separation of predictable and unpredictable stimuli is made on the basis of frequency content. A stimulus is deemed to be predictable if its frequency composition is a simple sum of harmonically related sine waves - single frequency sine waves, square waves, triangular waves. A stimulus which can not be decomposed to such a simple series is deemed to be unpredictable.

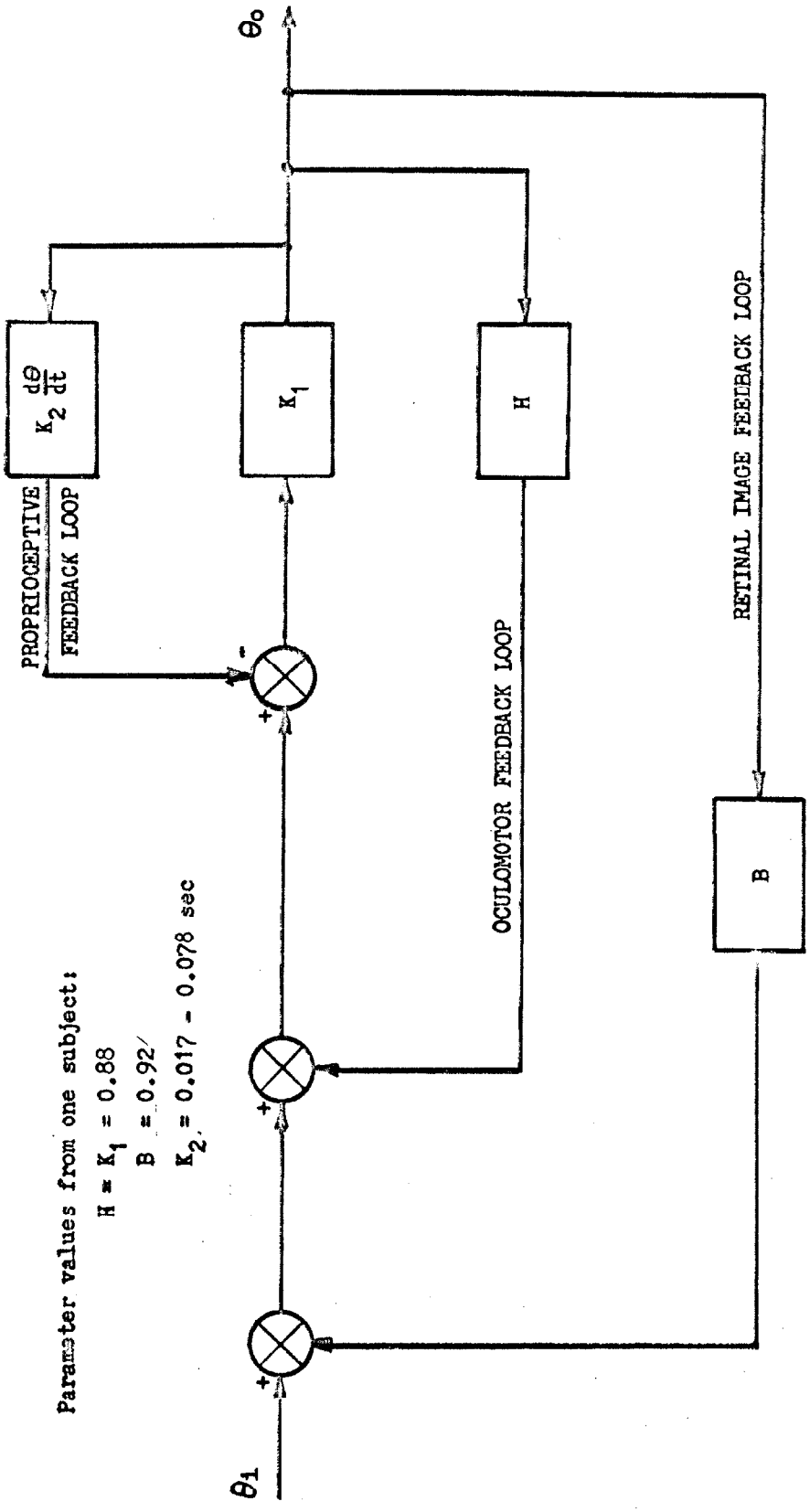

Fig. 4.2 - Smooth-following control system model redrawn from Fender and Nye.

general, for the reasons mentioned earlier, and should have been replaced by some unit which represents the ability of the cortex to learn the stimulus pattern. As a result, the model which they present is a first approximation to the portion of the overall system which tracks predictable sinusoids. Later models of the system have all included such a mechanism in parallel with the normal tracking mode.

The second objection to this smooth-following model is the fact that it ignores the saccadic component of the eye motion. In reducing their data, Fender and Nye did not account for the presence of the flicks in any way. Fortunately, this has little effect on the model which resulted. Fender (26) later showed that subtraction of the flicks from the record produced little effect on the phase of the response. The amplitudes of their responses are not appreciably altered by the presence of the flicks at stimulus frequencies less than one cps, but at frequencies higher than this value, the response they observed frequently degenerated into a saccadic following mode, with the result that the gain values which they measured are probably larger than the true gain of the smooth-following system.

Sampled Data Model

Experiment. - Young (61), working in 1962, attempted to present a model of the eye movement control system which would remove the majority of the objections to the simpler Fender and Nye model. The most important aspect of his experiment was the use of unpredictable stimulus wave forms for the extraction of the frequency response characteristics. These unpredictable waveforms were generated by adding three sinusoids of non-integrally related frequencies. The responses to these stimuli were analyzed on a digital computer which extracted the gain and phase of the system for each frequency component. Using the response curves which resulted, he concluded that the system could best be modelled by a sampled data system

with a 200 msec sampling period. Further, he noted that the responses of the smooth-following system and those of the saccadic system could be separated. The resulting model consisted of two sampled data systems in parallel, one controlling each of the eye movement components.

Saccadic system. - Young's model for the saccadic system is shown in Fig. 4.3a. Briefly, the retinal position error is sampled at a rate characterized by the sampling interval T. The dead zone effect at the fovea is accounted for by the second unit in this system. The error sample which results is then delayed for one sample period, a "computing delay", and then the sample is integrated to produce the step desired of the system. The final unit of the system is the "muscle and eye dynamics". This function amounts to a filtering of the desired step, but the effect is small in that the time taken by a saccade (less than 30 msec) is small with regard to the sampling interval, 200 msec. Young also includes in this system an input labelled "disturbance" which is to account for the small flicks and drifts that are observed as uncorrelated to the stimulus. However, he makes no attempt to characterize this "disturbance.

Pursuit system. - The second half of Young's model is comprised of the pursuit, or smooth-following system, as shown in Fig.4.3b. The action of this system is quite similar to that of the saccadic system except that it responds to the velocity component of the target. The retinal position error is sampled at about the same rate as before, and the error rate is estimated as the difference between the current error sample and the preceding error sample, divided by the sampling interval. This rate is passed through a limiter which effectively opens the pursuit loop whenever an error rate of greater than 30 deg/sec is detected, corresponding to a target displacement step of greater than six deg arc occurring in a sample period. The output of this unit is a velocity sample which is integrated to produce a step equal in magnitude to the desired velocity change. This function is

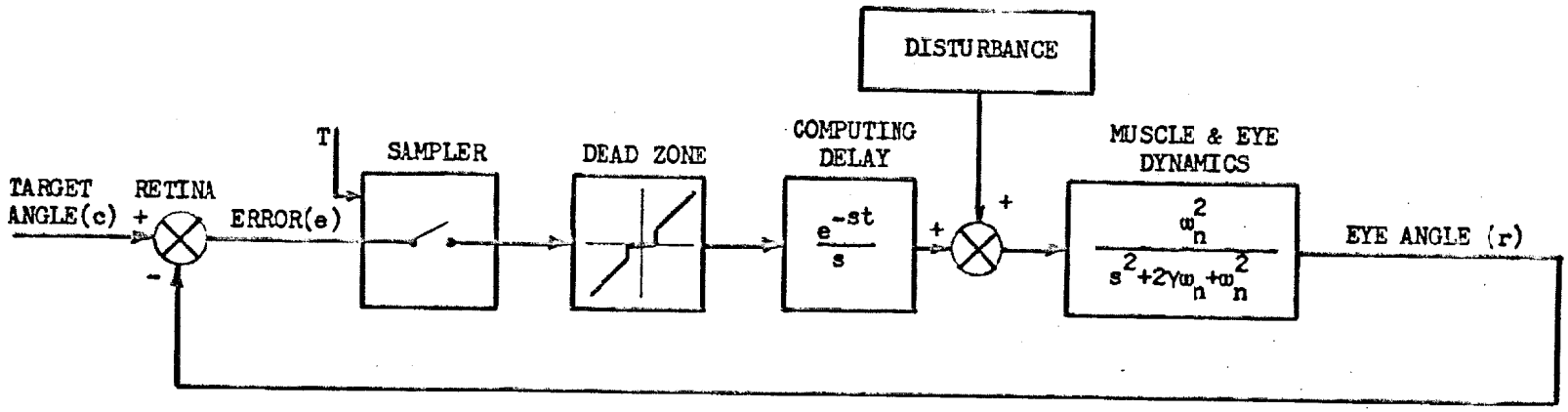

a) The saccadic system.

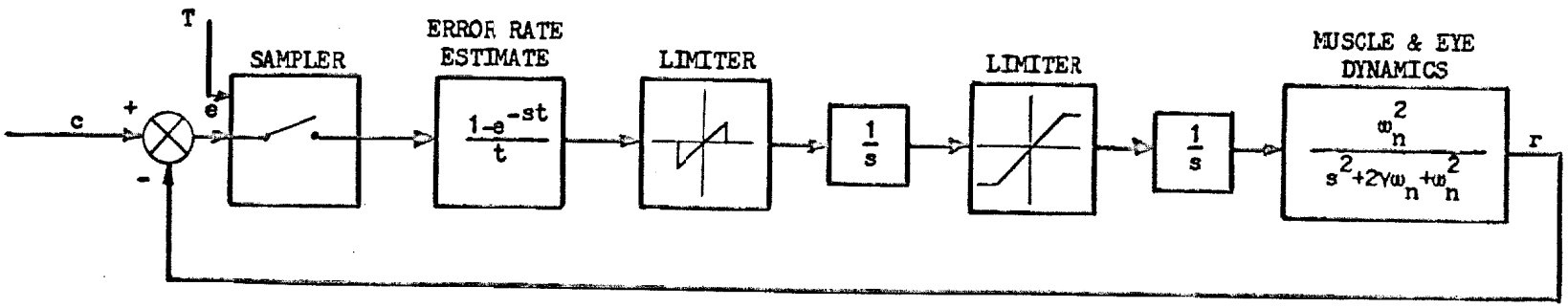

b) The pursuit system.

Fig.4.3 - The sampled data model of the human eye movement control system, redrawn from Young.

passed through a second limiter which reflects the maximum rate capabilities of the extraocular muscles, on the order of 25 to 30 deg arc/sec. Finally, the resultant step is integrated to produce a velocity change in the eye movement.

Objections. - The most obvious point in Young's model is the use of a sampled data system. The evidence which he cites to conclude that this is a good representation is convincing, but the sampler itself is one of the weakest points in the model. The source of this problem lies in the fact that the model is an attempt to fit a stochastic system with a fixed model. The result is that the exact nature and timing of the sampler is not at all clear in the system Young describes. He assumes that the sampler is always closed (information passing through) except when a sample of interest, one to which the system has responded, has passed through the sampler within the preceding 200 msec. Secondly, he assumes that the sample interval, T, is constant on the average; that is, that the sample interval will vary about a mean interval, but that this mean value never changes for any given subject. Experiments to test these two points have been performed, and are reported in later chapters of this thesis; they effectively refute both points. Moreover, these experiments point to the form, or source, of the "sampler", whereas Young's model does not.

A second objection to the sampled data model lies in the fact that it ascribes a sampling mechanism to the smooth-following system. The evidence presented to support this derivation is not convincing because of the inability to test this function in the absence of saccades. The tests used by Young consisted of measuring the velocity of the eye in response to a parabolic stimulus, one which had constant acceleration. The smooth-following system will attempt to track the velocity of the target, but the phase lag of the system produces position errors which are corrected with saccades. As a result, his velocity records are contaminated with "spikes"

representing the saccades, and these make the evaluation of the pursuit velocity difficult. Examples of such records are presented as Fig. 4.4 redrawn from Young. The assertion that the plot of orb velocity is constituted of a series of flat steps separated by spikes is questionable. Judgement on this point should be reserved until a definitive experiment has been performed. There is no reason, a priori, to assume that both systems should be of the sampled data form.

Integrated Model

Dallos (14) performed experiments very similar to those of Young, but arrived at a totally different model. Dallos' model is extremely complex, but its primary characteristic is that it is a system in which the saccadic and pursuit mechanisms are combined in an integrated model. Moreover, his model uses saturable elements to provide a form of sampled data response in the saccadic system while still allowing a continuous tracking in the smooth-following system. In addition to the non-predictive states of the following system, Dallos remeasured the predictable smooth-following system that was tested by Fender and Nye. He includes this in his model as paths parallel to the normal tracking functions. The primary objection to Dallos model is the same as that expressed to Young's saccadic system; a simple sampling effect does not appear to be the governing feature of this system.

Steady Fixation Model

One major objection to all three of the models presented above is that they fail to account fully for the spontaneous flicks and saccades - those eye movement components which are not correlated with the stimulus movement. Fender and Nye ignore these effects, and Young notes their existence, but does not attempt to characterize them. Dallos, on the other hand, attempts an analysis and includes the results of this analysis in his model but the work

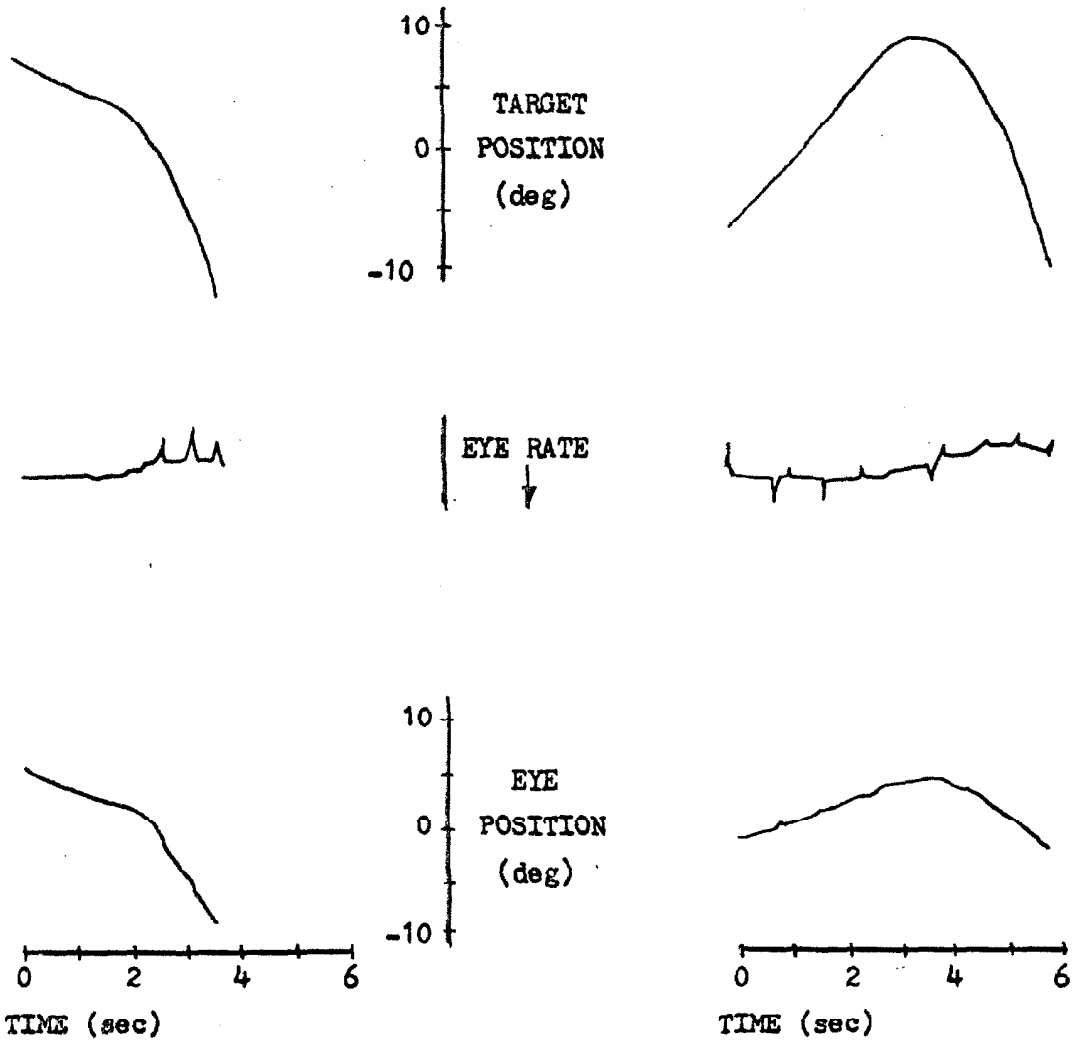

Fig. 4.4 - Records of eye position and velocity while tracking parabolic target motion, redrawn from Young.

performed by Dallos in this respect was performed earlier and more completely by Krauskopf, Cornsweet and Riggs (36).

The technique used in this type of analysis is straight-forward; the subject is asked to fixate a stationary point target, and the spontaneous flicks and drifts which occur are measured. The results obtained by Krauskopf, et al. indicated strongly that the relationship of these components was simple - the drift occurred at random and created fixation errors which were corrected by the flicks. The experiments performed in this respect, however, measured only the horizontal component of the eye position. The author of this thesis subsequently attempted a similar analysis on these spontaneous movements using both dimensional components. The experiment, which is reported in full in Chapter VIII, reveals that the primary emphasis of the earlier work was wrong, and a re-evaluation of the spontaneous components appears necessary.

General Model

Utilizing the information detailed above, a general model of the human eye position control system can be laid out. It would appear from the descriptions given above that the modelling of this system should be complete, and yet each model derived to date has certain faults which hinder the general application of that model. Without exception, the objections appear to arise from the fact that deterministic systems were used to model what is basically a stochastic process. The responses measured and reported are, in every case, a representation of the average response, whereas the specific response of the eye to any given stimulus may be quite different from the mean response. Moreover, those portions of the system which have not been adequately modelled in the past are just those areas where these random processes are most prevalent. Thus, a study of those sub-systems which are not well specified will as a matter of course establish the primary random processes involved in the general system.

A general model for this system is shown in Fig. 4.5. This model differs from that presented in Fig. 4.1 only in that four sub-systems have been displayed in parallel. These four units - a predictable and unpredictable control for both the smooth-following and saccadic systems - are all located in the cortex and reflect the separability of the saccade and pursuit systems shown by Rashbass (50), and the separability of the predictable and unpredictable modes, shown by Stark, Vossius and Young (56). Within each block in this diagram is a symbol indicating by whom that sub-system has been modelled, or, when applicable, where the attention of this thesis will be directed. In addition, various sources of noise, representing the spontaneous eye movements, are indicated in likely locations. These sources will also be examined here.

Recapitulation of the objections raised earlier in this chapter to the various models will indicate the basis on which the choice of experiments to be performed was made. In the saccadic control system, the two stimulus modes should be dealt with separately. Several experimental reports (14, 56, 61) have noted the fact that the saccadic system is capable of a predictive response when tracking single frequency square waves. Yet, none of these reports has included an analysis of the form of that prediction. Studies on the smooth-following predictive loop (14, 25) have shown that the phase delay in that loop is constant for each cycle at any given frequency. The experiments to be reported in Chapter V study the equivalent measure in saccadic tracking - the response delay to stimulus steps. This delay, however, will be shown to be far from constant and a probabilistic model to this effect will be generated. The non-predictive saccadic tracking model produced by Young is felt to be a good representation of this sub-system with the singular exception of the specification of the sampler. This problem is studied in depth in Chapter VI. The resultant model responds in a similar fashion to the system described by Young for many stimulus conditions, but the

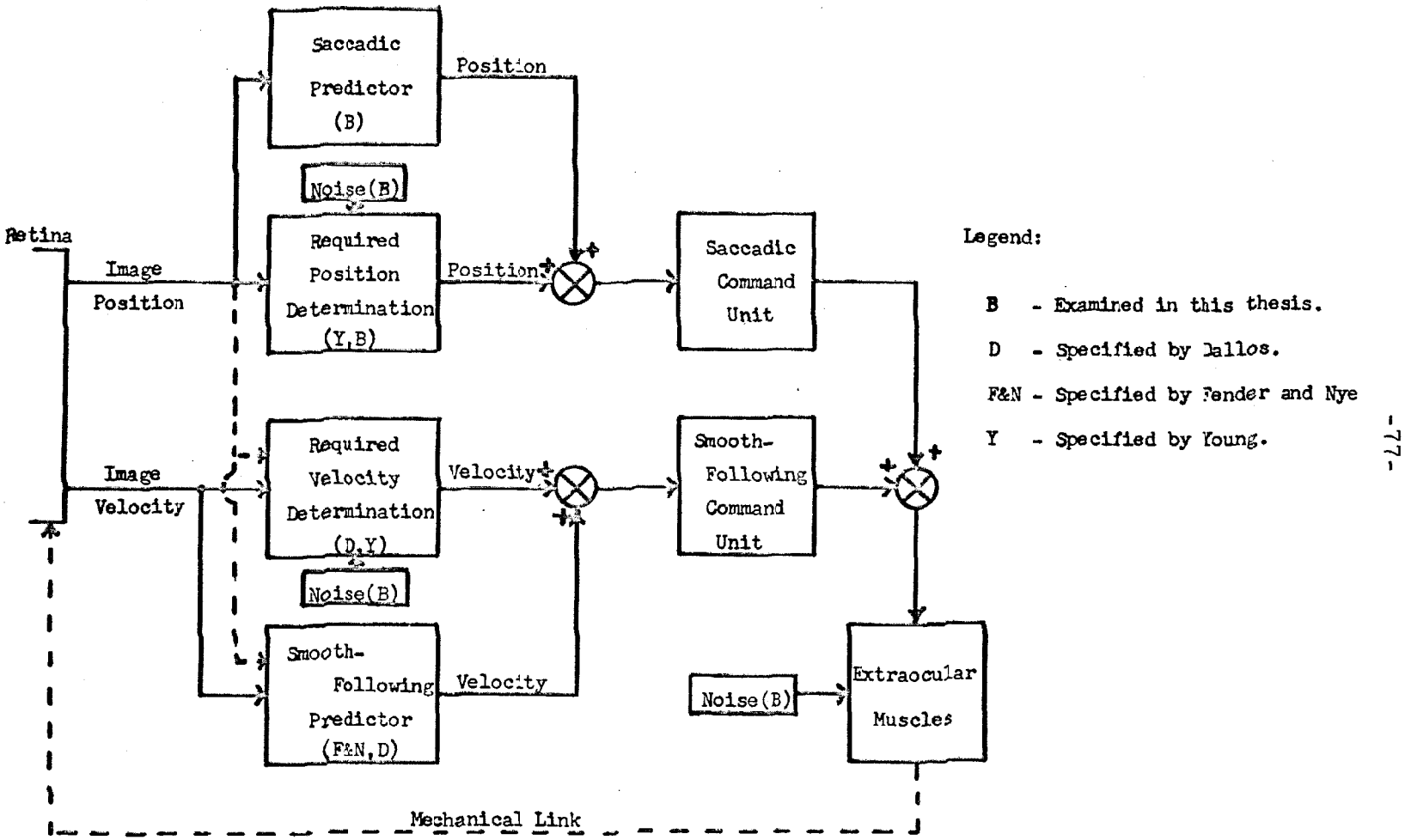

Fig. 4.5 - General model of the eye movement control system showing the separation of various response functions, and indicating by whom these functions have been modelled.

exceptions on which those experiments are based produce important insights into the mechanisms involved in the sampled data model. Finally, the major issue that was raised with regard to the smooth-following models was the presence of drift and flick components which could not be accounted for by the target motion. The statistics of these spontaneous movements will be investigated in Chapter VIII.

CHAPTER V

TEMPORAL ANTICIPATION IN SACCADIC TRACKING

Introduction. -As noted in the previous chapter, the major unspecified sub-system of the eye positioning system is the predictive loop in the saccade channel. The fact that such a loop exists has been well established (14,56,61), but no determination of the mechanism which supports this prediction has been forthcoming. This chapter presents experimental data and a model derived from that data which show the primary mechanisms involved in saccadic prediction.

In testing a sub-system of this type, it is necessary to assure that the stimulus chosen will elicit responses only from that sub-system. It will be shown that simple square waves of constant amplitude do, in fact, elicit a response in which the saccades are the only correlated component of the eye movement. Furthermore, the predictability of the stimulus must be specifiable. Under the definition of predictable stimuli presented earlier, a predictable square wave is one which has a constant period, while an unpredictable square wave is constituted of alternately directed stimulus steps whose separation in time is variable. Finally, some definition of what is meant by prediction will be necessary. Prediction in general implies that the subject has learned the stimulus wave form sufficiently well that he can anticipate the subsequent motion of the target and thereby generate a response that is closer in time, or phase, to the stimulus than a simple reactive response would be. Saccadic prediction involves two factors with respect to a square-wave, the amplitude and time of the response step. The factor of interest here is the time of occurrence of the response step, and the

experimental discussion which follows is aimed at investigating this factor.

The Experiment

Apparatus.-A schematic of the stimulus drive equipment is provided in Fig. 5.1. The stimulus mover is a linear motion, solenoidal transducer which carries the target slide, a pinhole, on its armature. The target position at any instant of time is determined by the state of the binary counter, A. The output state of this binary counter is fed, via a power amplifier, into the target transducer. For accurate positioning and maximum target transition speeds, the power amplifier is provided with a negative feed-back loop. A knife edge attached to the target slide interrupts a secondary light beam which is incident on a photocell; the effect is to produce illumination at that photocell which is proportional to the target position, and the output voltage of the cell is fed back for comparison with the stimulus drive voltage. In this configuration the target transducer can step through a maximum displacement of 12.5 mm in 10 msec. The target is placed in the primary position in the optical apparatus, position T in Fig. 3.5, and viewed by the subject in normal vision. The target used was a two min arc diameter pinhole illuminated at 13 mlumens per steradian, and the step amplitude was set at 1.25 deg arc, which was achieved in eight msec with no overshoot.

The driving pulses to the binary counter determine the time course of the stimulus wave form being presented. A low frequency square wave generator was used as the input to the counter in those experiments where a predictable, constant period, stimulus was necessary. Several control experiments utilizing unpredictable stimuli were also performed, however. These required a device which could generate a reproducible stimulus wave form whose time sequence was of such complexity that the subject would be incapable

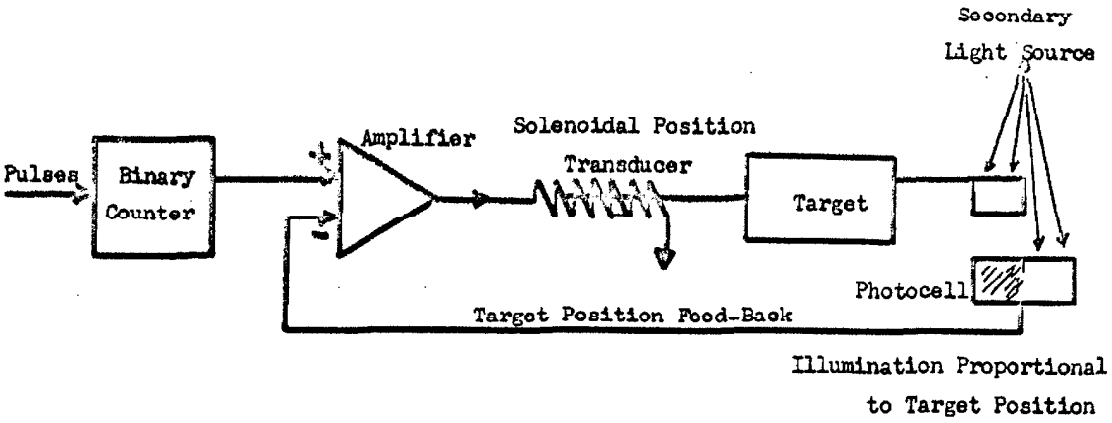

Fig. 5.1 Schematic diagram of target motion system.

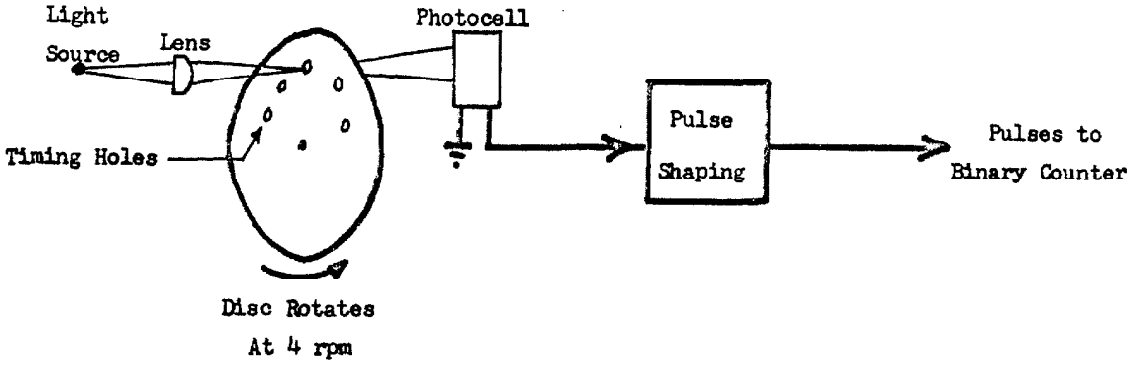

Fig. 5.2 - Schematic diagram of "random" period generator for unpredictable square wave stimuli.

of learning the wave form through replications of the experiment. This device, shown in Fig. 5.2, consists of an aluminum timing disc placed on a four rpm turntable. Twenty holes are drilled in the periphery of the disc, and these pass between a light source and a photocell. The output pulses of the photocell are shaped and used to drive the binary counter. The spacing of the holes in the disc determines the timing of the stimulus. Preliminary trials indicated that the range of inter-step periods from 500 to 1100 msec was that in which the anticipation of the predictable stimulus was most effective; as a result, twenty time intervals in this range were selected and randomized in two different orders. Two discs were made to correspond to these two lists, so that by inverting or replacing the discs, four different unpredictable stimulus regimes were available.

Experimental course. - The experimental course for the predictable stimuli consisted of two runs at each period (defined here as the time between subsequent steps, rather than the mathematical period which would be twice this number). Each run included 100 stimulus steps. Twenty periods were chosen in the range from 500 to 1100 msec, and an additional six were used in the range from 1100 to 4000 msec. The order of presentation of the periods was randomized to prevent systematic accommodation. For the unpredictable experiments, each subject was presented with forty 75 sec runs, ten runs with each of the four possible disc configurations. The result was that for each experimental configuration, predictable and unpredictable, approximately 200 responses were obtained at each stimulus period.

Data recording. - The data taken during the course of the experiments were recorded on the analog magnetic tape recorder for subsequent transmission to the computers. The data channels consisted of two stimulus and two response channels. Given that the stimulus amplitude was a constant, only the times of stimulus

transitions were necessary to specify its wave form. Accordingly, a simplified version of the flick detector was built to detect target steps, and the right and left transitions of the stimulus were recorded on two separate channels as pulses. The two response channels recorded the right and left flick detector outputs, a right flick being defined as one in which the horizontal rotation of the eye is from left to right. The actual eye position was not recorded in these experiments. Justification for using only the saccade time as a measure of the subjects's response is given below.

Data reduction. -Figure 5.3 shows oscillograph records of experimental segments for two subjects in both experimental conditions. The data displayed here are the stimulus wave form, the flick detector outputs, and the subject's response. Several points are worth noting on these records. First, the larger saccades which occur in response to stimulus steps are by no means the only saccades in the records; rather numerous spontaneous flicks can be seen scattered throughout the records. Secondly, there are a few places where large, erratic eye position traces are seen; these represent blinks. Despite the effects of the spontaneous flicks and the blinks, the saccades that are a part of the following motion are readily identifiable by eye, but an algorithm has to be developed so that this recognition can also be made by a computer program. From records such as these, several pilot computations were performed to determine the method of data reduction to be used. On the basis of these, it was decided to use the properly directed saccade that was nearest in time to any given stimulus step as the response to that step, provided that the magnitude of the time difference between stimulus and response was less than 400 msec (twice the normal reaction time to an unpredictable stimulus). The saccade chosen by this criterion was found to have the same amplitude as the stimulus more than 95 per cent of the time for stimulus periods below one sec. At stimulus periods greater than this, spontaneous flicks or blinks probably

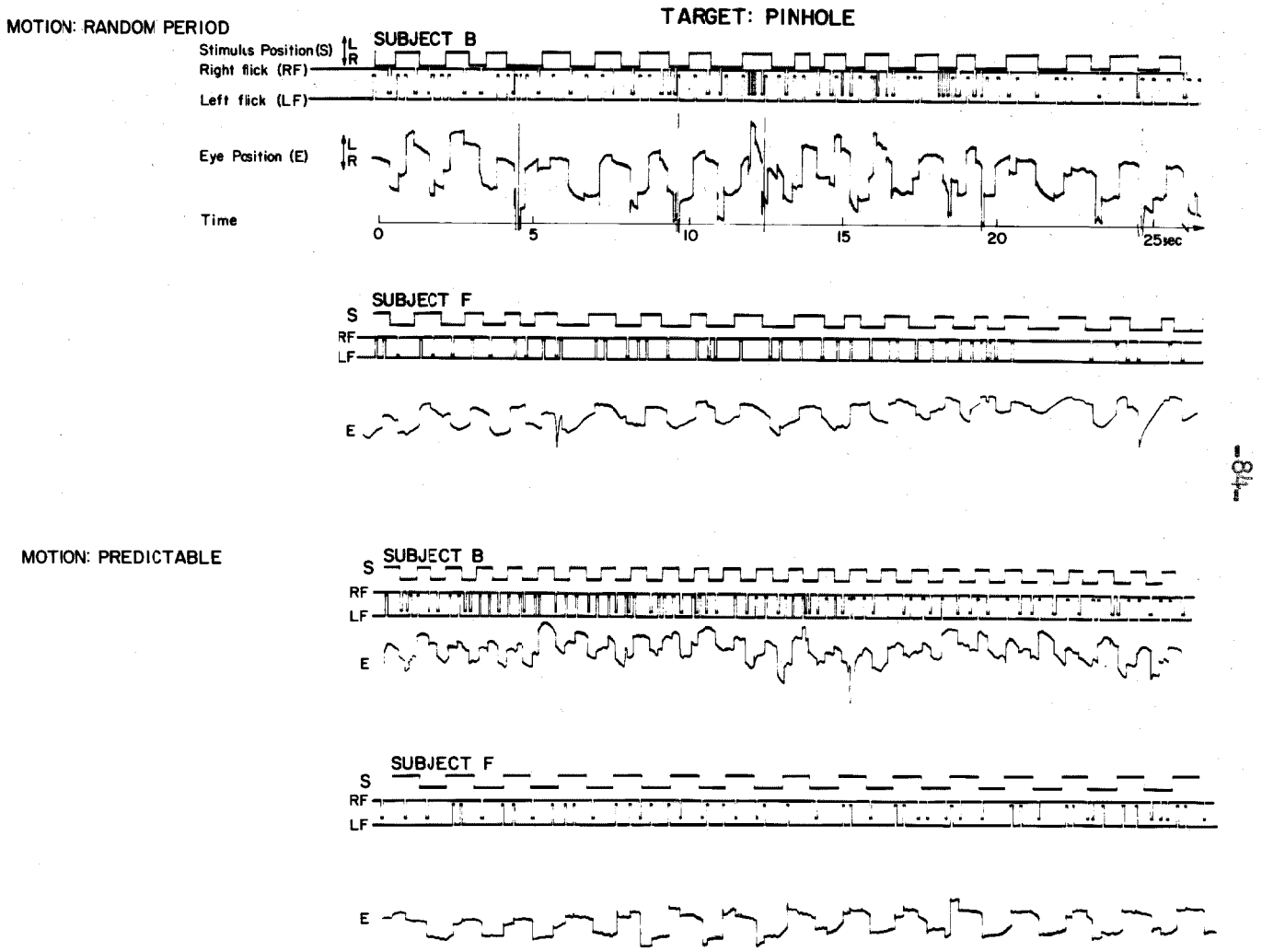

Fig. 5.3 - Sample recordings from square wave following experiments.

accounted for up to 15 per cent of the responses determined by the criterion. This effect will be seen in the discussion of the results. The choice of this response criterion permitted the use of the flick detector to perform a first order data reduction, and the recording of only the flick detector outputs. This, in turn, represented a reduction factor on the order of 400 in the amount of data which had to be considered. It was felt that the great saving in computer expense justified the small loss in accuracy.

The data reduction for the full experimental course was performed on the digital computers. The pulses from both the stimulus and flick detectors were transmitted to the machines in the TOE mode. For each stimulus time, the processing program determined the time of occurrence of the nearest, properly directed saccade. From these data, it computed a response time defined as the time at which the saccade occurred less the time at which the stimulus step took place. Thus, if the response followed the stimulus, the response time was positive. The data for each run were stored by the computer in two ways. First, the mean response time for each stimulus period was computed and compiled for the set of runs performed on any given day. Secondly, a histogram showing the frequency of occurrence of each response time was compiled for each run.

When the data were complete for a given subject, the average response times from each run or set of runs were plotted as a function of stimulus period (stimulus period in the unpredictable runs being defined as the inter-step time immediately preceding the stimulus step in question). These data points, as will be seen later, showed the general character of the results, but were sufficiently scattered as to make hand-fitting of a line to them risky. In order to avoid subjective effects in these curves, they were fitted with the least-squares technique described in Appendix III. To this end, fourth-order polynomials were chosen to represent the data, as it

was clear that the function was even, but it was further felt that second-order polynomials might not display fine structure in the data. In many cases, however, the true order of the data was lower than fourth-order. In such an instance, the least squares method attaches undue weight to the data points at the extremes of the range; hence, the reliability of the fitted curve falls off at the ends. As a result, the curves to be presented later have been plotted only over the central 80 per cent of the data range, although all the raw data points are included to permit judgement of the fit.

Results

Individual runs. - The first form of data presentation to be considered is the histograms of response time occurrences which were compiled for each experimental run. Examples of these histograms are given for three subjects in both experimental conditions in Fig. 5.4. Histograms a and b show the typical results from tracking unpredictable steps. Here, the majority of the samples are clustered in a distribution in the neighborhood of 200 msec. The comparable histogram, c, for subject B shows a somewhat different form. There is still a hump in the distribution at 200 msec, but there is an appreciable number of responses at all other values; the reason for this will be discussed later.

The second set of histograms, d through f, shows the response times resulting from a predictable stimulus period of 750 msec. Histograms d and f, for subjects F and B, show the typical form observed in predictive tracking. In these plots, the majority of the response times are contained in a broad distribution centered in the neighborhood of -100 msec, and the rest of the responses are located in a smaller peak at about 200 msec. These distributions within each histogram were readily identifiable in all the predictable runs performed on these two subjects. The smaller distribution is located at the same response time as the primary distribution in the unpredic-

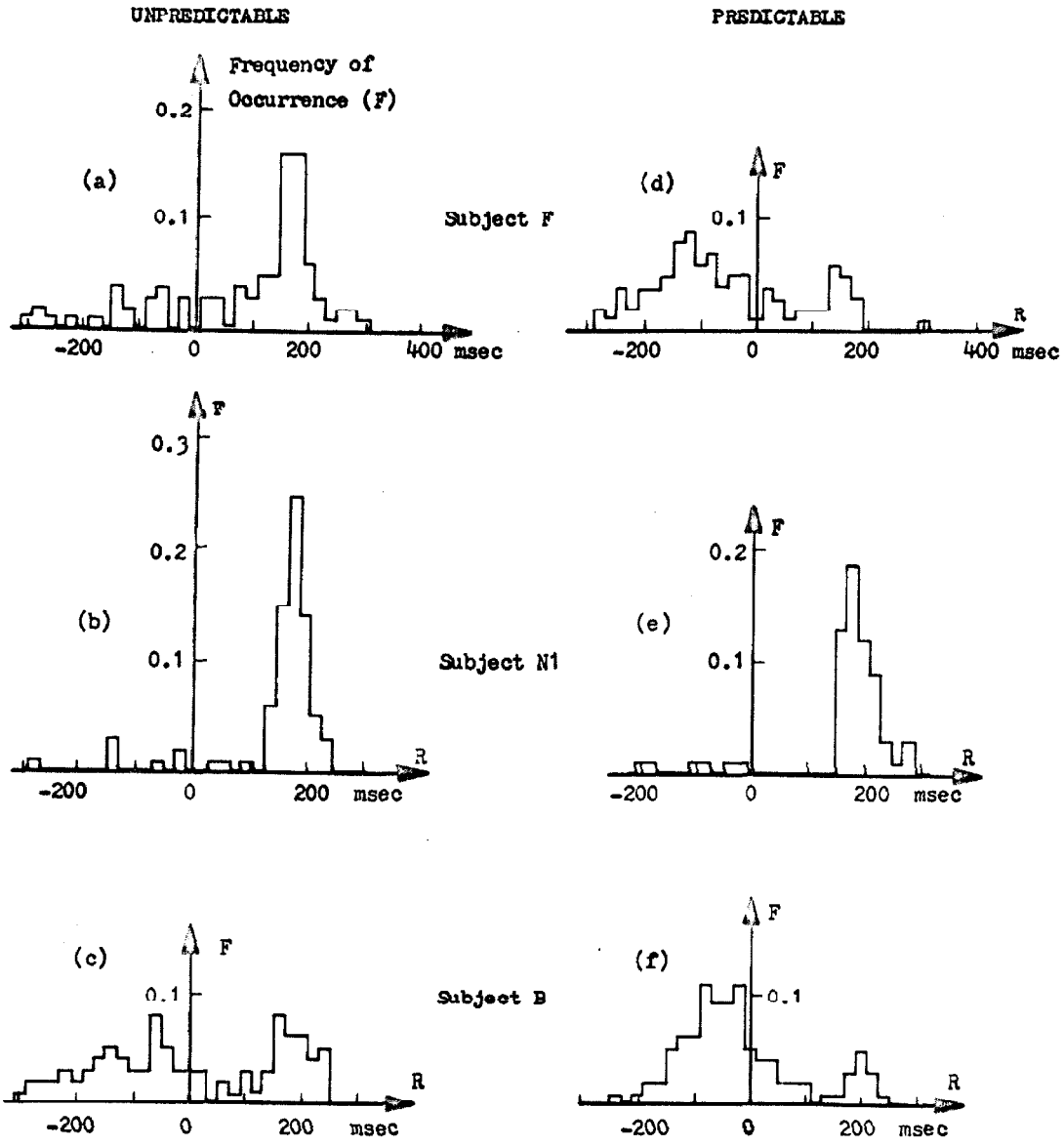

Figure 5.4 - Histograms of response times from individual runs of the square wave following experiments. Predictable stimulus period is 750 msec.

table experiments; thus it represents responses for which the subject has failed to anticipate the stimulus, and has responded at a normal reaction time after observing the step. As a result, this sub-distribution will be called the reactive distribution. The larger distribution, centered around a response time which occurs before the target step, is the result of prediction, and will be referred to as the predictive distribution.

Finally, attention should be drawn to the predictable histogram, e, for subject N1. The predictive sub-distribution is totally lacking in this histogram, and this subject, who was presented a somewhat abbreviated course of experiments, never showed signs of predicting the stimulus. The implication is clear. There is undoubtedly learning involved in this task, a fact not brought out in previous reports of this form of tracking. Subjects B and F gained considerable experience while performing the pilot experiments, but apparently the shorter experimental course used on N1 did not provide sufficient training. Further discussion on this learning process will be given in the conclusion of this chapter.

Predictive tracking. - The primary result of this experiment is contained in Fig. 5.5, which shows the mean response times from individual experimental runs plotted as a function of the stimulus period. The curve represents the fourth-order least-squares fit made to these data. The range of periods shown, from 500 to 1100 msec, represents the region in which the predictive effect was most apparent and for a considerable portion of this range, the average response actually precedes the stimulus.

Response times to unpredictable stimuli. - The plots of mean response times as a function of the stimulus period during the unpredictable runs are given in Figures 5.6 and 5.7 for the three subjects. The results for subjects F and N1, Fig. 5.6, are straightforward. Although the fitting technique produced minor variations in each curve, the most that can be said of these curves is that they demonstrate fairly constant response time to these stimuli.

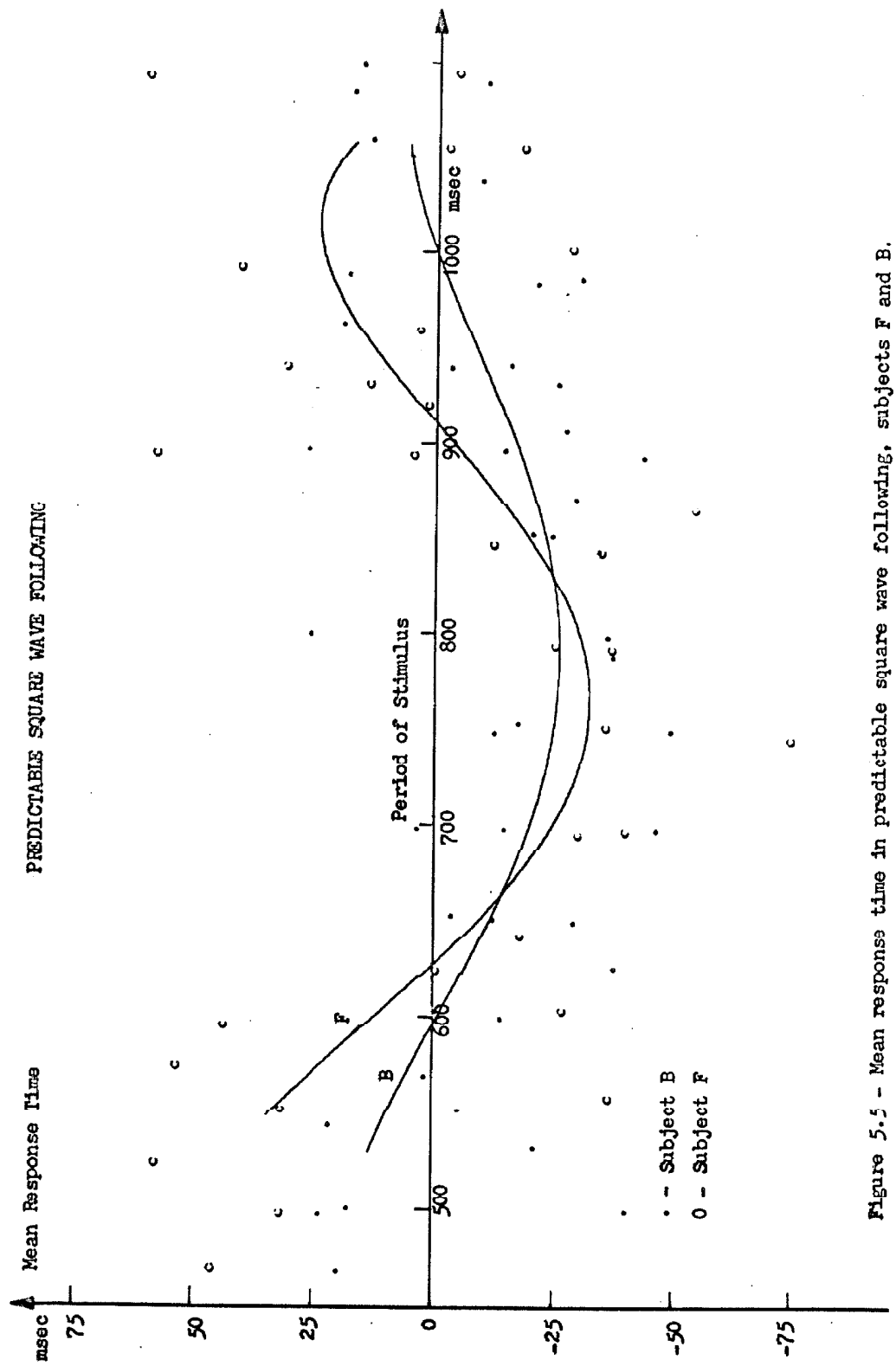

Figure 5.5 - Mean response time in predictable square wave following, subjects F and B.

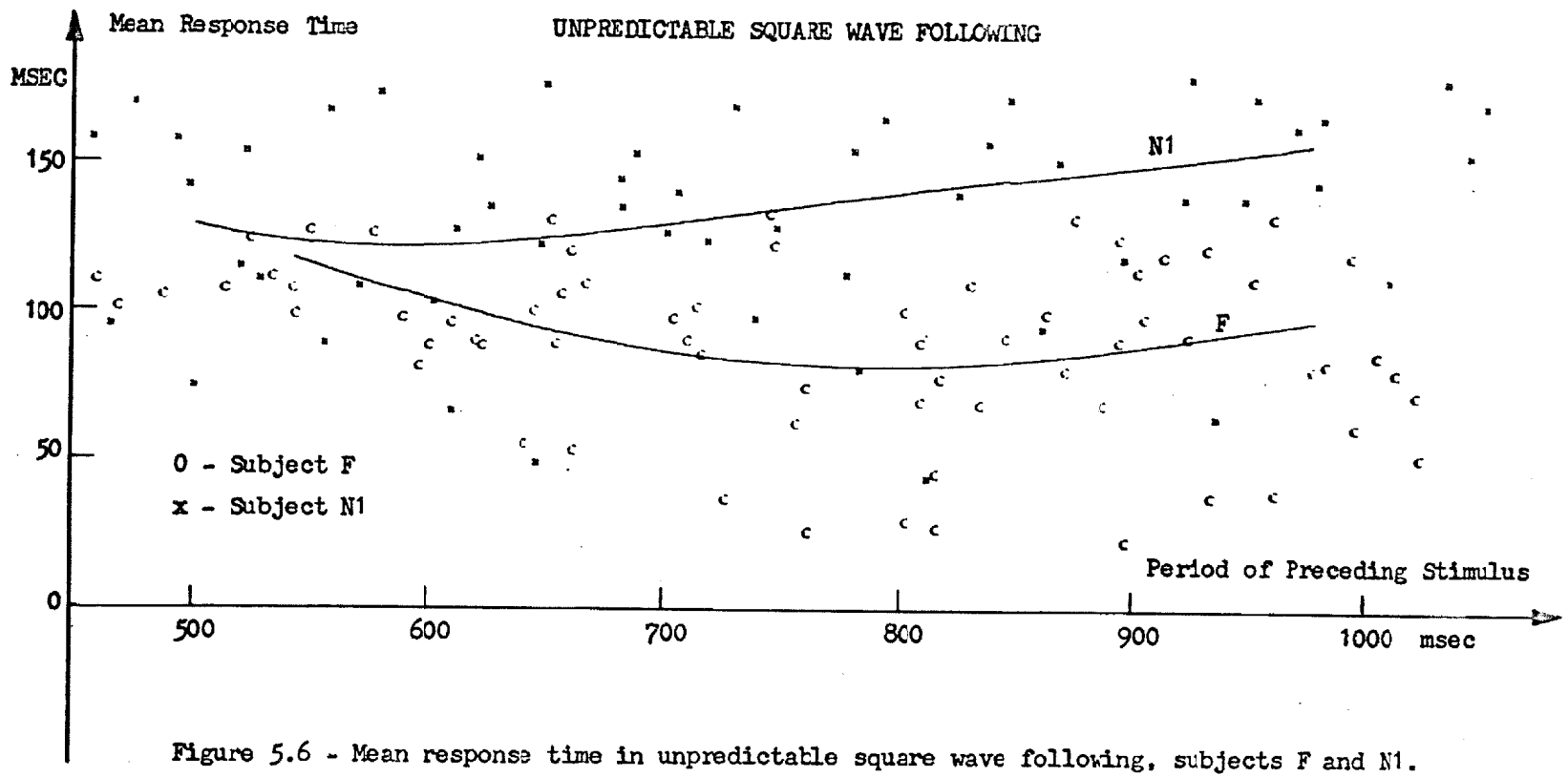

Figure 5.6 - Mean response time in unpredictable square wave following, subjects F and N1.

The equivalent curve for subject B, Fig. 5.7, has a completely different character, as the average response precedes the stimulus for stimulus separations greater than about 730 msec. This effect is puzzling, and several explanations can be tested. The first of these, clearly, is that the subject learned the time course of the discs. This would seem unlikely as the correspondence between Fig. 5.7, and the curve for his predictable response in Fig. 5.5 is poor. An alternative explanation might be that the effect is due to spontaneous flicks being judged as the response under the criterion established earlier, but the pilot experiments which were quoted above belie this conjecture. The final explanation is the one that the author feels is most plausible. This is that the subject soon established the average period of the unpredictable stimuli, 750 msec, and attempted to predict on that basis. This conjecture is partially supported by the linear nature of the curve in Fig. 5.7, and by the fact that it crosses the abscissa in the neighborhood of 750 msec. A test of this hypothesis was performed by altering the average period to one sec, and performing similar experiments on the subject. The results are shown in Fig. 5.8. A tendency towards prediction is seen, and the curve strikes a minimum at approximately 1150 msec. The strong predictive effect seen in Fig. 5.7 is lacking. This result, however, is not unexpected; the fact that the linear curve in Fig. 5.7 does not have unity slope indicates that this form of prediction is ineffective, and that many of the responses actually occur at a normal reaction time. The final piece of evidence on this hypothesis is contained in histograms c and f of Fig. 5.4, comparing the predictable and unpredictable runs for this subject. While histogram c does show the reactive peak, the sharp formation of a predictive peak is lacking; rather, the rest of the samples appear to be fairly uniformly distributed. It will be shown later that the predictive distribution is a definite manifestation of the predictive mechanisms. Thus, the lack of this peak in histogram c provides further evidence

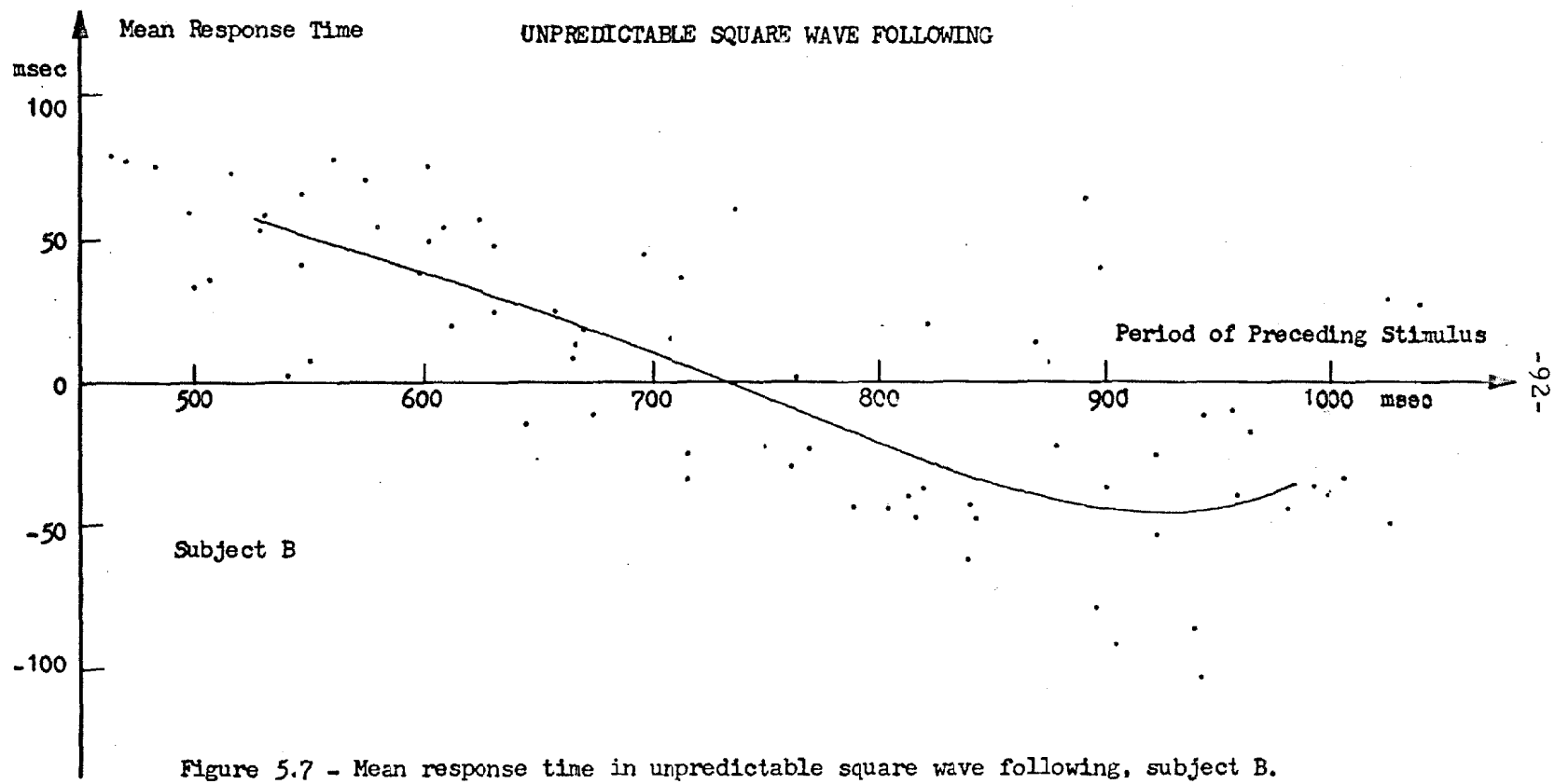

Figure 5.7 - Mean response time in unpredictable square wave following, subject B.

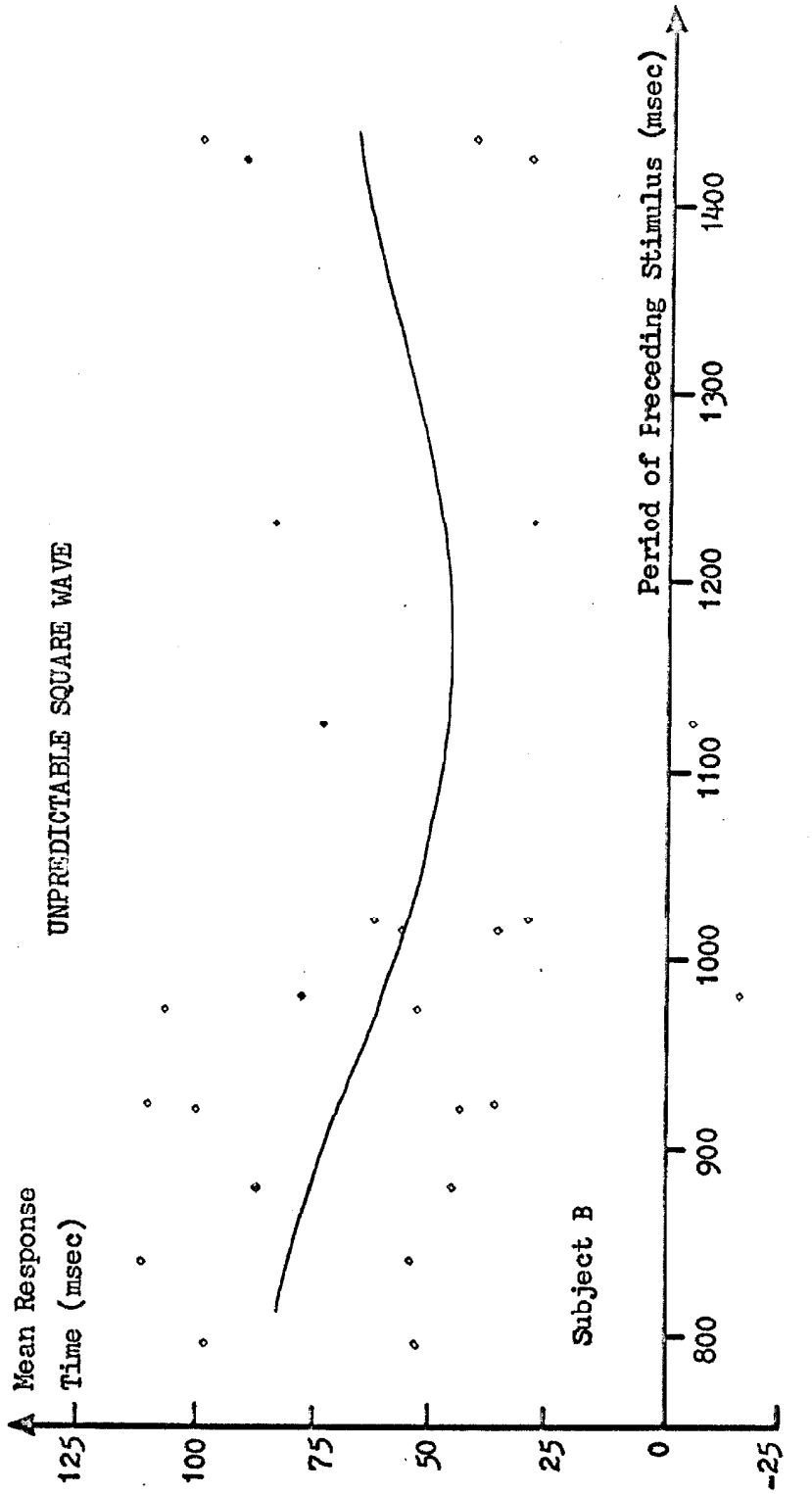

Figure 5.8 - Response to unpredictable square wave where mean stimulus period is 1000 msec.

that learning of the precise stimulus timing did not take place. The uniform distribution that is seen is compatible, however, with the hypothesis that he learned the average period.

The purpose of the unpredictable experiment was to obtain a measure of the effects of unpredictability and then to apply this to the predictable results, in order to show when anticipation of that form of stimulus failed. Subjects F and N1 show the unpredictability effect well; in the unpredictable runs, the major peak of the distribution always occurs in the neighborhood of 200 msec, a fact that Young's sampled data model would predict. As a result, the two sub-distributions in the predictable histograms can be allotted to two different sub-systems in the saccade control loop. The predictive sub-distribution is the result of the predicting loop being investigated, but at times, even when tracking a predictable stimulus, this predicting loop fails to function. In such instances, the response is generated via the normal path of the saccadic system, creating the reactive sub-distribution in the neighborhood of 200 msec.

Expanded Data Range

The results presented in the preceding section are in agreement with those determined by earlier researchers (14, 56), but these results provide little insight into the functioning of the predictor, or into the failure of this system at both the shorter and longer stimulus periods. In order to make a determination of this sort, the data range was extended to include larger stimulus separations, and a more detailed analysis was initiated. The results of these efforts are presented in this section.

Full data range. -In order to characterize the failure of the predictive mechanism at the longer stimulus periods, it was necessary to extend the range of stimulus periods out to four sec. To this end, six stimulus periods in the range from one to four sec were selected, and a full experimental course based on these periods was

presented to subjects B and F. The results from these experiments are presented in Fig. 5.9, along with the results reported earlier. The curves which are fitted to these data are separated into two segments. The lower section from 500 to 1000 msec, is similar to the curve of Fig. 5.5. An independent fourth-order fit has been made to the data points above the one second level. In order to assure that the two curves would join approximately, they were fitted to overlapping segments of data points. The choice of two separate curves was based on two reasons. First, the relative sparsity of data points in the region above one sec results in a single fourth-order fit being most inaccurate in this range. Secondly, if the points are weighted so as to overcome this problem, the resultant curve does not reveal the sharp predictive effect in the 650 to 900 msec range, as it is seen in Fig. 5.5.

Little comment is needed on Fig. 5.9, except to note that the mean response time appears to be asymptotic to a value on the order of 150 msec for the two subjects as the period is made longer; indicating that even though the situation is predictable, the subject is unable to exploit this fact at the longer stimulus intervals. The data were not extended to periods less than 500 msec, because, as will be seen, the data at hand are sufficient to specify the apparent lack of anticipation at short periods.

Integrated histograms. - The histograms of Fig. 5.4 indicated that the predictive mechanisms could be deduced from the two sub-distributions. In order to obtain a measure of these distributions, the individual histograms were collated to provide distributions with greater numbers of samples. The individual predictive and reactive distributions were segregated during this collation. The separation of these distributions was done for each of the smaller histograms before collation. In the majority of the cases, this separation was straightforward, as the distributions contained a zero between the two sub-distributions; where this was

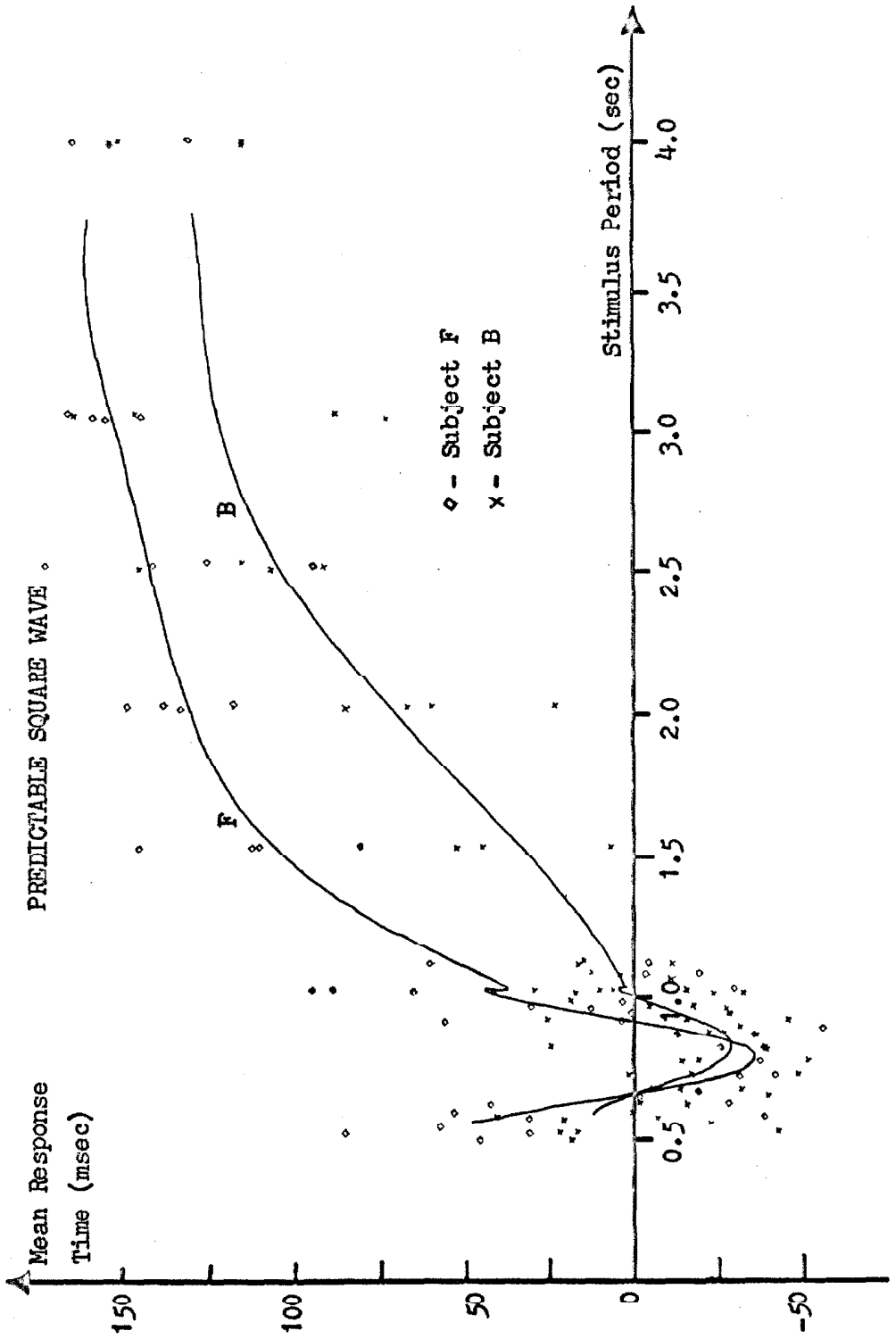

Figure 5.9 - Responses in square wave following, for stimulus periods from 0.5 to 4.0 sec.

not the case, a subjective judgement was made.

Figures 5.10 and 5.11 show six representative collated histograms for subjects B and F, respectively. These are chosen at equally spaced intervals over the range where prediction is most effective. The vertical axes in these figures represent the number of samples at each response time, and the total number of samples in the distribution is provided to permit correlation with the frequency of occurrence. In addition to the basic information contained in the distributions, three arrows have been plotted above these histograms. These represent the mean value of the predictive distribution, T_p, the mean value of the total histogram (mean response time), T_m, and the mean value of the reactive histogram, T_r. The general trend of the predictive mechanism can be deduced directly from these markers. First, the mean response time, T_m, drops with decreasing stimulus period to a minimum in the neighborhood of 800 msec after which T_m again increases; this has already been seen in the curves presented earlier. The cause of this shift, however, is now apparent. The larger mean response times at the longer periods are due to the appearance of a greater percentage of the points in the reactive distribution, while the response time change at shorter periods is due to a shift in position of the predictive distribution. These effects can be more easily seen in the data presented in the following section.

Distribution characteristics.-From the data just presented it would appear that the overall response time histograms can best be characterized by five parameters. These are the mean and deviation of the predictive sub-distribution, T_p and S_p; the mean and deviation of the reactive distributions, T_r and S_r; and the proportion of the total number of samples which is encompassed by the predictive distribution, π.

Of the five parameters, three can be seen to be constant functions of the stimulus period. These three, T_r, S_r, and S_p, are

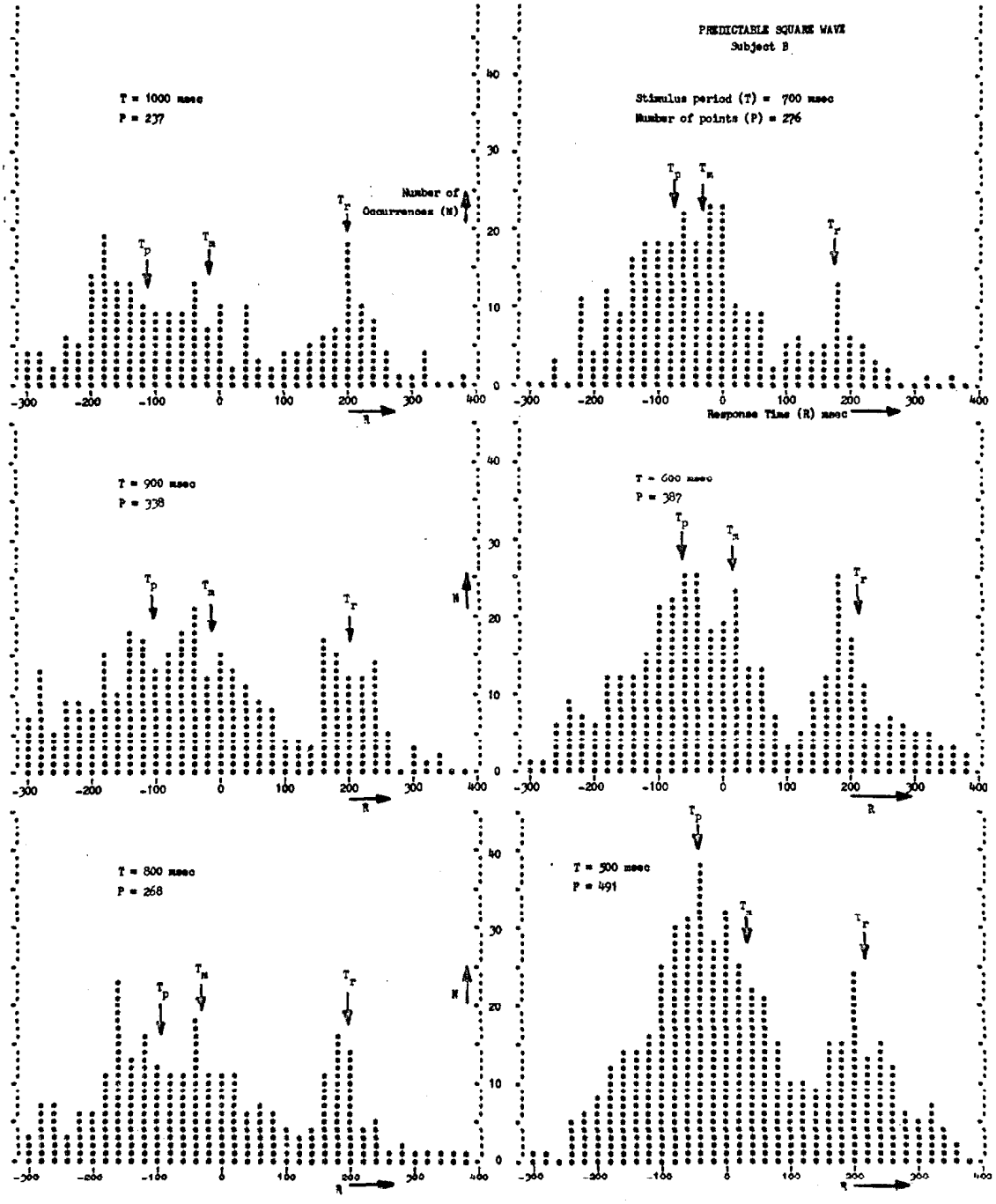

Fig. 5.10 - Collated histograms of response times for subject B in predictable square wave following. Three parameters are indicated by arrows: T_p, mean of predictive sub-distribution; T_m, mean of whole histogram; and T_r, mean of reactive sub-distribution.

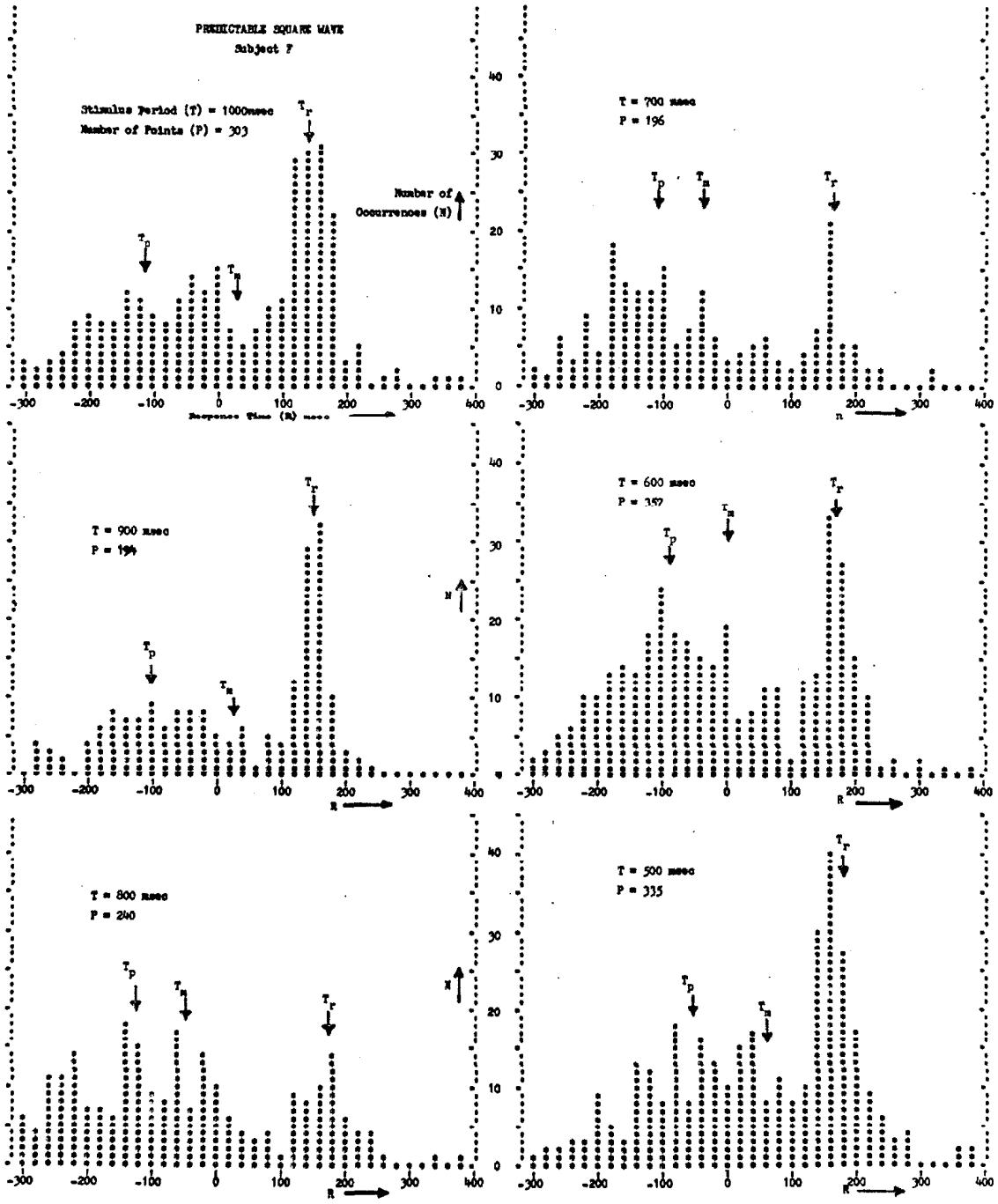

Fig. 5.11 - Collated histograms of response times for subject F in predictable square wave following. Three parameters are indicated by arrows: T_p, mean of predictive sub-distribution; T_m, mean of whole histograms; and T_r, mean of reactive sub-distribution.

plotted as a function of the stimulus period in Fig. 5.12, for both subjects. The constancy of these parameters is apparent from those plots, and the straight lines drawn through them represent the average values in each case. It should be noted that the data for the reactive distribution are not extended beyond the 1100 msec stimulus point, either in Fig. 5.12 c, or in the figures to follow. The reason for this is simply that the smaller experimental course, and the decreasing number of points in this sub-distribution combine to produce too few samples in this region to permit a reasonable determination of these parameters.

The fourth parameter to be considered is the mean value of the predictive distribution, T_p. This parameter is plotted for the two subjects in Fig. 5.13. These plots clearly contain two regimes, a rising portion for stimulus periods less than 750 msec. and a relatively constant section above that value. Although there are several mathematical functions which could be fitted to these curves- such as hyperbolae or exponentials- it is felt that the data do not justify a determination of such a form. As a result, they have been characterized by two straight line segments. No implication is intended, however, that this is the precise mathematical form of the curves.

The proportion of samples contained in the predictive distribution, π, is the final parameter that was extracted from the histograms. and is plotted in Fig. 5.14. The curves drawn through these points simply represent the best reasonable fit to the data. These consist of a constant portion at stimulus periods less than about 800 msec, and a decreasing segment out to a zero asymptote for larger periods. It will be noted that both curves are drawn asymptotic to zero, whereas the values at four sec are greater than 0.1 for both subjects. This rather arbitrary step has been taken because it is felt that these points represent an artifact in the data arising from the response criterion cited earlier, and that they are

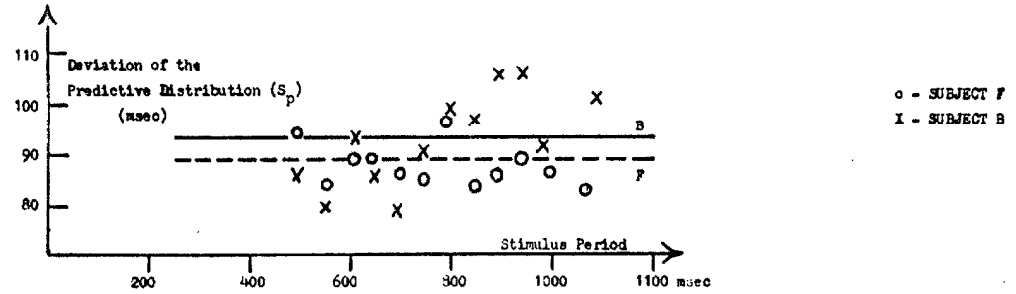

Fig. 5.12c - Deviation of the predictive sub-distribution as a function of stimulus period.

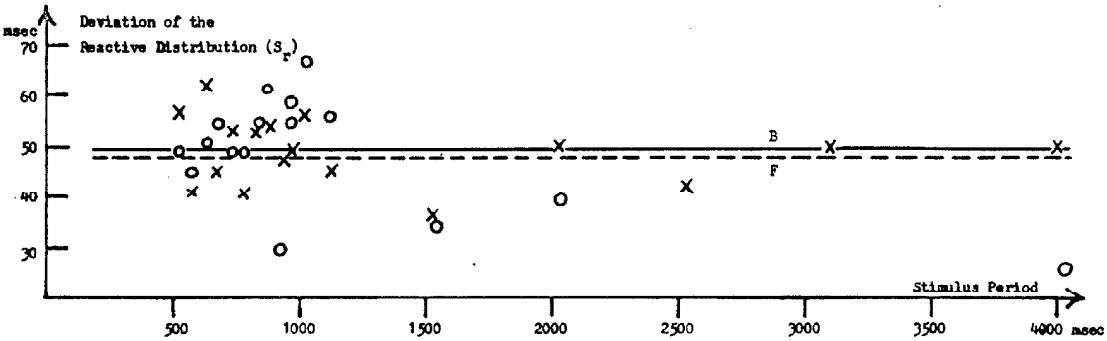

Fig. 5.12b - Deviation of the reactive sub-distribution as a function of stimulus period.

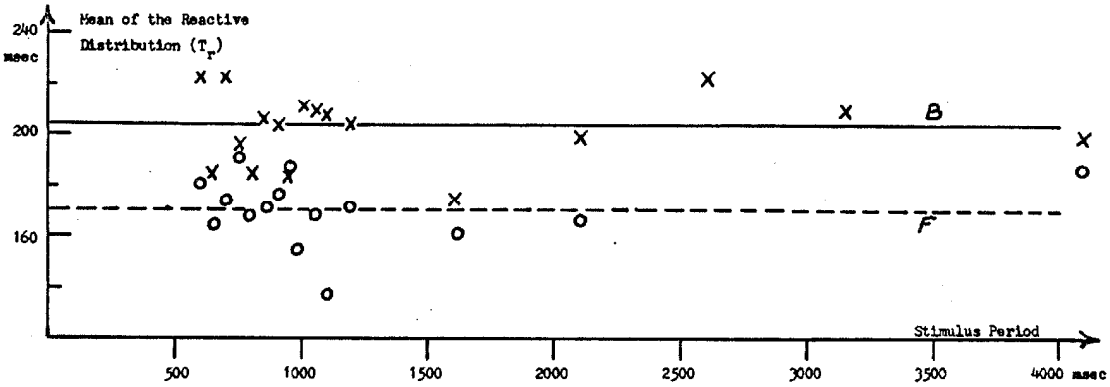

Fig. 5.12a - Mean response time of reactive sub-distribution as a function of stimulus period.

Figure 5.12 - Three parameters (T_r, S_r, & S_p) of predictive responses plotted as a function of predictable stimulus period. Plots reveal no apparent functional dependence on the stimulus period.

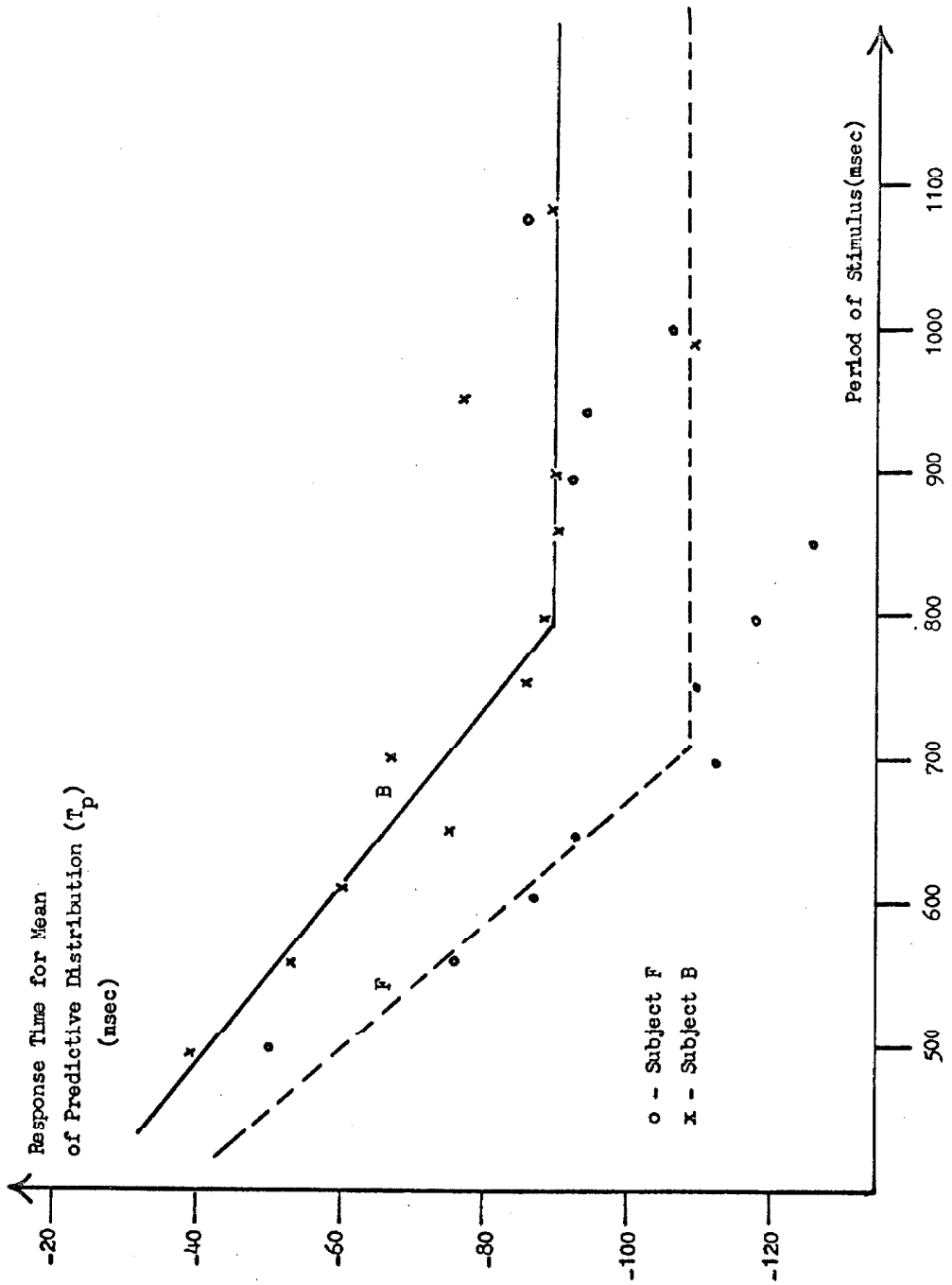

Figure 5.13 - Mean response time of the predictive sub-distribution as a function of stimulus period.

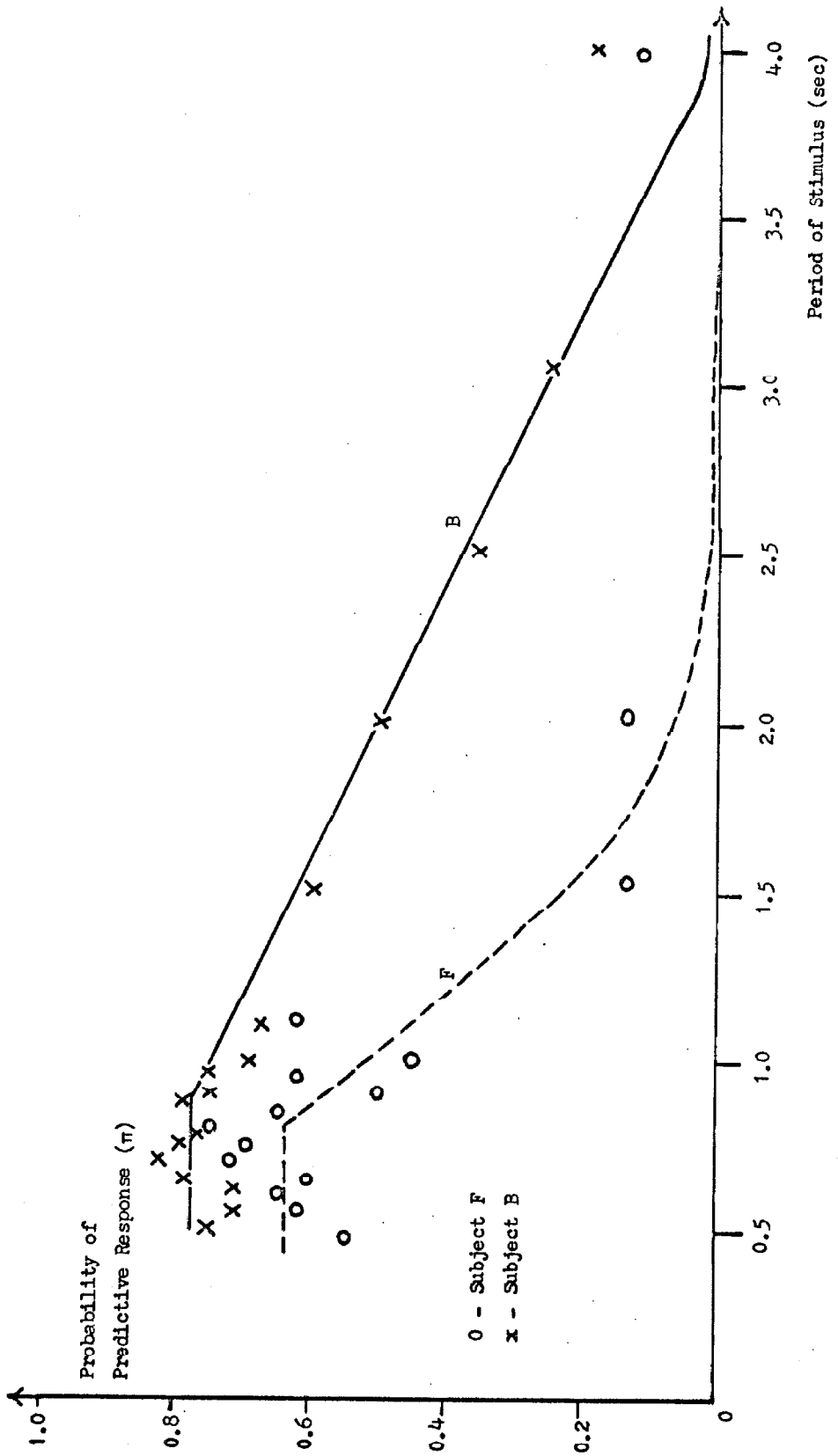

Figure 5.14 - Probability that the predictive mechanism will generate a response saccade, as a function of the stimulus period.

probably representative of spontaneous flicks being detected as responses. Spontaneous flicks will be considered in detail in Chapter VIII, and it will be shown that they serve to prevent retinal adaptation. The response saccades are equally effective in this function, however, so that the rate of generation of spontaneous flicks is probably reduced when many responses are being produced. The result is that the effect of the spontaneous flicks on the measured response in this experiment is not manifested until fairly low stimulus frequencies are reached.

The Model

The data presented above clearly indicate that a linear model of the form used in previous approximations to the eye positioning system can not represent the mechanism in effect here. Rather, the continuous mean response time changes which have been measured are simply the result of the averaging of two separate stochastic processes, true prediction and simple reaction. As a result, the model must include both of these control paths for the saccade loop.

The model chosen is shown in Fig. 5.15. Although this model will be modified in the conclusion to the thesis, Fig. 5.15 represents the basic elements in their simplest form. As presented, the model consists of a series of smaller units, each of which performs a separate function and is characterized by an individual mean operation time, although there are insufficient experimental parameters to specify all of these operation times.

Pattern analyzer. -The predictive function in this model is served by two units. The first of these is the "pattern analyzer" which generates the "required position" signals for the predictor once it has recognized the square wave, and determined its amplitude. While this recognition process is equally as important to the predictor as is the determination of the proper response time, this unit has been made subsidiary to the time determination, and its

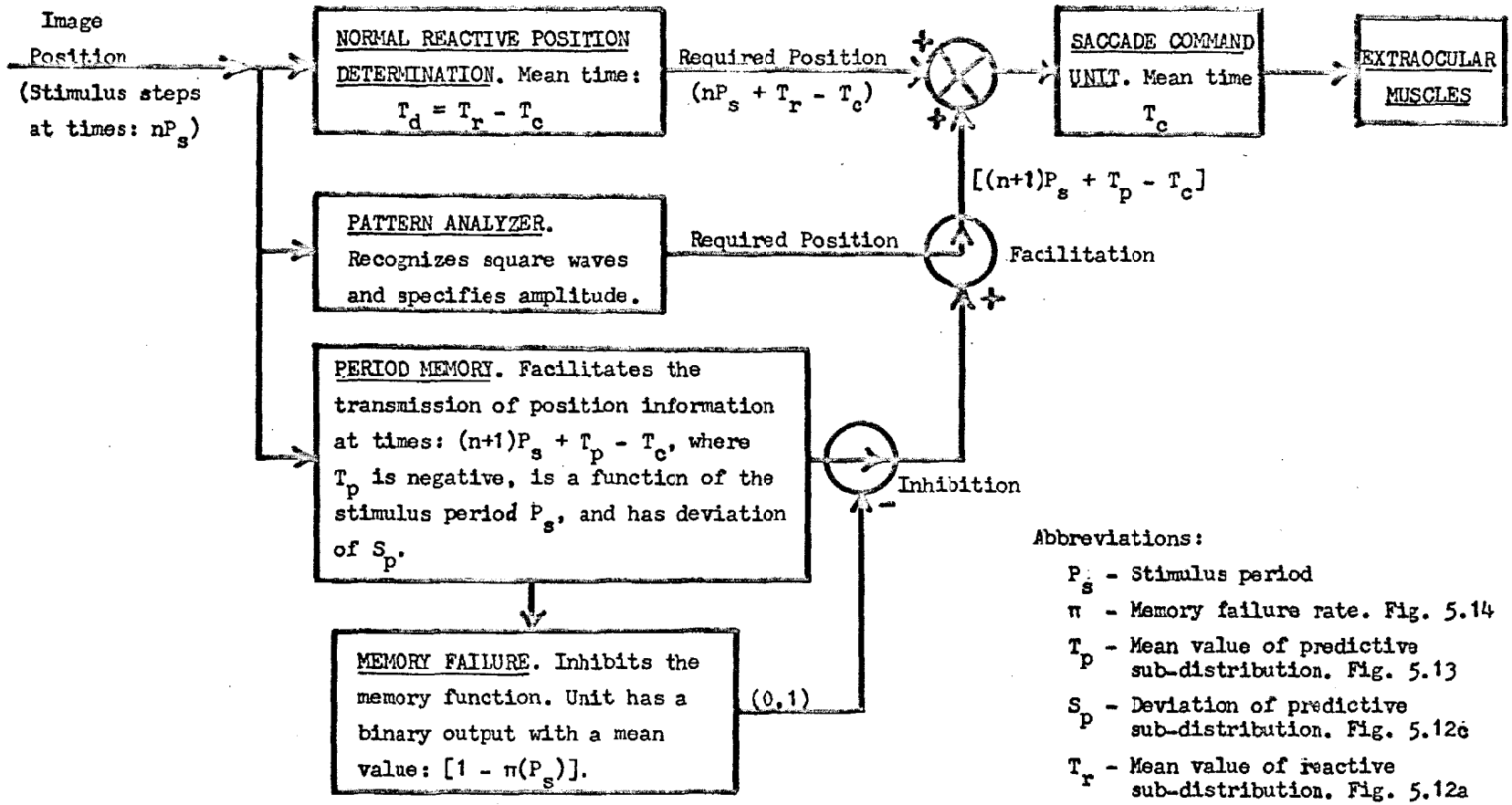

Figure 5.15 - Block diagram of proposed saccadic prediction model. Complete discussion of each unit is provided in text.

output, the required position information, is assumed to be correct at any given time. This output is only transmitted to the rest of the system, however, at times specified by the period memory.

Period Memory. -The period memory is truly the heart of the predictive mechanism in the form which has been measured here. In order to be able to anticipate a subsequent stimulus step, the system must recognize and learn the basic period of the stimulus function. The assumption is that once the stimulus time course has been learned, this unit facilitates the transmission of the position information at such a time as to produce a saccade which will correspond to a sample in the predictive distribution. Once the memory facilitates this transmission, the information must still pass through the saccade command unit which effects the saccade a mean time T_c later. As a result, the memory output must occur at a time $(T_p - T_c)$ before the next stimulus step in order that a mean predictive time of T_p as measured from Fig. 5.13 can result. The deviation of this prediction is assumed to be the same as deviation for the distributions, S_p. Thus this unit contains the primary characteristics necessary to produce the predictive sub-distributions seen in Figures 5.10 and 5.11.

The overall response histograms, however, indicate that simple reactive responses also occur during this following regime. The implication that must be drawn, then, is that the memory unit fails periodically to perform its predictive function. The cause of such failures is not clear, but the effect is represented in the model by an inhibitory effect on the memory. The output of the inhibitory unit is assigned the binary value one for failure, and zero for success; the mean value of this output is $(1-\pi(P_s))$, where π is the proportion of samples in the predictive distribution for any given stimulus period, P_s, as measured from Fig. 5.14. The curves in this latter figure clearly indicate that the failure of this unit is a direct function of the length of the period that must be remembered.

In the description presented above, two effects of stimulus period are included - the functional dependences of T_p and π on this period. The assessment of these effects is best left to the final portions of this chapter where potential mechanisms are put forward.

Saccade command unit. -Once the information about the required eye position is passed on by the pattern analyzer and period memory, it passes through the saccade command unit which generates the signals to the extrocular muscles. The experiment performed here permits very little to be said about this unit, but it is considered further in Chapter VII. The important fact to be drawn from that analysis is that this unit is refractory for a period after a signal has passed through it. The effect of this is to block any saccades that the reactive unit might generate if a predictive saccade has been transmitted in response to the stimulus step. The mean response time of this unit, T_c, and the deviation of this time, S_c, can not be determined from the data available here, but the effect of this time has been included in the predictive loop.

Normal reactive path. -The normal reactive path included in this model is not properly a unit of the predictive loop. It has been seen, however, that the prediction system fails at times, and the responses on such occasions must be obtained through the normal saccadic response loop. As a result, the "position determination" unit that was included in the general model of Chapter IV has been included here as a parallel path. The mean time for this unit to function is $(T_r - T_c)$, with the result that the overall mean response time through this unit is simply T_r, the mean of the reactive subdistribution. Moreover, the deviation in mean times from this unit and the saccade command unit combine to produce the measured deviation S_r.

Model Response

The response characteristics of the model just described can be fairly simply summarized. The combination of the pattern

analyzer and the period memory unit generates signals which cause response saccades to occur at a mean response time of T_p, where T_p is a negative number, and is a function of the stimulus period P_s. This system, however, only succeeds with a frequency specified by the probability factor π, also a function of P_s. When failures occur, a response is elicited through the normal reactive channel at a mean response time T_r. The deviations from the means in the two paths are S_p and S_r, respectively. Thus the mean response time T_m that is measured by the experiment is simply given by the equation:

$$T_m = \pi \cdot T_p + (1 - \pi) \cdot T_r,$$

where the functional dependences of π and T_p on the stimulus period are determined from Figures 5.14 and 5.13, respectively.

The mean response time curves that are predicted from this model are shown in Figures 5.16 and 5.17, for subject B and F, respectively. Also plotted in these figures are the least-squares curves shown in Fig. 5.9, and the mean response times determined from the histogram collation. These are provided for comparison with the model. The major deviation of these curves from the measured responses occurs at the long stimulus periods, where the apparent asymptotes of the two curves are different. This effect is a direct reflection of the curve fit which was used in Fig. 5.14, where the asymptotic value of π was forced to zero even though spontaneous flicks maintained an unrealistic level in the experimental data.

Conclusion

Up to this point, the work presented in this chapter represents the measurement of an effect, and the generation of a model which fits those measurements. This model is useless, however, if portions of it cannot be justified, and some potential mechanisms which might perform the assigned tasks are not offered. In the concluding section of this chapter, three major characteristics of the system are discussed - the form of the memory unit, and the source of its

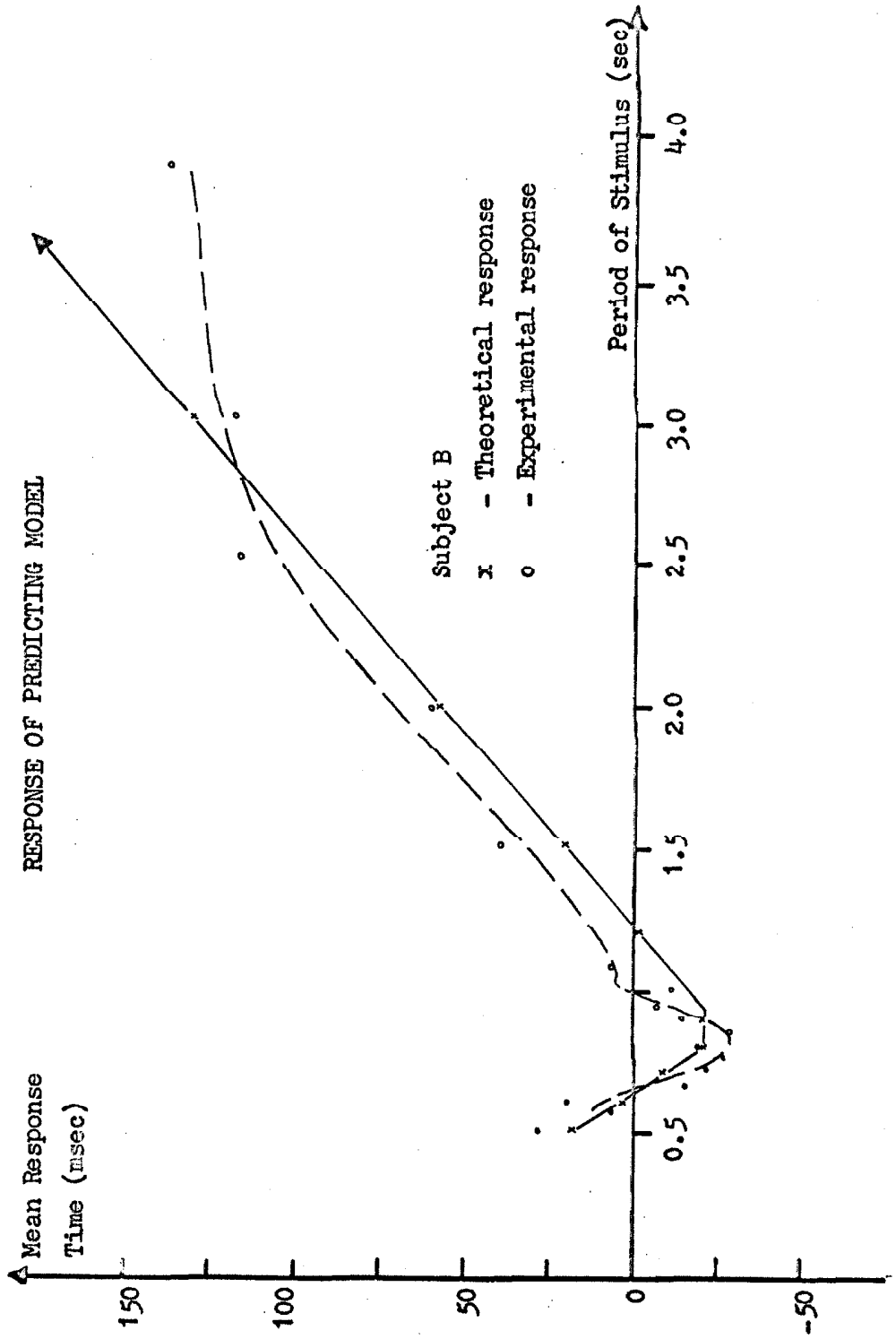

Figure 5.16 - Comparison of model and experimental responses for subject B.

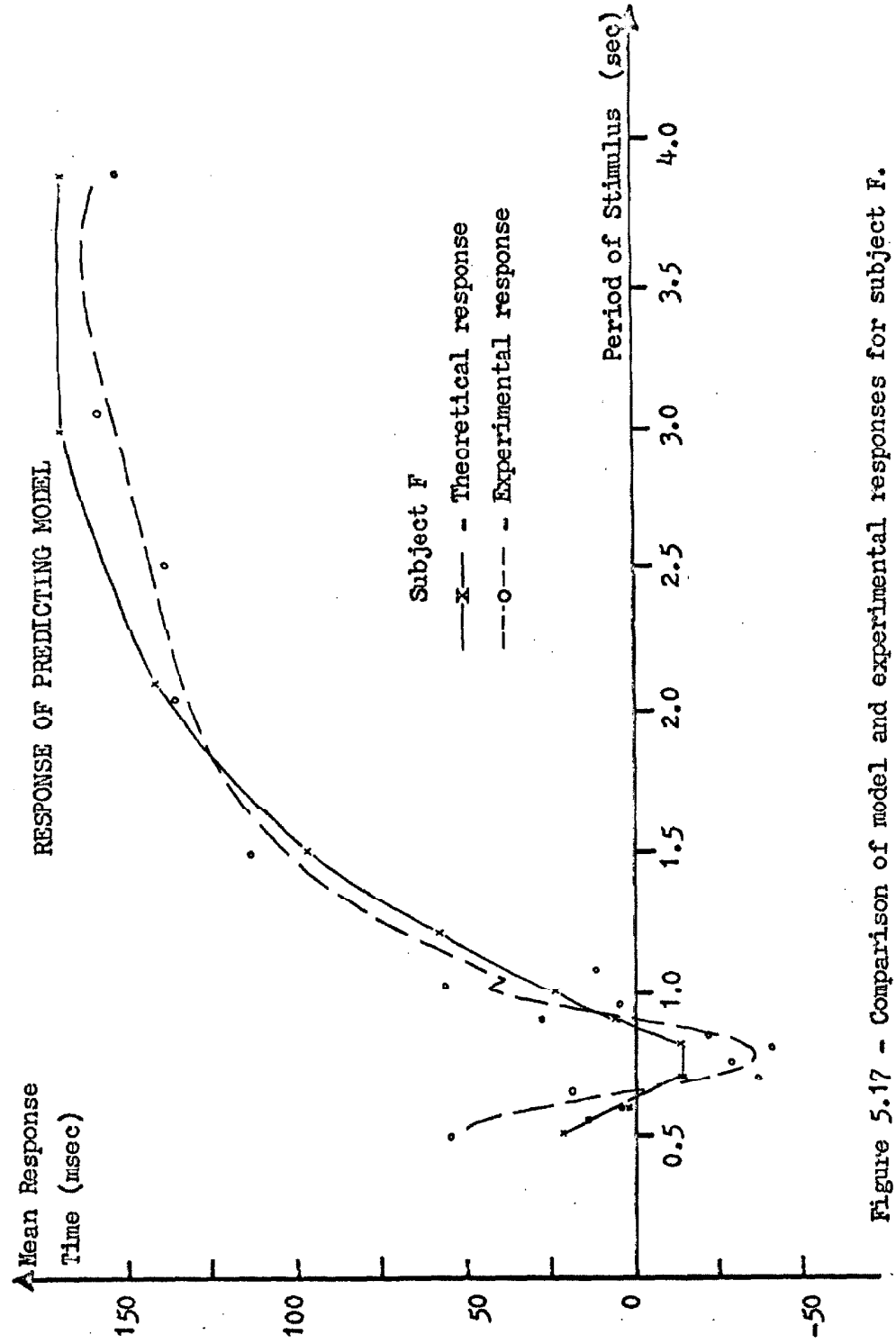

Figure 5.17 - Comparison of model and experimental responses for subject F.

failure; the cause of the apparent functional dependence between T_p and the stimulus period; and the factors which cause the mean predictive responses to lead the stimulus.

Memory mechanisms. -In this section, two memory mechanisms will be postulated. This speculation is intended to serve a dual purpose. First, it shows the feasibility of building such units out of neural elements, although the details of such a neural construction are entirely beyond the scope of this thesis. Secondly, it shows the form of the errors which might arise from any system utilizing neural elements.

The primary function of the memory unit, as defined earlier, is to produce an output signal a fixed time delay after the preceding stimulus step. The memory process in this case is involved with establishing a time delay of the appropriate length. One method of realizing this function might be the establishment of a pulse delay line whose length is determined by the stimulus period. The transmission rate of pulses along axons, and the pulse delay at the synapse are relatively constant for any given neuron; thus it would be possible to establish a delay line of mean length $(P_s + T_p - T_c)$, and use this to transmit a pulse which is synchronized with the occurrence of a stimulus step; the arrival of this pulse at the end of the delay line could then initiate the response to the subsequent stimulus step. An alternative method might utilize an internal, high frequency oscillator (a spontaneously firing neuron), and a counter. The counter could be reset at each stimulus step occurrence, and then when the counter reached a value equivalent to $(P_s + T_p - T_c)$, the next response saccade could be elicited.

Although either of these two mechanism might serve the purposes of the memory unit, speculation as to the mechanisms which produce anticipation of the stimulus must be based on two of the measured experimental parameters, the failure rate, and the

deviation of predictive responses. The curve of Fig. 5.14, shows that the failure rate of this unit is constant at low stimulus periods, but increases with increasing stimulus periods, eventually becoming asymptotic to 100 per cent. The deviation of the predictive response times does not appear, from Fig. 5.12c, to be a function of the time course, however. The two mechanisms which have been postulated do not fulfill the latter criterion. If one assumes that the basic neural elements of each method respond with only a mean value, then the deviation of these units from that mean will be reflected in the result. In the case of the delay line, random variations in the mean pulse delay time will produce a deviation in the output time that is proportional to the square root of the number of elements involved, and, therefore, also proportional to the square root of the stimulus time. The oscillator-counter system is even worse in this sense, as a slow drift in the frequency of the oscillator, will result in an error that is proportional to the stimulus period.

The lack of functional variations in the experimental results implies a far more sophisticated mechanism than either of the two proposed. Moreover, neither of these accounts for the failure rate that is observed. The hypothesis of a confidence test in this unit can account for both effects. Under this hypothesis two memory units, of either type, are assumed to exist in parallel. The output of one of these units is not used, however, unless the second unit also produces an output signal within a specified interval of time. The resultant distribution of output times is the conditional probability that both units agree within the specified time interval. The assessment of the distribution which results from such a test is difficult, as its deviation is a dual function of the individual deviations and the selected confidence interval, and is more closely related to the smaller of these two values. Nevertheless, the fact that the predictive unit continues to fail even at short stimulus periods, and that the deviation of the predictive times is relatively constant with stimulus

period, indicates that such a mechanism exists, and that the established criterion is smaller than the deviations of the parallel delay mechanisms.

Period learning. -Any mechanism which might be proposed including those suggested above, must be predicated on the ability of the system to learn the stimulus period, and this learning process will clearly require the assessment of several cycles of the stimulus. In order to test the duration of this learning, several experiments were attempted. These included simple presentation of predictable stimuli, interspersal of predictable and unpredictable runs at random, and the mixing of predictable and unpredictable segments within a single run. The results of the first test, which was entirely parallel to the experimental technique used earlier, were straightforward. A sample run is shown in Fig. 5.18, in which the mean response time obtained from ten trials, is plotted for each stimulus step in the sequence. The change in response times which occurs between the sixth and seventh steps is a clear indication that the stimulus period has been learned. Similar results were obtained for subject F.

The important fact, however, is that no such learning was apparent in the other forms of presentation for less than 20 stimulus steps. When predictable stimuli were mixed at random with the unpredictable steps, the subjects reported that they were only able to determine which form was being presented by the process of elimination. They could detect the lack of unpredictable steps, but could not recognize predictable steps unless they were apprised ahead of time of the type of stimulus being used. Thus, precognition of the predictable nature of the stimulus would appear to be prerequisite of the system operation.

Dependence of T_p on stimulus period. -One important aspect of the model is the change in the time of occurrence of the predictive saccades as the stimulus period is reduced. In order to simplify the discussion earlier in this chapter, this relationship was

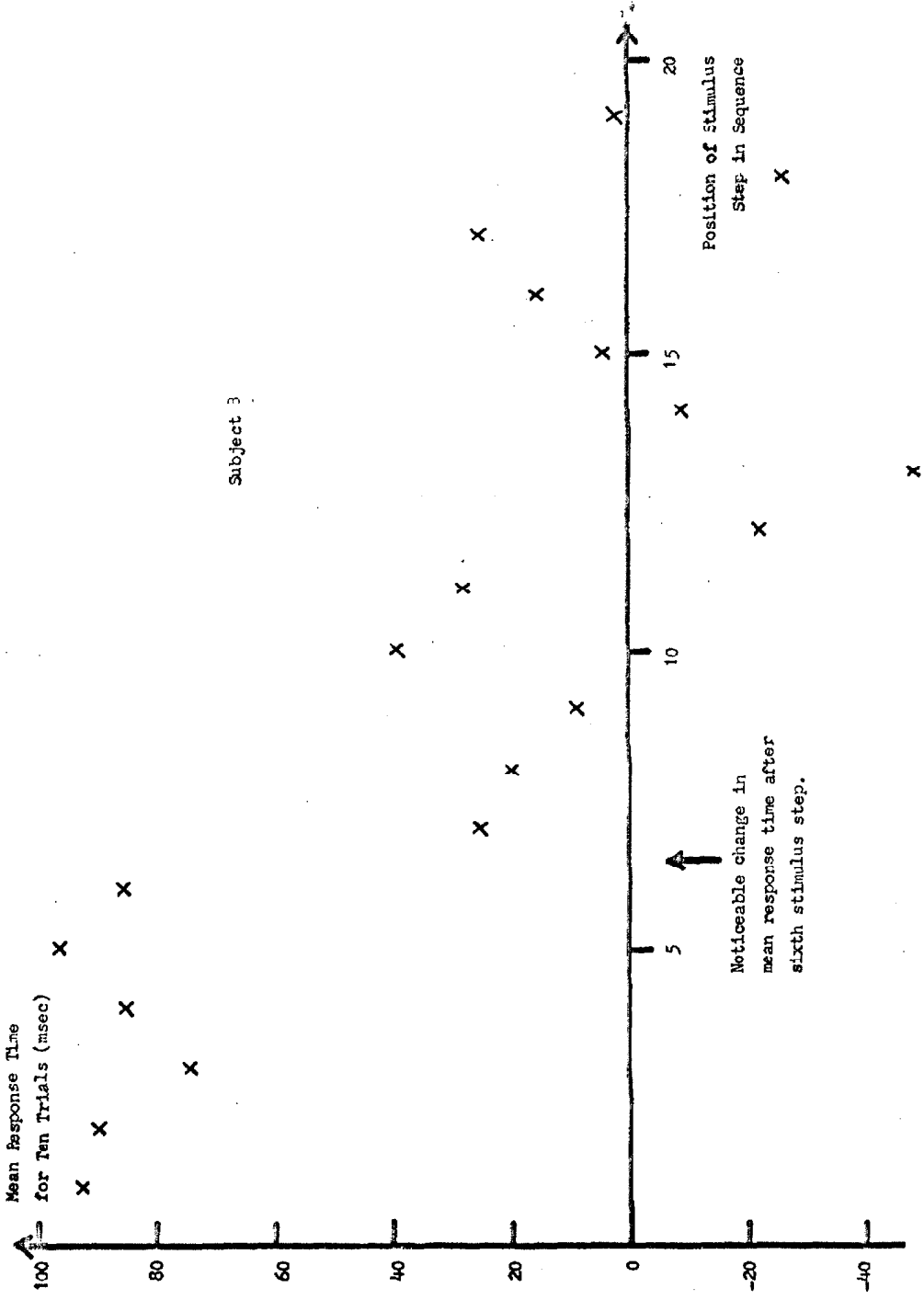

Figure 5.13 - Plot of the mean response time to individual stimulus steps in a predictable sequence. The sequence was repeated ten times to obtain the means shown. Drop in response time between sixth and seventh steps indicates where the stimulus period was learned.

attributed directly to the period memory, but it should be recognized that this assignment is not necessary. The effect observed in this case simply represents an additional delay in the predictive system when the stimulus separation is small. If this delay occurs anywhere along the system it can be combined with a constant predictive time to produce the effects observed.

Predictive lead. - The most obvious question that can be raised about this system is why the average predictive saccade precedes the stimulus by about 100 msec, when a more accurate prediction would be obtained by centering the predictive distribution on the stimulus step.

A complete answer to this question requires the experimental results which are presented in the next chapter, but the effect can be summarized by noting that the visual information available to the system is drastically curtailed for a period of about 50 msec before and after a saccade. This restriction on the information flow to the system is the combined result of a change in the visual threshold and an interruption of the efference copy mechanism. Regardless of the source, the end result is that the system is probably incapable of assessing a stimulus step which occurs closer than 50 msec to a saccade. The anticipation of a stimulus step however, has been predicated on the ability of the system to note the occurrence of the preceding step. This being the case, it is clear that the predictive response saccades must occur either before or after the stimulus, if prediction is to be sustained. The reason that the system response precedes the stimulus rather than follows it can not, however, be reasonably established.

CHAPTER VI

SACCADIC EFFECTS ON PERCEPTUAL THRESHOLDS

Introduction. -One of the more interesting aspects of the model presented in the preceding chapter is the fact that when the eye positioning system predicts a stimulus step, it generates a response that is substantially ahead of that step. It was noted there that this effect might well represent an attempt of the system to overcome a loss of visual information caused by the saccades. This chapter will present experiments designed to investigate this possibility.

Brightness perception. -The effects of saccades on perceptual thresholds have been measured, or noted, several times in previous experiments. One of the earliest of these was reported by Ditchburn (18). In that experiment, a subject was asked to fixate a spot on the face of an oscilloscope. The apparatus was arranged so that whenever a flick occurred, the spot under observation jumped momentarily. It was noted that the subject was incapable of perceiving this jump, while an observer standing by the subject's side could readily perceive the motion. Unfortunately, no thresholds were measured in this experiment.

Volkmann (58) subsequently attempted to quantize the effect that had been reported. Her technique involved asking the subject to produce large changes in fixation direction, thereby eliciting saccades, and then presenting a short, 20 μsec, flash at the fovea as the eye swept past a strobe light. By using very short stimulus presentations, she was able to eliminate image motion during the flash. The effect she noted was an 0.5 log unit increase in the perceptual brightness threshold.

In an attempt to extend the range of these measurements,

Latour (37) performed an experiment which was similar in many ways to Volkmann's. The primary difference was that he triggered his stimulus flash at random times with respect to the fixation change, and was able to measure the time course of the threshold change. The results that Latour reported indicate that the elevation of the threshold begins in the neighborhood of 40 msec before the start of the eye movement, and finishes about 80 msec after the start. Unfortunately, the very large saccades he elicited were on the order of 150 msec in duration. Moreover, the stimulation technique which he used caused the majority of the stimuli to be presented in extrafoveal areas. The fact that the rods become predominant in the periphery, and that the rods are the more sensitive of the retinal elements, casts doubt on his observations. The time course which he measured might well be equated with the interaction between these sensitivities and the time course of the eye movements.

There would seem to be good reason to question the results that have been reported as they deal with quite large eye movements, and the study of the time course of suppression was not restricted to stimuli in the foveal region. One of the experiments to be reported in this chapter determines both the threshold changes and the overall time course of the brightness threshold at the fovea during small, spontaneous flicks.

Position perception. - There exists the possibility of a secondary information suppressing phenomenon which has not been accounted for by previous experiments. It is entirely possible that information from the retina is ignored by the cortex when a flick is in progress. It has been shown by previous workers that the maximum brightness threshold change which is created by flicks is quite small, and this is confirmed by the present work. Nevertheless, Ditchburn reported that his subjects did not perceive the jump in the CRO spot, which was presumably several log units above this threshold. It is important to note that the experiment he reported required the subject to detect a motion in the stimulus; this suggests that an alternative mechanism prevents the cortex from detecting target motion which

coincides with a flick. The second experiment to be reported here investigates this possibility.

Brightness Threshold Change - Time Course

Experimental apparatus. - The aim of this experiment was to measure the time course of the brightness threshold change, and to perform this experiment foveally using spontaneous flicks. In order to assure that the stimulus was presented only on the fovea, and that the image should remain fixed on the receptors during the stimulus flash, the experiment was performed in stabilized vision. In this condition, the experimenter adjusted the target on the subject's instructions until the subject was satisfied that he was fixating the flash stimulus foveally.

The visual field for this experiment consisted of three segments. The first of these was a uniformly illuminated background, six deg arc in diameter, illuminated at 0.12 mlumens per steradian. Superimposed on this field was an annulus of 90 min arc inner diameter and 110 min arc outer diameter. This target was oscillated horizontally at six cps with a peak-to-peak amplitude of six min arc, to prevent it from fading as a result of stabilized vision. The annulus, which was continuously illuminated at 0.68 mlumens per steradian, served to locate the flash stimulus at all times. The flash stimulus itself was an 80 min arc diameter disc centered in the annulus. The disc had a nominal illumination of 0.65 mlumens per steradian, and all data were taken in terms of log units of attenuation below this level.

The optical formation of the stimulus disc was achieved by the apparatus shown in Fig. 6.1. Two short focal length lenses, A and B, were positioned a distance exactly the sum of their focal lengths apart with the second lens occupying the target position of the projection system (see Fig. 3.5). The portion of the source beam outside of the field of the lenses was occluded by masks. With this arrangement the second lens, A, appeared to the subject as an

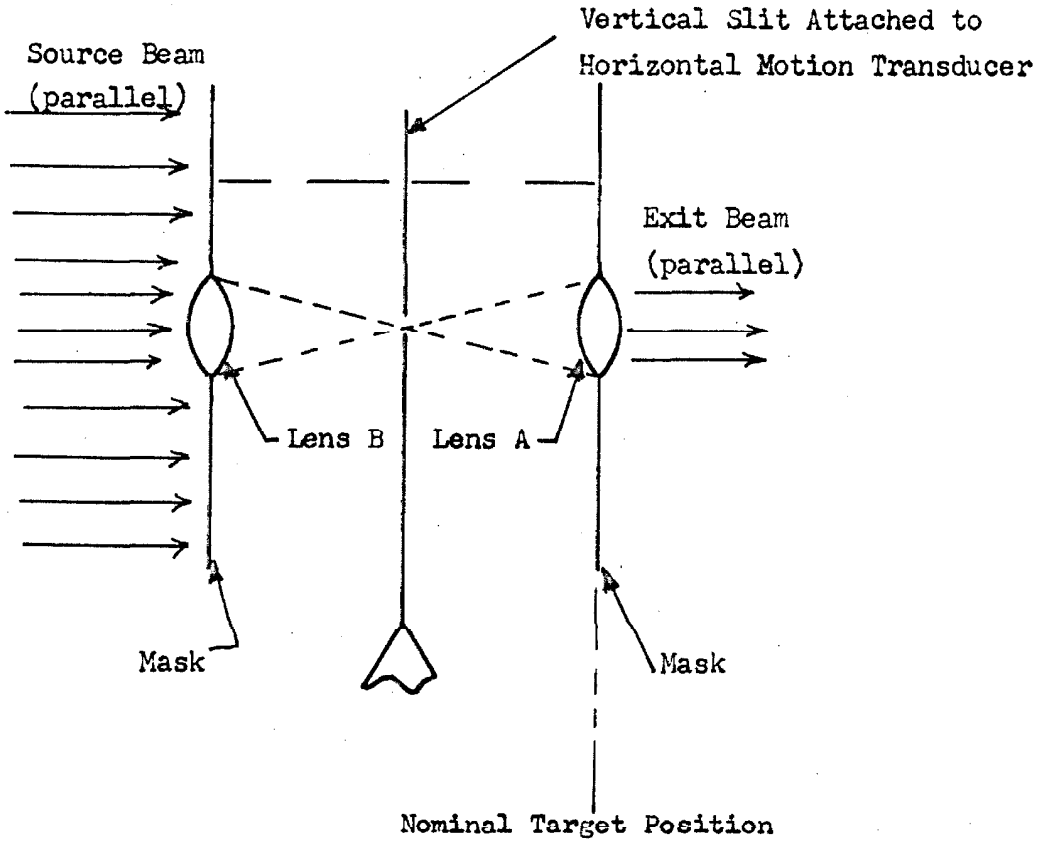

Figure 6.1 - Optical sub-system which generates the flash stimulus.

illuminated disc with a diameter equal to that of the lens. The use of lenses, rather than simple masks, to generate this image created an equivalent source point midway between the two lenses. In order to darken the disc, it was only necessary to occlude this point source from either direction, and the illumination of the disc decreased uniformly at all points. Moreover, the small size of the source point allowed the total rise time of the light pulse to be very short. To flash the disc illumination, a vertical slit was attached to the target motion transducer described in Chapter V. When at rest, one side of this slit blocked the source beam; when the slit was stepped rapidly across the source point, however, a flash of 5 msec duration was obtained with a rise and fall time of 0.2 msec. The subjective impression of a stimulus presentation was that of a flash of light covering the area located inside the stabilized reference annulus.

In order to obtain the desired time relationship between stimulus presentations and flicks, a variable delay circuit was used in conjunction with the flick detector. Pulses from the latter unit were delayed, and then led into the binary counter which controlled the target position (Fig. 5.1). With this apparatus, the stimulus could be presented anywhere from 20 to 800 msec after the initiation of a flick. The flick detector outputs for horizontal motion were added together in order that a flick in either horizontal direction could trigger the stimulus.

Experimental procedure. - The individual experimental runs were comprised of 23 stimulus presentations. The construction of the presentations was performed by a logical control unit which divided the session into 46 time intervals averaging three sec in duration, this timing being obtained from the turntable timer described in Chapter V. Alternate intervals were designated as stimulus and response periods. The first flick which occurred after the beginning of a stimulus period triggered a flash presentation after a fixed delay. The experimenter could vary this delay at will, or could inhibit the

flash to provide a measure of false-positive responses. The subject was provided with an indicator lamp which signalled him via the eye not being tested for 0.5 sec at the beginning of each response period. The subject was instructed to report at that time whether or not he had observed a stimulus flash in the preceding period.

Some care was taken to prevent the subject from obtaining external cues which might assist him in the perception. First, he was deafened to activity in the experiment room by requiring him to wear acoustically insulated earphones into which white noise was played. Secondly, there was the chance that the response signal light might allow him to predict when the next presentation would occur. This possibility is remote, however, as the period duration was not constant, but rather averaged three sec. Also, the flash itself was triggered by spontaneous eye movements, and it will be demonstrated in Chapter VIII that these are random events.

In order to be able to measure the subject's response to a stimulus which occurred before a flick, it was necessary to make use of one characteristic of these spontaneous movements. It will be shown in Chapter VIII that each subject has a characteristic mean inter-flick time. If the stimulus is delayed by this mean time then the flash stimulus will occur at approximately the same time as the subsequent flick. The subject's eye movements and response were recorded on the oscillograph along with the stimulus flash for later analysis.

Using the method described above, it was found that 45 per cent of the stimuli occurred within the range of interest, $\pm$100 msec with respect to the start of the flick. As the time of the stimulus presentation varied continuously with respect to the flick, it was necessary to subdivide this range and to lump all presentations within each subdivision into a common statistic. These subdividions yielded approximately equal numbers of samples.

The fact that the experimenter had to rely on a random process to obtain the desired stimulus-flick relationship made the measurement of a perceptual brightness threshold for each subdivision impractical. Instead, the experiment was performed at a single luminance level which produced approximately 50 per cent response to the total number of presentations. The measurement of thresholds was carried out in an experiment to be described later in this chapter. The experiment here was performed on two subjects for a total of 20 experimental runs.

Results. -The results for this experiment are presented in graphical form in Fig. 6.2. The horizontal axis in that plot is the time of the stimulus presentation with respect to the time of initiation of the flick. Thus, a negative time on this axis implies that the test flash preceded the flick. An indicator on this axis running from 0 to 15 msec shows the actual duration of the eye movement. The vertical axis represents the percentage of the stimulus presentations that the subject perceived. As noted above, these are computed over a range on the time scale. In every case, the midpoint of the subdivision has been plotted. Finally, the percentage of responses which were elicited for all the presentations outside of the range of interest are lumped together and plotted at the ends of the graph. Approximately five per cent of the stimulus presentations were inhibited, and of these, less than one per cent false-positive responses resulted. As this number was very small, no correction for false-positive responses was made in Fig. 6.2.

In order to permit the assessment of the significance of these results, 99 per cent confidence bands have been plotted around each point. The interpretation of these bands is that if the experiment were repeated 100 times, the percentage measured would fall within the range of the band 99 times. It will be seen that it is not possible to draw a horizontal line that would intersect all of these bands for either subject; thus, the overall effect measured is significant at greater than the 99 per cent level.

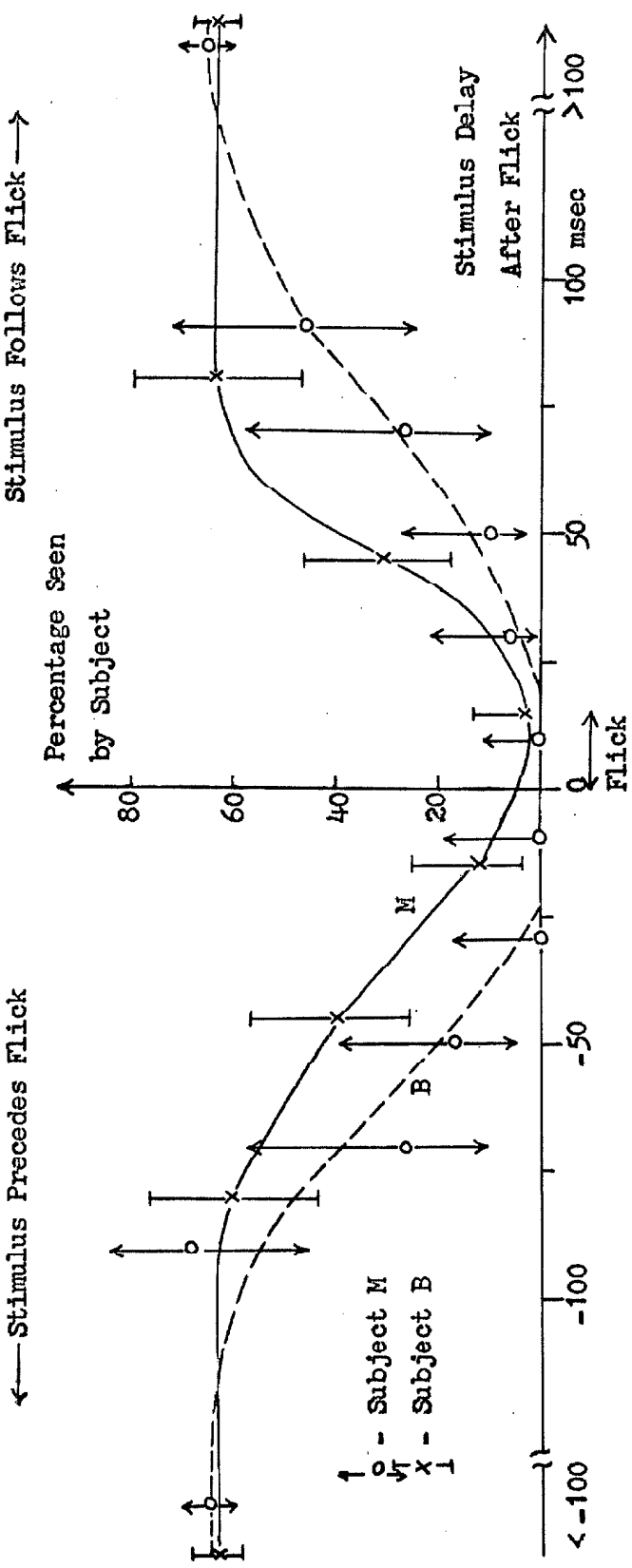

Fig. 6.2 - Plots showing time course of brightness threshold change relative to flick initiation time. Vertical marks around data points indicate 99 per cent confidence intervals.

Brightness Threshold Change - Amplitude

Experimental Procedure. - The experiment presented above clearly demonstrates that a flick causes a change in the perceptual characteristics of the visual system, and that this effect exists both before and after the eye movement. It was not practical, however, to measure the amplitude of this change at each point in terms of the brightness threshold, because of the low percentage of stimulus presentations which were in the range of interest. In order to measure this amplitude, the following experiment was performed in which the stimulus presentation times could be accurately controlled by the experimenter. This, of course, limited the testing range to post-flick stimuli.

Four standard stimulus delays were chosen; 20, 60, 100 and 220 msec. The basic experimental run, described above, contained 23 stimulus presentations. These presentations were arranged so that each of the four standard delays was presented five times, and the stimulus was inhibited three times. The order of presentation was randomized in several different sets, and the experimenter changed sets several times during each session.

The level of the flash illumination was changed for each experimental run. This was done in such a manner that the total number of responses in individual runs eventually spanned the possible range from 0 to 20. As a result, the experimenter was assured that he had bracketed the 50 per cent threshold for each of the stimulus delays.

Data reduction. - In order to achieve significant statistics, it was necessary to collate the data from all the experimental sessions. The validity of this step was confirmed by the fact that the overall threshold level, where the total number of responses from a single run was 50 per cent, changed by less than 0.1 log units from day to day.

In order to obtain the best estimation of the threshold value for

each stimulus delay, a fitting technique known as probit analysis was used. The basic assumption within this form of analysis is that the statistical threshold fluctuation is normally distributed with the log luminance as the distribution parameter. Figure 6.3a shows the percentage of responses at all log luminance levels for the 60 msec stimulus delay for subject M, along with the 99 per cent confidence intervals for those measures. The probit assumption, in terms of this figure, states that the gradual change in percentage of responses seen is the result of fluctuations of the perceptual threshold.

Under this assumption, the mathematical formulation of the data point spread can be achieved. If λ denotes the log unit attenuation of the stimulus, and $N(\lambda)$ is taken as a normal distribution with a mean value equal to the threshold value sought, then the fraction of responses which will be elicited at any given luminance level λ_o, is

$$\rho(\lambda_o) = \int_{-\infty}^{\lambda_o} N(\lambda)\, d\lambda. \qquad \text{Eq. 6.1}$$

In order to obtain a fit to this functional form, it is necessary to transform the experimental parameter ρ into some form that has a linear relationship to λ. In particular, the equation

$$\rho = \int_{-\infty}^{t} N_o(\omega)\, d\omega, \qquad \text{Eq. 6.2}$$

where $N_o(\omega)$ is a normal distribution with unit deviation, can be solved for t uniquely for any given value of ρ. Thus, t specifies the value of ρ, and also is linearly related to the luminance λ.

The probit analysis requires the solution of Eq. 6.2 for each experimental value of $\rho(\lambda)$, and the plotting of t versus λ. This transformation has been done on the experimental values of Fig. 6.3a,

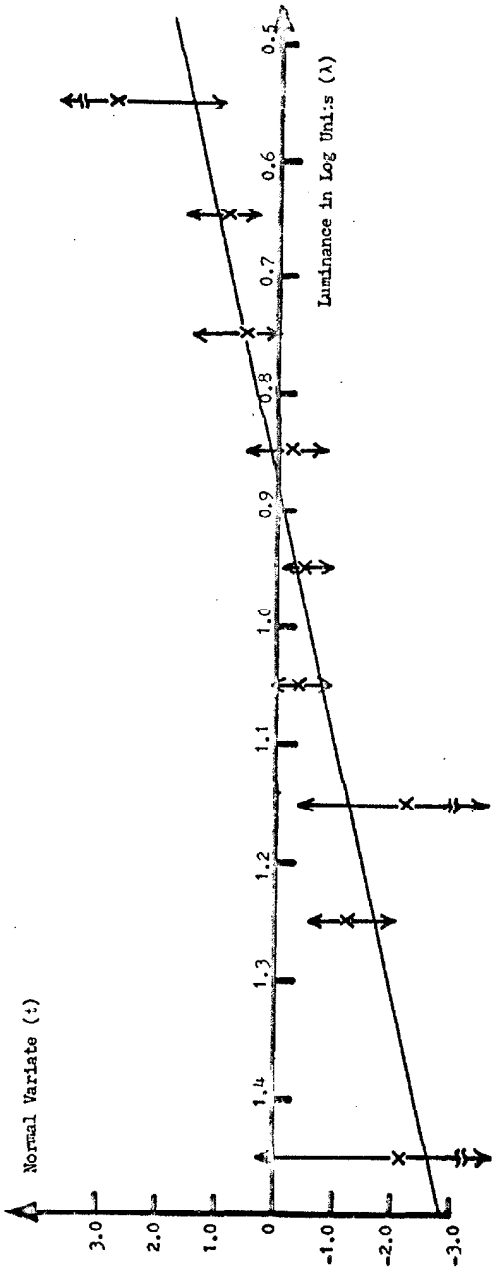

Figure 6.3b - Response percentages of Fig.6.3a transformed into normal deviates by probit analysis. (See text)

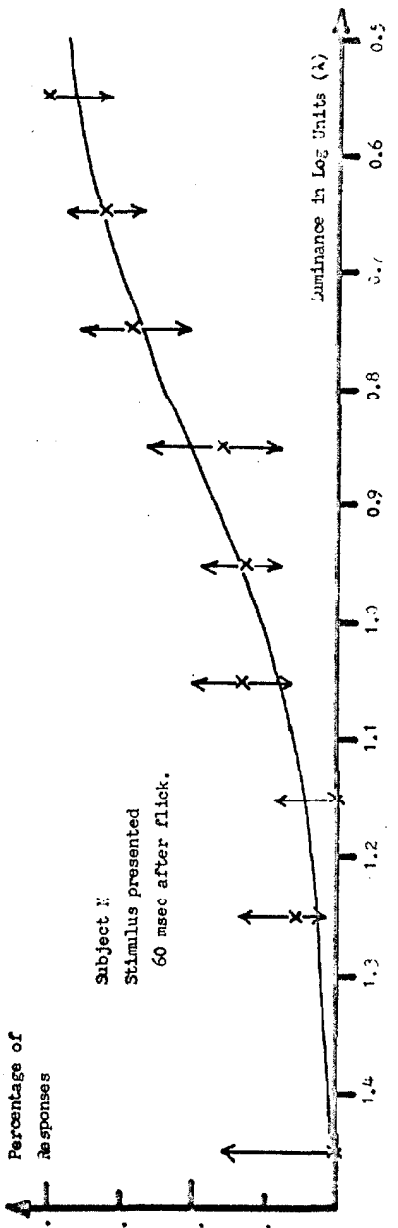

Figure 6.3a - Percentage of responses to stimulus flashes delayed 60 msec after a flick, plotted as a function of flash luminance. Arrows indicate 99 per cent confidence bands.

and the resultant plot is shown in Fig. 6.3b, along with the straight line fit. The sigmoid curve that was plotted on Fig. 6.3a, simply represents the inverse transformation performed on that straight line. This last step, however, is unnecessary, as it can be seen that the 50 per cent threshold level, the parameter sought, is the value of λ where t is zero in Fig. 6.3b.

Results. - The probit analysis was used on the data for both subjects, and the results are plotted in Fig. 6.4 as the threshold value versus the time delay. While the magnitude of the threshold change for the two subjects is different, the effect of the flick on the visual threshold is clear. Unfortunately, the experimental apparatus used did not permit the sampling of the threshold during the course of the flick itself. The data derived by Volkmann, however, can be used in this respect. The results from her Fig. 5 (58) have been used to calculate an equivalent threshold change during the flick itself, for each of her three subjects. This threshold difference was then related to a non-flick threshold level of 0.97 log units, and plotted as three circles in Fig. 6.4. As her data were always taken in the middle of the saccade, they have been plotted in that same location on this curve, 7.5 msec after the initiation of the flick. Despite the differences in technique, the experimental results are clearly similar, and it can be concluded that the maximum threshold difference which occurs due to a flick is on the order of 0.5 log units.

Variation in Motion Perception

While the two experiments just reported show clearly that there is an interaction between brightness threshold and flicks, they do not directly answer the question as to whether this would affect the predicting loop investigated in Chapter V. The reason for this doubt lies in the small threshold changes which were measured. The pinhole target which was used in the square wave experiments was approximately three log units above the thresholds measured above,

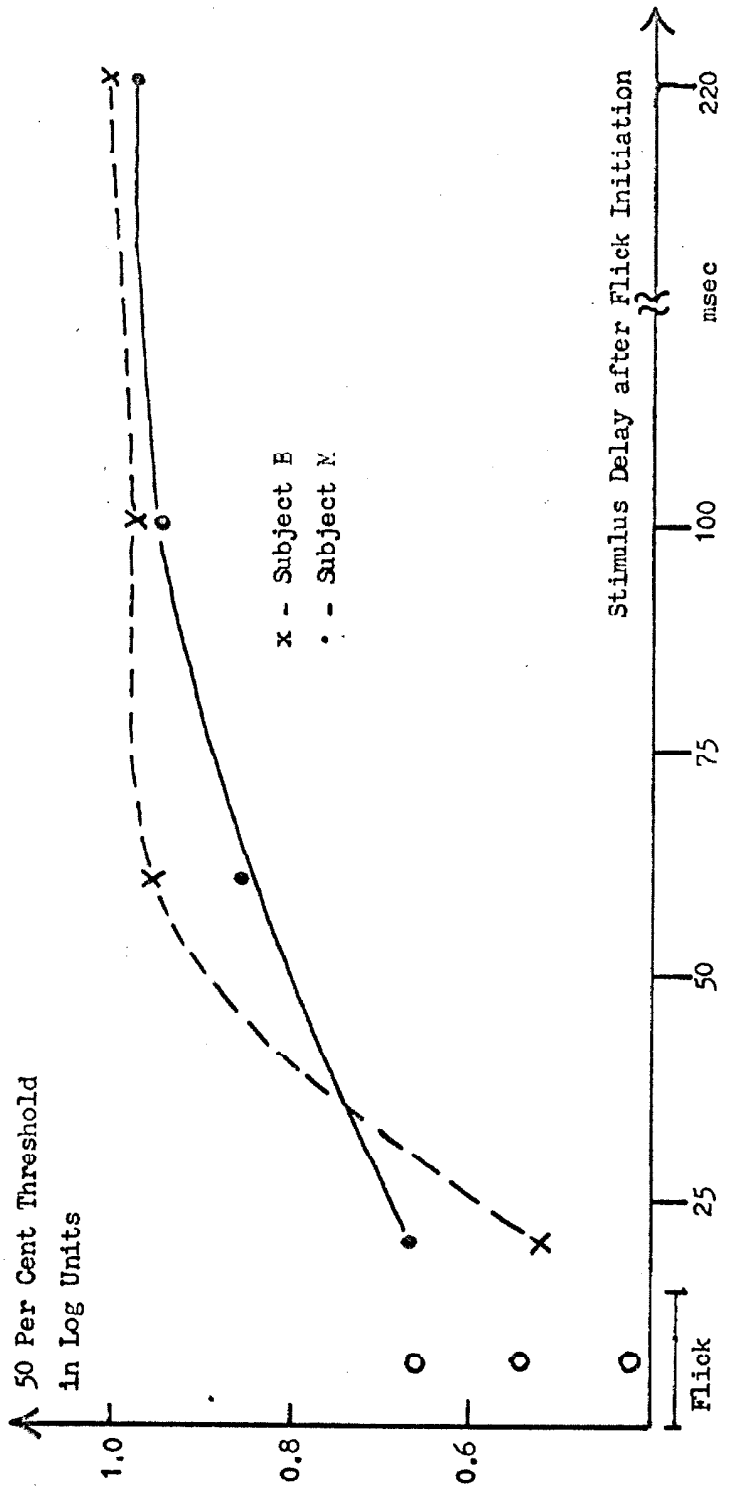

Figure 6.4 - Brightness threshold in log units as a function of time delay between stimulus and a flick. The o's plotted at 7.5 msec delay are data recalculated from Volkmann.

and these experiments show a maximum threshold change on the order of only one half log unit. It would appear, then, that if the occurrence of a saccade interfered with the information transfer in the previous experiments, it would have to do so by some means other than by elevation of the perceptual threshold. The following experiment was devised to test that possibility.

The experiment. - The experiment performed was similar to that used to test the time course of the threshold change, except that the stimulus condition was changed. The target, which in this instance was presented to the subject in normal vision, was the small pinhole used in the predicting experiments. Instead of flashing the target, the stimulus presentation consisted of a small step change in the target position. Thus, the subject was asked to report the perception of a small target motion which occurred at random times with respect to his spontaneous flicks. In order to prevent the target step from eliciting following movements, the amplitude of the step was held to 15 min arc. Rashbass (50) has shown that this is below the level which will produce saccadic following.

Results. - The results of this experiment are plotted in Fig. 6.5. The form of this plot is very similar to that of Fig. 6.2. The horizontal axis represents the time difference between the flick and the stimulus, negative times representing a stimulus before the flick. The vertical axis represents the per cent of presentations perceived, and 99 per cent confidence bands have been plotted around the data points. The effect is quite clear. The subjects, M and B, saw 99 and 93 per cent of the stimulus steps, respectively, when these steps occurred at a time separation of greater than 100 msec from a flick. When the stimulus steps coincided with the flick, however, neither subject saw any of the target motions. This alone would not be surprising were it not for the fact that this perceptual failure starts about 40 msec before the flick, and lasts from 25 to 60 msec after the flick is complete.

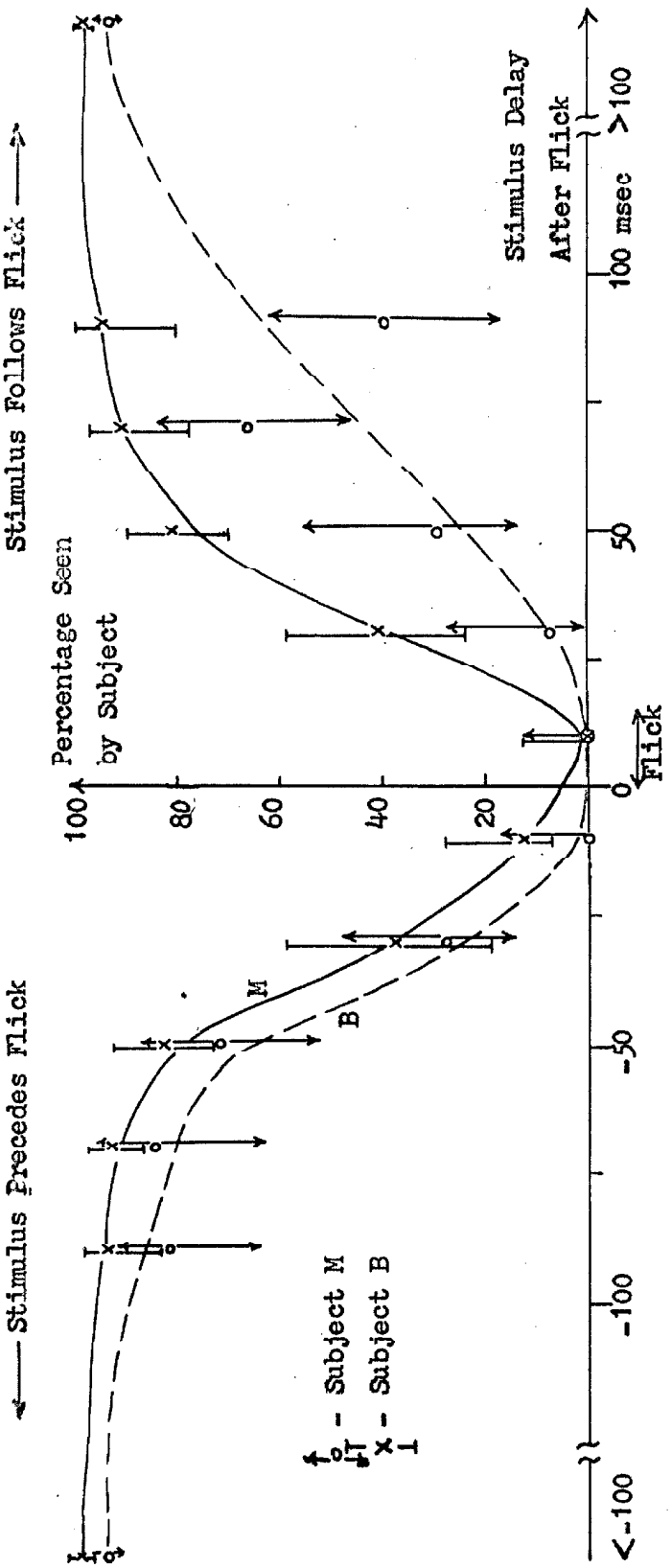

Fig. 6.5 - Plots showing time course of suppression of position detecting ability relative to time of flick initiation. Vertical points around data points indicate 99 per cent confidence intervals.

Conclusion

Before drawing conclusions from the experiments of this chapter, let it be understood that the author is aware that the third experiment reported is hardly complete. A proper evaluation of the interaction between flicks and motion perception would require the determination of an amplitude threshold, the correlation of flick and stimulus step directions, and the inclusion of some brightening of the stimulus during the step to cancel the effect of the reduced threshold.

In spite of the above restrictions, the indications of this experiment are very strong - the retinal information that is available to the cortex is altered as the direct result of a flick. Although the brightness threshold changes which were measured in the previous experiment are probably not large enough to perturb the functioning of the eye positioning system, an extrapolation of the effect which was measured in the third experiment of this chapter could easily necessitate the lead seen in the predictive response mechanism.

The results reported here provide an interesting insight into the functioning of the efference copy mechanism. Moreover, the effect must be considered as a potential sampling mechanism. The discussion of these considerations, however, requires experimental evidence to be presented in later chapters, and is, therefore, reserved for the conclusion of the thesis.

CHAPTER VII

SACCADIC RESPONSE MECHANISMS

Introduction

When eye positioning systems models were discussed in Chapter IV, it was noted that the author felt that further attention should be cast on the sampled data model presented by Young (61) for the saccadic response system. Although no specific points were raised at that time, it is felt that there are two general aspects of this model which should be checked.

Sampler. -First, there is the question of the use of a sampler in the model. There are many examples in neurological systems of units which possess characteristics similar to a sampler, such as absolute refractoriness of axons and neurons. Various combinations of refractoriness and pure transmission delays could be used to effect a sampler of the form Young describes, but none of these would have the precise mathematical function of that form.

To be more exact, the responses of Young's sampled-data system must be considered in two distinct categories. The first of these exists when stimulus functions require responses more widely separated in time than the sample period. In this condition, the model which he proposed responds with a reaction time delay about 200 msec after the stimulus. This is based on his constraint that the sampler only blocks the transmission of information for 200 msec after a stimulus motion which requires a saccadic response. The second category, of course, is the case where the stimulus requires responses closer together than the 200 msec interval. In such instances, the sampled data model produces a series of responses that are separated by 200 msec, rather than by the time separation defined by the

stimulus. This is the characteristic of a refractory system. The important point is that the sampled data model requires that the time delay for widely separated stimuli be the same as the refractory period seen in response to rapid stimuli.

Within either stimulus category, the model probably provides an accurate measure of the response, as the sampled period can be adjusted to match either the delay or the refractory period. When stimuli of the two categories are mixed, however, the differences between the two mechanisms will be revealed. The experiments to be presented in this chapter have been designed, in part, to test this transition region. The technique involves presenting stimulus steps in pairs with the time interval between them varied from values less than the sampling period up to values approximately three times this parameter. Moreover, the presentations of the pairs are separated by relatively long intervals. The effect of this choice is to require two responses from the saccadic system; the first of these responses is always to a stimulus widely separated from the preceding one, while the target step which elicits the second response varies between the two categories, closely and widely spaced. The mean response times to these stimuli will differentiate between the delay time and refractory effects.

Predictability effects. - The second point which these experiments are to test is the effect of varying orders of unpredictability in the stimulus. To date, the class of predictable stimuli for the saccade system has been restricted to square waves of the form used in Chapter V. In those experiments, the stimulus motion was totally predictable. It is entirely possible, however, that if a subject has advanced knowledge of part of the stimulus function, he can respond in less time than would be required for the response to a totally unknown function. Specifically, if he knows the next position to which the target will move, but does not know the time at which this step will take place, he might well react faster than if he knew neither the

next position nor the time.

In the experimental course presenting the stimulus pairs to test the mechanisms mentioned earlier, it was possible to constrain the target motions in such a way as to establish a test of predictability effects also. Thus the experiments to follow will investigate both questions.

Experiment

The experimental condition. - The target to be tracked was allowed to assume only three positions, right, left, or center of the visual field, and these positions were equally spaced 1.5 deg arc apart. (Fig. 7.1) Secondly, target transitions were only permitted between adjacent positions. When the target was at rest in the center of the subject's field of view, it might move left or right with equal probability; hence, he was unable to determine to which of the two extreme positions it would move in the next step. When the target rested at one of the extremes, however, the subsequent position was automatically specified as being the center. Finally, the subject was told that the stimulus steps would always occur in pairs, that the time separation (T) between pairs was on the order of three sec, and that the separation between the members of each pair (PW) was variable from 20 to 650 msec. The combination of these constraints provided two distinct forms of experiments, containing a total of three stimulus configurations.

In the first experimental form, arbitrarily referred to as the normal form (Fig. 7.1a through c), the stimulus was at rest between stimulus pairs in one of the extreme positions. At the beginning of the pair presentation, the target stepped to the center position, and proceeded to one of the extremes. The two stimulus steps of each pair differed in predictability. Prior to the first step, the subject knew the direction and amplitude of the stimulus step, but did not know the time at which it would occur. This condition will be referred to as

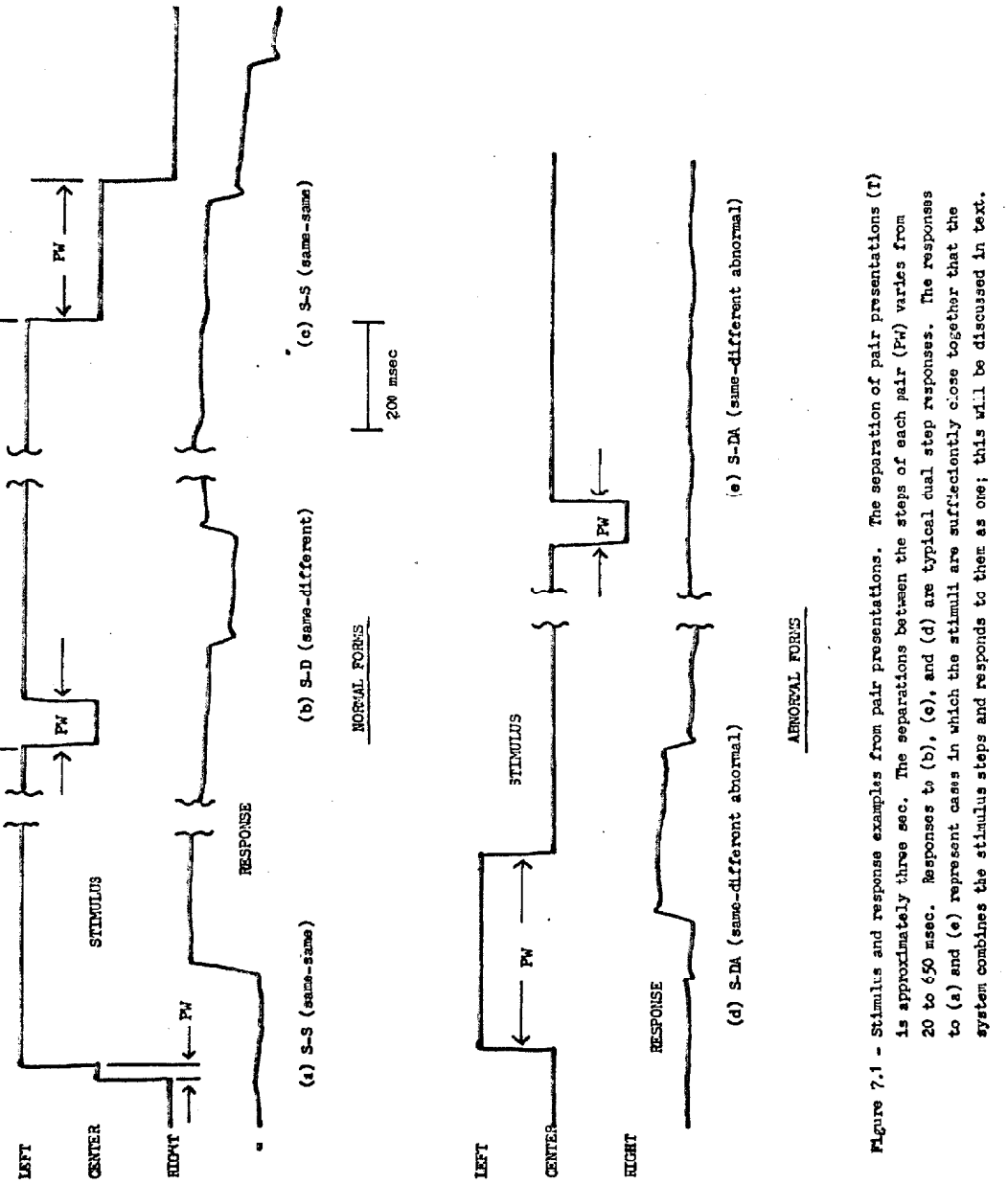

Figure 7.1 - Stimulus and response examples from pair presentations. The separation of pair presentations (T) is approximately three sec. The separations between the steps of each pair (PW) varies from 20 to 650 msec. Responses to (b), (c), and (d) are typical dual step responses. The responses to (a) and (e) represent cases in which the stimuli are sufficiently close together that the system combines the stimulus steps and responds to them as one; this will be discussed in text.

first-order unpredictability. The second step of the stimulus pair, however, represented a second-order unpredictability in that the subject again did not know the time at which the step would occur, and further, he did not know to which of the extremes the target would move. The stimulus configurations within the normal form were further subdivided as to whether or not the second step in the pair was in the same direction as the first. These classifications are called 'same-same' or S-S (Fig. 7.1a and c) and 'same-different', or S-D (Fig. 7.1b).

The second experimental form, called the abnormal form, started with the stimulus at rest in the center. It can be seen that the orders of predictability for the two stimulus steps are therefore the reverse from the normal form. Here, the stimulus was equally likely to step to either extreme at the start of the stimulus pair, but had to return to the center at the end of the pair. This constrained the stimulus to the 'same-different' class, and will be referred to as S-DA (Fig. 7.1d and e).

Equipment. - The stimulus generator in this experiment was designed so that the experimenter had complete control over the stimulus being presented. A schematic of the equipment is shown in Fig. 7.2. The occurrence of each stimulus pair was triggered from the turn-table device described in Chapter V (Fig. 5.2). The holes in the disc on the turn-table were set to give pair separations which were approximately, but not exactly three seconds. These pulses were then used to trigger a pulse generator. This unit consisted of a one-shot multivibrator which produced a pulse P_1 at the start of its cycle, and a pulse P_2 at the end of the cycle. The time separation of the pulses was a function of the time constant of the one-shot. Plug-in units were provided, each of which produced sixteen different time constants, these time constants being selectable by a rotary switch on the unit. The pulses from the generator were then fed into two binary counters whose outputs were added algebraically to provide

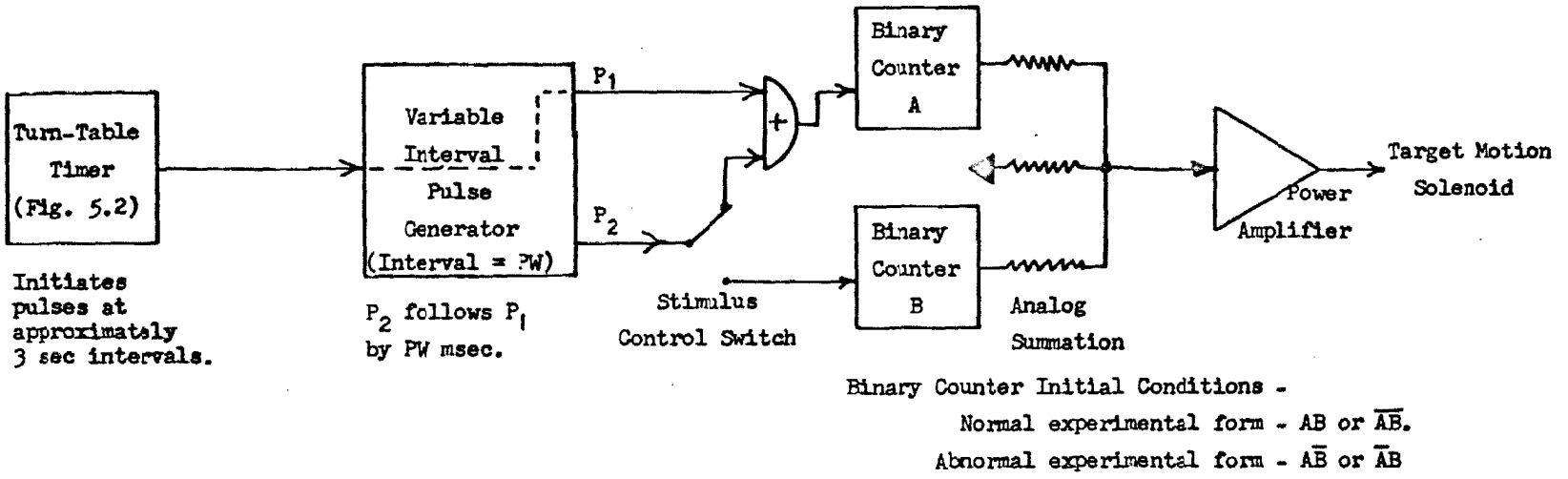

Figure 7.2 - Schematic diagram of stimulus pair generator.

the three required voltage levels. Finally, the output sum from the binary counters was used to drive the power amplifier and target motion solenoid described earlier; the target was the pinhole used in the experiments reported in Chapter V.

It was the initial state of the binary counters, A and B, and the routing of the pulse pairs which determined the experimental form and stimulus type which were presented. For normal experiments, the binary counters were initially set in the same state (AB or $\overline{A}\overline{B}$). The first pulse was always fed into binary counter A, thereby driving the stimulus to the center. The second pulse could be routed to either counter A or B. If it was routed to A, the stimulus created was S-D, while routing to B produced stimulus S-S. During the abnormal experiments however, the initial condition of the binary counters was different, either $A\overline{B}$ or $\overline{A}B$. In this form, the switching of the second pulse controlled the direction of the subsequent stimulus pair. If the second pulse was continually routed to counter A, a series of stimulus pairs to one side was created, whereas if the switch was left in position B, alternate stimulus pairs were oppositely directed.

The individual experimental runs were two minutes in duration; 24 runs were performed on each subject in the normal form, and 12 in the abnormal form. A total of 32 time constants were selected in the range of interest; with the result that each stimulus type was sampled approximately 30 times at each pair width. The fact that the switch which routes the second pulse, and the rotary switch which selects the separation were controlled at random by the experimenter prevented a totally uniform distribution, but the subjects all reported that they were unable to anticipate the experimenter. Variations in the final number of presentations were accounted for as weighting functions when obtaining averages etc.

Data processing. - The variable of interest in these experiments was the time relationship between the stimulus and response. For

this reason, the flick-dector was used to pre-process the data, and four tracks of pulses were recorded on the analog tape recorder. These marked the times of occurrence of right and left stimulus steps, and right and left saccades of the eye. These pulses were subsequently transmitted to the digital computers in the TOE mode.

The data reduction routines separated the stimuli by class, S-S or S-D, and by stimulus separation, PW; and then determined the subjects response. First, the lists of stimulus times were searched to find the first two times which were as yet unprocessed. From these, the stimulus was classified as R-R (right-right, one of the two S-S types), R-L, L-L, or L-R. Next, the appropriate saccade time list was searched to find the first properly directed flick following the first stimulus. This was considered to be the initial component of the response. If this saccade followed the stimulus step by more than 400 msec (twice the normal reaction time), the response was stored as an 'infinite' lag, and processing of that stimulus pair was terminated. These 'infinities' occurred frequently with S-D type stimuli at small pair widths where no response was elicited(as in Fig. 7.1e) and were seldom seen for S-S stimuli. If an initial response was found, the second half of the response was determined as the first properly directed saccade which followed both the second stimulus step, and the initial response saccade. Again, if this response followed both events by more than 400 msec, it was deemed to be infinite. This latter condition occurred most frequently in response to S-S type stimuli with small pair widths, where the total response to the two stimulus steps might be embodied in a single eye movement as in Fig. 7.1a. These processing steps were repeated for each stimulus pair in the run, and the results for each run collated with all other runs to provide the final averages.

The variables saved can be described as four lists, each list containing 32 entries, one for each stimulus pair width for both S-S and S-D type stimuli. These four lists are the mean 'lag', the reaction

time to the first stimulus step; the percentage of infinite lags; the mean response width, the time separation between the first and second response steps; and the percentage of infinite response widths.

Results

Curve fitting to the response. -In order to evaluate the results of these experiments, it is useful to consider the response to these stimuli that is predicted by the sampled data model. First, the sampled data model does not predict infinities of the type to be found in the experiments. The fact that some were, in fact, found could be the result of noise in the system, and is not an a priori reason to condemn the model. The variables of interest, then, are the lag, reaction time to the first stimulus step, and the response width. According to the sampled data model, the first response to the stimulus pair will occur one sample period, approximately 200 msec, after the first stimulus. Thus the lag should be a constant function of the pair width, with a value on the order of 200 msec. The model further predicts that the second response will occur one sample time after either the second stimulus step, or after the initial response step, whichever event occurs earlier. Thus the response width should be constant at about 200 msec for pair widths less than 200 msec, and equal to the pair width for all values of that variable greater than 200 msec.

The possible variations in the true response which were mentioned earlier in this chapter should now be considered in light of this predicted response. These variations were concerned with two elements. The first was the difference between the refractory period and the response delay; and the second was the change that a basic reaction time might undergo if the predictability of the stimulus varied. As these are simply constant effects, it would seem reasonable that they might at most change the value of any constant response, or change the slope of the response width at larger pair widths. For this reason, the experimental data were fitted with straight line approximations similar to the curves which the sampled data model predicts.

The experimental response lags were simply fitted with a constant value, the appropriately weighted average of the experimental points. The response width was least-squares fitted with two straight line segments by an iterative procedure. An arbitrary break point of 200 msec was chosen, and a constant function was fitted to the data for pair widths less than this value, while a straight line was fitted to the points at greater pair widths. From these two lines an intersection point was calculated in terms of pair width. This intersection was used as the next break point, and the process repeated. This iteration continued until two break points were within 10 msec of each other. In practice anywhere from three to six iterations were needed to pass this test.

An example of these curves, and of the basic experimental results is given in Fig. 7.3. This figure contains the computer printed plots for subject F in the normal experiments. The legend at the top of the page describes what is plotted by each symbol. The vertical axis in this case is the stimulus pair width in msec. In Fig. 7.3a, the S-S and S-D lags are plotted along with the percentage of infinite S-D lags. The constant functions for the fitted lines are approximately equal, at an overall average of 195 msec. The response widths are shown in Fig. 7.3b, along with the percentage of infinite S-S response widths. Again, the constant portions of the two curves, S-S and S-D, are similar, but the break points and the slopes in the upper portion of the two curves are quite different. These curves have been presented only to convey a picture of the form of the data being dealt with. Future considerations of this form of response will use only the best-fit curves.

It can be seen from Fig. 7.3, that the percentage of infinite samples in the two classes shown are far from random, as they would be were noise the causative factor. Rather, it would appear that the second stimulus step is capable of modifying the response to the first stimulus if the pair width is sufficiently small.

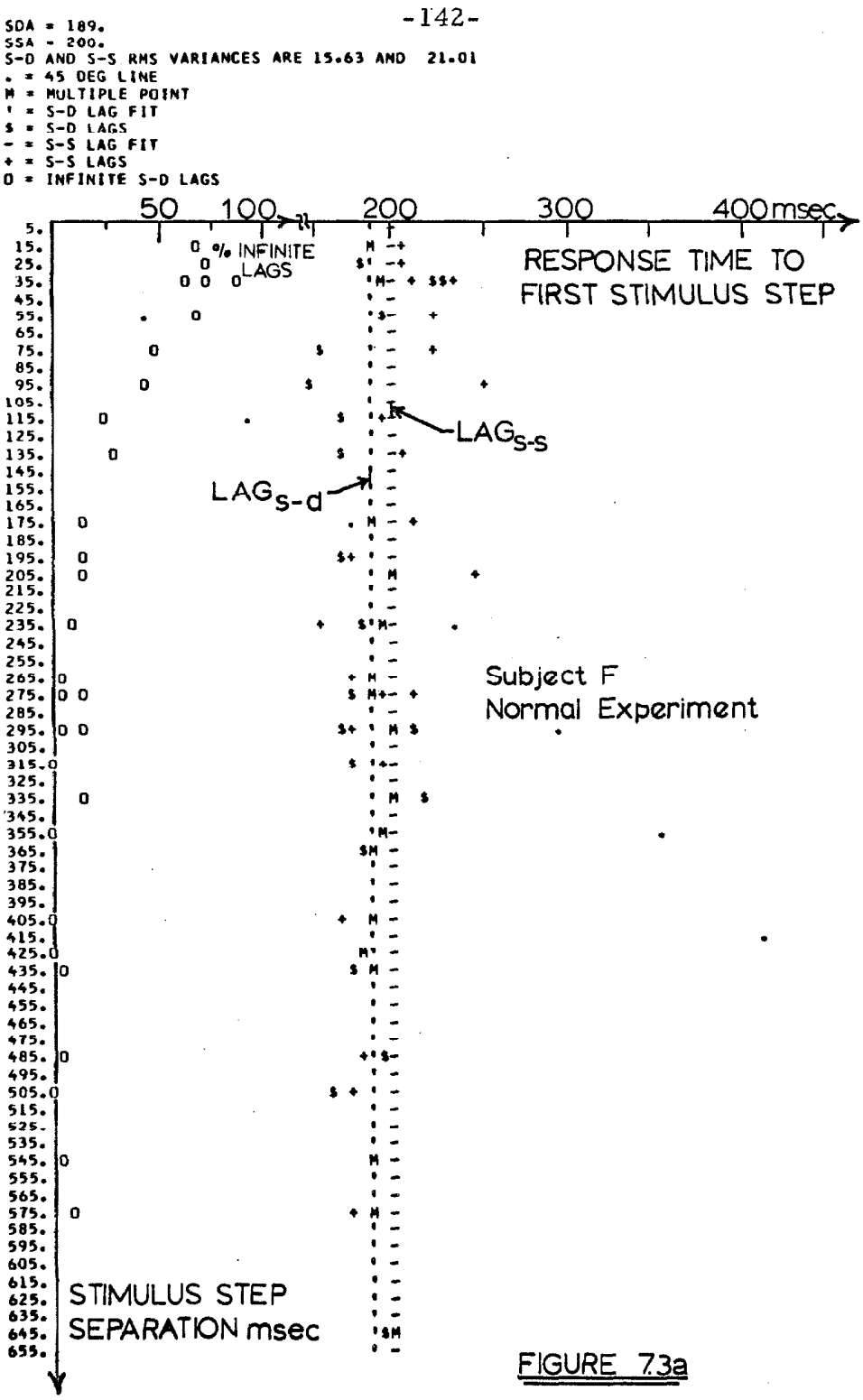
SDA = 189.
SSA = 200.
S-D AND S-S RMS VARIANCES ARE 15.63 AND 21.01
. = 45 DEG LINE
M = MULTIPLE POINT
' = S-D LAG FIT
$ = S-D LAGS
- = S-S LAG FIT
+ = S-S LAGS
0 = INFINITE S-D LAGS
50
100
200
300
400 msec
0 % INFINITE LAGS
RESPONSE TIME TO FIRST STIMULUS STEP
LAG S-S
LAG S-d
Subject F
Normal Experiment
STIMULUS STEP SEPARATION msec

FIGURE 73a

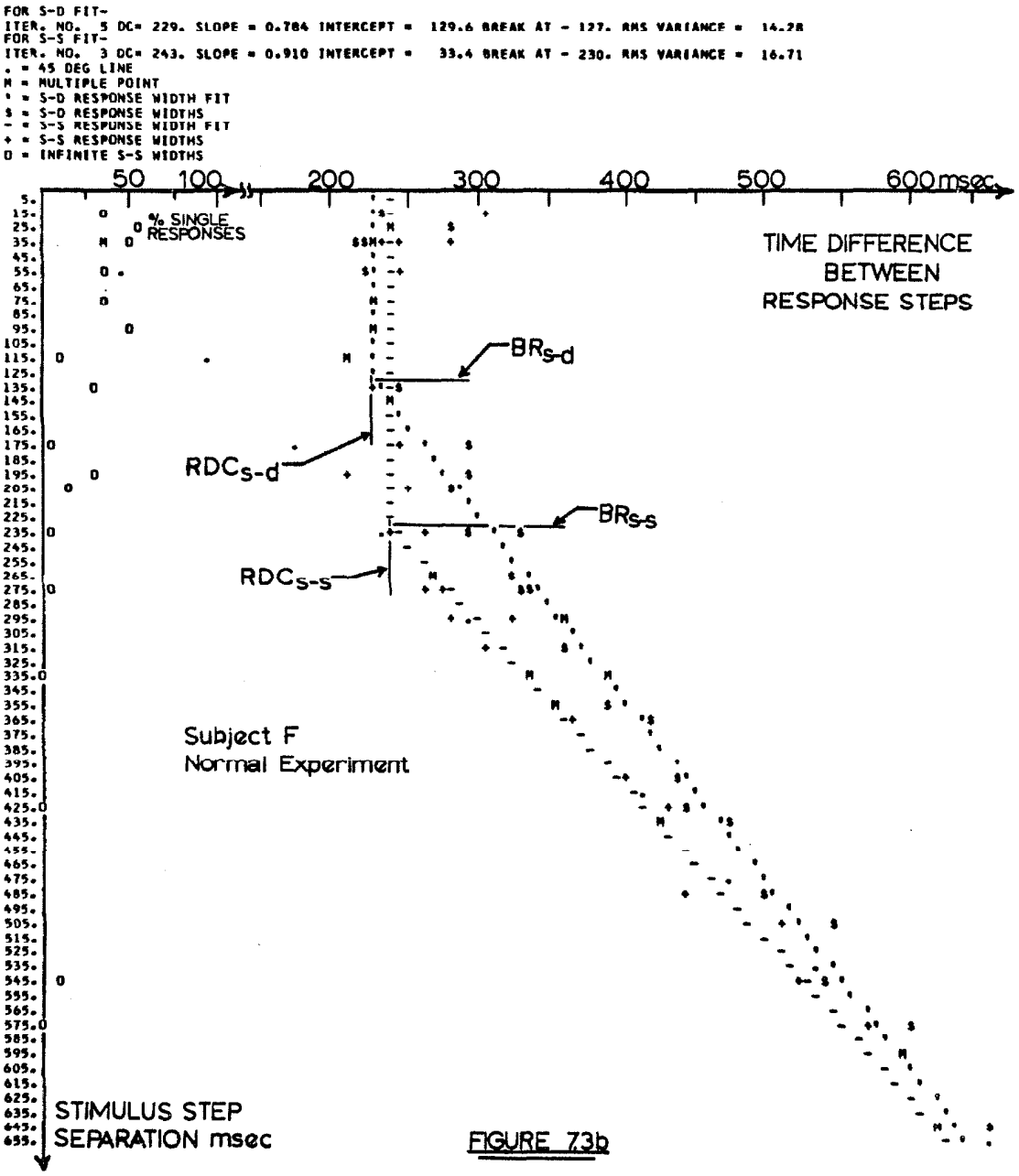
FOR S-D FIT-
ITER. NO. 5 DC= 229. SLOPE = 0.784 INTERCEPT = 129.6 BREAK AT = 127. RMS VARIANCE = 14.28
FOR S-S FIT-
ITER. NO. 3 DC= 243. SLOPE = 0.910 INTERCEPT = 33.4 BREAK AT = 230. RMS VARIANCE = 16.71
. = 45 DEG LINE
M = MULTIPLE POINT
' = S-D RESPONSE WIDTH FIT
$ = S-D RESPONSE WIDTHS
- = S-S RESPONSE WIDTH FIT
+ = S-S RESPONSE WIDTHS
0 = INFINITE S-S WIDTHS
50 100 200 300 400 500 600 msec
% SINGLE RESPONSES
TIME DIFFERENCE BETWEEN RESPONSE STEPS
BRs-d
RDCs-d
BRs-s
RDCs-s
Subject F
Normal Experiment
STIMULUS STEP SEPARATION msec

FIGURE 7.3b

This being the case, there is undoubtedly some threshold pair width that can be identified with the 50 per cent point. To determine these threshold points, the percentage curves were fitted using the probit analysis mentioned in Chapter VI.

Primary Results. - The results for each of the three subjects F, B, and N1, are shown in more comprehensive form in Figures 7.4, 7.5, and 7.6, respectively. In each of these figures, six curves are plotted. The horizontal axis is the pair width (separation of the stimulus steps), while the vertical axis is the time in msec following the start of the pair. The curves plotted for each subject are:

i) the time of occurrence of the second stimulus (a 45^{o} straight line);
ii) the time of the first S-S and S-D response;
iii) the time of the first S-DA response, and
iv), v), and vi) the times of the second response for each type stimulus.

The initial response times for S-S and S-D have been combined as these stimuli were randomly mixed in the same experimental runs, and the subjects had no way of knowing which type would occur after the presentation of only the first stimulus step. The statistical risk involved in this step is assessed in the next section. One other piece of experimental data has been included in the figures for each experimental condition. This is the time threshold below which more than 50 per cent of the response were contained in a single saccade; this threshold is indicated by terminating the appropriate second response curve at the pair width. Finally the time of the second response which is predicted by the sampled data model is shown on each graph as a series of x's.

The data represented by these plots can be summarized by extracting pertinent parameters from the curves. These parameters will be used from here on and are marked on Fig. 7.3. They are

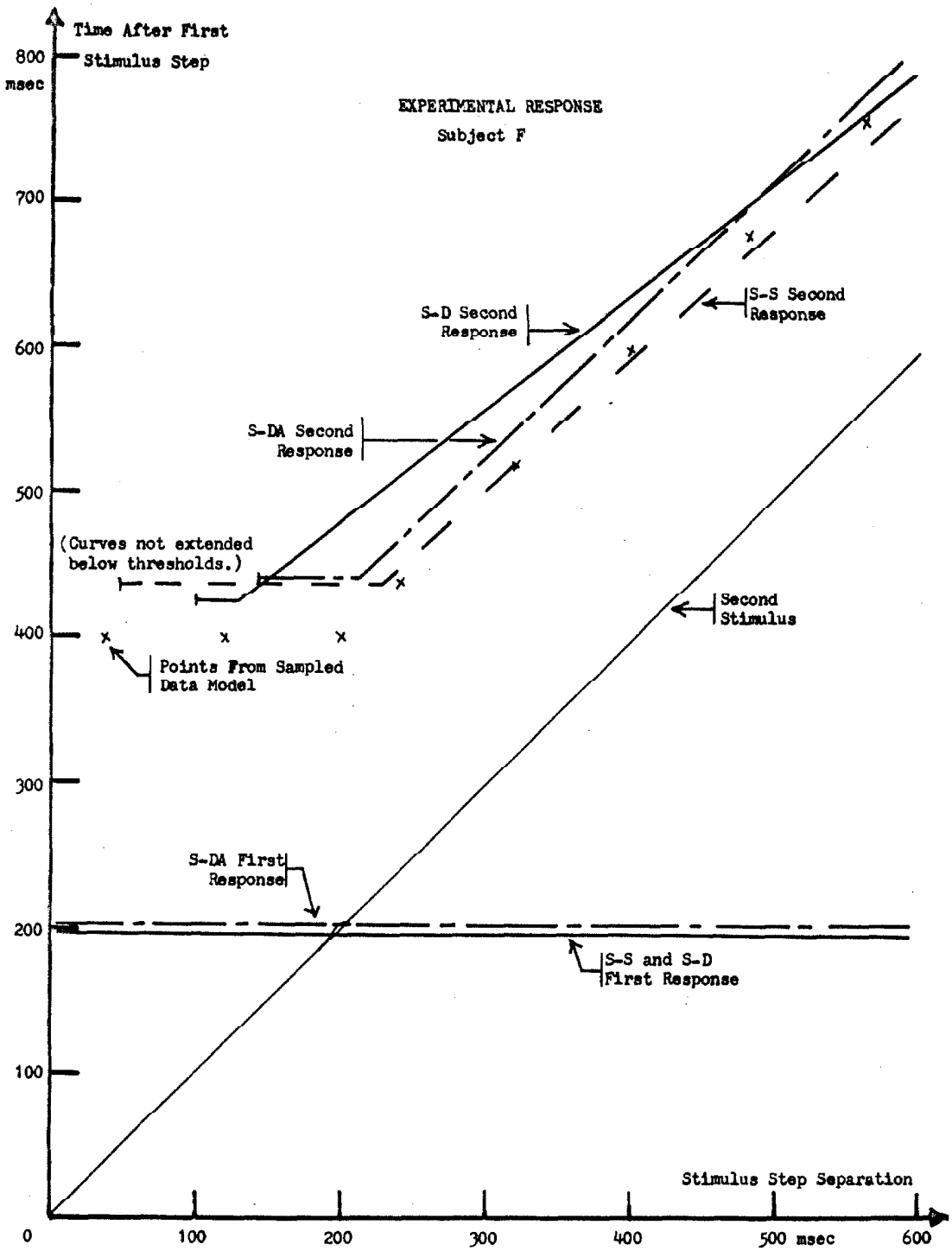

Figure 7.4 - Fitted curves to experimental response of subject F. Abbreviations: S-S, same-same stimulus in normal experiment; S-D, same-different stimulus in normal experiment; S-DA, same-different stimulus in abnormal experiment.

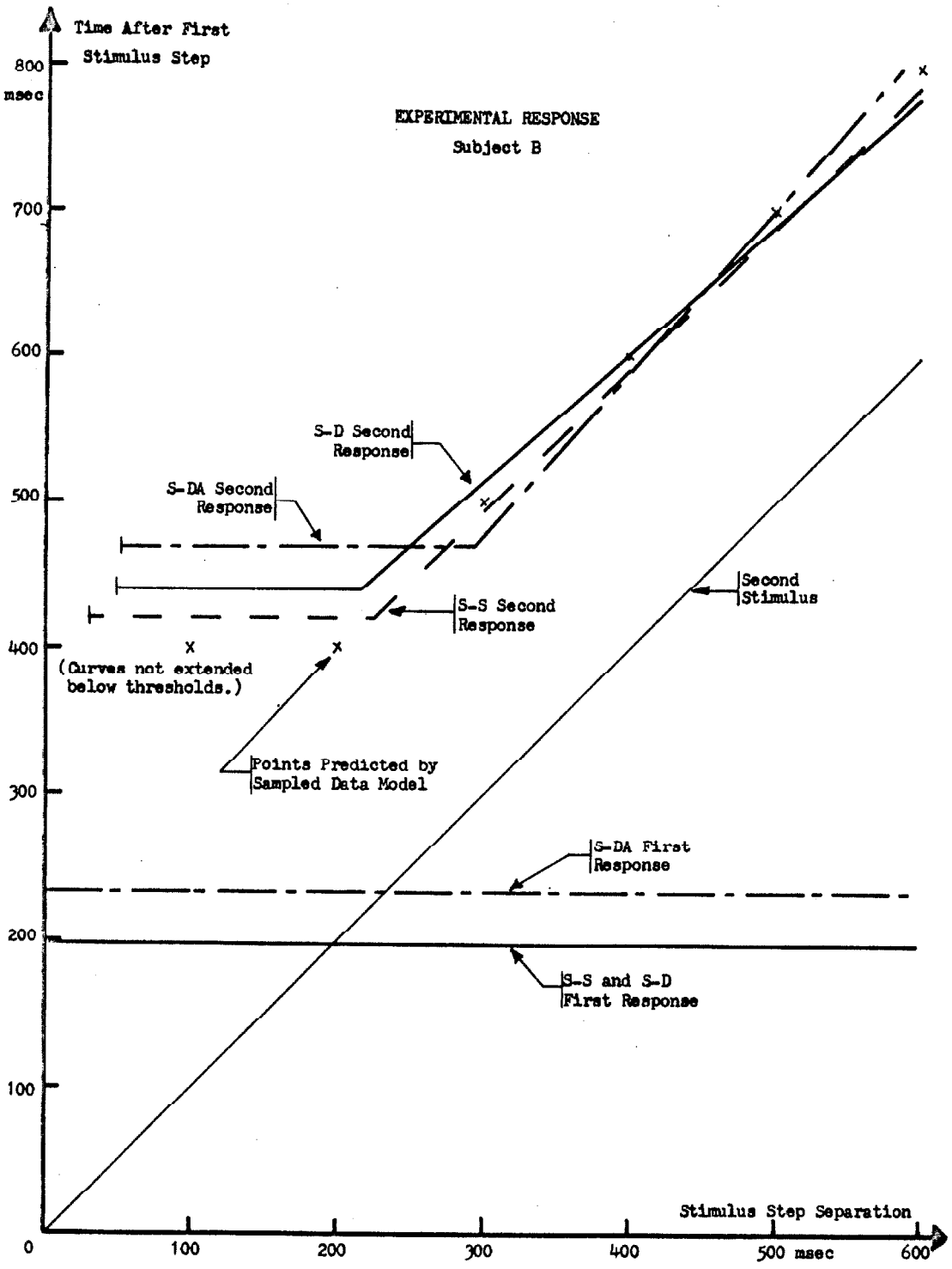

Figure 7.5 - Curves fitted to experimental response of subject B. Abbreviations: S-S, same-same stimulus in normal experiment; S-D, same-different stimulus in normal experiment; S-DA, same-different stimulus in abnormal experiment.

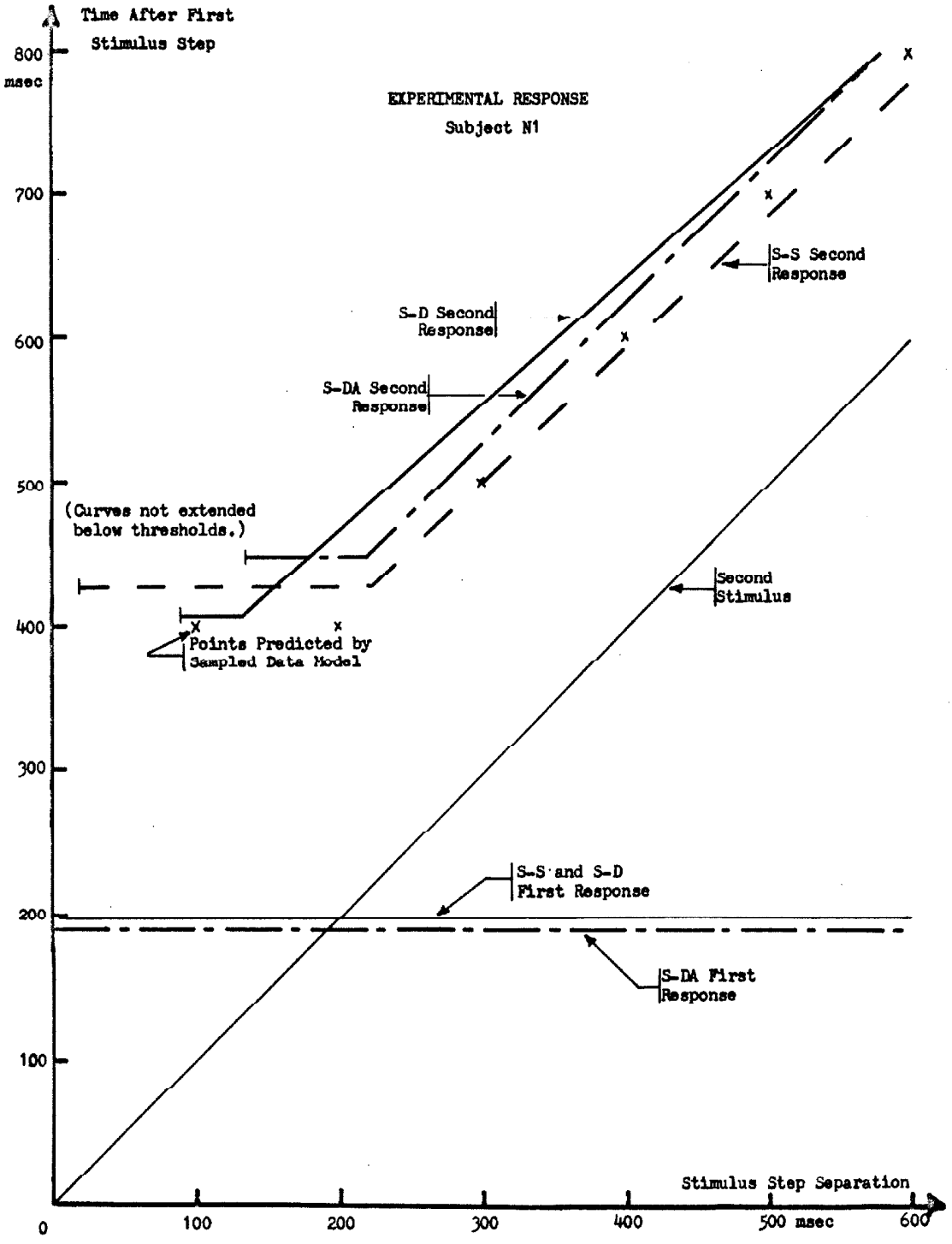

Figure 7.6 - Fitted curves to experimental response of subject N1. Abbreviations: S-S, same-same stimulus in normal experiment; S-D, same-different stimulus in normal experiment; S-DA, same-different stimulus in abnormal experiment.

the LAG, the mean first response time; the time differential between the response steps in the region where it is a constant, RDC; and the break point, BR, which is the pair width at which the response separation becomes a function of the stimulus pair separation. These data are presented for the two normal stimulus forms in Table 7.1.

Significance of experimental results. -It is very tempting at this point to attempt to fit the observed results to a preconceived model. This proposition is chancy, however, without first assessing which portions of the experimental curves should be considered as significant, and which deviations within these curves might simply be a chance variation in the data.

The first question to be answered is the comparability of the abnormal and normal experimental regimes. As stated earlier, one purpose of this experiment was to assess any change in reaction time which might arise as a result of changes in stimulus unpredictability. If such an effect is obvious, it will show up as changes between the two forms of experiments. That is, the initial reaction times in the two experiment sets will differ by this effect, the abnormal initial reaction being longer; and the RDC value will be similarly affected, that for the normal experiments being larger. Comparison of the initial reaction times, LAG shows little effect for subjects N1 and F, and in fact, the abnormal LAG value is smaller than the normal LAG for subject N1. The significance of all the LAG value differences for each of the three subjects is given in Table 7.2. The measure presented in this table is the probability that the derived means, different though they may be, arise from the same distribution. The comparison of the S-S results with those for the S-D, represents the risk involved in combining these two as was done in Figures 7.4 through 7.6, and in Table 7.1. The important combinations however are those in which the LAG values for the S-DA stimuli are compared with those for the S-S stimuli. Only for subject B can the difference in lags be said to possess significance. A

TABLE 7.1

Response Parameters Derived From Experimental Data

Subject	F		N1		B	
Stimulus	S-S	S-D	S-S	S-D	S-S	S-D
LAG (msec)	195	195	195	195	200	200
RDC "	245	230	210	235	220	240
BR "	230	130	220	135	225	215
Threshold (msec)	45	100	20	90	30	50

Abbreviations: S-S, same-same stimulus in normal experiment; S-D, same-different stimulus in normal experiment; LAG, mean response time to first stimulus step; RDC, mean response time difference between first and second steps for stimulus separations less than BR; BR, stimulus separation at which second response time becomes a function of that separation; Threshold time is the stimulus separation below which both stimulus steps are responded to by a single saccade more than 50 per cent of the time.

TABLE 7.2

Significance of The LAG Values

The table entry is the probability that the two LAG values compared arise from the same distribution.

Subject	F	N1	B
S-D vs S-S	.68	.67	.80
S-DA vs S-D	.70	.90	.15
S-DA vs S-S	.90	.70	.18

TABLE 7.3

Confidence Band Widths for the Second Response Curves

The table entry is the value of ρ for a 90 per cent confidence interval of the form $(x \pm \rho)$.

Subject	F	N1	B
ρ for S-S Response (msec)	28	27	33
ρ for S-D Response (msec)	24	36	32

Abbreviations: S-S, same-same stimulus in normal experiment; S-D, same-different stimulus in normal experiment; S-DA, same-different stimulus in abnormal experiment.

similar comparison of the RDC values reveals that all possible differences for these cases are insignificant at the 0.9 level or greater. Thus the unpredictability effect, if it exists, is not large enough to be revealed by these measurements alone.

The overall significance of the results can be measured in another manner. The calculations by which the various curves were fitted to the experimental results produced a mean square error for the data points with respect to the curve. This error is essentially the standard deviation of the means of the distributions which comprise these curves. The fact that the curve fitting was performed by including the sample weight of each experimental point allows the use of this deviation in assessing a uniform confidence band for each of the curves. This band is expressible in the form $(x \pm \rho)$, such that if the value derived from the original experiment is x, subsequent repetitions of the experiment will produce results which fall within a band of $(x \pm \rho)$ a given percentage of the time. The 90 per cent confidence bands for the S-S and S-D second response curves are given in Table 7.3 for each of the three subjects. The value of ρ is given in msec, and should be applied vertically around the appropriate curves in Figures 7.4 through 7.6.

Use of the confidence bands allows determination of the deviations between individual curves which may be deemed significant. The most important assessment here is that the predicted response values derived from the sampled data model fall outside these bands in some portion of the curves for each of the three subjects. This is sufficient justification for seeking an alternative model of the system. Secondly, the constant portions of all curves fall within the confidence interval of at least one other curve; this is an alternate statement of the confidence separations mentioned above. Further, for subject B, all three curves coincide in this manner over their whole range. This, however, is not typical of the three subjects. For subjects N1 and F, there is a large portion of the data range

in which the S-S and S-D curves are significantly separated, over pair separations from 200 msec to 650 msec for the former, and from 175 msec to 570 msec for the latter. Thus, for these subjects, the S-S and S-D responses must be treated independently within any model to be used. The primary difference between these two curves would seem to be the break point, the constant levels and end points being roughly the same. For the two subjects, F and N1, these break points differ by more than 85 msec, the S-D break point being the smaller. This same amplitude relationship is seen for subject B, but the difference is only ten msec.

The normal experimental forms, S-S and S-D, have been shown to be significantly different over a large portion of the stimulus range and the major difference can be seen to lie in the break points. This will necessitate some mechanism in the model being derived which will differentiate on the basis of stimulus direction, S-S vs S-D. However, consideration of the S-DA break points, as seen in Figures 7.4 through 7.6, will reveal that this directional sensitivity was not present in the abnormal experimental form. The S-D and S-DA break points differ consistently by more than 75 msec, the S-DA break point being the larger. Moreover, for subjects F and N1, the S-DA break point is very nearly the same as for S-S stimuli. Finally, the 50 per cent thresholds for the S-D and S-DA cases differ for each subject, the abnormal threshold being the larger in each case. The implication here is that the subjects, being in a different experimental regime, adopted a different stratagem for tracking the abnormal stimuli. No instructions were given in the experimental sessions other than that the subjects were to follow the targets to the best of their ability. The model to be derived in this experiment reveals that the difference seen between the abnormal and normal responses is a direct result of the predictability of the stimuli overcoming the directional sensitivity in the system, but the abnormal cases will not be used during the construction of the model.

Saccade Response Model

Basic model elements. - The model presented here includes both elements with simple time delays, and refractory elements. At the heart of the model is the saccade command unit, a 'computer' element which takes a measure of the error existing in the visual axis, and computes the saccade which must reduce this error to zero. The assumption is made that this unit is totally preoccupied with the problem at hand, and thus will not start computing on a subsequent saccade until the current computations are complete, and some recovery time, reset time, has been allowed. As with any computer, this system needs input and output units, in this case, the retina and visual cortex, and motor units and extraocular muscles. In the model to be used, the visual cortex is assumed to take the visual information from the retina, and use this to generate a description of the error in the visual field. Any alteration of basic responses that is to take place must occur in this unit, and once the information has been transferred to the command element the saccade is irrevocable. Thus the threshold effects noted earlier will be embodied in the input unit. The output, or effector unit is assumed simply to follow the commands of the computer, and produce the appropriate saccade. Thus, the saccade command unit is the refractory element, while all three segments - input, computer, and output - contribute to the overall time delay.

It should be noted that it would be possible to derive a substantial portion of the detector and effector elements from anatomy and electrophysiological experiments. This has not been done because these elements probably extend higher into the nervous system than does reliable information about the CNS. That is, the time functions for retinal and muscular conversions of nervous signals, and for transmission times along the nerve fibers, are all smaller than the corresponding time parameters which are derived for the model. Also, refractory effects in the nerves and muscles

have been ignored. This is justified for two reasons. First, the stimuli never occurred at intervals less than 16 msec, which interval is greater than normal receptor or nervous refractory periods; secondly, flicks are seldom initiated closer together than 160 msec, a time which is larger than normal muscular refractoriness.

Model description. -The system to be used is shown in block diagram form in Figure 7.7, along with the primary times associated with each unit. The error detector, as described above, has been divided into two sub-units to provide for the two forms of response alteration observed in the experiments. The first of these units, labelled "cortical 'integrator'", delays the stimulus information and combines, integrates, all retinal information arriving during that delay time. These functions are the result of a two step process. First, a disparity is noted in the relative positions of the target image and the fovea. The retinal information about this disparity is not transmitted to the next unit in the system until a time TCI later, at which time the latest retinal information is transmitted. Thus, if the two stimulus steps of an S-S pair are separated by less than TCI, they will generate a single, combined response. This effects a form of "sampling" on the data, but this sampling interval is quite small in comparison to the overall system response time. A further discussion of this mechanism is provided in the conclusion to this thesis, where a relationship to efference copy will be postulated.

The second unit in the system provides the error determination. It is assumed to have the task of actually describing the error that exists at the retina and passing this description along to the command unit where the corrective saccade is generated. The basic time to perform this function is TED. The saccade is inevitable once the information leaves this unit; thus, the threshold value for which S-D stimulus pairs generate no response is a separation equal to (TCI + TED). An interesting aspect of this unit is that it contains a

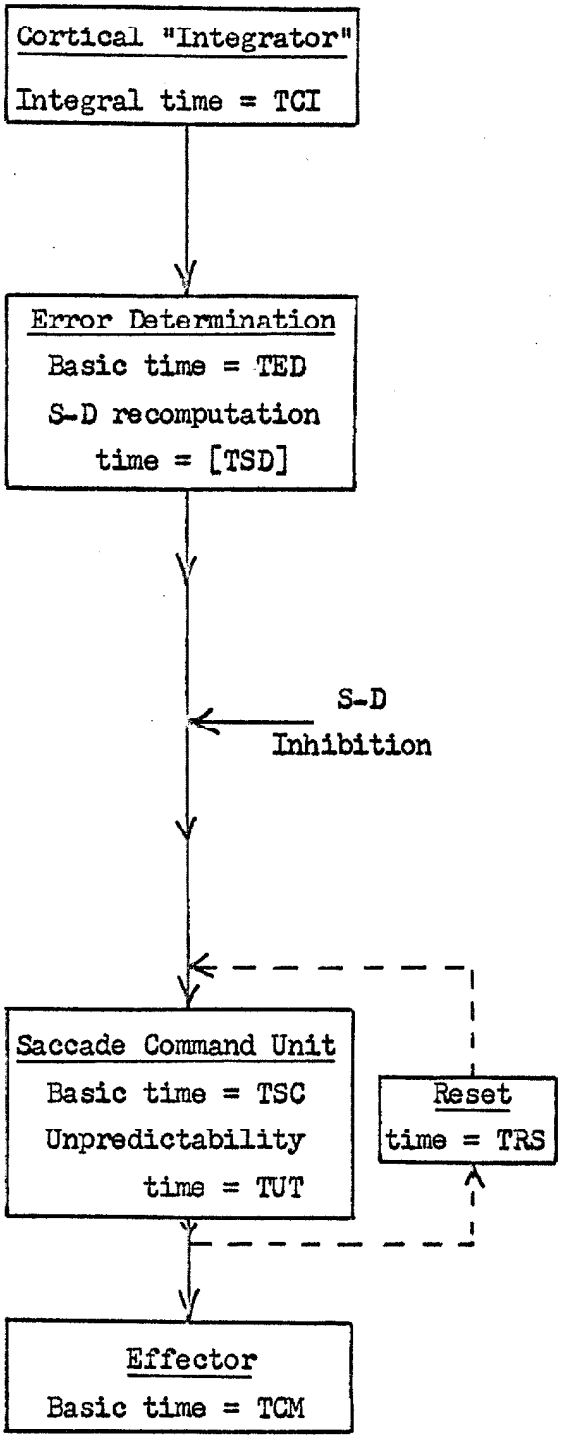

After stimulus motion creates an image-fovea disparity, this unit delays a time TCI and then transmits latest retinal information.

This unit sets up a description of the error correction needed in a time TED. The second stimulus of S-D pair requires an additional time [TSD].

If the second stimulus of S-D pair occurs before information about first step passes here, the initial response will be inhibited. Otherwise, first response saccade is inevitable.

Command unit will not accept information about a second stimulus step until computation on first is complete, and an added reset time, TRS has passed.

Takes command from preceding unit and produces a saccade a time TCM later.

Figure 7.7 - Saccadic response model. Complete description of units is in text.

recomputation time, [TSD], which applies only to the second stimulus of an S-D stimulus pair such that the total error determination time for such a stimulus is (TED + [TSD]). This factor is crucial to fitting the experimental data, for it provides a difference in the break points for the S-S and S-D second response curves. Even though this function is necessitated by the experimental results, it is possible to speculate on the cause of the specificity to S-D stimuli. If the unit were of a form such that the error description is changed only when a new, non-zero error occurs at the retina, then a situation would prevail at the second step of each stimulus pair wherein the description would need to be changed only if the second stimulus step were oppositely directed to the first, S-D. The S-S stimuli create identical errors under the experimental regime that was used. The stress time might well be a function of time, a deduction from the non-unity slope of the S-D curve above the break-point, but judgement on this aspect of the model will be withheld until later. If, in fact, a function of time is used, the basic amplitude of this function will be assigned the value TSD, and the parameter [TSD] will be interpreted as that function evaluated at the appropriate time.

The saccade command unit is the third element in the model. The basic computation time has been assigned to the parameter TSC, and needs no further elucidation. Combined with this parameter, however, is the unpredictability effect as represented by the time, TUT. This is one of the variables that the experiment was designed to measure. The assumption is that lower order unpredictabilities require less computation time than do higher orders, for the simple reason that advance information about the stimulus to be presented can be processed ahead of time. Thus the saccade in response to a stimulus step of first-order unpredictability is calculated in time TSC, while a second-order unpredictable response is computed in a time (TSC + TUT). Finally, this unit is characterized by a reset time, TRS. This factor simply says that the computer is not ready

to calculate a new saccade as soon as computation is complete on the preceding one and the information has been passed to the effector. There are many possible interpretations of this time, and the visual inhibition mentioned in Chapter VI is the most tempting of these. However, it will be seen later that it is not possible to determine this time exactly from the data at hand, and therefore speculation on this point is withheld here.

The fourth and final stage in the system is the effector or motor unit. This section is characterized as a slave unit, responding only to input stimuli from the command unit. As such it is represented by the response time, TCM.

Model response. -Using the above interpretation of the unit functions, the response of the model to S-S and S-D stimulus pairs can be determined. In the equations below, TR1 and TR2 represent the time of occurrence of the first and second response sacades, and ST2 represents the time of the second stimulus step; all times are referred to the time of the first stimulus step. Now,

$$TR1 = TCI + TED + TSC + TCM. \qquad \text{Eq. 7.1}$$

for all stimuli. In order to specify the response time to the second stimulus step, it is convenient to introduce another time, TACC, which represents the time at which the command unit accepts the information about the second stimulus. This time can be defined as:

$$TACC = MAX(ST2 + TCI + TED,\ TR1 - TCM + TRS), \qquad \text{Eq. 7.2}$$

for the second step of an S-S pair. The function MAX(A, B) assumes the value of the larger of its two arguments so that this equation simply states that the computer will not accept an early stimulus until it has been reset (+TRS), and cannot accept a late stimulus until it arrives (ST2 + TCI + TED). It is the changeover from the constant second argument to the variable first argument which determines the break point in the second response curves. The parameter TACC for the second stimulus of an S-D pair is:

$$TACC = MAX(ST2 + TCI + TED + [TSD],\ TR1 - TCM + TRS). \qquad \text{Eq. 7.3}$$

Finally, TACC permits the calculation of the actual second response time for both stimuli as:

$$TR2 = TACC + TSC + TUT + TCM. \quad \text{Eq. 7.4}$$

For convenience, these equations are recast in terms of the experimental variables given in Table 7.1 as :

$$BR_{s-s} = TSC + TSR \quad \text{Eq. 7.5}$$

$$BR_{s-d} = TSC + TSR - [TSD], \quad \text{Eq. 7.6}$$

and, $$RDC = TSR + TSC + TUT, \quad \text{Eq. 7.7}$$

where RDC is the average of the RDC values for S-S and S-D. Of course the experimental parameter LAG is simply the first reaction time, TR1.

Fit to experiment. -Equations 7.5 through 7.7, allow the fitting of this model to the experimental data. Using the interpretation given to the two detector blocks, the associated times for these blocks can be derived directly as:

$$TCI = \text{S-S threshold}, \quad \text{Eq.7.8}$$

and $$TED = (\text{S-D threshold}) - (\text{S-S threshold}). \quad \text{Eq.8.9}$$

What remains at this point, then are five unknown parameters, and four knowns. Solution of the equations shows that of the five remaining system parameters, TSC, TRS, and TCM cannot be specified uniquely utilizing the data at hand. This is simply mathematical recognition of the fact that one is unable to place, either physically or in time, the location of the interface between the saccade command unit and the effector. Rather than attempt this feat, the parameters will be specified as sums, and some comments on possible solutions will be provided in the conclusion of this chapter. Thus, the final set of equations is:

$$(TSC + TCM) = LAG - TCI - TED, \quad \text{Eq. 7.10}$$

$$(TSC + TRS) = BR_{s-s} \quad \text{Eq. 7.11}$$

$$[TSD] = BR_{s-s} - BR_{s-d}, \quad \text{Eq. 7.12}$$

and $$TUT = RDC - BR_{s-s}. \quad \text{Eq. 7.13}$$

These equations have been solved for each of the three subjects, and the results are given in Table 7.4.

Upon comparison of the theoretical responses, equations 7.1 through 7.4, with the experimental responses, it becomes clear that all aspects of the experiment have been matched save one. The LAG, DC, and BR values are all matched, but nothing has been done to assure the mating of the slope of the second response curve above the break point. Rather the model has unity slope in this region. When the model response is plotted in this form, it is found to lie within the significance bands for the RDC values, and for the upper portion of the S-S response. Unit slope on the upper portion of the S-D curve, however, crosses the significance bands at pair separations of 200 and 380 msec for subjects F and N1 respectively. Thus, unit slope can not be deemed satisfactory for this response. The only solution for this is to postulate a linear decay function for the S-D stress time, of the form:

$$[TSD] = TSD(1 - t/T_o), \qquad \text{Eq. 7.14}$$

where t is the elapsed time since the passage of the first stimulus, and the function is constrained to be identically zero for values of t greater than T_o. The choice of a linear function is not intended to exclude some other form, such as an exponential; the experimental data, however, are sufficiently scattered as to make the determination of the precise functional form difficult, and the linear fit which has already been made is therefore felt to be satisfactory for the purposes of the model.

A decaying expression implies that the extra time, [TSD], is in fact a function of the time proximity of the two stimuli in addition to existing only for the S-D second stimulus. Given such a function of time it is possible to match the slope of the upper portion of the S-D second response curve, as:

$$SLOPE_{s-d} = 1 - TSD/T_o. \qquad \text{Eq. 7.15}$$

TABLE 7.4

Model Parameter Values Derived From Experimental Data

(See Table 7.1 and Equations 7.8 through 7.15)

Subject	F	N1	B
TCI	45	20	30
TED	55	70	20
(TSC + TCM)	95	105	150
(TSC + TRS)	230	220	225
TUT	6	6	2
[TSD] ↗	103	87	10
[TSD] ↘	130(1 - ST2/605)	110(1 - ST2/655)	- - - -

Note: See text for symbols used in this table. All parameter values are quoted in msec.

Under the interpretation of t in Eq. 7.14, ST2 specifies t, and the value of the function [TSD] to be used for any given calculation can be evaluated at the time of entry of the signal into the error determination unit. With this stipulation, it can be seen that the value of [TSD] determined earlier from Eq. 7.12, is the function of Eq. 7.14 solved for a value of t equal to BR_{s-d}. Using this figure, Equations 7.14 and 7.15 were solved simultaneously for TSD and T_o, and the functional form of this parameter is also given in Table 7.14 for subjects F and N1. Such a solution was not made for subject B, because it was felt that the value of [TSD] derived from his response is too small to allow the legitimate introduction of this effect (it makes an insignificant contribution).

Experimental-model comparison and evaluation. - The first criterion that any model of this nature must meet is that all associated delay, or refractory times be positive. Although this might seem a trivial consideration, there is no guarantee that it will be met. The results in this case do fulfill that requirement. Secondly, and more important, is that the model response agree with the data that this model is to fit. Using measured deviations between the experimental and theoretical curves, it is possible to derive a confidence range for each of the nine curves. According to the derivation of the model parameters, the model fit to the LAG values is exact, and derivation of confidence has no meaning. For the six second response curves, however, the calculation has been performed, and the minimum and maximum confidences for each curve is listed in Table 7.5. A table entry of (100) implies that the theoretical and experimental curves crossed somewhere in the range under consideration.

Finally, the theoretical responses have been plotted in Figures 7.8 through 7.10, for subjects F, N1, and B respectively The outer limits of the 90 per cent confidence intervals for the experimental curves are plotted on the same sheets for comparison.

TABLE 7.5

Significance Limits of Model Response

Table contains the maximum and minimum significance levels for the comparison of the model response to the experimental response. (100) indicates that the two curves cross at some point.

Subject		F	N1	B
S-D	MAX	85	73	82
	MIN	85	73	57
S-S	MAX	(100)	(100)	(100)
	MIN	48	86	74

Abbreviations: S-S, same-same stimulus in normal experiment; S-D, same-different stimulus in normal experiment.

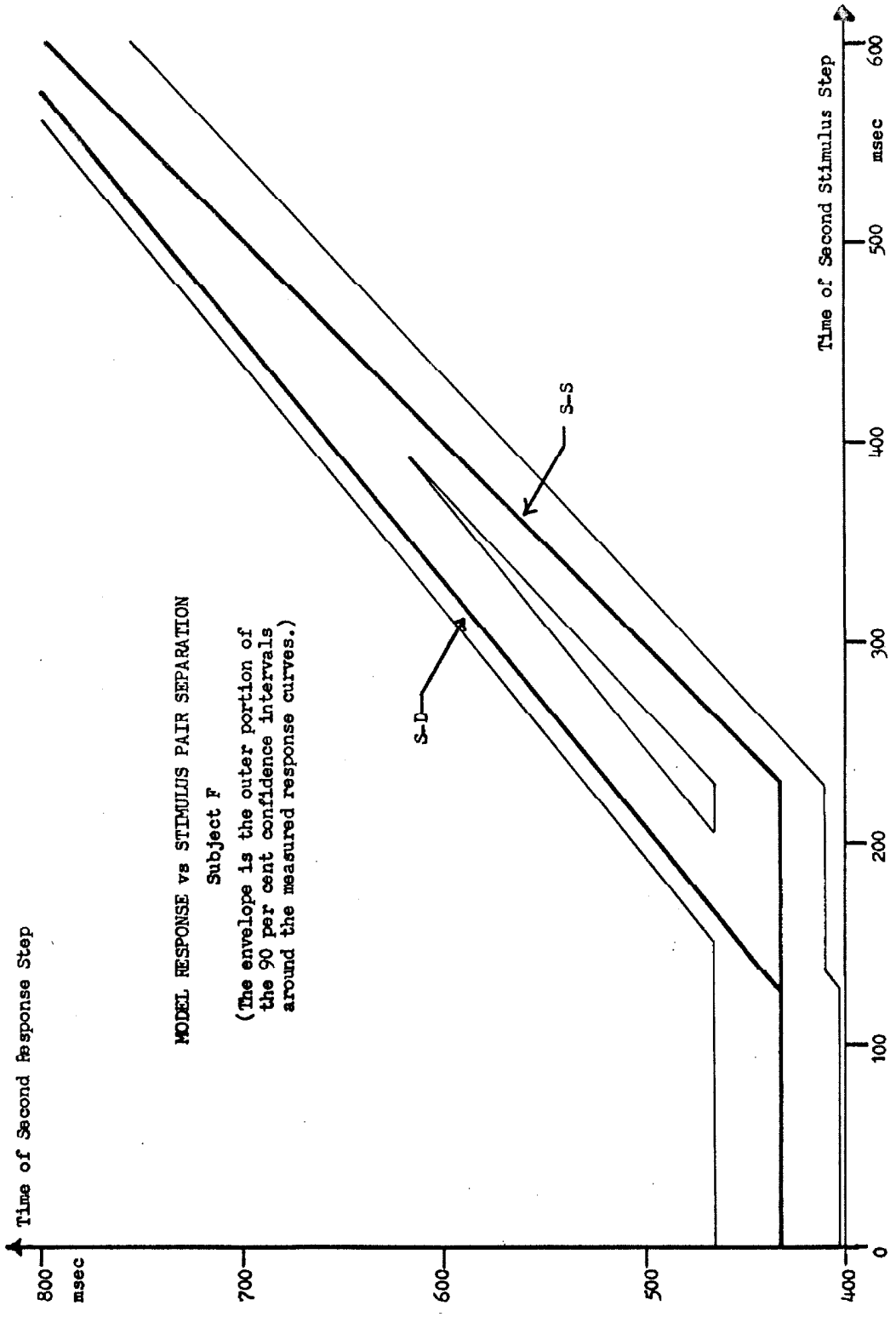

Figure 7.8 - Saccadic model response for subject F.

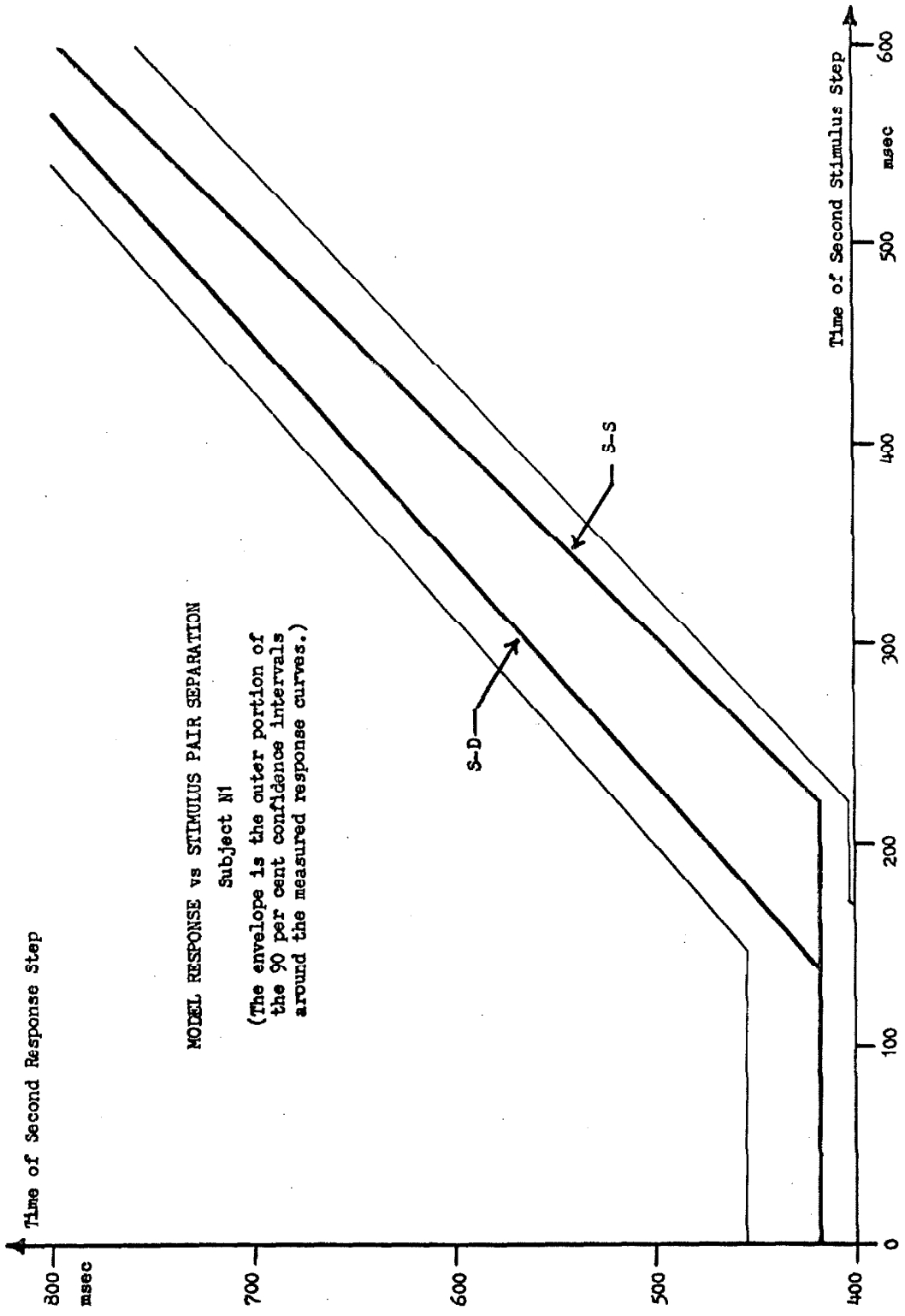

Figure 7.9 - Saccadic model response for subject N1.

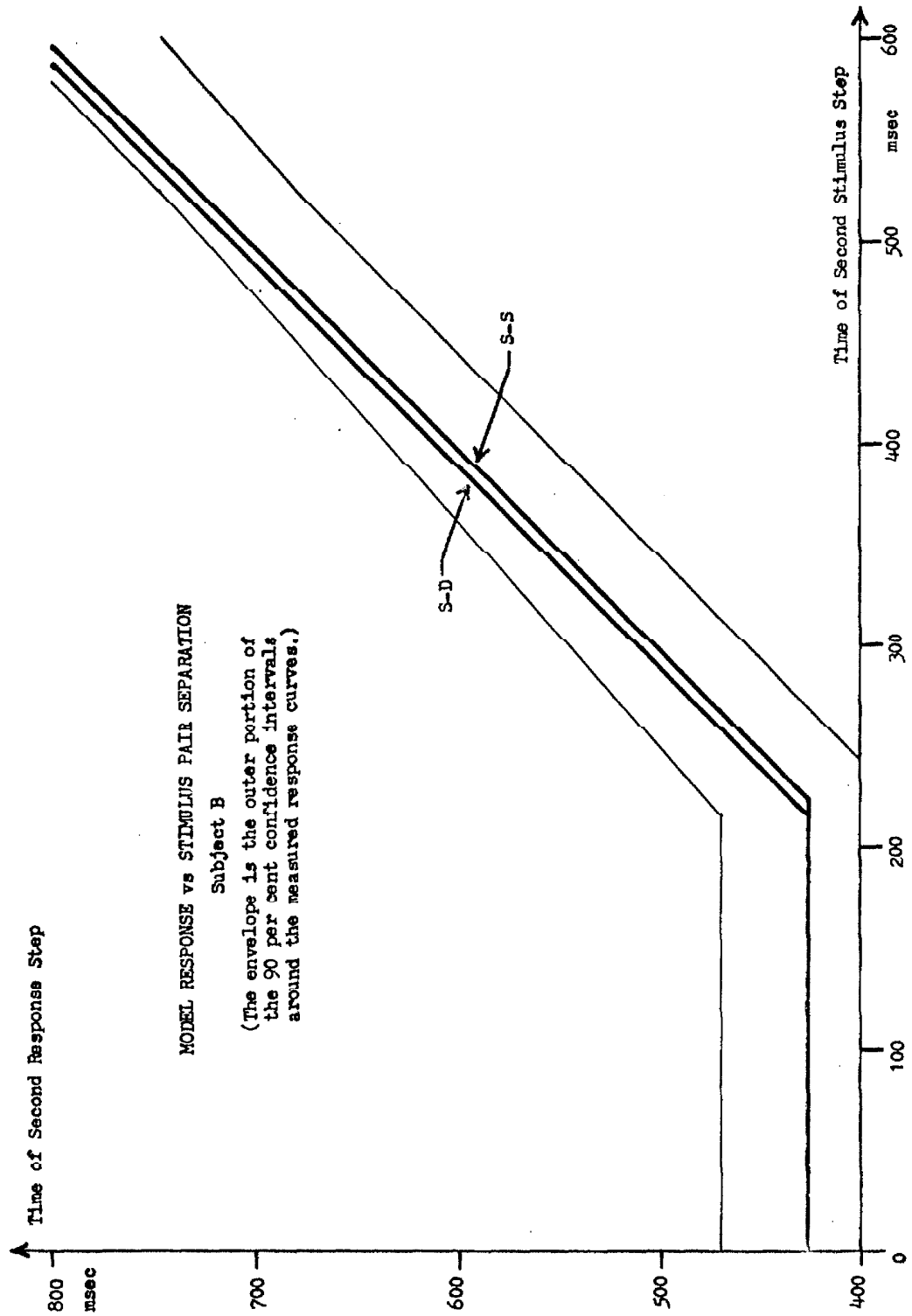

Figure 7.10 - Saccadic model response for subject B.

Conclusion

The final proof of any model, however, is not its significance to the experimental data, but rather its plausibility. This aspect of the system here presented can be considered from several directions. In the discussion which follows, the more important sections of the model will be considered individually.

TCI and TED as thresholds. - The experimental effect that was noted of aborted or altered responses is not surprising. In the limit, as the stimuli become closer spaced, some effect on the response should be expected. If nothing else, the pause between stimulus steps will become so short as to be unnoticeable. Further, the effect is noted for all three subjects that the decision (unconscious) to halt a response can be made later than the decision to alter it. Thus, the thresholds to S-S stimuli (TCI) are uniformly shorter than the thresholds to S-D stimuli (TCI + TED), where in the latter case, the initial response need only be inhibited. In this line, it is interesting to note that the threshold for the abnormal experimental condition was also longer than for the S-D stimuli in the normal runs. This is truly an effect of predictability. The subject, knowing that the only alteration he will ever need to make to a response is to inhibit it, manages, again unconsciously, to postpone this decision. How this effect would enter into the model is not clear. On the face, it implies that the response can be altered after the initial information enters the command unit, and no provision has been made for this in the model.

[TSD]. - This parameter, with its specificity to the second step of an S-D pair was the most suprising development of the model to the author. A speculation as to its source has already been made to the effect that this represents the extra time necessary to alter a description of the error. This interpretation of the effect accounts for the differences noted between the S-D and S-DA experiments. In the case of the latter experiment, where the subject knew that the target

would return, the error description could be changed independently of the signal, before the stimulus step occurred. Likewise, the first step of any normal pair could be prepared in this manner. This is a predictability effect which explains the fact that [TSD] does not appear in the initial response time, and that the S-DA curves are much more similar to the S-S curves for subjects F and N1, than they are to the S-D curves.

This recomputation time is not, however, solely a result of the required change in error description. The fact that the S-S curves are nearly unit slope, and that the S-S and S-D curves converge in all cases forces a time decay onto the variable [TSD]. Thus, [TSD] is the result of the necessity to perform the recomputation a short time after the passage of the preceding stimulus. The time constants for this term in the case of the two subjects in which it could be evaluated is quite close to the maximum stimulus separation used in the experiments. Nevertheless, it should be expected that the two response curves ultimately coalesce along the forty-five degree line predicted by the sampled data model.

It should be noted that this problem is not simply a fluke of the model chosen. Several alternative hypotheses, which might be more acceptable from the logical point of view, have been tested, but none of these is capable of matching the experiment. For instance, a negative specificity could be attached to the S-S responses, and allowed to decay to zero as the system 'forgot' the error description from the previous stimulus step. Such an effect would account for the difference in break points, but would reverse the slope relationships. Also, it can be seen that the [TSD] term must exist prior to any refractory units in the system - the saccade command unit with its ability to handle only a single stimulus at a time. If this condition is not met, the break point relationship of the experimental data cannot be maintained with a common RDC level.

TSC, TCM, and TRS. - These three parameters are of the group that cannot be determined uniquely from the experimental data at hand, and probably, owing to the rote action of TCM, can never be determined by purely psycho-physical experiments. The inclusion of the effector unit is in no way required from the data. The values of (TSC + TCM), and (TSC + TRS) in Table 7.4 show that TCM could be set to zero, and the system would perform in an equally satisfactory manner. The inclusion of an effector is strictly a logical attempt to indicate a separation between higher, reasoning, and lower, almost mechanical, regions of the CNS.

Secondly, there is no reason strictly based on the results why the detector units could not be included in the refractory computer unit, except the restriction mentioned earlier that TSD must remain ahead of this unit. Such a system, with the total response time included in the computer section, is simply the sampled data model with two important exceptions, the first of which is the restriction on TSD. The second restriction, however, is that even if TCI and TED are set to zero (the threshold functions could be performed inside the command unit) along with TCM, the resulting value of TSC would be only on the order of 195 msec for each subject. This leaves a residual value of some 25 msec in the reset time, TRS, and such a refractory factor is not compatible with the predictions of the sampled data model.

TUT. - The discussion of this parameter has been held for last, because it was the determination of such a parameter which the experiments were designed, in part, to achieve. In this sense the experiments were discouraging to say the least. The most significant fact that one can state about this parameter is that it was found as a positive factor for each of the three subjects tested. The confidence limits which the experiment produced, however, reduce the confidence in this parameter to a negligible level. If the parameter exists, and first indications (the positive sign in three of

three cases) are that it does, then the effect is in all probability a very small one. The other effects that have been measured serve to mask any effect based on unpredictability.

CHAPTER VIII

SPONTANEOUS EYE MOVEMENTS

Introduction. -Up to this point, the concern of this thesis has been primarily with the role of saccadic eye movements in tracking situations. It has already been pointed out in Chapter IV, however, that spontaneous eye movements occur in all regimes of tracking as components of the eye position that are uncorrelated with the stimulus. The most obvious manifestation of these spontaneous movements occurs when a subject is asked to fixate a small stationary target - a task which nominally requires no eye movements. It was the question of what the eye was doing during these steady fixation tasks that lead many of the early investigators to develop accurate methods of measuring eye position (1, 32, 39, 52); for visual observation could determine the large voluntary changes in fixation position, but not what was occurring during steady fixation.

The initial studies of fixation in which accurate measurement techniques were available tended to concentrate on two aspects of the spontaneous eye movements. The first problem was to determine what components of eye movements existed, and what their relative magnitudes and frequencies were. (2, 17) Ditchburn and Ginsbourg (17) provide a good summary of these measurements. The second aspect brought under consideration was the functional relationships which exist between the spontaneous movements and perception. The evidence on these points has already been cited in Chapter II.

It has been demonstrated that eye motion during these periods of steady fixation is a primary factor in maintaining clear vision, and the role played by each temporal component - flick, drift, and tremor- has been examined independently; the next question which might be asked is of the relationships between the flicks and the drifts in this

spontaneous regime. It is this aspect of eye movements that is investigated further in this chapter.

Previous Studies

Many researchers interested in control mechanisms of the eye have pointed to minor aspects of the interrelationships between flicks and drifts during steady fixation. Fender(24)notes that drift movements are started in random directions, but tend to maintain their initial direction. During fixation of a point target that is not in the primary position (along the reference axis defined in Chapter II) he notes a tendency of the eye to drift towards that position, and then to flick back to the correct target position. Nye(47)analyzes the "wander" of the fixation position in terms of the feedback system that he derives for smooth following. He concludes that the fixation wander in normal vision is primarily a function of the position insensitive region at the fovea of the eye. Specification of a precise interrelationship between slow and fast movements, however, has been best presented in two studies, one analyzing the horizontal component of the orb position only, and the other dealing primarily with the drift, but using two dimensional analysis.

One dimensional statistics. -The drift-flick interactions, as detected from the horizontal component of eye position, have been thoroughly studied by Cornsweet (13), and by Krauskopf, Cornsweet, and Riggs (36). The conclusions reached from their studies can be simply stated. The drift movement of the eye happens at random; as this drift moves the image across the retina, and away from foveal regions, a threshold is crossed which initiates a flick to move the image back to the center of the fovea. They find that the probability of flick initiation increases by a factor of three as the position error of the fixation axis from the center of the fovea increases from zero to six min arc. Further, they find a tendency for the flicks to overcompensate this error. This last is a most interesting finding.

From studies of the tracking mechanism, such as in Chapters V and VII, one expects a time delay between error detection and flick initiation on the order of 200 msec. In this case, the flicks should undercompensate by the amount of the additional error that the drift generates between the detection of the error, and the initiation of the saccade.

Two dimensional study. -Nachmias (45) studied the fixation movements using a measurement technique which obtained both the horizontal and vertical components of eye position. He concluded that the role of flicks in compensating drift errors was not as clear-cut a causal relationship as the earlier studies had found, but that there were specific directions from the fixation center along which this direct effect could be measured. In other directions, however, he found little compensatory action by the saccades. In a later paper, Nachmias (46) studied further the origin of the drift. Whereas earlier work by Fender, Nye, and Krauskopf et al. had assumed that the drift direction was a random function, Nachmias' initial study had indicated a definite preferential direction for this component. The subsequent analysis which he performed tended to reveal two effects. First, the eye did tend to drift in a preferred direction, and this direction was oriented upward and temporally for both subjects. This effect he speculatively allotted to instabilities in specific eye muscles. The second effect he noted was a definite interaction between the preferred drift direction and the position of the target relative to the primary position of the eye. A deviation in the target position from the primary position tended to orient the preferred drift direction towards the primary position.

Objections to these studies. -While these two studies would appear to produce a definitive statement on the interplay between the drifts and flicks in this situation, there are several possible objections. First, Nachmias' fixation patterns, as well as similar patterns produced by Nye(47) and others, show that the vertical component of

fixation wander is usually greater than the horizontal. This would tend to cast doubt on the statistics produced in the one dimensional studies. Although such an analysis could be presumed to show the proportional relations between flicks and drifts, the threshold errors measured would be incorrect. Also, the previously noted over-compensation by the flicks would appear to be a suspicious aspect of a system in which this component serves a solely corrective function.

Finally, Nachmias' second study tends to cast doubts on the results he had measured before. If the primary position and target position were not the same in his earlier experiments, it would seem likely that this misalignment could account for the strong corrective tendencies he noticed in certain directions. It should be noted that such a misalignment occurs more often than not, unless care is taken to avoid it.

With these objections in mind, the author undertook an experiment to restudy these questions. The intent was to obtain statistics, similar to those of Cornsweet, which could be applied in two dimensions. The initial results, however, showed that the whole subject deserved review and re-emphasis. The primary finding, as will be seen, is that the majority of the flicks, far from being corrective, are in fact random.

The Experiment and Data Processing

The design of the experiment is aimed at obtaining records in the computer from which a wide variety of statistics relative to the origin and role of drifts and flicks can be obtained. The experimental condition sought is one in which the subject fixates a stationary target steadily while his eye movements, spontaneous by definition, are measured. The data reduction techniques then allow the specification from these records of the eye positions at the beginning and end of each flick, the drift being simply specified as the eye movement which occurs between the flicks.

Experimental procedure. -Although the experimental condition was simple, as the subject was placed in the apparatus and instructed to fixate a pinhole (two min arc in diameter), great care had to be taken to eliminate two potentially confounding effects - eye fatigue and off axis fixation. Observations were carried out for two minutes each, and the subject was continually urged to abandon the experiment if at any point he felt fatigued. In addition, the experimenter kept close watch on the eye movements displayed on an oscilloscope. If any signs of fatigue appeared, such as excessive drifts or a high blink rate, the session was terminated.

In order to avoid the pitfalls of placing the targets elsewhere than in the primary position, use was made of a subjective measure of this error. The experiments in Chapter VI would indicate that a subject should be able to perceive his spontaneous drift, as it disagrees with efference copy, but should not be able to detect the flicks. In an experimental condition where the primary position and the target position differ and thus generate systematic drift with corrective flicks, the subject perceives the target continually drifting away from his primary position as in the autokinetic illusion. When such systematic wander was noted by the subject, and it generally required a minute to become apparent, he was told to move the target in the opposite direction to the perceived systematic drift until it ultimately ceased. The experimental runs in which this occurred were discarded. In subsequent runs, the subjects reported that the target still drifted, but that they could not detect a systematic tendency in this motion.

Recording and transmission. -The recording of the experimental runs was controlled by the Biosys Data Terminal (BDT) so as to allow the calibration of the eye position signal at both ends of each experimental record. The BDT was wired to produce an experiment 122 sec long. The first and last two seconds of each run were reserved for calibration, the calibrating unit executing a 1.5 sec pulse movement at time zero and 120 sec. The remaining 118 sec constituted the

useful data record. The analog signals representing the eye positions for each run were transmitted directly to the computer using a time-multiplexor; this A/D conversion was executed at the rate of 50 samples per channel per second. In addition to the eye position, the logical sum of the four flick detector outputs - temporal, nasal, up and down - was required by the data processing programs. This information was recorded on the analog tape recorder, and subsequently transmitted in the TOE mode.

Basic data processing. - The forms of data processing that were applied to these experiments were as varied as the desired statistics, but there was a common initial processing for all sessions. The information to be derived from the data require the following:

i) that a true calibration, from voltage transmitted to min arc, be achieved;

ii) that a mean position which could be designated as the center of fixation be established for each run;

iii) that blinks be eliminated from the records;

iv) that each flick be identified and categorized as to initial position, final position, and time of occurrence; and

v) that the overall pattern of fixation be stored.

Utilizing the data derived from items (iv) and (v) above, it is possible to generate the majority of the statistics needed. Accordingly, these data were stored on an intermediate storage tape, so that the varying forms of statistical analysis could be performed on subsequent computer runs without the necessity of reperforming the basic processing.

The program which satisfied the above requirements is outlined in the steps that follow. These steps are laid out in some detail in an attempt to eliminate any question as to the meaning of the statistics to be presented later.

i) The data for each run were collected from the storage tape on which they had been saved during data transmission from the BDT.

ii) For each component, the four calibration steps were located and averaged, and the resulting calibration factor was used for multiplicative scaling of the raw data.

iii) The mean of each directional component was found and subtracted from the data.

iv) Then, all data points for which either directional component was greater than 40 min arc were flagged and ignored in subsequent computations. This limit was determined from initial runs, and can be shown to be more than twice as large as any expected eye position.

v) The mean of the remaining data points was again subtracted. At this point, the data were ready for reduction into flick and inter-flick drift components. The following five steps were performed cyclically until the end of the data lists was reached.

vi) The current flick (as designated by the TOE list) was checked for time proximity to the next flick and the previous one. Tests in the laboratory showed that blinks were revealed by the flick detector as a series of "flicks" separated by about 75 msec, whereas true flicks seldom occurred closer together than 100 msec. As a result, flicks from the TOE list which were closer than 85 msec to each other in time were discarded, and the program stepped to step x.

vii) If the time separation was satisfactory, the flick was identified in the vertical and horizontal eye position lists as the maximum displacement occurring over a 40 msec interval within 60 msec of the time indicated by the flick detector. This technique eliminated the necessity of obtaining the mathematical derivative of the eye position, and permitted the broad, 20 msec, sampling interval to be used. In this manner, very little position information was lost between samples, and a maximum number of samples could be compared in the computer for any given run.

viii) Once the flick had been identified, it was checked for minimum and maximum amplitudes to avoid either false detections, or small blinks. If it failed either test, the program moved to step x.

ix) For each valid flick, the following six parameters were stored to characterize the flick: whether or not a blink had occurred since the preceding flick was found (such an occurrence invalidates the corresponding drift segment); the polar coordinates of the starting and finishing points of the flicks; and the time of initiation.

x) The TOE list was advanced by one to pick up the next detected flick, and the program looped to step vi.

This loop was continued for all flicks, with the limitation that not more than 266 valid flicks could be stored in the computer, owing to space limitations. When the flick storage was complete, the program proceeded.

xi) The "matrix" containing the six parameters for each flick was written on the intermediate storage tape.

xii) The routine generated a two-dimensional fixation histogram for each run. This represented the number of samples during which the fixation axis corresponded to any given coordinate pair. The cell size used was one min arc square. This histogram was written on the storage tape and also printed to allow the experimenter to check the run for signs of fatigue. Typically, fatigue caused the fixation histogram to spread to about twice the linear size of a normal pattern.

xiii) Finally, the routine returned to step i for the next run.

Scope of the experiments. - Extensive experiments were performed on three subjects, and shorter sessions of a confirmatory nature were run on a fourth. The primary conclusions can be drawn with equal validity from any of the four subjects, but histograms will generally be presented for only one or two subjects at a time - for the sake of clarity and compactness. The data to be presented

represent varying viewing periods, and therefore varying numbers of samples. The minimum length of experiment which is combined for these results is 8 minutes, and the maximum length is 22 minutes. While the 50 cps sample rate determines the number of A/D fixation samples obtained from these data, the components of major interest are the flicks and the inter-flick drift. The number of these observed during any experimental session is a function of the subject's spontaneous flick rate, and this figure varies widely among individuals. In the tables to be presented later, the number of samples on which the figures are based will be included.

The experiments were performed utilizing both the normal and stabilized vision conditions. All experiments tested the left eye of the subject.

Results

The results to be presented can be broken down into three broad categories. The first presentation is designed to demonstrate the general characteristics of fixation, and of the flicks and drifts in fixation. The second section will investigate the evidence on the corrective role of flicks. That section will show that the majority of the flicks are random events. The final section, then, will investigate the characteristics of this stochastic process with the intent of postulating a model of that process.

General Characteristics

Fixation characteristics. -The overall wander of the eye during a simple fixation task can best be represented by a two-dimensional histogram showing the frequency of occurrence of fixation at any point in the visual field. The center of the histogram may be assumed to be the target location for the purposes of expressing fixation error. The frequencies of occurrence are proportional to the time that the primary fixation axis of the eye dwelled in any particular position in the target plane.

Such a fixation pattern is shown in Fig. 8.1 for subject B. The pattern contains 5787 samples representing 115.7 sec viewing time. The numbers printed in the pattern represent the total number of samples which fell within a two min arc square located in that relative geometric position. Limitations in the printing technique restrict the maximum number that can be printed in any cell to two digits. For this reason, cells in which greater than 99 samples were found are printed as zero, and cells in which no samples were found are left blank.

It will be noted that this pattern is basically elliptical in shape with the major axis oriented vertically and skewed to the left, temporally for the left eye. Henceforward, this will be referred to as temporal skew rather than in directional terms. The source of the skew will be considered later.

The simplest manner in which to treat such an elliptical pattern is to consider an equivalent bivariate normal distribution, which has the form -

$$P(v,h) = K \cdot EXP[\,-.5(A_{vv}(v-\bar{v})^2 + 2A_{vh}(v-\bar{v})(h-\bar{h}) + A_{hh}(h-\bar{h})^2)\,], \qquad \text{Eq. 8.1}$$

where v and h are the horizontal and vertical coordinates, $\bar{v}$ and $\bar{h}$ are the mean values of these coordinates, or the center of the distribution, and K is a normalizing constant. Further, one can define the expectation values:

$$\bar{h} = \frac{1}{N} \sum_{i=1}^{N} h_i, \qquad \text{Eq. 8.2}$$

$$\bar{v} = \frac{1}{N} \sum_{i=1}^{N} v_i, \qquad \text{Eq. 8.3}$$

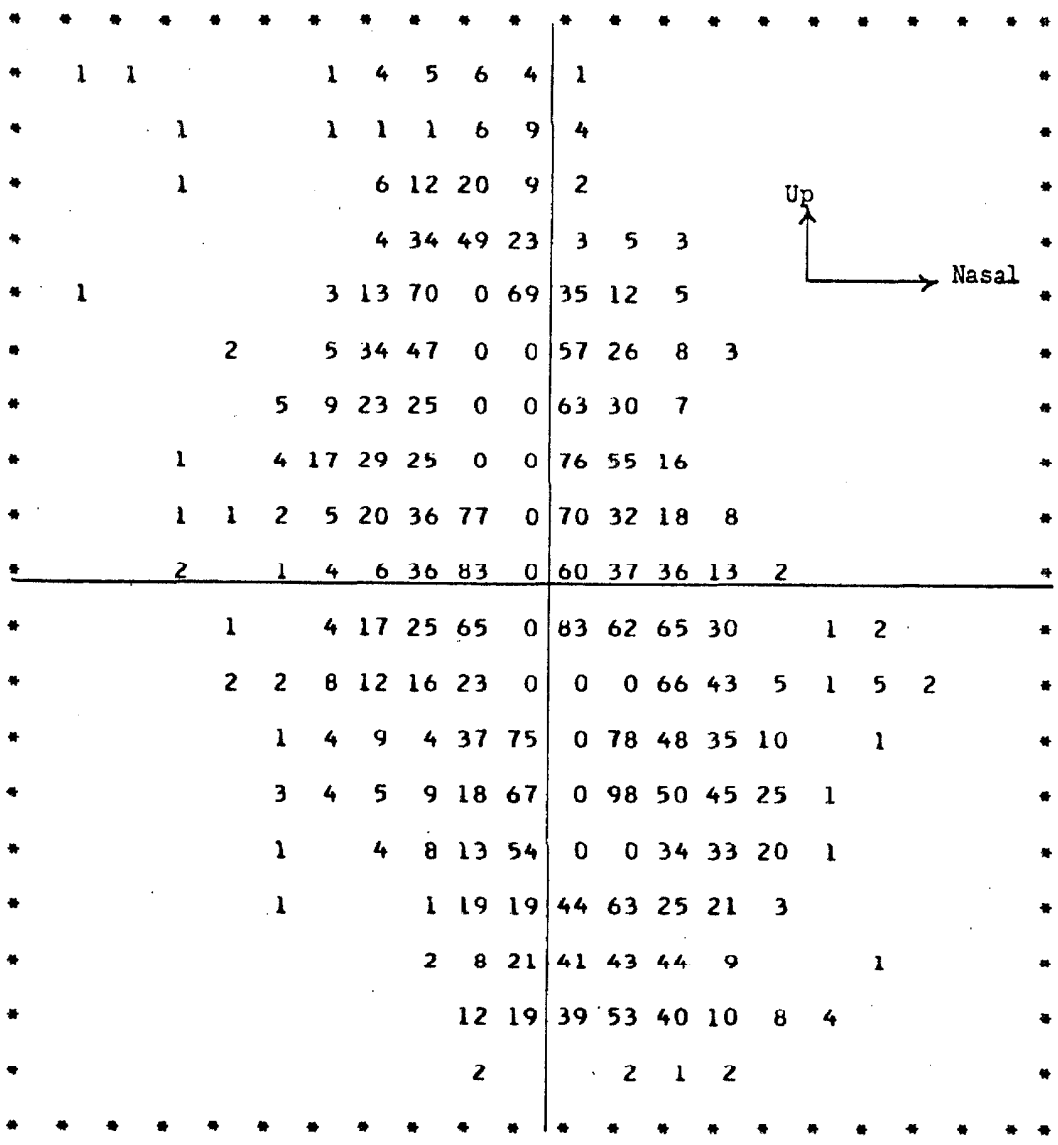

	1	1				1	4	5	6	4	1										
			1			1	1	1	6	9	4										
			1				6	12	20	9	2										
							4	34	49	23	3	5	3								
	1					3	13	70	0	69	35	12	5								
				2		5	34	47	0	0	57	26	8	3							
					5	9	23	25	0	0	63	30	7								
			1		4	17	29	25	0	0	76	55	16								
			1	1	2	5	20	36	77	0	70	32	18	8							
			2		1	4	6	36	83	0	60	37	36	13	2						
				1		4	17	25	65	0	83	62	65	30		1	2				
				2	2	8	12	16	23	0	0	0	66	43	5	1	5	2			
					1	4	9	4	37	75	0	78	48	35	10		1				
					3	4	5	9	18	67	0	98	50	45	25	1					
					1		4	8	13	54	0	0	34	33	20	1					
					1			1	19	19	44	63	25	21	3						
								2	8	21	41	43	44	9			1				
									12	19	39	53	40	10	8	4					
									2			2	1	2							

Cells in fixation histogram are 2.0 min arc square.
The squares of the deviations are:
Horizontal- 13; Vertical- 65; and Cross- -14.
The total number of points is 5787.
The temporal skew angle is 14 deg from the vertical.
The ratio of the axes of the ellipse is 2.7:1.

Fig. 8.1 - TWO-DIMENSIONAL FIXATION HISTOGRAM
(Subject B, left eye)

$$\sigma_{hh} = \frac{1}{N} \sum_{i=1}^{N} (h_i - \bar{h})^2, \qquad \text{Eq. 8.4}$$

$$\sigma_{vv} = \frac{1}{N} \sum_{i=1}^{N} (v_i - \bar{v})^2, \qquad \text{Eq. 8.5}$$

and, $$\sigma_{hv} = \frac{1}{N} \sum_{i=1}^{N} (v_i - \bar{v})(h_i - \bar{h}) \; . \qquad \text{Eq. 8.6}$$

The last three parameters are the mean squared variances for h and v, and the covariance, respectively. If the parameters of Equations 8.2 through 8.6 are determined from the samples of the distributions, then the coefficients for Eq. 8.1, can be found from the matrix equation:

$$\begin{bmatrix} A_{vv} & A_{hv} \\ A_{hv} & A_{hh} \end{bmatrix} = \begin{bmatrix} \sigma_{vv} & \sigma_{hv} \\ \sigma_{hv} & \sigma_{hh} \end{bmatrix}^{-1} \; . \qquad \text{Eq. 8.7}$$

Having determined these coefficients, the following equation generates the family of ellipses which represent loci of equal probability:

$$A_{vv}(v-\bar{v})^2 + 2A_{vh}(v-\bar{v})(h-\bar{h}) + A_{hh}(h-\bar{h})^2 = C. \qquad \text{Eq. 8.8}$$

These ellipses can be represented in general terms by the ratio of the lengths of their major and minor axes, and by the temporal skew angle of the major axis; the latter being defined as the angle between the vertical and the major axis measured in the temporal direction. The legend of Fig.8.1 includes the values of σ_{hh}, σ_{vv}, σ_{hv} the temporal skew angle, and the ratio of the axes, for the distribution in that figure.

Figure 8.1 shows the largest number of samples which can be assessed from a printout of the form shown, but the characterizing parameters have been computed for the total fixation patterns of all experimental runs performed on each subject, and these are listed in Table 8.1. It will be noted that there is considerable difference between the constants for the four subjects. First, the elliptical

TABLE 8.1

Parameters For The Fixation Ellipses

Subject	B	M	N1	F
σ_{hh}, mean squared horizontal variance (min arc)^2	15.	63.	17.	19.
σ_{vv}, mean squared vertical variance (min arc)^2	54.	40.	16.	51.
σ_{vh}, mean squared covariance (min arc)^2	-11.	-5.	-6.	-1.
θ, temporal skew angle of major axis (deg)	15.	78.	47.	2.
R, ratio of axis lengths	2.2	1.3	1.5	1.6
Minutes of experiment	20.	22.	16.	12.

ratios vary from 1.3 to 2.2. Secondly, the squared variances vary from 63 (subject M, σ_{hh}) to 16 (subject N1, σ_{vv}). It is of interest to cast these variances into terms of standard deviations. The result is that these deviations vary from four to eight min arc. This measure is seen to correspond to Polyak's "central bouquet of cones" in the fovea. (See Chapter II.) The radius Polyak determined for that region is on the order of eight min arc. Thus, the correlation between the fixation pattern and the central fovea would indicate that the fixation image is constrained approximately to this central area. The final note to be made from Table 8.1 is that although the skew angles vary widely from subject to subject, they are all less than 90 deg, so that the major axis of the fixation pattern is always pointed temporally and upwards.

Flick and drift characteristics. -In order to be able to characterize the flicks and drifts, some form of coordinate system in the target plane must be adopted. The system to be used here is a polar coordinate system with the target at the origin of coordinates. The zero angle line is in the nasal direction, and angles will be measured from $-\pi$ to $+\pi$ from this line, positive angles being in the counter-clockwise direction. In the histograms that follow, radial and angular positions will be measured directly in this system. Whenever the amplitude or direction of a component, such as a flick, is described, the numbers quoted will be the amplitude and direction of the equivalent vector in this system. The data to be presented in this section, and in following ones, are frequently in the form of histograms generated from the computer. Figure 8.2 is such a histogram. These plots are meant to be read from the side. Viewed as a vertical page, however, the ordinate is the parameter being histogrammed, increasing upward, and the abscissa is the probability of occurrence, increasing to the left with zero at the right-hand edge. The probability scale factor is printed at the top of the page along with numbers representing the one-tenth inch points.

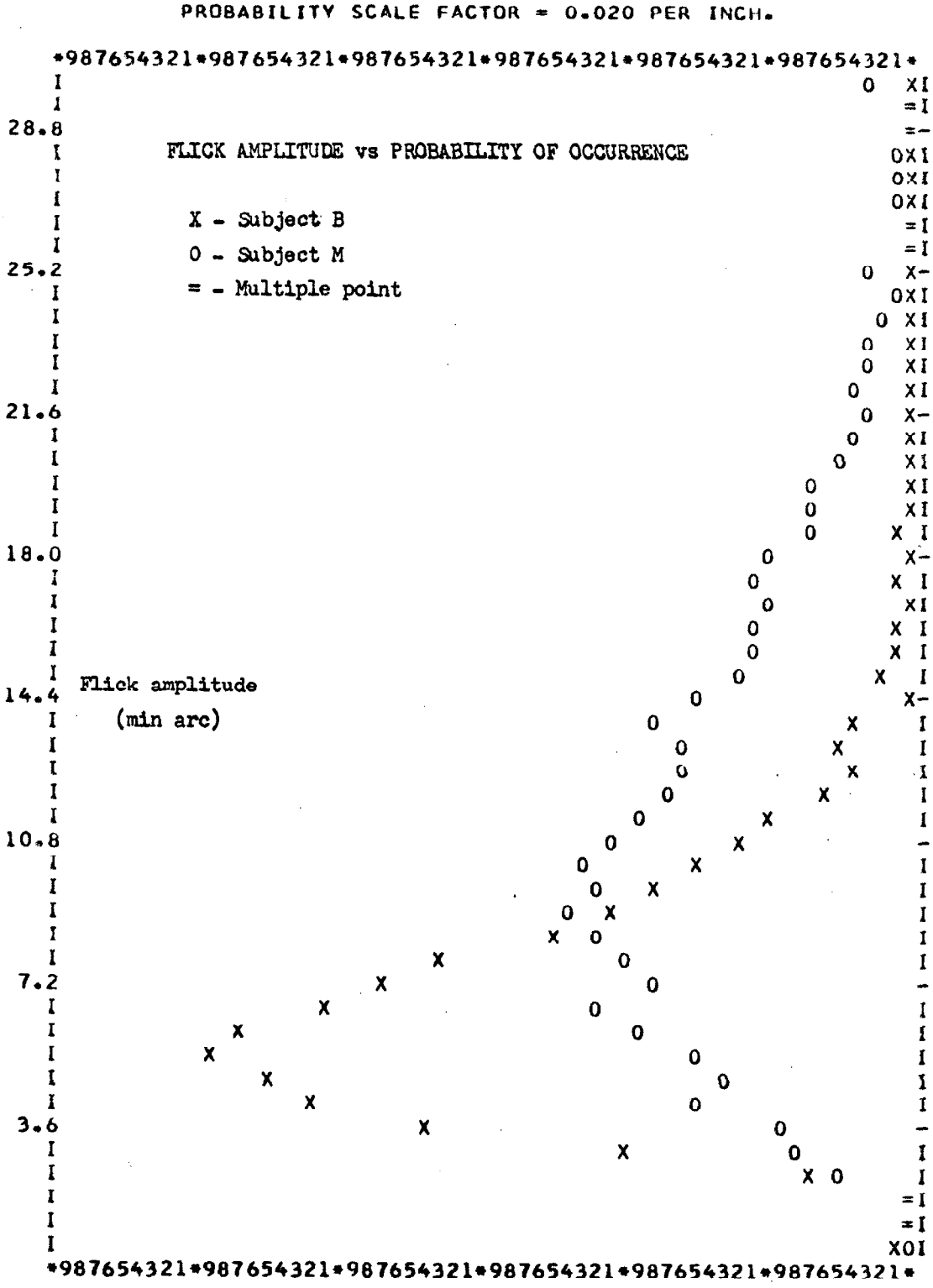

Fig. 8.2 - Flick amplitude histograms.

The overall statistics of the flicks and drifts are best represented by histograms of their amplitudes and directions. Figures 8.2, 8.3, 8.4, and 8.5 are these histograms, presenting the flick amplitude, drift amplitude, flick direction, and drift direction, respectively. These plots are shown for two subjects in order that the general shape of the distributions and the variations between subjects may be assessed. The curves for all subjects are similarly shaped; the primary variation in the amplitude histograms is a matter of scaling on the component amplitude axis, and the difference in the directional histograms is in the locations of the maxima of probability (peaks). For this reason, the histograms can be characterized by tabulating parameters extracted from them. Table 8.2 gives the following parameters for three subjects: the mean and most probable values (peaks) for the amplitude histograms, and the locations of the peaks in the directional histograms. Two values in this table are questionable. The second peak in the drift direction distributions for subjects M and N1 are quite a bit smaller than the first peak. As a result, the determination of the location of this peak is difficult for subject M, and impossible for subject N1.

These data are presented here to form a general picture of the process as it was measured. The significance of these data to that process will be evaluated shortly.

Starting positions. - The final data to be presented in this section are the starting and ending points of the flicks. Histograms of the radial starting and finishing positions of flicks for all three subjects are very similar to those shown in Fig. 8.6 for subject B. The function plotted in that figure is the probability that a flick will be initiated (or terminated) at the radial distance, R, from the center of fixation. This radial distance is equivalent to the magnitude of the error which exists at the start (or end) of the flick. Moreover, as the drift in this study has been defined as the total eye movement occurring between flicks, the histogram of flick end position is also

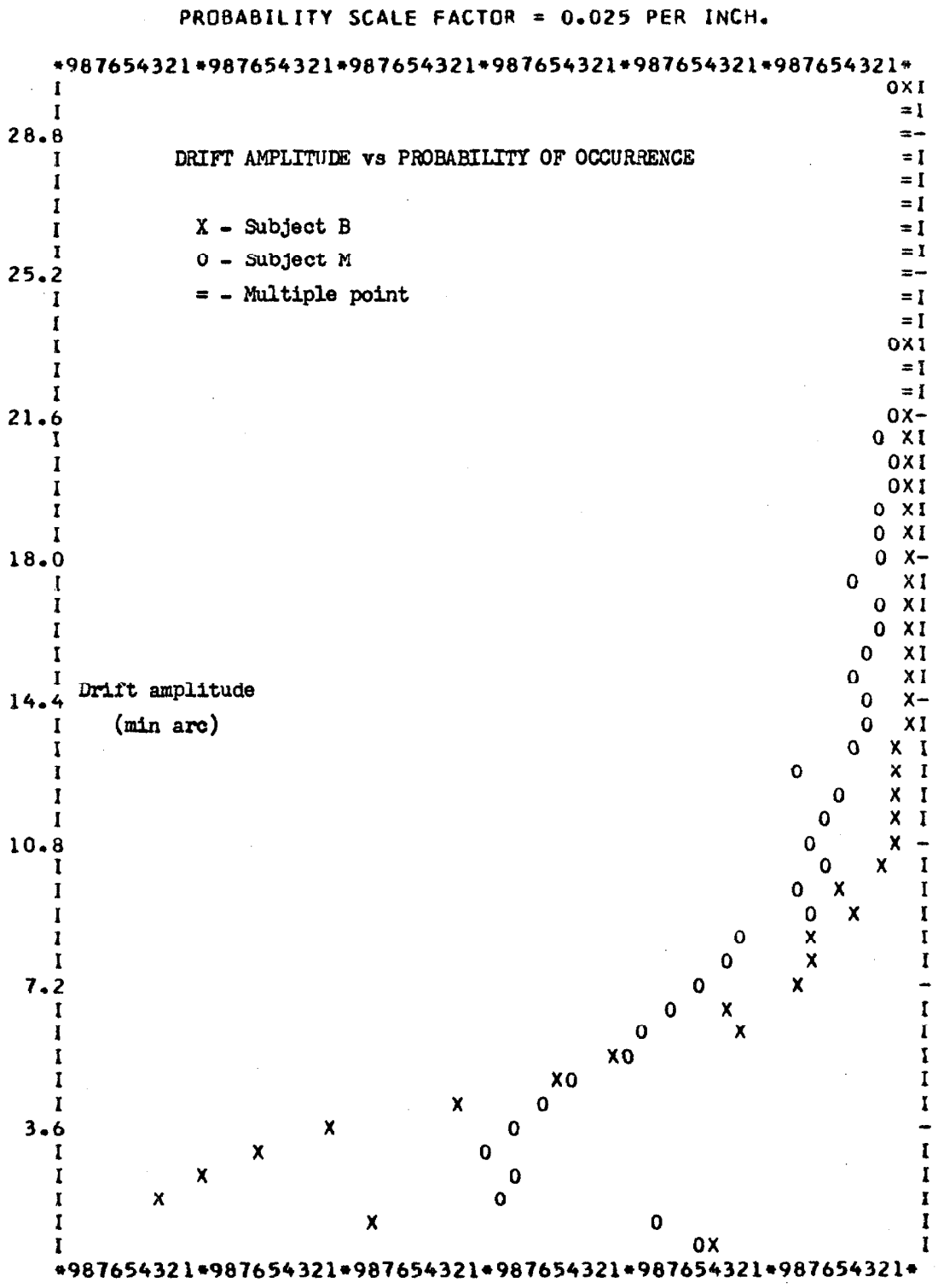

Fig. 8.3 - Drift amplitude histograms.

FLICK DIRECTION vs PROBABILITY OF OCCURRENCE

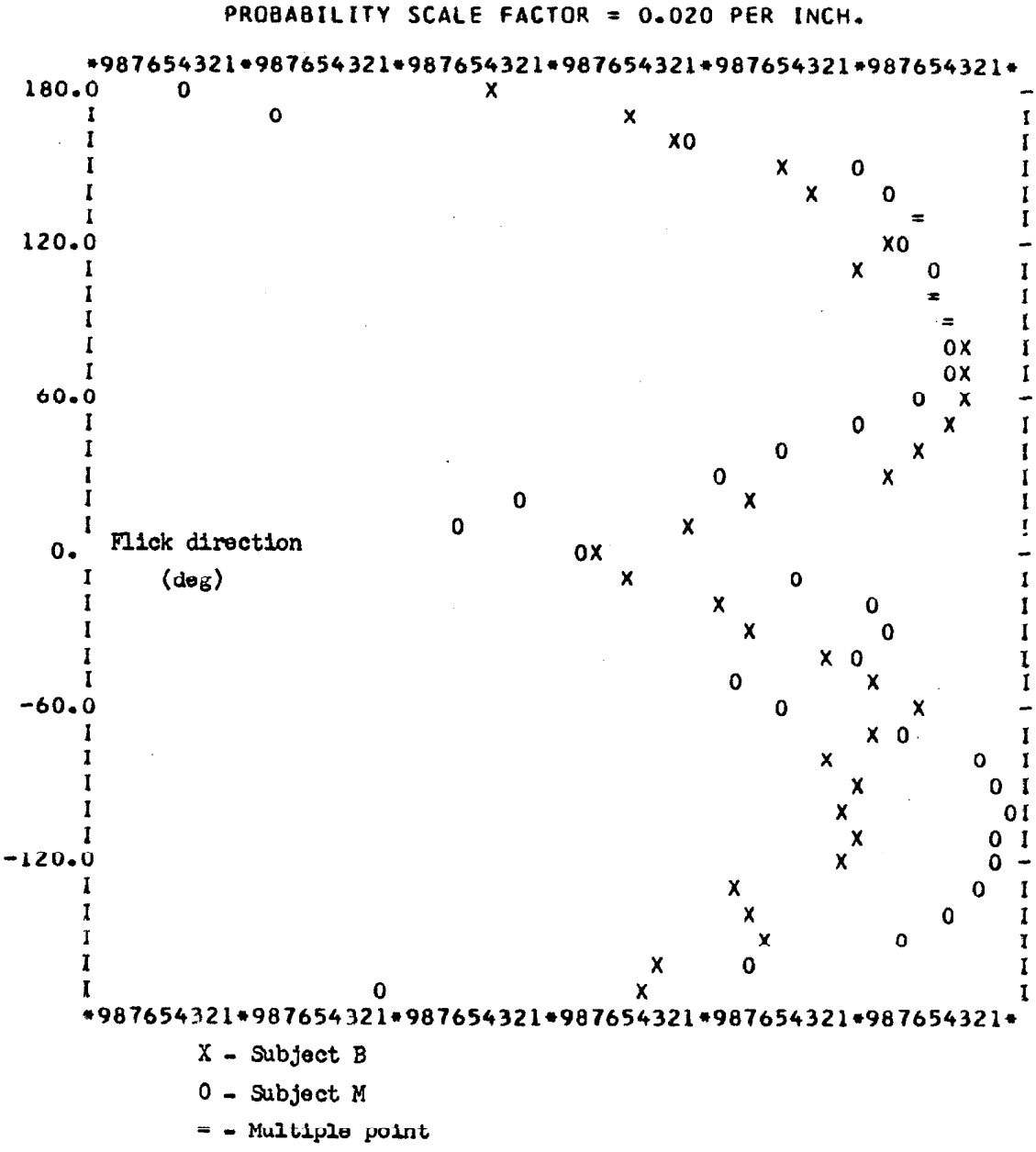

Fig. 8.4 - Flick direction histograms.

DRIFT DIRECTION vs PROBABILITY OF OCCURRENCE

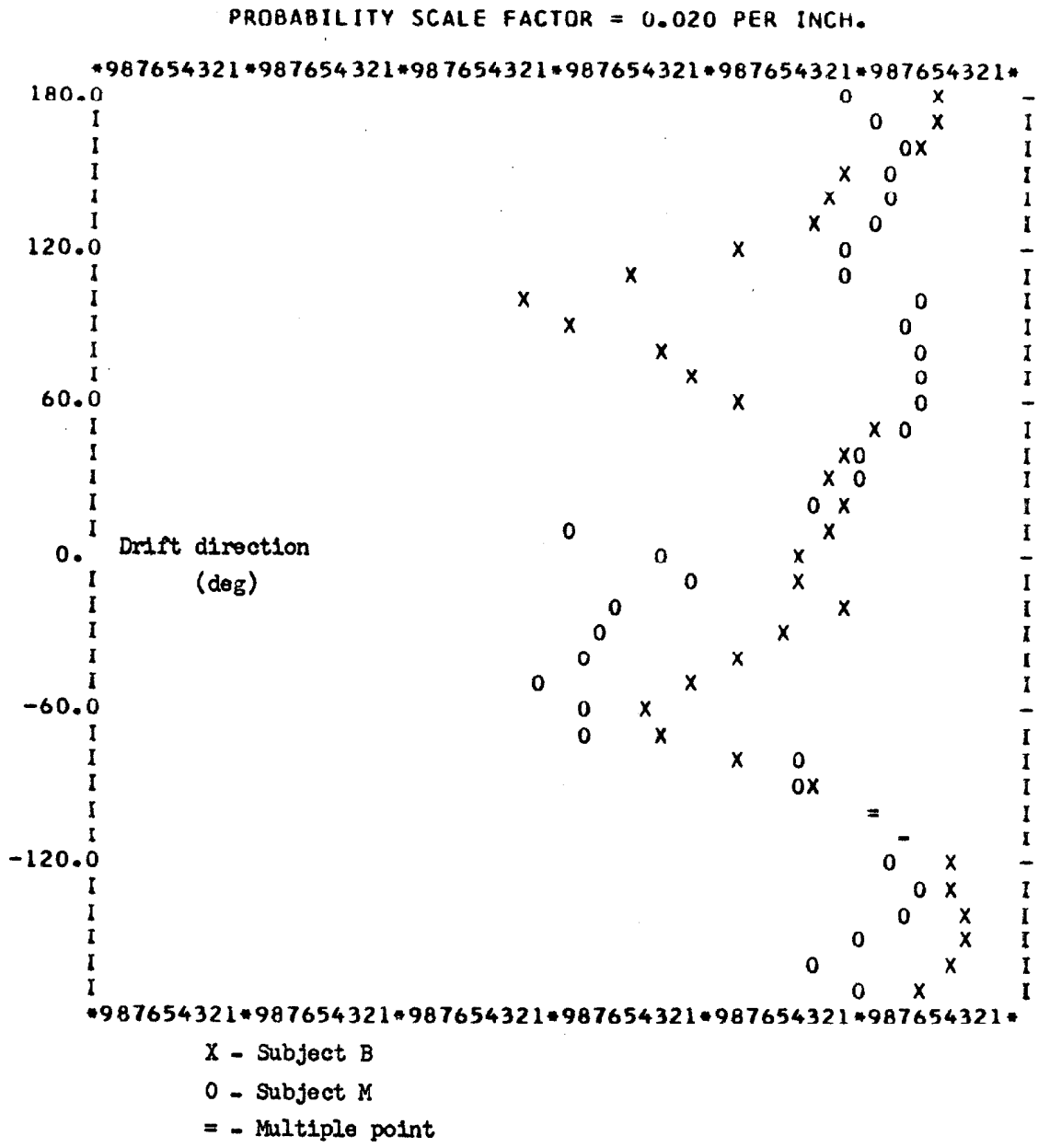

Fig. 8.5 - Drift direction histograms.

TABLE 8.2

Parameters Characterizing Flick and Drift Histograms

Subject	B	M	N1
Mean flick amplitude (min arc)	6.6	11.4	6.6
Most probable flick amplitude (min arc)	5.4	9.0	6.0
Number of flick samples	2240.	3114.	1128.
Mean drift amplitude (min arc)	3.6	6.6	4.8
Most probable drift amplitude (min arc)	1.8	3.0	3.6
Number of drift samples	2208.	2969.	1118.
First flick direction peak (deg)	0.	10.	10.
Second flick direction peak (deg)	180.	180.	170.
First drift direction peak (deg)	-60.	-50.	-20.
Second drift direction peak (deg)	100.	(110.)	- -

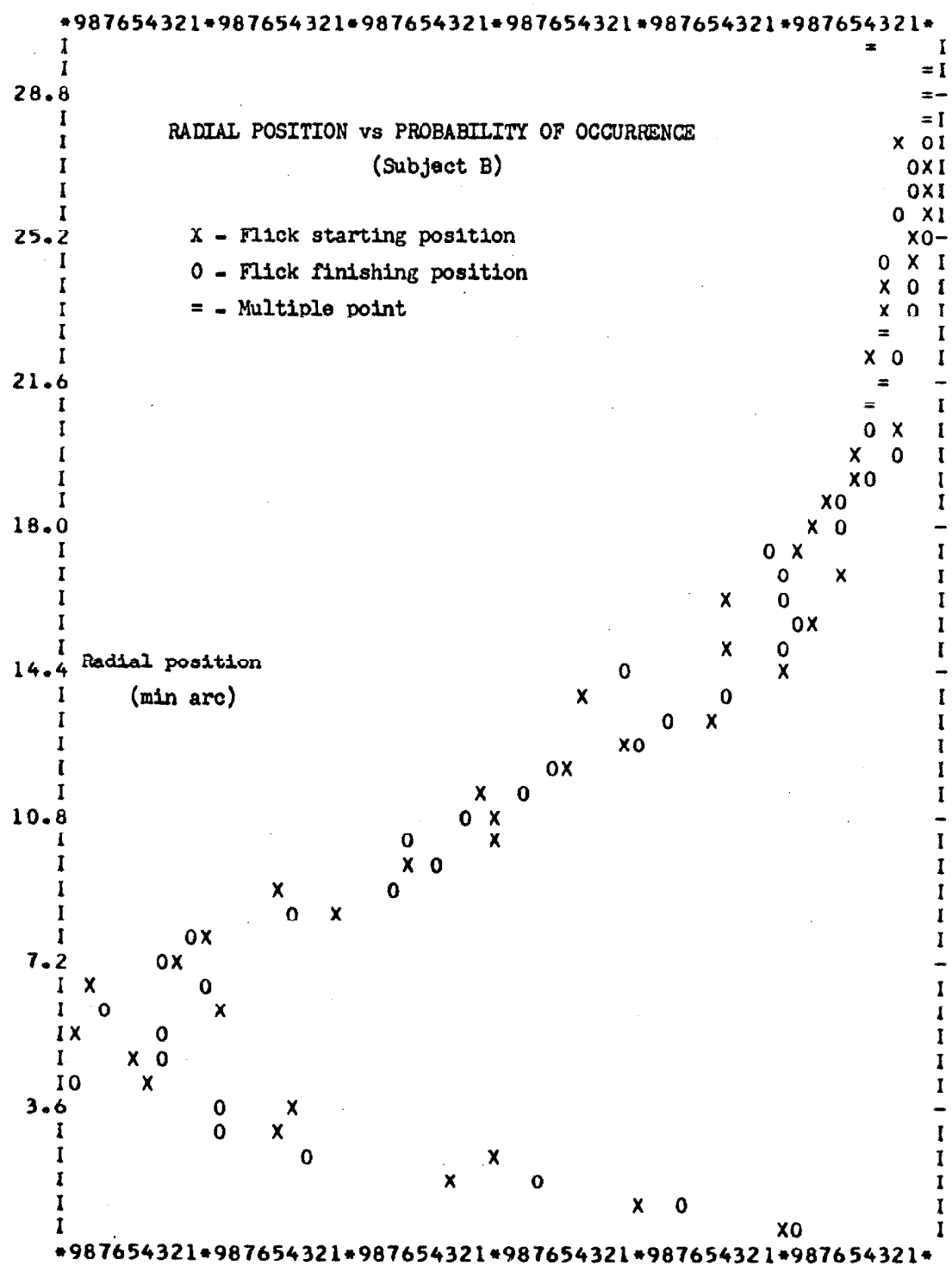

Fig. 8.6 - Position histograms showing equivalent error magnitude at start and end of flicks.

the histogram of drift start position, and vice versa. The mean and peak values for these histograms are presented in Table 8.3 for all three subjects. Two other parameters relating to these histograms are presented in that table, and will be discussed shortly.

While the mean and peak values of these histograms are useful, the form of the histogram in Fig. 8.6 is misleading. The parameter plotted is equivalent to a probability per unit radius. Thus each histogram cell represents the sample taken from an annulus whose area is proportional to the radial position of that cell. In order to present a readily understandable plot, the histograms of Fig. 8.6 have been translated to a probability per unit area by dividing the probability in each cell by its radial position and renormalizing the distributions. The resultant plots in Fig. 8.7 provide easier visual correlation with the fixation histogram of Fig. 8.1, although Fig. 8.7 contains no more information than did Fig. 8.6.

Evidence on Corrective Role of Flicks

Component relations. - The first assessment of the flicks as the corrective component in spontaneous fixation movements can be made from the overall character of the flicks and drifts, as represented by the parameters in Table 8.2, and Figures 8.2 through 8.5. If each flick serves to correct the error in the fixation position created by the single preceding drift segment, then one would expect two relationships to be revealed in the histograms. First, the mean flick and drift amplitudes should be approximately equal, unless, as Nachmias suggests, the flick is generated from information occurring about a reaction time before the flick is initiated. In the latter case, the flick amplitudes should be smaller than the drift. Secondly, if the drift exhibits any preferred direction, then the flicks, in order to correct would have to be oppositely directed.

Searching Table 8.2 for the above relationships would tend to belie the conjecture that the flicks correct the preceding drift. For all three subjects the mean flick amplitudes are substantially larger

TABLE 8.3

Parameters From Histograms of Flick Starting and Ending Positions

Subject	B	M	N1
Mean flick starting position (min arc)	8.4	10.8	6.0
Most probable flick starting position (min arc)	5.4	7.8	4.8
Mean flick finishing position (min arc)	7.8	10.8	5.4
Most probable flick finishing position (min arc)	6.0	7.8	4.2
Maximum integrated percentage difference	1.5	2.6	3.6
Position of maximum percentage difference (min arc)	4.2	6.6	3.6
Number of samples	2240.	3114.	1128.

Note: All positions in this table are in terms of radial distance from the center of fixation.

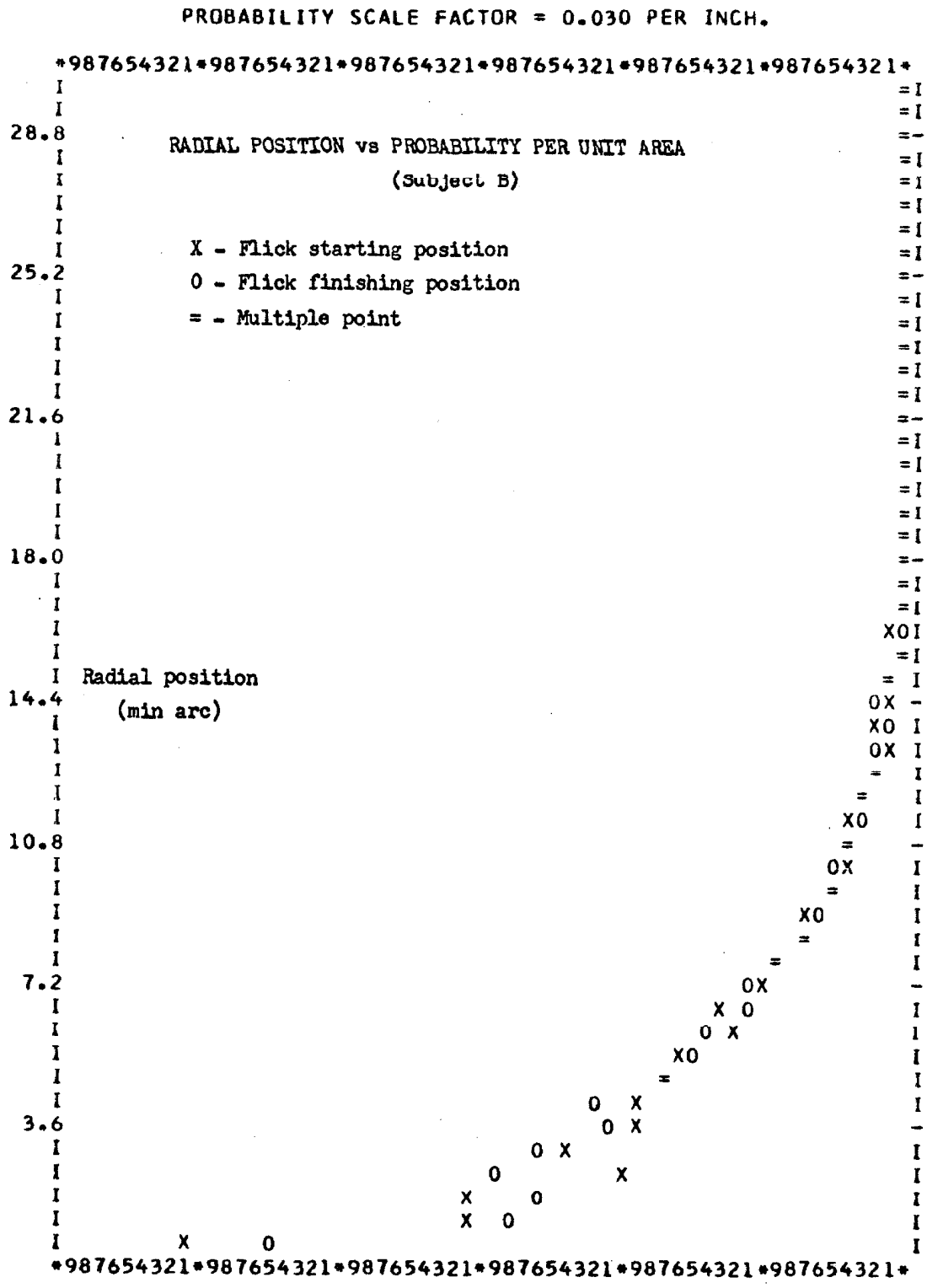

Fig. 8.7 - Position of flick starts and ends histogrammed on a per unit area basis, and renormalized.

than the mean drift amplitudes, in ratios varying from 4:3 for subject N1 to 2:1 for subject B. Moreover, the amplitudes of maximum probability for the two components possess even larger ratios. The directional evidence is just as strong. Only for subject N1 is the primary flick vector oppositely directed to the primary drift vector. Subjects B and M show a mixed directional relationship, such as can be seen from Fig. 8.8. This figure plots the flick and drift direction histograms together for subject M. Six peaks have been identified in this plot; these represent the first and second drift peaks, D1 and D2, the first and second flick direction peaks, F1 and F2, and two subsidiary peaks in the drift distribution, DS1 and DS2. It will be seen that the two axes determined by D1-D2 and F1-F2 intersect at about 60 deg. and therefore the corrective relationship does not exist between these peaks. However, the subsidiary drift peak DS1 is separated from F2 by 180 deg, as is DS2 from F1. Similar subsidiary peak relationships exist in the flick histogram. The point to be made, however, is that these related peaks are definitely smaller than the unrelated peaks.

These results show that the typical flick does not correct the preceding drift segment on a one-to-one basis. However, this does not prove that flicks are non-corrective. The distributions presented separate the angular probabilities from the amplitude probabilities, and the corrective effects must be assessed using joint probabilities measured with respect to the fixation position error, as in the discussions which follow.

Starting positions. - The histograms, and parameters, which represent the starting and ending points of the flicks have already been presented in Figures 8.6 and 8.7 and in Table 8.3. If the flicks are truly executing a corrective function, it would be expected that the ending points would be clustered around the center, while the starting

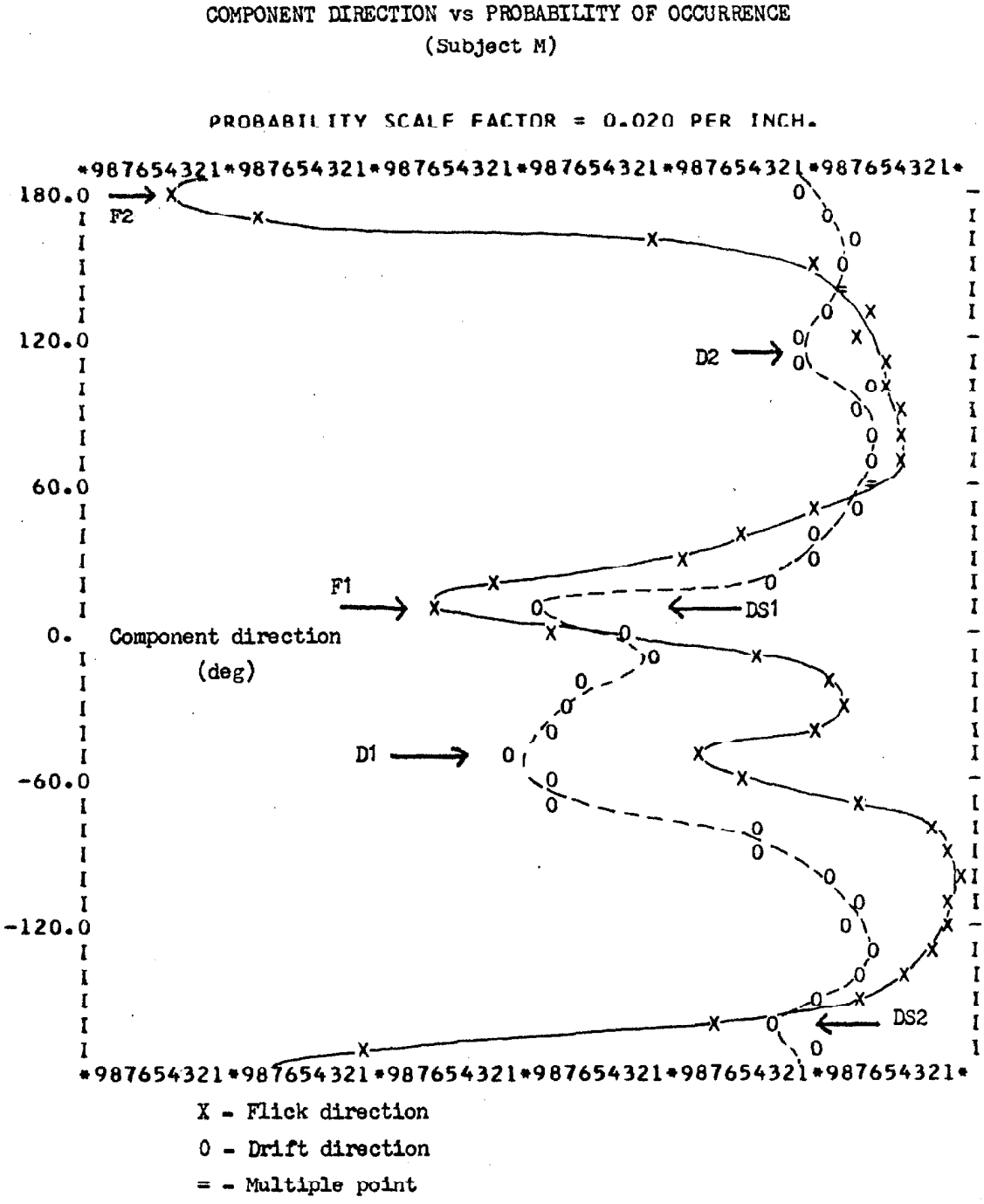

Fig. 8.8 - Direction histograms for flick and drift components.

points would be found primarily in an annular ring near the edge of the fixation pattern. Figure 8.6 shows no such effect. Furthermore, the difference between the mean starting and ending values is never greater than 0.6 min arc for any of the three subjects, although, where a difference is detected, the mean ending position is always smaller than the mean initiation position.

The information contained in Fig. 8.6, and similar distributions for the other two subjects, can be considered in another way. By integrating the probabilities represented by the two curves from the origin out to any radius, R, one arrives at curves which represent the percentage of all flicks which start or finish at a radial position less than R. When this is done, the resultant curves for the initiation and termination positions are very similar, but a definite small corrective tendency can be seen, as the percentage of flicks which end inside a given circle is always slightly greater than the percentage which start within that circle. The maximum percentage differences, and the radii at which these maxima occur are given for the three subjects in Table 8.3. The indication of these differences is that the flicks do tend to correct fixation position, but the corrective role is surely a minor one, as only four per cent of the flicks at most are correcting with respect to any given error.

Probability of flicks reducing error.-While the data just presented show that there is a corrective trend in the flicks, they represent an integrated measure of the process, that is, they are the percentages of all flicks which correct with respect to a given position. Of more interest in this line, is the individual probability that a flick initiated at any given radial position will reduce the error, the radial distance from the center. This proportion has been plotted in Fig. 8.9 for subject B. The function plotted is the proportion of the flicks initiated at a radius R which terminated within the circle of that radius. The curve would indicate that for radial errors greater than about six min arc the error is reduced, on the average, by flicks.

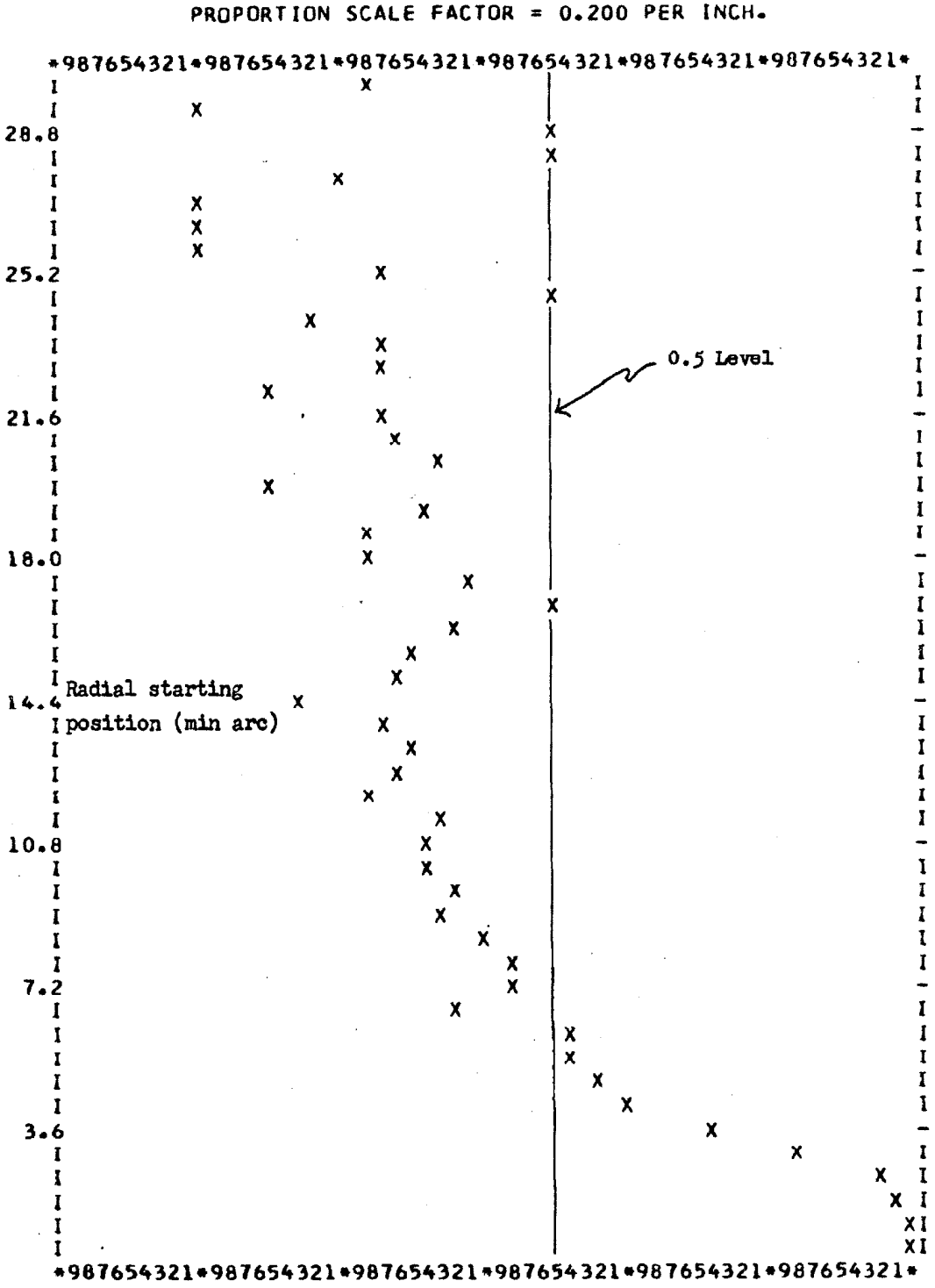

Fig. 8.9 - STARTING POSITION OF FLICKS vs PROPORTION WHICH REDUCE FIXATION ERROR (Subject B)

The relationship between position and probability of correction, however, is not the important element to be drawn from this plot. The important fact is that some of the flicks initiated at all radii do increase the fixation error. In fact, as the radial error gets larger, where 100 per cent correction would be expected, the curve of Fig. 8.9 is asymptotic to a value less than unity. This is true for all three subjects, the asymptotic values being 0.74, 0.84, and 0.82 for subjects B, M, and N1, respectively. The overall percentage of flicks which actually increase the fixation error, can be found from integrating the product of the probability of flick initiation (Fig. 8.6), and the probability of flicks reducing the error (Fig. 8.9). The results of such integration show that 48 per cent of all flicks increase the error for subjects B and M, and 46 per cent do for subject N1.

Section conclusion. - The conclusions to be reached from the data presented in this section, then, are two-fold. First, a certain percentage of the flicks do decrease the fixation error which exists at their initiation. The important fact, however, is that a large proportion, on the order of one half, of the flicks actually increase the error. Moreover, the fact that the flick amplitudes are larger on the average than the drift amplitudes would imply that most of the correcting flicks are probably compensating for error created by flicks. The results then, are that a large portion of the flicks are of random origin, and simply serve to bring a new area of the retina to bear on the target.

Ditchburn et al. (20) in their study with stabilized vision tentatively assigned the role of preventing adaptation to the spontaneous drift. They noted, however, that the drift rates which were of benefit to clear vision were abnormally large, and that flicks were actually more beneficial. It has been shown here that the flicks are about three times as large as the drift on the average, and that a large number of the spontaneous flicks are not performing a corrective function. Hence, the conclusion can be drawn that the random flicks

serve to prevent retinal adaptation by bringing fresh receptors to bear on the target image.

Before concluding this section, it should be noted that one obvious method of testing the corrective role of the flicks would be to present the target in stabilized vision, where no correction should be necessary if the stabilized image is located at the fovea. This experimental condition was used on all three subjects. The results, however, were confounded in every case by some spurious form of fixation error cue. This was evidenced by the fact that the fixation patterns expanded very little in this condition, whereas the true stabilized vision condition should have been unbounded. There are several possible explanations for this effect. Dallos (14), in performing a similar experiment, concluded that the subject generated a mental fixation point, and used efference copy to provide the error measure. The results of Chapter VI, however, would make this unlikely. More probably the optical apparatus in the experiments here provided visual cues. The field of view of the system is limited to about six deg arc by the lenses. It is impossible to keep the lenses of such a system absolutely clean, so that the subject actually perceives the stabilized image as "moving" about on a six deg arc disc of dim illumination. This disc, of course, is not stabilized, and therefore provides him with a continual measure of his fixation position.

The stabilized vision results which were obtained supported all the arguments presented in this chapter, but they have been omitted because correction of the data for the unexpected visual cues is an involved process, and it is felt that the data which are presented are more than sufficient for the argument.

Evidence on Flick and Drift Sources

Percentage of flicks which are correcting. - The data just presented indicate that a high proportion of the flicks are of random origin. The statistics presented showed that never less than 45 per

cent of the flicks serve to increase the fixation error. In order to assess what percentage of the flicks are actually correcting, it is necessary to note that the presence of random flicks which increase fixation error implies the presence of apparently correcting flicks which are actually due to the stochastic process. The assumption that something on the order of 55 per cent of the flicks are programmed to be corrective would be incorrect from a mechanistic point of view, even though the end result is error reduction.

In order to determine how many flicks are the result of a true corrective mechanism, it is necessary to determine how many perform a corrective function due only to the random process. This latter measure can be determined approximately by using the histograms presented earlier, and making suitable simplifications of these curves.

The assumptions to be used are as follows. First, the flick amplitude histogram (Fig. 8.2) is approximated as a square distribution function. Such an approximation is diagrammed in Fig. 8.10a. The points at which the true histogram crosses a probability equal to one half of the maximum (points R_o and R_i) are taken as the limits of the square function; between these limits, all flick amplitudes are assumed to be equi-probable, and zero probability is used outside the limits. Secondly, the assumption is made that all flick directions are equi-probable. This is the weakest assumption, but it reduces the difficulty of solving the problem by several orders of magnitude. The effect of this assumption will be considered shortly.

Within these assumptions, the end point of a flick will lie with uniform probability within an annulus whose inner and outer radii are R_i and R_o, and whose center is the flick initiation point. The probability that a random flick will reduce the error for any given radial position, then, is the proportion of the flick end-point annulus which falls within a circle of radius R, when the center of the annulus is positioned on the circumference of that circle. Figure 8.10b illustrates this point; the proportion being sought is B divided by

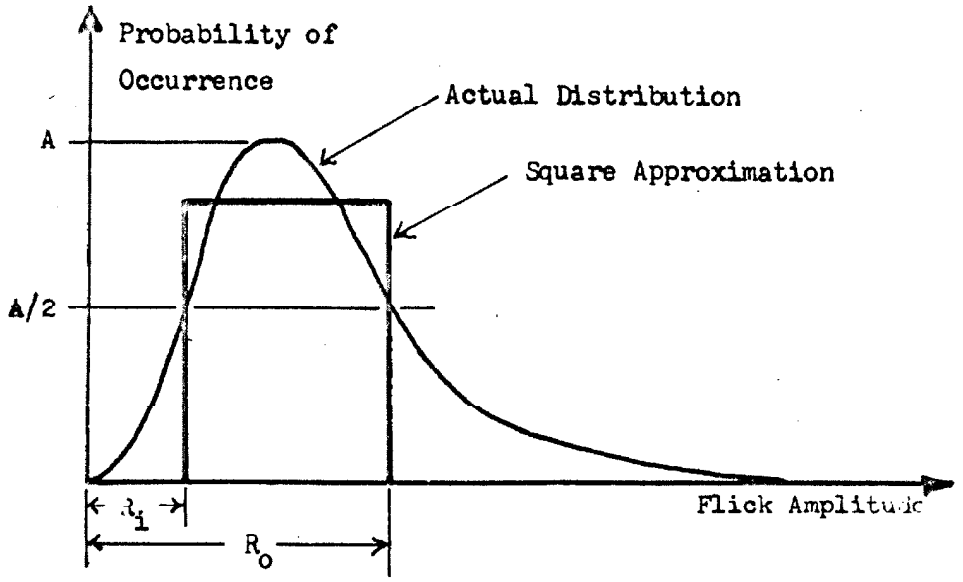

Fig. 8.10a - Square approximation to flick amplitude histogram.

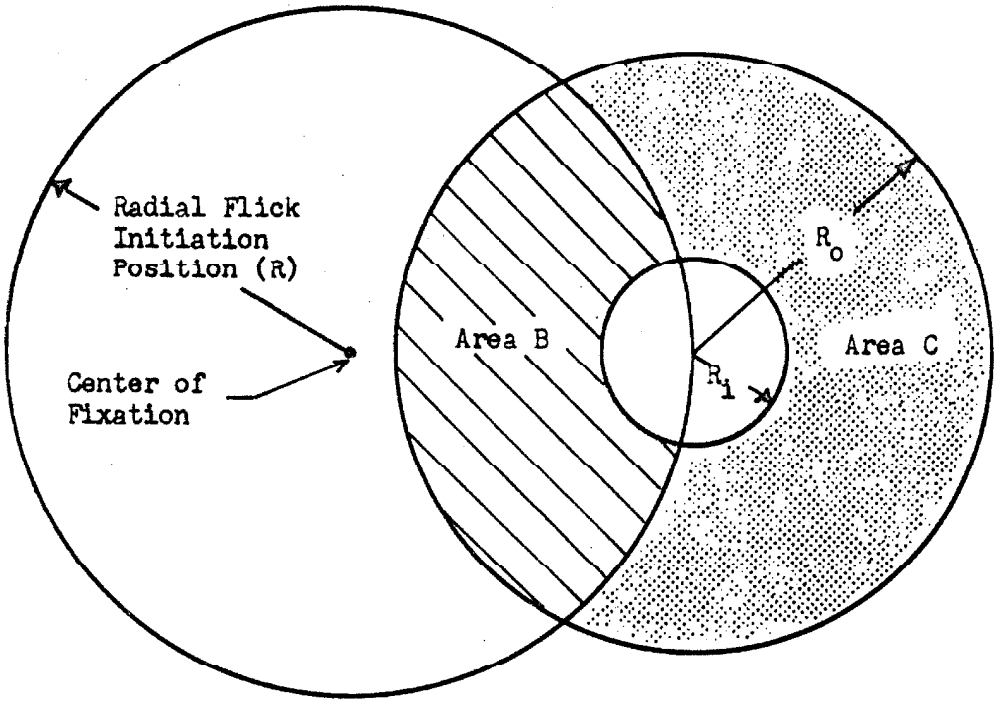

Fig. 8.10b - Geometric representation of the probability that a random flick will reduce the fixation area. This probability is - B/(B + C).

(B + C). For radii, R, less than R_i, this proportion will be zero. For values of R greater than R_i, the curve increases monotonically and becomes asymptotic to 0.5. The shape of this curve, then, is very similar to the experimental curve of Fig. 8.9, and the difference between the derived curve and the experimental curve at any point represents the percentage of flicks initiated at that point which are truly correcting, rather than simply reducing the radial position due to a stochastic generation process.

Curves such as described above are found in Figures 8.11 and 8.12, for subject B. The 0's in Fig. 8.11 are the same experimental curve shown in Fig. 8.9, and the X's are the derived curve from the approximation above. Figure 8.12 displays the difference between these two curves. These plots were very similar for all three subjects, and the first two entries in Table 8.4 summarize the results for the three subjects. These parameters are the maximum value for the difference curves, as in Fig. 8.12, and the radial position at which this maximum occurs.

In order to assess the overall percentage of flicks which are non-randomly corrective, the following definition and procedures are used.

P_{rr} is the total percentage of flicks which would be corrective if all flicks were random, and is found from the theoretical curve of Fig. 8.11 by the integration process used earlier to find,

P_{er} which is the total percentage of flicks which reduced the fixation error in the experiments.

P_{ri} is $(1 - P_{rr})$, the theoretical percentage which would increase the radial position if all flicks were random.

P_{ei} is $(1 - P_{er})$, the percentage of experimental flicks which increased the radial position; this has been assumed to be due entirely to random flicks. Using these values, one can calculate

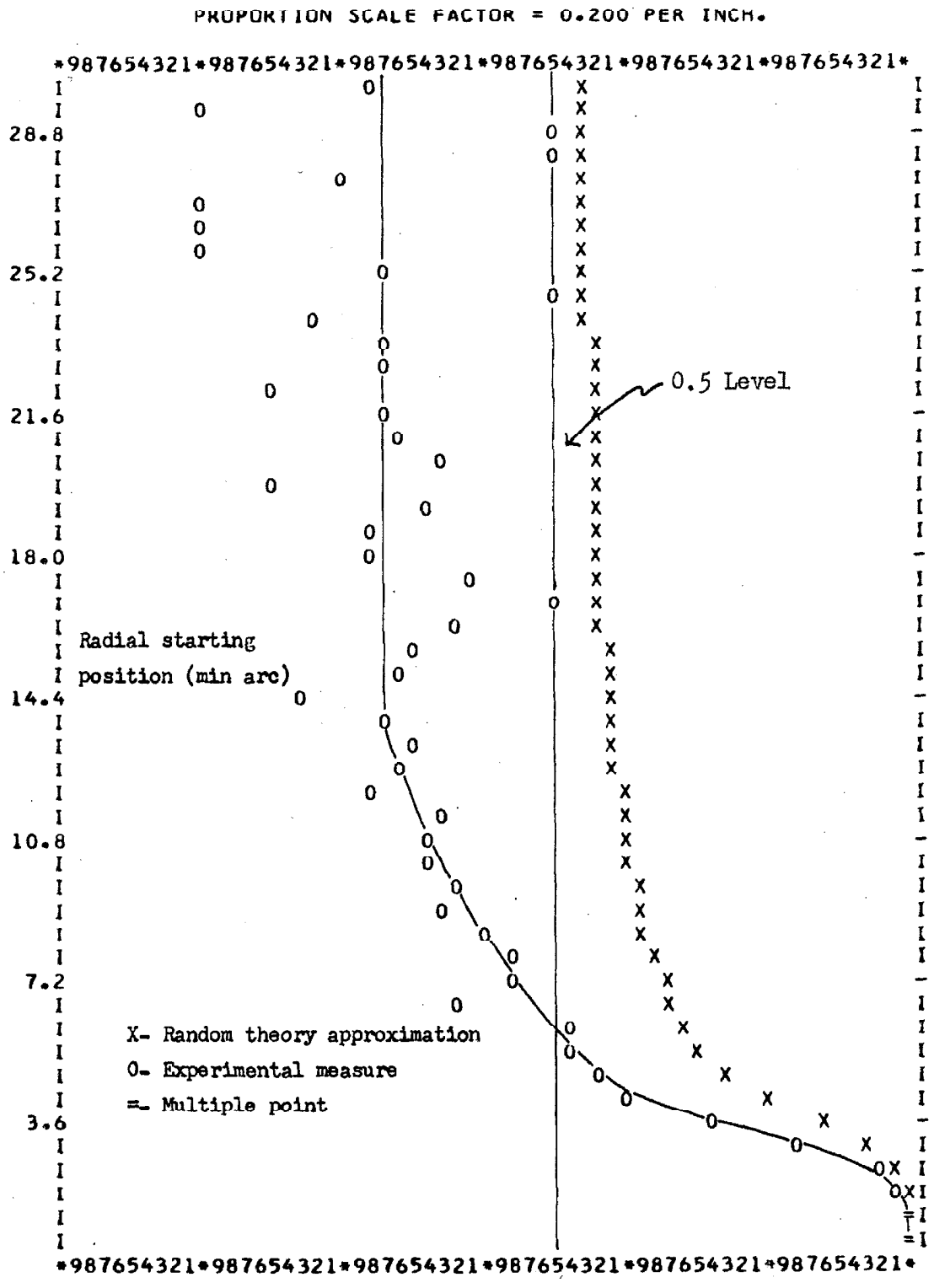

Fig. 8.11 - STARTING POSITION OF FLICKS vs PROPORTION WHICH REDUCE ERROR
(Subject B)

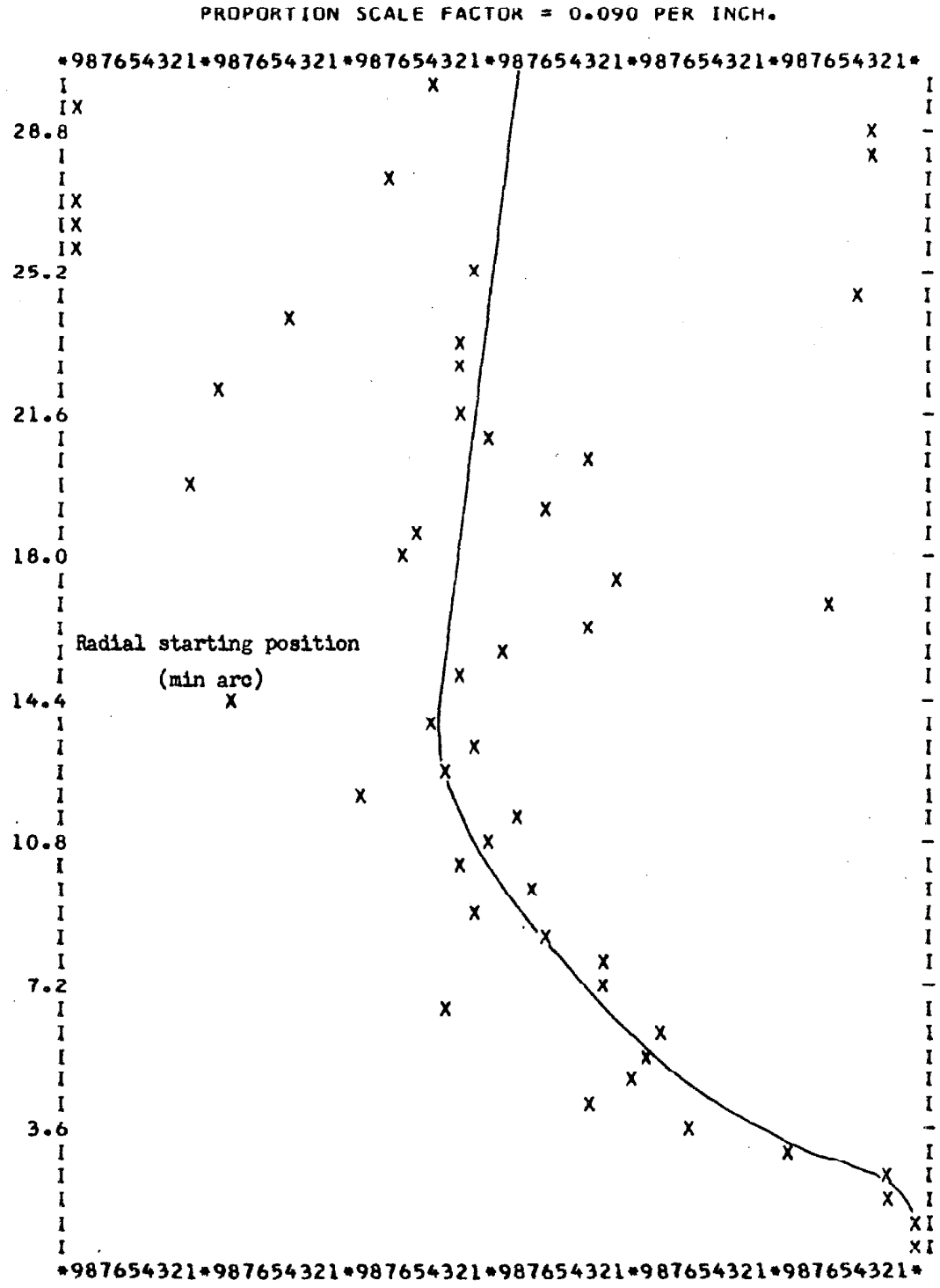

Fig. 8.12 - RADIAL STARTING POSITION OF FLICKS
vs
PROPORTION WHICH NON-RANDOMLY REDUCE FIXATION ERROR
(Subject B)

TABLE 8.4

Parameters Relating to "Programmed" Corrective Flicks

Subject	B	M	N1
Maximum proportion of flicks which non-randomly reduce fixation error	.33	.45	.50
Radial flick starting position at which maximum occurs (min arc)	12.	18.	12.
Percentage of all flicks which non-randomly reduce fixation error	30.	35.	39.

P_{rer}, the percentage of randomly reducing flicks in the experiment, from the equation,

$$P_{rer} = P_{rr} \cdot \frac{P_{ei}}{P_{ri}} .$$

Finally, P_{ce}, the total percentage of experimental flicks which are programmed to be corrective (non-random), can be found as

$$P_{ce} = 100. - P_{rer} - P_{ei}.$$

These percentages are listed for the three subjects as the third entry in Table 8.4. The indications of this approximation are that somewhat more than 60 per cent of the flicks are of random origin.

It should be noted that the integral process used above assumes that the fixation pattern is round, and Fig. 8.1 shows that this is not the case. The interaction of the most probable flick direction, and the direction of the major axis of the fixation ellipse determines the validity of the approximation given above. If the primary flick direction is oriented perpendicular to the major axis of the fixation histogram, then the measure of corrective flicks above will be an underestimate, whereas a parallel configuration will create an overestimate. In fact, however, consideration of the values in Tables 8.1 and 8.2 will show that the angular difference between the major axis and the primary flick direction varies from 75 deg for subject B to 12 deg for subject N1. The percentages of truly correcting flicks for these two subjects was calculated as 30 and 39 per cent, respectively. The difference in these percentages agrees with the conclusions about the validity of the approximation, the more parallel case producing higher percentages, with the result that an overall approximation to the effect that 35 percent of the flicks are actively correcting fixation error is probably reasonable.

Inter-flick intervals. - The conclusion has been reached that the majority of the flicks are of random origin. The statement that this

represents simple noise in the eye positioning system, however, would be naive. The innervation pattern at the extraocular muscles which is required to produce a flick is complex, as was seen in Chapter II. This patterned innervation precludes simple neural or muscular errors as the source of the random flicks. Rather, they must arise from some form of flick generator which initiates a complex reaction to produce these spontaneous movements. The form of this random flick generator can be inferred to some extent from the nature of the inter-flick interval histograms. Figure 8.13 shows the probability of occurrence of flick separation times for all three subjects. Although these curves differ greatly, they possess a common form which can be characterized as - a dead time, a rapid rise to the most probable interval, and a decay from that point to the axis. This form of interval histogram is characteristic of a system which generates events at a fixed probability per unit time, and is refractory for a period after each event is generated. On this basis, a model has been evolved which can satisfy all three of the histograms in Fig. 8.13.

The model being postulated is shown in schematic form in Fig. 8.14. This system is characterized by two basic blocks; a random pulse generator which produces pulses at a mean rate α per sec such that for small Δt, the probability of generating a pulse is $\alpha\Delta t$; and an absolute refractory section, whose refractory period is determined by a "log normal" distribution. (This form of distribution is detailed below.) The refractory unit is arranged such that pulses which arrive at the unit during the refractory period are lost, and the first pulse passing through it after such a period initiates a new refractory regime. The pulses are then assumed to initiate the process by which the innervation pattern for a flick is produced.

The log normal distribution which characterizes the refractory period is the Gaussian distribution using a transformed distribution

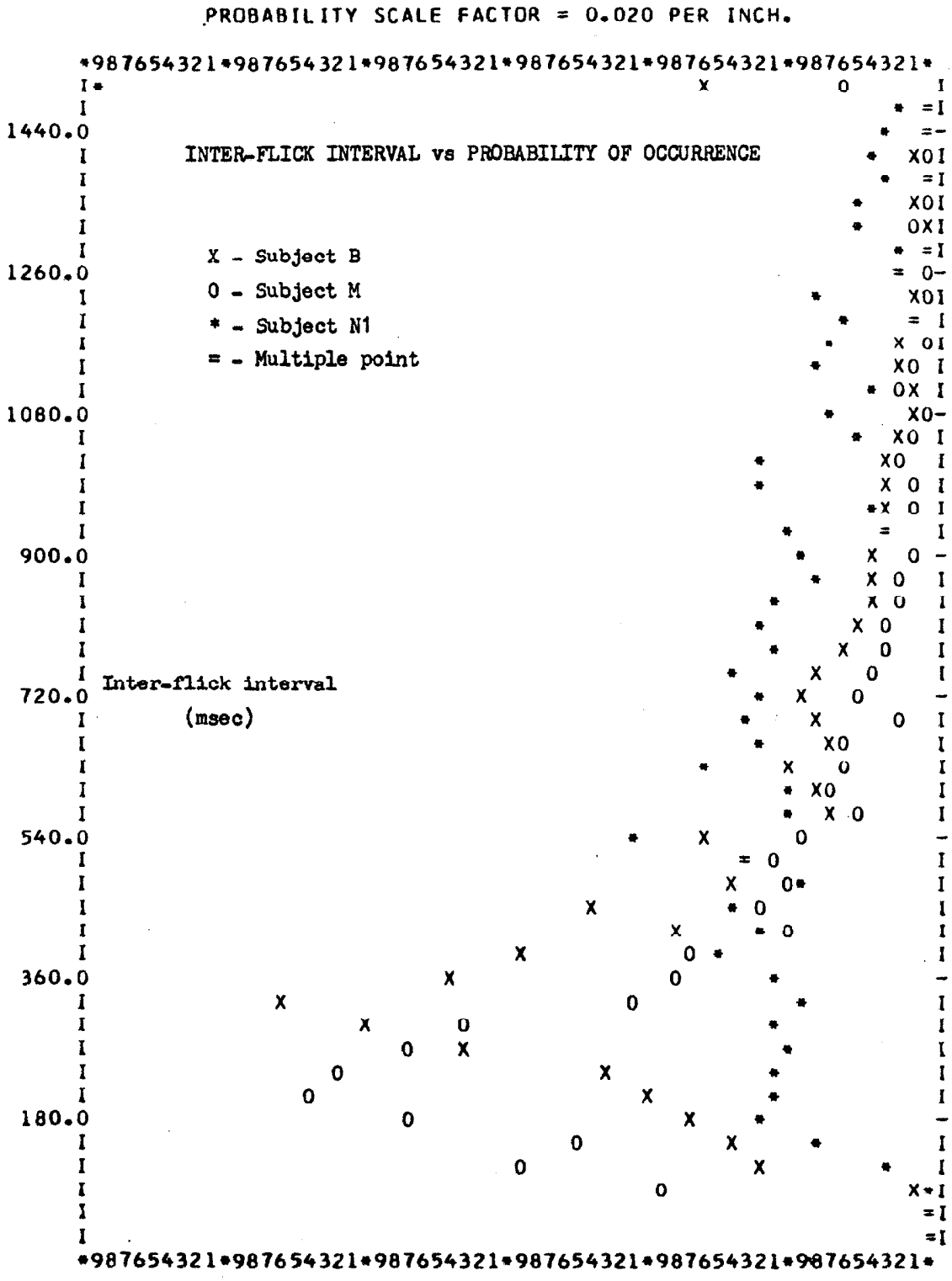

Fig. 8.13 - Inter-flick interval histograms for three subjects.

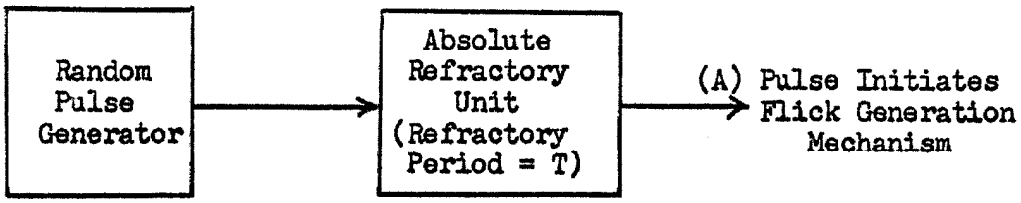

$P_{sp}(t) = \alpha \cdot t$ -

The probability that the pulse generator produces a pulse in the time interval ($t_o = t$ $t_o + t$) is $\alpha \cdot t$, where t_o is arbitrary.

$$P_T(T=\tau) = \frac{1}{(2\pi)^{1/2}} \cdot e^{-(s^2)/2}, \text{ where } s = \beta \cdot \ln(\tau/T_o) \text{ -}$$

The probability that the refractory period, T, is equal to the value τ, is determined by the log normal distribution. On the logarithmic scale, T_o is the mean value of T, and β is a scaling factor which determines the deviation.

Figure 8.14 - The stochastic flick initiation mechanism with the corresponding probability equations.

parameter,

$$S = \beta \ln(t/T_o) \qquad \text{Eq. 8.9}$$

instead of the parameter t. This represents a transformation, with arbitrary scaling factors, from the semi-infinite interval, t equal zero to infinity, to the infinite interval over which the Gaussian is defined, and represents the fact that negative refractory periods can not exist. A plot of this distribution for T_o of 150 msec, and β of 2. is shown in Fig. 8.15a.

In order to calculate the interval histogram which the system of Fig. 8.14 would produce, it is best to treat the functions initially on a segmented time basis, where the time at the n'th segment is $n\Delta t$. In this system, Eq. 8.9 becomes

$$S_n = \beta \ln(n\Delta t/T_o). \qquad \text{Eq. 8.10}$$

Using this function, the probability that a pulse arrives at the point A in Fig. 8.14 during the time interval, t_n, assuming that a pulse did not arrive during the preceding (n-1) intervals, is given as

$$\gamma_n = \alpha\Delta t \int_{-\infty}^{S_n} \frac{e^{-S^2}\, dS}{(2\pi)^{1/2}} \cdot \qquad \text{Eq. 8.11}$$

Now, the value of the time interval histogram at any given t_n, is the probability that a pulse does not occur during the (n-1) intervals multiplied by the probability that the pulse will occur in the n'th interval. This can be shown to be

$$H_n = \gamma_n \left\{ \prod_{i=1}^{n-1} [1 - \gamma_i] \right\} \cdot \qquad \text{Eq. 8.12}$$

Before allowing Δt to approach zero so that a continuous distribution can be found, it is convenient to express

$$\ln(H_n) = \ln(\gamma_n) + \sum_{i=1}^{n-1} \ln(1 - \gamma_i) \cdot \qquad \text{Eq. 8.13}$$

Using the power series approximation to the logarithm, this becomes

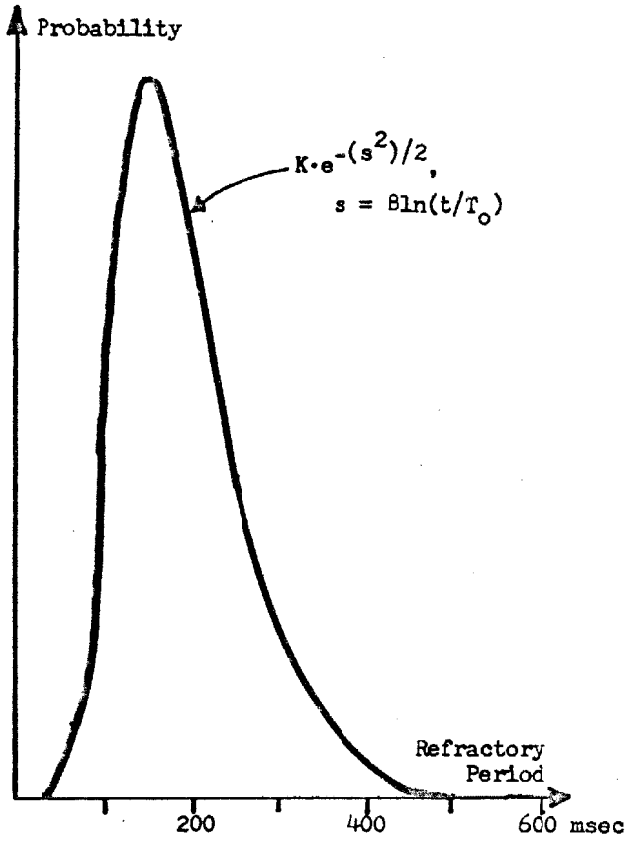

a) Log normal distribution.

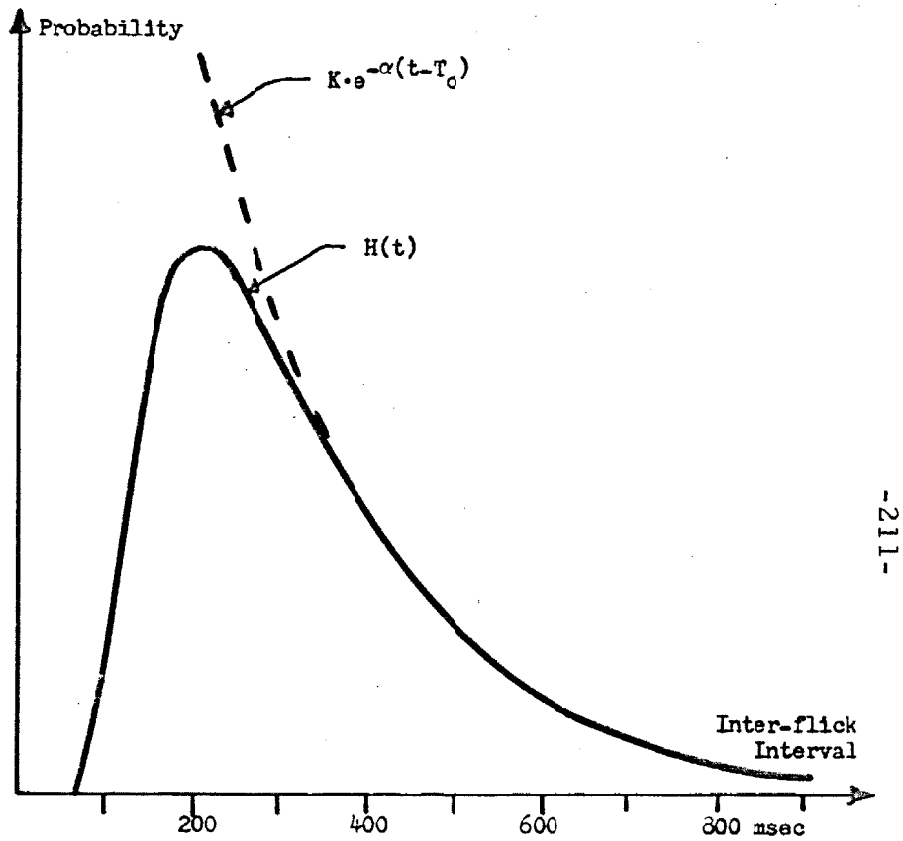

b) Theoretical histogram and exponential decay for comparison.

Figure 8.15 - Log normal distribution for the refractory period, and a histogram of inter-flick intervals from the stochastic flick generator. T_o = 150. msec; β = 2.0; α = 4.6 pps.

$$\ln(H_n) = \ln(\gamma_n) - \sum_{i=1}^{n-1} (\gamma_i + \gamma_i^2/2 + \gamma_i^3/3 + ...). \qquad \text{Eq. 8.14}$$

Now, Δt is reduced to zero as n approaches infinity so that $n\Delta t$ remains constant at t. It will be seen from Eq. 8.11 that γ_n approaches zero in this instance, so that terms in Eq. 8.14 of order higher than unity may be neglected. Thus, the integral equivalent of Eq. 8.12 becomes

$$H(t) = \gamma(t)\, e^{-\int_0^t \gamma(\rho)\, d\rho}\, dt, \qquad \text{Eq. 8.15}$$

where,

$$\gamma(t) = (\alpha/\sqrt{2\pi}) \int_{-\infty}^{\beta \ln(t/T_o)} e^{-S^2/2}\, dS. \qquad \text{Eq. 8.16}$$

Note that for values of t greater than T_o, and for large β, $\gamma(t)$ approaches the constant value, α, and H(t) becomes an exponential with a decay constant $1/\alpha$. This relationship is seen in Fig. 8.15b, where H(t) and the exponential function are both plotted. The function plotted was generated from the log normal distribution of Fig. 8.15a, using a value for α of 4.6 pulses per sec.

Now it is possible to return and consider the inter-flick interval histograms of Fig. 8.13. The statement has been made that these curves are all characterized by a dead zone, where the interval probability is low, followed by an exponential decay. This assertion would seem reasonable for subjects B and M, but the smaller number of samples in the histogram for N1 makes it difficult to assess the validity of the statement. Unfortunately, the solution for the three parameters of the model from the experimental data is difficult. Instead, three parameters have been extracted from these histograms and are presented as Table 8.5. The first of these is α in pps. This parameter was determined by plotting the logarithm of the histograms

TABLE 8.5

Characteristics of Inter-Flick Interval Histograms

Subject	B	M	N1
α, slope constant (sec^{-1})	3.7	4.6	2.2
Mean inter-flick interval (msec)	480.	330.	780.
Most probable inter-flick interval (msec)	315.	195.	195.

as a function of time, and measuring the resultant slope. The equating of this parameter with the value in the model would appear, from the sample plot of Fig. 8.15, to be a reasonable step. The second parameter in Table 8.5 is the inter-flick interval of maximum probability. This number is similar to T_o in the model, but is always greater than T_o. The final parameter is simply the mean interflick time for the subject.

An attempt to fit this model to the experimental data can be made using an iterative process and checking by eye. Such an attempt has been made to fit the data for subject M. The resulting model parameters for this subject are:

T_o = 150. msec

β = 2.0, and

α = 4.6 pps.

The resultant fit is shown in a combined plot with the original data for that subject in Fig. 8.16. The agreement would appear to be good. Interpretation of the parameters of the fit, however, is not straightforward, owing to the transformed variable, s, in the log normal distribution for the refractory unit. The plot of Fig. 8.15a, showing the log normal distribution which was used for the fit to subject M, can be characterized in the untransformed time axis, in order to provide comparison with other units in the eye positioning system. If the mean and deviation of this non-Gaussian function are calculated, the resultant values are 210 msec, and 80 msec, respectively. It has already been shown in Chapter VII, that the saccadic system possesses a refractory period which is of the order of 200 msec. The deviation measured here is slightly higher than that measured in Chapter V for the normal response time; 50 msec was the deviation arrived at in the latter case. Nevertheless, the obvious argument is that the refractory unit involved in the generation of the random saccades is very similar to the overall characteristics of the saccade command system, and might well be ascribed to the necessity of the saccades being generated through that unit.

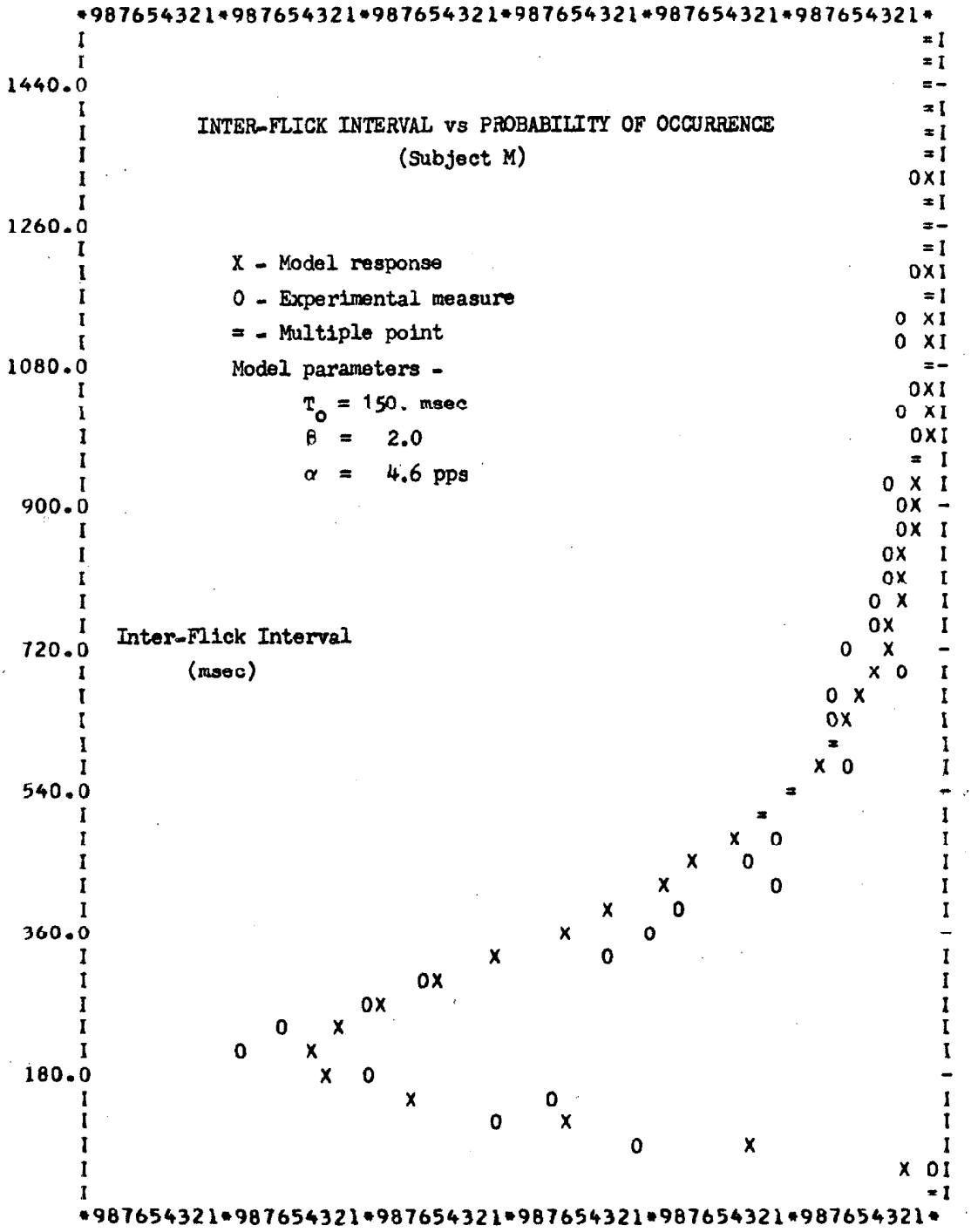

Figure 8.16 - Inter-flick interval histograms for comparison between the experimental response and the response of the model in Fig. 8.14.

The more interesting component in this model is the random pulse generator which initiates the formation of the spontaneous saccades. The mean rate for this unit varies widely among the subjects tested, from 4.6 pps for subject M, to 2.5 pps for subject N1. The general characteristics of the flicks, being much the larger spontaneous component, suggest that they are responsible for relocating the retinal image in order to prevent adaptation. This being the case, the mean generation rate might well be expected to be a function of the intensity level of the stimulus. This relationship was not tested here, however.

Drift correlations.-Having sought a potential source for the random flicks, attention should now be directed towards the drift component. The available information on this component, however, is not as tractable as that for the flicks. Nevertheless, directional correlations for the drift do provide insights as to its origin.

Comparison of the overall fixation histograms, such as Fig. 8.1, with the drift directional characteristics, Fig. 8.5, reveals an important element of the drift. First, the most noticeable characteristic of fixation patterns (see Table 8.1) is the fact that the fixation ellipses are not aligned parallel to the muscular coordinate system. The muscle-position transformation derived in Appendix I is solved there for small fixation deviations, and it is demonstrated that the pairs of recti produce independent horizontal and vertical displacements for small eye movements. Thus the fact that the fixation patterns derived here all possess a measurable covariance means that the rectus pairs must receive some common noisy innervation pattern. This covariance could be attributed to the random flicks, if the primary flick directions were either parallel or perpendicular to the fixation ellipse axes; this is not the case, as these directions differ by angles of from 12 to 30 deg. Moreover, the primary drift direction is parallel to neither the muscle coordinate system nor to the primary fixation axis. Hence, the drift must arise from two

sources, one which is common to the two sets of recti, and one that is independent for these sets.

The Model

Utilizing the data that have been presented, it is now possible to postulate an overall model for the stochastic processes which generate the spontaneous eye movements. Figure 8.16 shows a flow chart of this model. The system presented relies on both the data that have resulted from this chapter, and several known characteristics of the eye.

It was mentioned in Chapter II that the primary, or neutral, position of the eye does not represent a position in which the extraocular muscles are at rest. The latter position is that which the eye attains when the extraocular muscles have been paralyzed and only the elastic properties of the muscles determine the position of the orb; this paralysis position is located temporally and upward with respect to the primary position. Furthermore, Bender (5, 6) in electrophysiological experiments performed on monkeys has been able to elicit an eye centering reflex. Using an electrical stimulus in the cerebrum, he can cause both eyes of the animal to center, regardless of the position of the eyes prior to stimulation. The implication of this work is that the neural control which overcomes the elasticity of the muscles has a common source for all six pairs of extraocular muscles.

The effect of this system in maintaining the proper muscular tone is shown in Fig. 8.16 for one eye only, and there only for the two pairs of recti. The input to the system is labelled "tone to balance muscular elasticity", and this signal is fed to both the vertical (superior and inferior recti) and the horizontal (medial and lateral recti) systems. The sign convention adopted in the model is such that positive signals from the cortex at the entry points for the "horizontal displacement signal" and the "vertical displacement signal" will

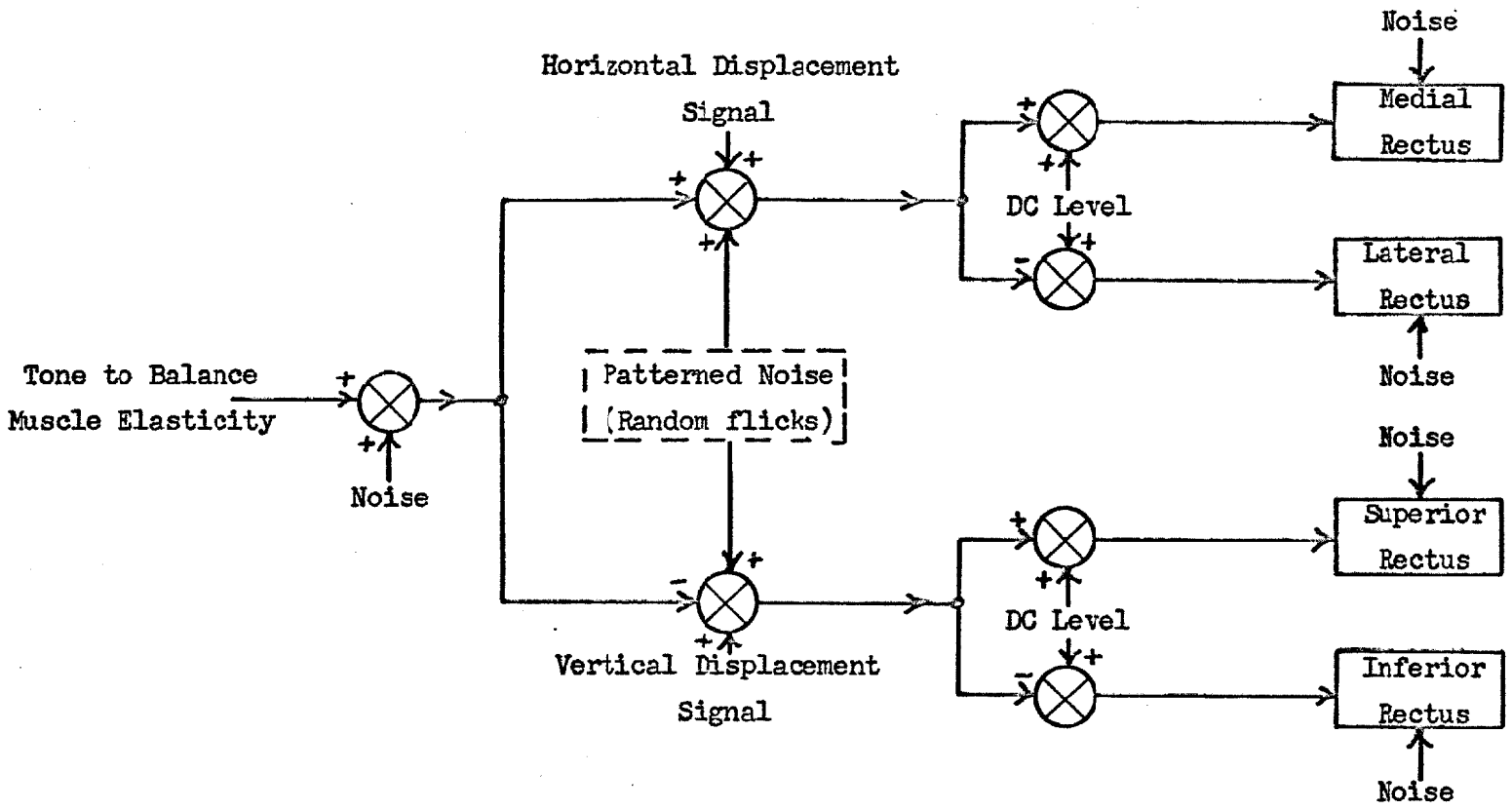

Figure 8.17 - Partial schematic diagram of the extraocular muscle innervation system showing potential sources of noise - eye movements not correlated with a fixational task. The patterned noise is the stochastic flicks generated by the system of Fig. 8.14; the noise source in the tone system creates drift motion with correlated vertical and horizontal components; and the noise sources at the muscles create independent drift directional components.

produce nasal and upward rotations of the eye, respectively. Thus, the tone maintaining signal must be subtracted from the vertical displacement signal, and added to the horizontal input to overcome the muscle elasticity. The resultant signal is then fed differentially to the extraocular muscles by mixing these signals with a DC level using the appropriate sign. The DC level has no significance in the system unless one wishes to consider that the basic signal is neural impulse frequency, in which case all signals must be positive, negative frequency having no real interpretation.

Thus, the primary system of Fig. 8.16 provides for both the centering system and the cortical control of the eye positioning system. Into the primary model, random functions are inserted at three levels. The first of these is from the command level. This "noise" represents the flick generating model which was discussed earlier. The second level at which noise enters the system is in the tone system. This noise is assumed to be random, and of relatively low frequency. It is this source which is the origin of the covariance in the drift motions, as it creates drift towards and away from the paralysis position, relative to the primary position. The final noise level presented is at the extraocular muscles themselves, and represents the inaccuracies and variations in sensitivity of these muscles and their associated synapses. These independent sources provide the uncorrelated drift components.

The final portion of this model, of course, is the correcting system which has not been shown. It is assumed that the majority, if not all, of this correction is performed by the non-random flicks. Figure 8.12, the plot of the percentage of non-random flicks as a function of radius, provides a measure of the sensitivity of this correcting system. It is not possible to measure the corrective function more specifically, because a substantial portion of the flicks which reduce position error are, in fact, of random origin, and these can

not be separated when analyzing the data. Presumably, the general method of error reduction is very similar to the control systems which have been considered in earlier chapters.

CHAPTER IX

CONCLUSION

The preceding four chapters have presented the experimental work which was done in support of this thesis. In each chapter, a model of the sub-system under investigation was presented as a result of the experiments, but no attempt has been made thus far to integrate those models. It would be possible to use entirely separate systems, noting that the stimulus conditions in each case were sufficiently different for parallel pathways to have been tested, each of which responded independently and exclusively to its own specific stimulus regime. While this relationship is correct to a degree, it is unrealistic to assume that none of the components are common to the various models. The attempt will be made in this chapter to present an integrated model which combines, where reasonable, elements from the separate models. In some cases, there are possible combinations which are speculative, and these will be noted in the discussion. Finally, when insufficient information is available to justify a given step completely, an experiment which might be used to test that question will be suggested.

Integrated Model

The model which the author would like to propose is drawn in schematic form in Fig. 9.1. Comparison of this figure with Fig. 4.5 will reveal that no changes have been incorporated in the smooth-following system as such. Within the saccadic system, and in the region of the extraocular muscles, however, the changes are obvious, and each unit bears an additional symbol indicating in which chapters that portion of the model was discussed. Note should also be taken of the inclusion of "inhibiting" and "facilitating" elements in the

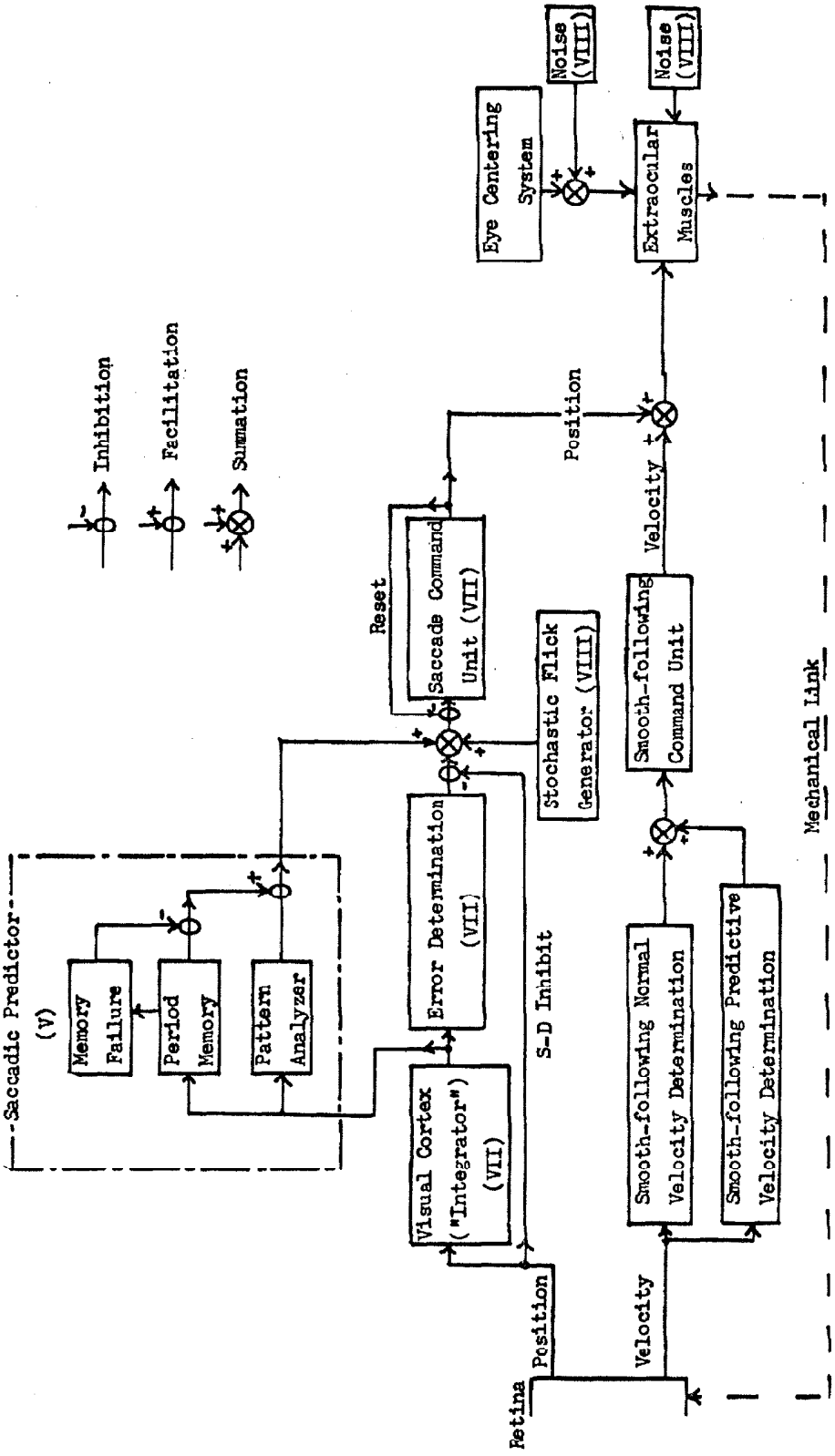

Figure 9.1 - The model of the eye movement control system from Chapter IV, redrawn to include those portions which were investigated in this thesis. Each unit which was tested here has a number in the box indicating in which chapter it was studies. Further consideration is given to these units in the text of this chapter.

information paths in this model. The implication of these is simply that a signal (undefined for this purpose) on the line feeding into the loop of these elements will either permit or forbid transmission of information through the direct path for some given amount of time - a process equivalent to digital "and" gates. The associated time course of this facilitation or inhibition is given in the chapter in which the specific unit was derived.

Normal saccade path. - The normal saccadic loop, that path through which the following of unpredictable stimuli is effected, has been little changed from the model derived in Chapter VII. The position information from the retina is passed through the visual cortex integrator, the error describer, and finally out to the extra-ocular muscles via the saccade command unit.

The testing in Chapter VII was carried out using a stimulus condition in which pairs of stimulus steps were presented. The steps which constituted these pairs were separated by times ranging from 20 to 650 msec, and the steps were of constant amplitude, although the direction, right or left, could vary between members of each pair. The factor of interest was the timing of the response process. The discussion in Chapter VII was cast in terms of those pairs, but generalizations of the stimulus conditions can be made and these will be presented with reference to each sub-unit as it is discussed.

The first element in the normal saccadic path is the visual cortex which performs a delay and integration function. This unit first detects a disparity in the retinal image position relative to the fovea, and then transmits the retinal image error after a delay time, TCI. The transmitted information is the image position which exists at the end of the delay period, with the result that the transmitted signal includes all image motion which takes place during that period-integration. The effect of this action is to produce a single response step to any series of target motions which are separated in time by

less than the delay time of the unit. The time associated with this action was determined to be about 30 msec, from the experiments of Chapter VII.

The second element in the normal system is the error determination unit. This element sets up a description of the retinal error which exists, and passes this error on to the command unit. The time delay, TED, involved in that process was determined in relation to the time at which the response could be terminated if the stimulus position error at the retina were reduced to zero. According to the model, the response saccade is inevitable once the information has passed this unit, but at any time before this transmission, a corrective motion of the target will inhibit the response via the line labelled "S-D inhibit" (Fig. 9.1). In addition to the primary time delay of this unit, a recomputation time, [TSD], was determined for stimuli which followed each other closely in time. If a second stimulus motion requires an error description which is different from the immediately preceding one, then the recomputation of the description requires an additional time delay. This extra delay, however, is a function of the stimulus separation. For the two subjects who exhibited this effect, it was found that this recomputation delay decayed to zero approximately 600 msec after the passage of the initial stimulus.

The third element in this system is common to all of the saccadic functions which were measured. This is the "saccade command unit", which computes the signals to be transmitted to the extraocular muscles. It is characterized by a constant computation time, TSC, and a refractory, or reset, time, TRS. The latter function is indicated in Fig. 9.1 as an inhibitive feed-back path around the element. This command unit is totally occupied in the process of computing a saccade, and will not accept information regarding a second saccade until a time (TSC + TRS) after it started processing the preceding saccade.

The final element in the loop is the extraocular muscles which were assigned a single response time, TCM. This represents the time delay between the transmission of the information from the command unit and the initiation of the saccade.

Saccade predictor. -The predictive loop for square wave following, which was shown as a single unit in Fig. 4.5, is here subdivided into the units derived in Chapter V. The image position information which this system needs to predict the stimulus is extracted from the visual cortex unit described above. This information is routed to two sub-units. The first of these is the "pattern analyzer" which generates the position error signal to be sent to the saccade command unit. This transmission takes place only when facilitated by the "period memory" unit. The period memory function is a form of timing delay in the system. The predictive response to a stimulus step occurs approximately 100 msec before the step, and is actually keyed to the time of occurrence of the preceding stimulus. Thus, period memory involves establishing a delay whose duration is determined by the stimulus period. The accuracy of this memory function decreases at both short and long stimulus periods. At shorter periods, the predictive lead is reduced from the normal 100 msec, thereby producing a larger mean response time. At the longer stimulus periods, the memory function fails more frequently. This failure, which is evidenced by a reactive response 200 msec after the stimulus, is thought to arise from the comparison of two identical delay units. As the stimulus period increases the accuracy of these units decreases, and the comparison of their outputs failsmore often. The failure of the memory unit is shown in Fig. 9.1 as an inhibitive function on the output of the memory.

Once the position information from the pattern analyzer has been transmitted (on cue from the period memory), the saccade is generated by the command unit described above. The refractory time of this unit serves to separate the predictive and reactive responses to a given stimulus step. If a predictive response has been elicited,

the reactive signal which is passing through the normal saccade response system will be inhibited at the saccade command unit by this refractoriness.

System noise. - The final area of investigation dealt with spontaneous eye movements as they represent noise in the eye position control system. The model which concluded Chapter VIII. contained very few elements which are directly attributable to the control system itself. The noise in the smooth system, random drift, arises from the eye centering system, and from the extraocular muscles themselves, as indicated in Fig. 9.1. The majority of the flicks, however, represent a stochastic process. Moreover, this process must be sophisticated, as the innervation pattern required to produce a saccade can be shown to be quite complex. For this reason the stochastic flick generator is placed at a higher level than the extraocular muscles. This generator consists of the flick initiation system described in Fig. 8.14, followed by a unit which generates an error measure for the saccade command unit. The statistics of this error measure are highly variable from subject to subject, but can be measured experimentally, as in Figures 8.2 and 8.4. The flick generation system presented in Chapter VII included a refractory unit after the random flick initiator. This refractory function is inherent in the saccade command unit in the model of Fig. 9.1.

Model Response

Generally speaking, the sub-systems in the integrated model presented here are unaffected by the integration. The primary elements of each have been retained as separate functional sub-units and the refractory nature of the saccade command unit provides the signal separation necessary to assure their integrity. There are, however, several aspects of the system which should be investigated further.

Information suppression. - The suppression of position information by the saccades was studied in Chapter VI. While it is clear that a more thorough study of that effect is needed, it is interesting to note the effects of such suppression on saccadic tracking. The interaction of suppression with predictive tracking has already been noted, and the notion was put forward that this is the reason why the predictive stratagem generates saccades prior to the stimulus step. An equivalent effect on the normal, reactive saccade control, however, was not seen. If this suppressive process is placed directly in the model, then the expected response to the stimulus pairs used in Chapter VII would be different from the response that was measured.

The suppressive effect that was measured is intimately linked to the efference copy theory, for it represents the inability of the system to detect a stimulus motion in the presence of eye movement, and one of the postulated functions of efference copy is to allow the discrimination between eye motion and stimulus motion (29). It is also tacitly assumed that efference copy continuously monitors the command information for eye movements in order to provide the cortex with a measure of the eye position. The author would like to suggest that this assumption is incorrect, and accordingly, would like to propose a redefinition of the efference copy mechanism.

Much experimental evidence has bearing on this question. It has been shown here that small target movements can not be detected in the presence of flicks. The equivalent test in the smooth-following system has not been made - whether small, slow target motions can be detected in the presence of random drifting motions of the eye. The converse effect in both the smooth and saccadic systems is seen in autokinetic motion experiments. In these experiments, the subject perceives a small stationary target to be drifting about his visual field. This apparent motion has been shown to be the direct result of eye motion. (42) In Chapter VIII it was shown that the fixation errors in such an experiment are corrected by flicks, but

this corrective effect is not noticed as an equivalent target motion in autokinesis. Finally, the experimental evidence is very strong that random flicks require a complex innervation pattern which comes through the saccade command unit, whereas the random drift is undoubtedly due to unprogrammed fluctuations in the neuro-muscular system.

A redefinition of the manner in which efference copy functions can account for all the effects mentioned above. This redefinition states that efference copy is a passive mechanism. Rather than continually processing the eye movement command information, the cortex interrogates the efference copy path only when rapid image motion or image-fovea disparity is perceived. If this interrogation yields the information that an equivalent eye movement has been executed within $\pm$40 msec of the perception, then the perceived motion is interpreted as being eye motion. Otherwise, the image motion is assessed as being the result of target movement.

Under this definition, the perceptual results noted above can be explained as follows. Small target motions, such as were used in Chapter VI to test the suppression effect, are interpreted as eye movements whenever they coincide in time with the flicks. Spontaneous drift is not a response to a system command, and therefore is interpreted as target motion such as is reported in autokinesis. Finally, the flicks which occur during fixation are the result of patterned innervation, and thus are properly interpreted as "commanded" eye movements, with the result that the perceived autokinetic motion is the cumulative effect of the drift. This accounts for the perceived motion being large, whereas it was seen in Chapter VIII that the image seldom left the central fovea.

The effect of this hypothesis on the eye positioning system is minimal. Under the assumptions, the interrogation must be made <u>whenever</u> a rapid image motion is perceived. Thus, no <u>additional</u> time is required in the assessment of image motion if it should be

the result of eye movement. Moreover, regardless of the origin of the image displacement, a corrective eye movement must be made. The interrogation process requires a constant time for all image motions, and this process is assumed to take place in the visual cortex unit previously described. The only instance in which the control system requires the differentiation between eye movement and target motion is in the case of predictive tracking, where the time of a stimulus step must be known in order to predict the next step. In order to avoid the confusion which arises when a saccade and a stimulus motion coincide, the predictive system programs the saccades to precede the stimulus by about 100 msec.

Predictive memory failure. -The period memory unit involved in saccadic prediction was discussed earlier, and it was noted that this memory unit fails to predict the stimulus motion at times, resulting in a reactive response. The rate of this failure was determined in Chapter V to be a function of the stimulus period, and therefore of the time delay which must be applied to a stimulus signal. Moreover, it was found that the deviation of the predictive saccade times was not a function of this delay. This experimental evidence led to the hypothesis that the failure was due to the comparison of two, parallel, fallible memory units. This hypothesis could be tested by measuring the sequential properties of the memory failure. If the source of the failure is as suggested, then the occurrences of reactive response should be random functions of the stimulus sequence. If, however, these occurrences should turn out to be systematic, then the failure is due to another cause.

The time course of the learning which is involved in this predictive process should also be investigated further. Several experiments were attempted and reported in Chapter V. The results of these tests indicated that the predictive function was only established when the subject had prior knowledge that the stimulus would have a constant period. In tests wherein predictable stimuli were mixed at

random with unpredictable forms, there was no evidence of learning within the first 20 stimulus steps. Whether or not this learning ever takes place should be investigated.

Noise characteristics. -Although the statistical determinations reported in Chapter VIII represent a great deal of information about the spontaneous eye movements, there is a wealth of statistical techniques which might be applied to this analysis with profit. Specifically, the source of the random drift was identified, but not well specified. The drift noise was assigned two separate sources, neither of which are involved in the smooth-following command system. These two sources, the eye centering system and muscle error, were assumed to account for drift which was respectively correlated and uncorrelated between the two directional components. Cross- and autocorrelation techniques should be applied to the horizontal and vertical drift components (with saccades subtracted) in an attempt to separate the drift sources. The arguments presented in Chapter VIII on this separation involved consideration of only the fixation histogram, and the presence of directional components which could be shown to possess both correlated and uncorrelated segments.

APPENDIX I

THE MUSCLE-POSITION TRANSFORMATION

In Chapter II, the problem of specifying the relationship between extraocular muscle tension and resultant eye position is discussed. Using purely geometrical considerations, and the coordinate system previously defined (see Fig. 2.6 and Fig. 2.7), it is possible to produce a mathematical transformation between eye position and angular muscle displacement. The angular muscle displacement is a convenient method of characterizing the muscle tension. For any given muscular set, the effect of each muscle-pair is expressed as the angular rotation which the tension in that pair would produce were they to cause pure rotation. (The pure rotation axis for each pair of muscles is shown in Fig. 2.6.) If one assigns the following variables:

v = the vertical angle of the resultant eye position;

n = the horizontal angle of the resultant eye position;

t = the resultant torsionsl position;

g = the angular muscle displacement of the superior and inferior recti about the axis 'a-a', defined in the same direction as v;

u = the angular muscle displacement of the medial and lateral recti about the vertical axis, defined in the same direction as n;

w = the angular muscle displacement of the superior and inferior obliques about the axis 'b-b', defined in the same direction as t;

a = $u + 23^{\circ}$;

and, b = $u - 51^{\circ}$;

then the following equations give the eye positions, defined within the

adopted coordinate convention, as a function of the angular muscle displacements:

$$n = u + \tan^{-1}\left[\frac{(\cos a)(\sin a)(1 - \cos g)}{(1 - (\cos a)^2(1 - \cos g)}\right] + \tan^{-1}\left[\frac{(\cos b)(\sin b)(1 - \cos w)}{(1 - (\cos b)^2(1 - \cos w)}\right]$$

$$v = \sin^{-1}[(\cos a)(\sin g)] - \sin^{-1}[(\cos b)(\sin w)]$$

and, $$t = \tan^{-1}[(\sin g)(\sin a)/(1 - (\sin a)^2(1 - \cos g))] - \tan^{-1}[(\cos b)(\sin w)/(1 - (\sin b)^2(1 - \cos w))]$$

The experimental work in this paper, however, never involved magnitudes of any of these angles greater than two degrees. In this region, first order approximations to the trigonometric functions can be made as $\tan\beta = \beta$, and $\cos\beta = 1$, without introducing an error greater than 0.1 percent in any of the trigonometric functions. Using these approximations, the equations above are greatly simplified to:

$$n = u,$$

$$v = g.\cos 23^\circ - w.\cos 51^\circ = .92g - .62w,$$

and, $$t = w.\sin 51^\circ + g.\sin 23^\circ = .39g + .77w.$$

It can be seen from these equations that in the region of interest the two pairs of recti, which produce the majority of the displacement in the line of sight, act independently in the vertical and horizontal directions.

APPENDIX II

THE FLICK DETECTOR

The majority of the experiments performed during the research for this thesis involved testing the flick component of the eye movements, and it was generally necessary to know the time of occurrence of these motions. For this reason, an electronic flick detector was designed which will produce a logical pulse output whenever a flick occurs in the eye position signal. In general, two flick detectors were used, one for the vertical position component, and one for the horizontal. The discussion to follow is limited to only one of these, but the construction and principle are identical for each.

Detection of the flicks makes use of their rather unique time course. This time position relationship was discussed in Chapter III, and is seen to be relatively constant for all flicks of amplitude less than about five deg arc. As noted, these movements typically displace the fixation direction the full amount of the flick in 15 msec. For many of the flicks, an overshoot of about 10 per cent of the size of the total movement is detected; these overshoots last another 15 msec. The smallest flick which the flick detector is called upon to recognize is three min arc, which produces a peak velocity of roughly three deg arc per sec. This velocity is substantially larger than the maximum drift velocity which the eye exhibited during any of the experiments performed, and thus allows the use of the eye velocity as the parameter which points out the flicks. Care must be taken in this approach, however, as the tremor component of the eye movements contains considerable power in the frequency range from 40 to 100 cps, and this might well be detected by a simple differentiator circuit.

A schematic diagram of the flick detector is shown in Fig. Apx 2.1. Basically, there are five elements in this network; the first

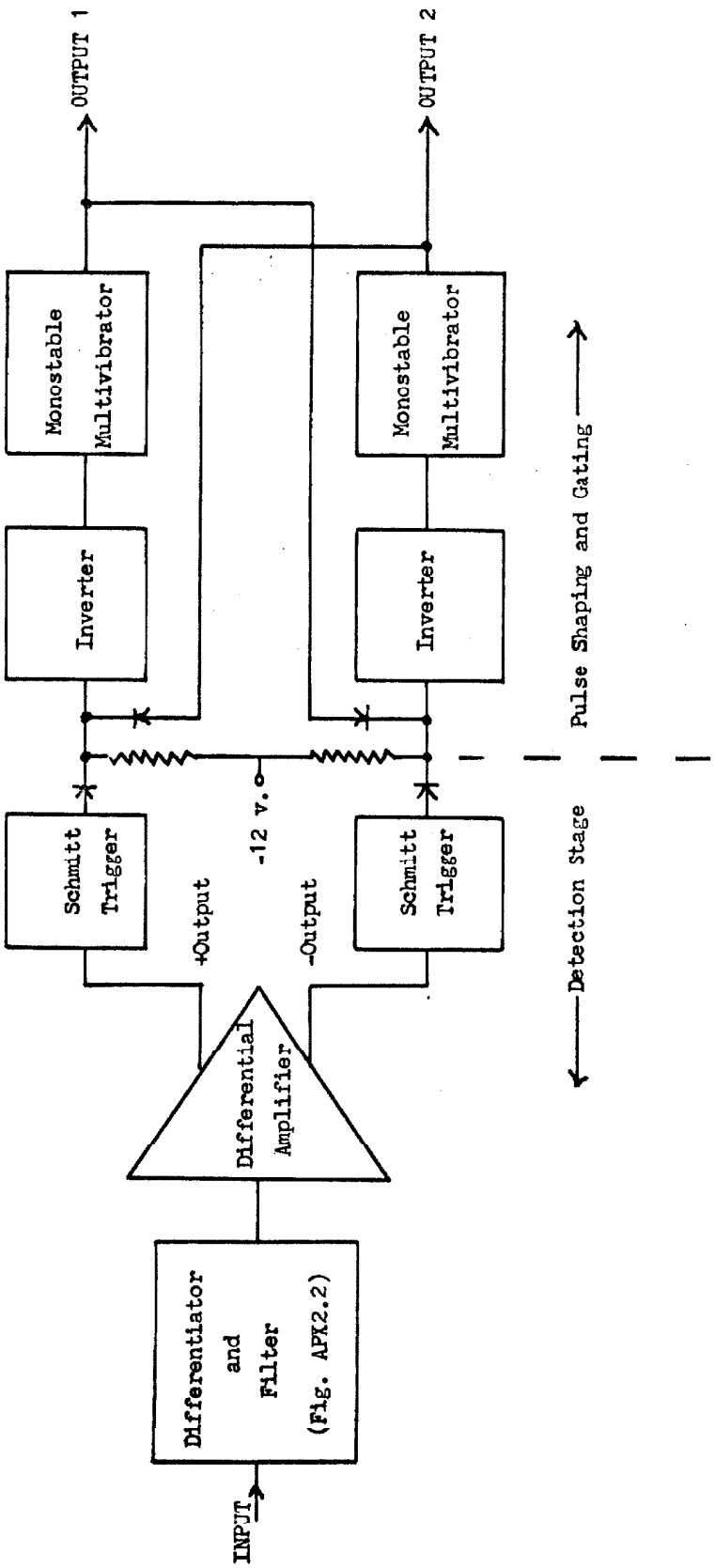

Figure APX2.1 - Schematic diagram of flick detector.

three perform the appropriate filtering and detecting, while the last two are pulse shaping circuits. The eye signal is fed into the filter circuit where a combination differentiator and low pass filter reduce it to a series of positive and negative pulses demarking the two possible directions of flicks. This pulse train subsequently passes through a differential amplifier to separate the two directions from each other. This amplifier has two adjustments which permit the experimenter to control the amplitude of the flicks which will pass through the detector for either direction. A balance control alters the relative DC level of the two outputs, while a level shift varies these levels together. The final portion of the detecting stage is constituted of two 'Schmitt' triggers which are set for a fixed firing level.

The pulse forming section is constituted of two monostable multivibrators driven by the 'Schmitt' triggers through inverters. These multivibrators are set for a pulse duration of 70 msec, and serve to prevent the flick detector from producing a pulse in any given channel when this pulse is actually only a measure of the overshoot of a flick in the opposite channel. This logical gating is performed by the diode gates shown at the input to the inverters. When a flick is detected in either channel, the opposite channel is prevented from producing an output pulse for the next 70 msec.

The filter circuit in the first stage of the flick detector is the heart of the network; the circuit diagram for this unit is shown in Fig. Apx 2.2, and the gain-frequency curve in Fig. Apx 2.3. The overall characteristic of this filter is a band-pass from 18 to 70 cps, with a 6 db per octave positive slope to about 40 cps, and an 18 db per octave fall-off above 60 cps.

The DC level of the basic filter unit was found to drift quite heavily when it was first tested, owing primarily to lack of temperature compensation in the transistor amplifiers. As a result, it was

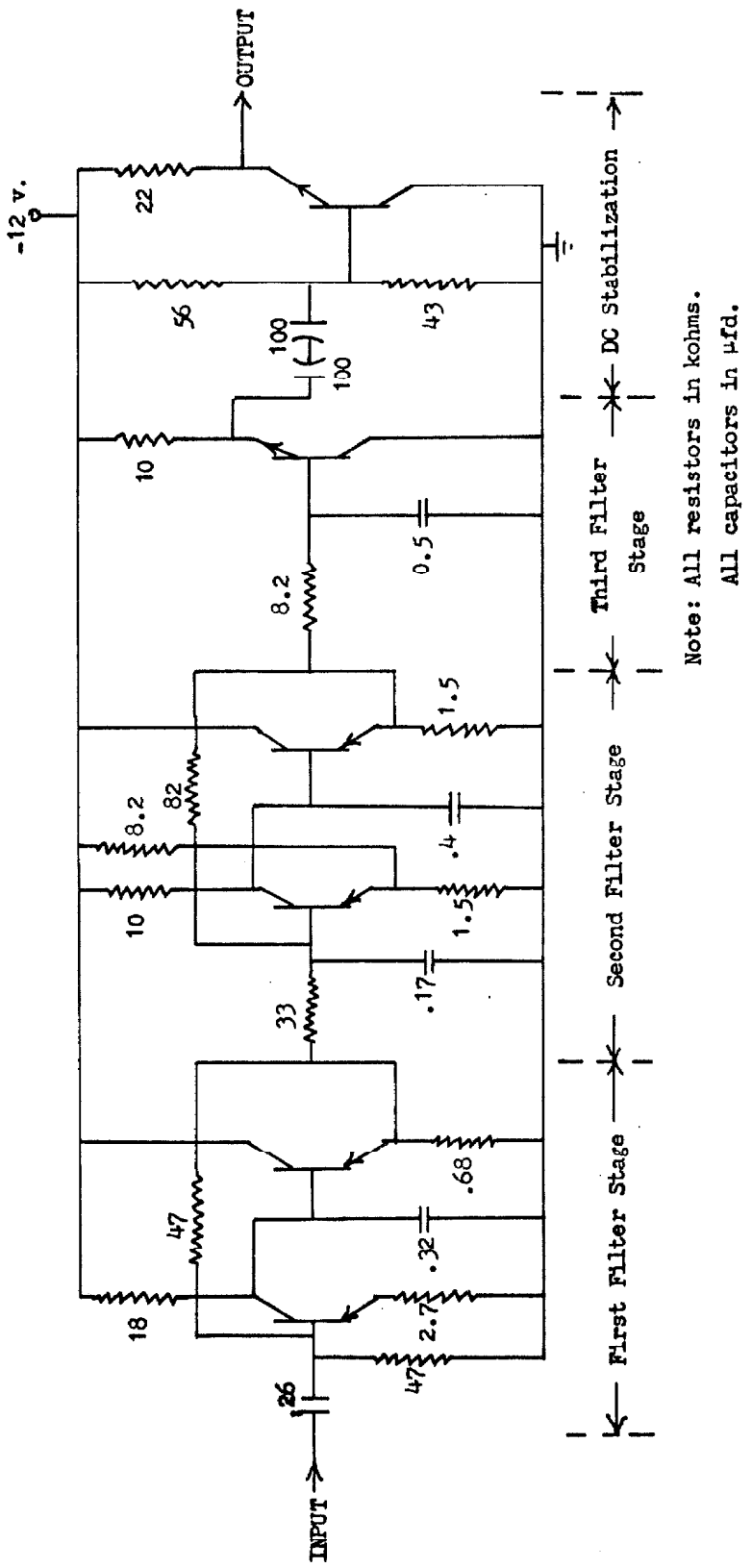

Figure APX2.2 - Circuit diagram of filter stage of flick detector.

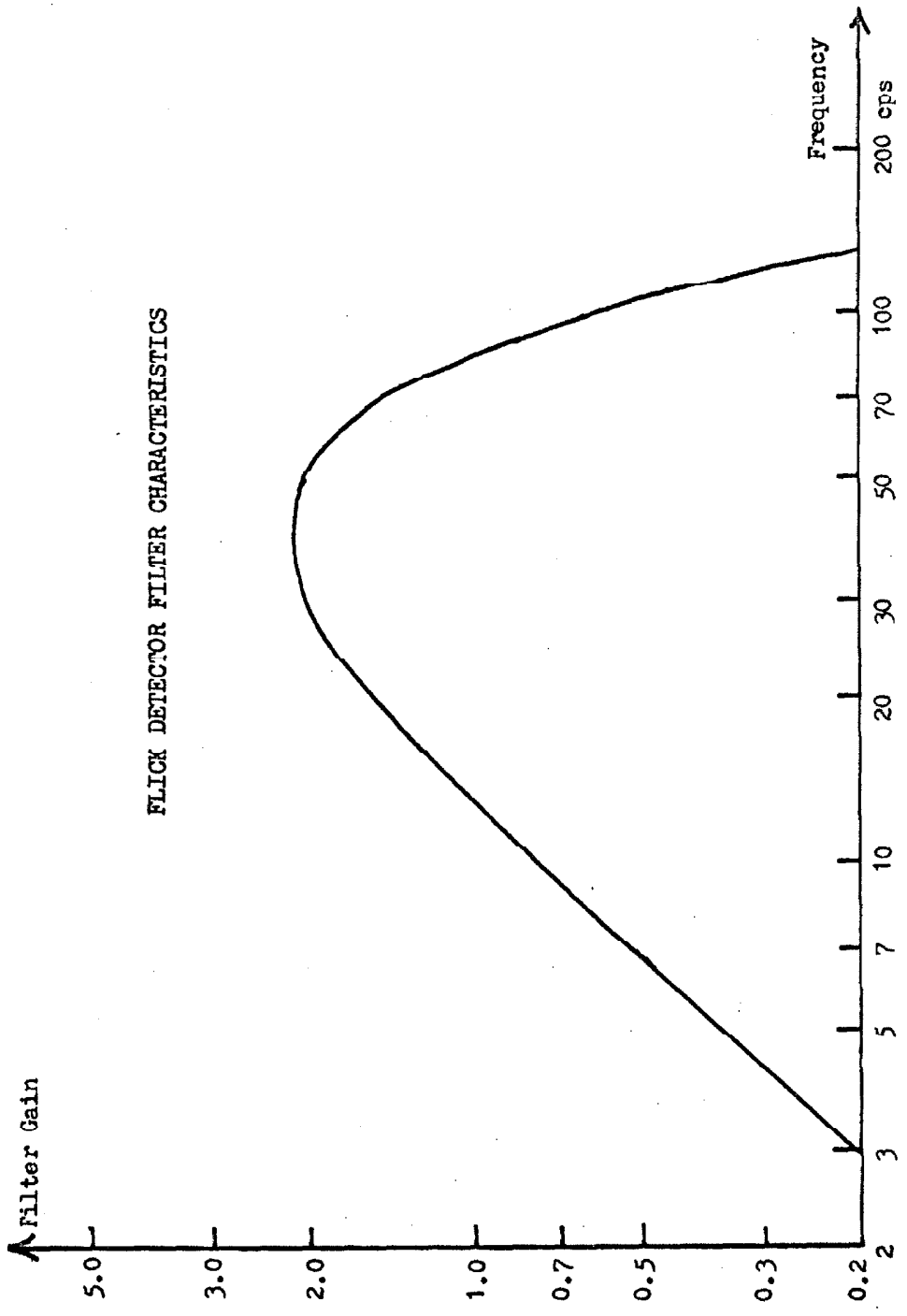

Figure APX2.3 - Gain-frequency plot for the flick detector filter-differentiator stage.

necessary to add the fourth section to the filter to block this drift. This unit contributes one pole-zero pair to the overall network, but the pole is sufficiently close to the origin that the zero has no effect on the filter characteristics in the range of interest, 30 to 40 cps.

APPENDIX III

LEAST-SQUARES FIT TECHNIQUE

Several of the data reduction methods used during the experiments described in this thesis necessitated obtaining a least-squares polynomial fit to the data - that polynomial which minimizes the squared error between the data points and the resultant curve. The technique described in this appendix obtains such a fit over a set of data points taken from arbitrary values of the independent variable.

In the derivation that is to follow, the following definitions are used. N, is the total number of data points to be fitted. Capital letters define vectors of length N, such as:

$$A = (a_1, a_2, a_3, \ldots\ldots, a_N).$$

Lower case letters are simply scalar numbers, but a scalar vector, can be defined as -

$$(c) = (c, c, c, \ldots\ldots,) \text{ out to N values.}$$

Finally the 'dot' product, is defined as:

$$(A, B) = \sum_{i=1}^{N} (a_i \cdot b_i),$$

and a form of vector multiplication as

$$(A)(B) = (a_1 b_1, a_2 b_2, a_3 b_3, \ldots\ldots, a_N b_N).$$

The first step in the fitting technique is to obtain a set of polynomials which are orthogonal over the independent variables. If the following elements are defined:

X = the vector of experimental independent variables, and

P^j = the vector of values of the j'th order polynomial evaluated at the corresponding points of the independent variable,

then, orthogonality requires that the following relationship hold true-

$$[P^j, P^k] \begin{cases} = 0 \text{ if } j \neq k \\ \neq 0 \text{ if } j = k. \end{cases}$$

The orthogonal polynomials are found from the following recursion formulae:

$$P^0 = (1),$$

$$P^1 = X - (a^1), \text{ and}$$

$$P^m = (X - (a^m))P^{m-1} - b^m P^{m-2},$$

where the coefficients a and b are found to be,

$$a^m = \frac{[XP^{m-1}, P^{m-1}]}{[P^{m-1}, P^{m-1}]}, \text{ and}$$

$$b^m = \frac{[P^{m-1}, P^{m-1}]}{[P^{m-2}, P^{m-2}]}.$$

Using these polynomials, the best fit, F, to the measured values of the dependent variable, Y, can be expressed as:

$F = \sum_{j=1}^{L} c^j p^j$, where L is the order of the fit, and the coefficients are found as:

$$c^j = \frac{[Y, P^j]}{[P^j, P^j]}.$$

The major advantage of this technique is that it places no restrictions on the selection of the independent variable, i. e., no requirement for a specified set of data points.

REFERENCES

1. Adler, F. H. and Fliegelman, F. "Influence of Fixation on the Visual Acuity," A. M. A. Arch. Ophth., 12:475, 1934.

2. Barlow, H. B. "Eye Movements During Fixation," J. Physiol., 116:290, 1952.

3. Barlow, H. B., FitzHugh, R. and Kuffler, S. W. "Dark Adaptation, Absolute Threshold and Purkinje Shift in Single Units in the Cat's Retina," J. Physiol., 137:327, 1957.

4. Baumgartner, G. "Kontrastlichteffekte an retinalen Ganglienzellen: Ableitungen vom Tractus opticus der Katze," The Visual System: Neurophysiology and Psychophysics., Edited by R. Jung and H. Kornhuber, Springer-Verlag, Berlin, 1961, p. 45.

5. Bender, M. B., Teng, P. and Weinstein, E. A. "Centering of Eyes," A. M. A. Arch. Neurol. and Psychiat., 72:282, 1954.

6. Bender, M. B. "The Eye-Centering System," A. M. A. Arch. Neurol. and Psychiat., 73:685, 1955.

7. Byford, G. H. and Stuart, H. F. "An Apparatus for the Measurement of Small Eye Movements," J. Physiol., 159:2P, 1961.

8. Byford, G. H. "The Fidelity of Contact Lens Eye Movement Recording," Optica Acta, 9:223, 1962.

9. Campbell, F. W. and Westheimer, G. "Dynamics of Accommodation Responses of the Human Eye," J. Physiol., 151:285, 1960.

10. Christman, E. H. and Kupfer, C. "Proprioception in Extraocular Muscle," A. M. A. Arch. Ophth., 69:184, 1963.

11. Clowes, M. B. and Ditchburn, R. W. "An Improved Apparatus for Producing a Stabilized Retinal Image," Optica Acta, 6:252, 1959.

12. Cogan, D. G. Neurology of the Ocular Muscles., Charles C. Thomas; Springfield, Illinois, 1956.

13. Cornsweet, T. N. "Determination of the Stimuli for Involuntary Drifts and Saccadic Eye Movements," JOSA, 46:987, 1956.

14. Dallos, P. J. "A Small Signal Analysis of the Human Eye Fixation Mechanism," Unpublished Ph. D. dissertation, Northwestern University, 1962.

15. Davson, H. Physiology of the Eye, J. and A. Churchill, Ltd; London, 1963.

16. Delabarre, E. B. "A Method of Recording Eye Movements," Am. J. Psych., 9:572, 1898.

17. Ditchburn, R. W. and Ginsborg, B. L. "Involuntary Eye Movements During Fixation," J. Physiol., 119:1, 1953.

18. Ditchburn, R. W. "Eye-Movements in Relation to Retinal Action," Optica Acta, 1:71, 1955.

19. Ditchburn, R. W. and Fender, D. H. "The Stabilised Retinal Image," Optica Acta, 2:128, 1955.

20. Ditchburn, R. W., Fender, D. H. and Mayne, S. "Vision with Controlled Movements of the Retinal Image," J. Physiol., 145:98, 1959.

21. Dodge, R. and Cline, T. S. "The Angle Velocity of Eye Movements," Psychol. Rev., 8:145, 1901.

22. Dodge, R. "Five Types of Eye Movements in the Horizontal Meridian Plane of the Field of Regard," Am. J. Physiol., 8:307, 1903.

23. Fender, D. H. "Torsional Motions of the Eyeball," Brit. J. Ophthal., 39:65, 1955.

24. Fender, D. H. "The Function of Eye Movements in the Visual Process," Unpublished Ph. D. dissertation, University of Reading, 1956.

25. Fender, D. H. and Nye, P. W. "An Investigation of the Mechanisms of Eye Movement Control," Kybernetic, 1:81, 1961.

26. Fender, D. H. "The Eye-Movement Control System: Evolution of a Model," Neural Theory and Modeling, Edited by R. F. Reiss, Stanford University Press, 1964.

27. Fender, D. H. "Contact Lens Stability," Biomedical Sciences Instrumentation, Proceedings of the Second National Biomedical Sciences Instrumentation Symposium, Edited by W. E. Murry and P. F. Salisbury, Published by ISA, Plenum Press: New York, Volume 2:43, 1964.

28. Helmholtz, H. von. Treatise on Physiological Optics, Vol. II, Translated from the Third German Edition, Edited by J. P. C. Southall. The Optical Society of America, George Banta Publishing Company; Menasha, Wisc., 1924.

29. Holst, E. von, and Mittelstaedt, H. "Das Reafferenzprinzip," Naturvissenschaften, 37:256, 1950.

30. Hubel, D. H. and Wiesel, T. N. "Receptive Fields of Optic Nerve Fibers in the Spider Monkey," J. Physiol., 154:572, 1960.

31. Hubel, D. H. and Wiesel, T. N. "Receptive Fields, Binocular Interaction and Functional Architecture in Cats Visual Cortex," J. Physiol., 160:106, 1962.

32. Huey, E. B. "On the Psychology and Physiology of Reading," Am. J. Psych., 11:283, 1899.

33. Jacobson, J. H. and Gestring, G. F. "Centrifugal Influence on the Electroretinogram," Photoreception, Annals of the New York Academy of Sciences, 74:362, 1958.

34. Johnson, L. E., Jr. "Human Eye Tracking of Aperiodic Target Functions," Systems Research Center, Case Institute of Technology, Cleveland, Ohio, 37-B-63-8.

35. Kuffler, S. W. "Discharge Patterns and Functional Organization of Mammalian Retina," J. Neurophysiol., 16:37, 1953.

36. Krauskopf, J., Cornsweet, T. N., and Riggs, L. A. "Analysis of Eye Movements During Monocular and Binocular Fixation," JOSA, 50:572, 1960.

37. Latour, P. L. "Visual Threshold During Eye Movements," Vision Res., 2:261, 1962.

38. Lehmann, D., Beeler, G. W., and Fender, D. H. "Changes in Patterns of the Human Electroencephalogram During Fluctuations of Perception of Stabilized Retinal Images." Electroenceph. Clin. Neurophysiol. (In press)

39. Lord, M. P., and Wright, W. D. "Eye Movements During Monocular Fixation," Nature, 162:25, 1948.

40. Marg, E., Jampolsky, A., and Tamler, E. "Elements of Human Extraocular Electromyography," A. M. A. Arch. Ophth., 61:258, 1959.

41. Matin, L. "Measurement of Eye Movements by Contact Lens Techniques: Analysis of Measuring Systems and Some New Methodology for Three-Dimensional Recording," JOSA, 54:1008, 1964.

42. Matin, L. and MacKinnon, G. E. "Autokinetic Movement: Selective Manipulation of Directional Components by Image Stabilization," Science, 143:147, 1964.

43. McCann, G. D., and Ray, C. B. "Computers and Data Processing for Nervous System Research," IEEE Trans. on Bio-Medical Elect., BME10:48, 1963.

44. Momose, H. "Methods of the Action of the Extraocular Muscles by Means of the Quantitative Measurements of Integrated EMG, Part I, Application of an Integrator to Behaviours of the Horizontal and Vertical Muscle in Monocular Movements," Acta Soc. Ophth. Japan, 61:1570, 1957.

45. Nachmias, J. "Two-Dimensional Motion of the Retinal Image During Monocular Fixation," JOSA, 49:901, 1959.

46. Nachmias, J. "Determiners of the Drift of the Eye During Monocular Fixation," JOSA, 51:761, 1961.

47. Nye, P. W. "The Cybernetics of Eye Movements and Their Relationship to Retinal Activity," Unpublished Ph. D. dissertation, University of Reading, 1962.

48. Orschansky, J. "Eine Methode die Augenbewegungen direkt zu untersuchen," Zbl. Physiol., 12:785, 1898..

49. Polyak, S. L. The Retina, University of Chicago Press, Chicago, Illinois, 1941.

50. Rashbass, C. "The Relationship Between Saccadic and Smooth Tracking Eye Movements," J. Physiol., 159:326, 1961.

51. Rashbass, C. and Westheimer, G. "Disjunctive Eye Movements," J. Physiol., 159:339, 1961.

52. Ratliff, F. and Riggs, L. A. "Involuntary Motions of the Eye During Monocular Fixation," J. Exp. Psych., 40:687, 1950.

53. Riggs, L. A., Armington, J. C., and Ratliff, F. "Motions of the Retinal Image During Fixation," JOSA, 44:315, 1954.

54. Robinson, D. A. "The Measurement of Eye Movement Using Magnetic Induction in a Contact Lens Coil," Biomedical Sciences Instrumentation, Proceedings of the Second National Biomedical Sciences Instrumentation Symposium, Edited by W. E. Murry and P. F. Salisbury, Published by ISA, Plenum Press: New York, Volume 2:97, 1964.

55. Stark, L. "Environmental Clamping of Biological Systems: Pupil Servomechanism," JOSA, 52:925, 1962.

56. Stark, L., Vossius, G. and Young, L. "Predictive Control of Eye Tracking Mechanisms," IRE Trans. On Human Factors in Electronics., HFE-3:52, 1962.

57. Tamler, E., Marg, E., and Jampolsky, A., and Nawratski, I. "Electromyography of Human Saccadic Eye Movements," A. M. A. Arch. Ophth., 67:658, 1959.

58. Volkmann, F. C. "Vision During Voluntary Saccadic Eye Movements," JOSA, 52:571, 1962.

59. Westheimer, G. "Kinematics of the Eye," JOSA, 47:967, 1957.

60. Whitteridge, D. "Central Control of Eye Movements," Handbook of Physiology, Section 1: Neurophysiology, Vol. II., American Physiological Society, Washington, D. C., p. 1089, 1960.

61. Young, L. R. "A Sampled Data Model for Eye Tracking Movements," Unpublished D. Sc. dissertation, Massachusetts Institute of Technology, 1962.